QUANTUM CORRELATIONS IN AND BEYOND QUANTUM ENTANGLEMENT IN BIPARTITE CONTINUOUS VARIABLE SYSTEMS

Richard Tatham

A Thesis Submitted for the Degree of PhD
at the
University of St. Andrews

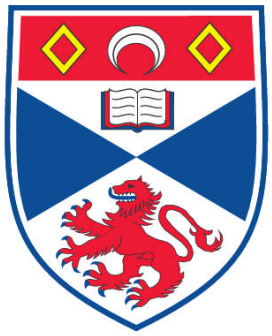

2012

Quantum correlations in and beyond quantum entanglement in bipartite continuous variable systems

Richard Tatham

School of Physics and Astronomy

This thesis is submitted in partial fulfilment for the degree of

PhD

at the

University of St Andrews

April 2012

Abstract

This thesis explores the role of non-classical correlations in bipartite continuous variable quantum systems, and the approach taken is three-fold. We show that given two initially entangled atomic ensembles, it is possible to probabilistically increase the entanglement between them using a beamsplitter-like interaction formed from two quantum non-demolition (QND) interactions with auxiliary polarised light modes. We then develop an elegant method to calculate density matrix elements of non-Gaussian bipartite quantum states and use this to show that the entanglement in a two mode squeezed vacuum can be distilled using QND interactions and non-Gaussian elements.

Secondly, we introduce a potential new measure of quantum entanglement in bipartite Gaussian states. This measure has an operational meaning in quantum cryptography and provides an upper bound on the amount of a secret key that can be distilled from a Gaussian probability distribution shared by two conspirators, Alice and Bob, given the presence of an eavesdropper, Eve.

Finally, we go beyond the realm of quantum entanglement to explore other non-classical correlations in continuous variable systems. We provide solutions for a number of these measures on two mode Gaussian states and introduce the Gaussian Ameliorated Measurement Induced Disturbance (GAMID). The interplay between these different measures and quantum entanglement is examined. We then attempt to take small steps into the non-Gaussian regime by computing these non-classicality measures on the three-parameter continuous variable Werner states.

Declarations

1. Candidate's declarations:

I, Richard Tatham, hereby certify that this thesis, which is approximately 30,000 words in length, has been written by me, that it is the record of work carried out by me and that it has not been submitted in any previous application for a higher degree.

I was admitted as a research student in October 2008 and as a candidate for the degree of Doctor of Philosophy in October 2008; the higher study for which this is a record was carried out in the University of St Andrews between 2008 and 2012.

Date 28/03/2012 Signature of candidate

2. Supervisor's declaration:

I hereby certify that the candidate has fulfilled the conditions of the Resolution and Regulations appropriate for the degree of Doctor of Philosophy in the University of St Andrews and that the candidate is qualified to submit this thesis in application for that degree.

Date: 28/03/2012 Signature of supervisor

3. Permission for electronic publication: (to be signed by both candidate and supervisor)

In submitting this thesis to the University of St Andrews I understand that I am giving permission for it to be made available for use in accordance with the regulations of the University Library for the time being in force, subject to any copyright vested in the work not being affected thereby. I also understand that the title and the abstract will be published, and that a copy of the work may be made and supplied to any bona fide library or research worker, that my thesis will be electronically accessible for personal or research use unless exempt by award of an embargo as requested below, and that the library has the right to migrate my thesis into new electronic forms as required to ensure continued access to the thesis. I have obtained any third-party copyright permissions that may be required in order to allow such access and migration.

The following is an agreed request by candidate and supervisor regarding the electronic publication of this thesis:

Access to printed copy and electronic publication of thesis through the University of St Andrews.

Date: 28/03/2012

Signature of candidate Signature of supervisor

Contents

Acknowledgements

There are several people that I would like to thank for supporting me during this thesis. Firstly, I would like to thank my supervisor, Dr Natalia Korolkova for her support and guidance throughout my time at St Andrews. I would like to thank my collaborators at the University of Nottingham, Dr Gerardo Adesso and Davide Girolami for the fantastic work that they have done. I owe a thank you to Dr David Menzies who assisted me greatly in my first year. Most of all, I would like to thank Dr Ladislav Mišta from Palacký University who has proven how patient a person can be when asked lots of stupid questions, and has provided a lot of direction. He has become a true friend and a fantastic collaborator. Finally, I would like to thank Anastasija and my family for indulging my non-stop talking about quantum information.

Publications

The following is a list of publications that have arisen as a result of the research of this thesis. They are presented in chronological order and are referred to throughout the thesis.

[I] R. Tatham, D. Menzies and N. Korolkova,
An approximate beamsplitter interaction between light and atomic ensembles,
Phys. Scr. **T143**, 014023, (2011)

[II] L. Mista, R. Tatham, D. Girolami, N. Korolkova and G. Adesso,
Measurement-induced disturbances and non-classical correlations of Gaussian states,
Phys. Rev. A **83**, 042325, (2011)

[III] R. Tatham and N. Korolkova,
Entanglement concentration for two atomic ensembles using an effective atom-light beamsplitter,
J. Phys. B: At. Mol. Opt. Phys. **44**, 175506, (2011)

[IV] R. Tatham, L. Mista, G. Adesso and N. Korolkova,
Nonclassical correlations in continuous-variable non-Gaussian Werner states,
Phys. Rev. A **85**, 022326, (2012)

[V] R. Tatham and N. Korolkova,
Entanglement concentration with quantum non demolition hamiltonians,
ArXiv:1111.4557. Submitted to Phys. Rev. A

Manuscripts in Preparation

- L. Mišta and R. Tatham,
  Gaussian Intrinsic Information
  June 2012
- R. Tatham, N. Quinn and N. Korolkova,
  The dispersion of quantum correlations in the distribution of entanglement via separable ancilla
  May 2012

Conference Presentations

The following is a list of conferences in which I have taken part.

1. 16$^{\text{th}}$ Central European Workshop on Quantum Optics (CEWQO 2009), Turku, Finland, 2009, Poster Presentation.
2. 11$^{\text{th}}$ International Conference on Squeezed States and Uncertainty Relations (ICSSUR 2009), Olomouc, Czech Republic, 2009, Poster Presentation.
3. Summer School on Scalable Quantum Computing with Light and Atoms, Cargese, Corsica, 2009, Poster Presentation.
4. Invited seminar at University of Nottingham, United Kingdom, 2010, Oral Presentation.
5. 17$^{\text{th}}$ Central European Workshop on Quantum Optics (CEWQO 2010), St Andrews, United Kingdom, 2010, Poster Presentation.
6. International Workshop on Continuous Variable Quantum Information Processing (CVQIP'10), Herrsching, Germany, 2010, Poster Presentation.
7. International Conference Photon10 QEP-19, Southampton, United Kingdom, 2010, Poster Presentation.
8. Quantum Information Scotland (QUISCO), Scotland, 2011, Oral Presentation.
9. Rank Prize Funds Symposium, Grasmere, United Kingdom, 2011, Oral Presentation.
10. International Conference on Quantum Information Processing and Communication (QIPC'11), Zurich, Switzerland, 2011, Poster Presentation.
11. Participant in Quantum Discord Workshop, Singapore, 2012

Research visits

- Palacký University, Olomouc, Czech Republic, April-May 2011
- Centre for Quantum Technologies, Singapore, January 2012

Part I

Introductory Material

Chapter 1

Introduction

The development of quantum theory can be regarded as the greatest revolution of the 20^{th} century, sweeping away the determinism of the preceding centuries and replacing it with inherent quantum uncertainty. In the years since, quantum mechanics has proven to be an undeniably successful theory. It began its journey explaining black body radiation and the photoelectric effect, and has since been used to explain the behaviour of elementary particles, chemical bonds, and the structural properties of crystals. The theory of light has not escaped the vast scope covered by quantum mechanics, with Maxwell's infamous equations now viewed as statistical truths.

One of the strangest things that quantum systems are capable of is to follow non-local dynamics [1] and to become correlated in non-local ways [2], unthinkable in the classical realm. Such phenomena are now regularly observed in laboratories worldwide, and any physical theories that claim to dispel non-locality are seen as increasingly quixotic.

Consider two people, Alice and Bob, separated by lightyears but sharing two particles from a common source. Each perform space-like separated experiments. That is, the experiments take a short time compared to the time period required for light to propagate from Alice and Bob and vice versa. Alice's experiment finishes before she could receive any classical communication from Bob, and Bob is likewise ignorant of Alice's experimental results. Only much later on, after Alice and Bob communicate classically, does it become apparent that their results are, in fact, correlated. Whatever the experimental results of one party, the other's have been non-locally influenced. These results should perhaps be expected to be correlated - after all, the two particles came from the same source. However, the beauty lies in the fact that Alice and Bob could choose to perform any measurement that they wished on their respective particles and the measurements of the other would be influenced. If they were to instead use classical objects then such correlations would require superluminal communication. This observation is at the core of all investigations into *quantum entanglement*.

That non-local correlations can exist at all without conflicting with Einstein's relativity, is possible only because all measurement outcomes are probabilistic in nature. Quantum mechanics is indeterministic, and as such can peacefully coexist with relativity. In fact, Aharanov and Shimony [3] have independently posited that relativity and non-locality are the only axioms required to uniquely define quantum mechanics amongst the myriad of other physical theories.

The indeterminacy enters at the most fundamental level - when we ask what is meant by a quantum state. Regardless of whether one holds to the Copenhagen interpretation, countless experiments have suggested that atoms may act like waves and light may act like a stream of particles. Add into the mix Heisenberg's uncertainty principle, in which after one measurement a second observable would give unpredictable results, and it is easy to see why there are so many interpretational traps to fall into. In the words [4] of Stephen Hawking: "Even God is bound by the uncertainty principle and cannot know position and velocity. He can only know the wavefunction."

The pragmatic approach is to sidestep the question and introduce a definition of a quantum state based on axiomatic principles that are born out in experiments. A quantum state $\hat{\rho}$ is a positive semi-definite, Hermitian matrix[1], inhabiting a Hilbert space such that $\mathrm{Tr}\left[\hat{\rho}\right] = 1$. This

[1]The "hat" above the ρ is used to denote an operator, as the density matrix can be viewed as an operator

last condition is to ensure that any probability distribution resulting from measurements of the quantum state normalise. At the first hurdle, it appears that the quantum theory is unclear, as there is no way that a single measurement on a single quantum object can yield an entire probability distribution. It is, then, implied that $\hat{\rho}$ denotes the statistical properties of an entire ensemble of identical quantum objects[2].

The only other important comment to be made on this is that a density matrix may be used to describe multiple systems. Two entirely statistically separate entities $\hat{\rho}_1$ and $\hat{\rho}_2$ can have their density matrices combined as $\hat{\rho} = \hat{\rho}_1 \otimes \hat{\rho}_2$ in a larger Hilbert space. Thus, we can largely remove any analysis of quantum correlations from specific experimental settings and instead analyse the properties of the abstract $\hat{\rho}$. Correlations between subsystems will be contained within the density matrix.

If a quantum state is examined entirely without any environmental interactions, i.e. we have complete statistical knowledge of the system, then the state is said to be *pure*. However, if there are interactions with any system not accounted for in $\hat{\rho}$, then $\hat{\rho}$ is said to form a *mixed state*. A mixed state is not a fundamental object. A mixed state is simply a sign of ignorance on the behalf of the researcher. If we have initially a pure state in a laboratory, but it is not closed off from the elements, it is clear that information will be lost to the environment.

Traditionally, one could verify the purity of their quantum state by checking that $\mathrm{Tr}\left[\hat{\rho}^2\right] = 1$. Another tool, much used in quantum information theory, is the von-Neumann entropy [6]

$$\mathcal{S}\left(\hat{\rho}\right) = -\mathrm{Tr}\left[\hat{\rho}\log\hat{\rho}\right] \tag{1.1}$$

where the definition is understood in terms of the eigenvalues of $\hat{\rho}$. $\mathcal{S}\left(\hat{\rho}\right)$ is zero if and only if $\hat{\rho}$ is a pure state. The von-Neumann entropy shall be used extensively throughout this thesis, particularly for defining the quantum mutual information that captures the total correlations between two subsystems $\hat{\rho}_A$ and $\hat{\rho}_B$ that make up the larger $\hat{\rho}_{AB}$

$$\mathcal{I}_q\left(\hat{\rho}_{AB}\right) = \mathcal{S}\left(\hat{\rho}_A\right) + \mathcal{S}\left(\hat{\rho}_B\right) - \mathcal{S}\left(\hat{\rho}_{AB}\right) \tag{1.2}$$

where $\hat{\rho}_A = \mathrm{Tr}_B\left[\hat{\rho}_{AB}\right]$.

Quantum entanglement has in recent years been identified as a potent resource in quantum communication and is now readily accepted. However, until fairly recently the physics community wrongly associated all non-classical correlations with quantum entanglement. However, in 2001 [7] a crude tool, the *quantum discord* was established that demonstrated a different type of non-local correlation that can be formed between quantum subsystems. These non-local correlations have recently found uses in quantum computing [8], but the full repercussions have not yet been seen.

The work carried out in the pursuit of this thesis has covered a wide range of topics. In this thesis are the best results from my studies into quantum entanglement and other non-local correlations. The main focus has been on continuous variable systems (that is, density matrices in infinite dimensional Hilbert spaces) as there remains far more to be explained than in the finite-dimensional setting. Gaussian states are a special case and shall be referred to a lot.

The structure of this thesis is as follows. In Part 1, Chapter 2 gives all of the required information for describing continuous variable systems. In Part 2, Chapter 3 details all of the relevant background information from entanglement theory. Chapters 4, 5 and 6 contain original work on entanglement distillation and measures. In Chapter 4 we detail a method for increasing quantum entanglement in two already entangled atomic ensembles. In Chapter 5 we explore entanglement distillation schemes using single quantum non-demolition interactions and non-Gaussian operations. In Chapter 6 we introduce a quantity that looks promising as an entanglement measure.

In Part 3, Chapter 7 contains relevant background information on quantum discord and related measurements of correlations in bipartite systems. Chapters 8 and 9 contain further original work on non-classicality indicators. In Chapter 8, we define a new non-classicality

---

acting in a Hilbert space.

[2]It is assumed throughout this thesis that the reader has a working knowledge of quantum mechanics and so it is unnecessary to outline all the axioms and implicit assumptions from which quantum theory follows. For a detailed analysis, I recommend [5].

measure on Gaussian states and find analytic solutions on two mode Gaussian states. In Chapter 9 we explore the quantum correlations in a simple non-Gaussian state.

The work in Chapters 4 and 5 is entirely my own. The investigation of the Gaussian Intrinsic Information in Chapter 6 is an ongoing project with Dr. Ladislav Mišta of Palacký University with most work being carried out in parallel so as to make sure thare are no errors. The work of Chapters 8 and 9 has been carried out in collaboration with Dr Mišta and Dr Gerardo Adesso at the University of Nottingham. In both chapters, all analytic work was carried out primarily by myself and Dr Mišta in parallel with Dr Adesso (and in the case of Chapter 8, his PhD student Davide Girolami) performing numerical calculations. My supervisor, Dr Natalia Korolkova, has provided guidance on all projects except for the measure discussed in Chapter 6.

In the final chapter we provide conclusions and suggest further work that could be done on the ideas in this thesis.

Chapter 2

Continuous Variable Systems

In recent years, as the drive for quantum computers and communication hurtles ever forward, more and more thought and attention has been given to how to implement quantum devices in practice. Atomic systems have long been thought of as great candidates for quantum memory and quantum repeaters [9, 10, 11]. To transmit signals, the obvious workhorse is light.

Light is a quantum object. If we shine a torch through two slits and onto a screen we see wave-like interference patterns. Light can be polarised and succumbs to diffraction and refraction. Light propagates in space and interferes with itself. Light is a wavelike object.

And yet, with suitable detectors we could consider the corpuscle nature of light in the guise of photons. Einstein was awarded the Nobel prize in 1921 for his explanation of the photoelectric effect, based on exactly that idea [12]. Light consists of particles.

The quantum nature of light has long been known. Planck's initial treatise in 1905 asserted just that! As light is such a useful resource in quantum information theory, we here give an introduction to quantum optics, as the quantum language of light provides the perfect playground in which to introduce continuous variable systems.

In what follows we discuss the basics of quantum optics, as has been described in lots of excellent references [13, 14, 15, 16, 17, 18, 19, 20]. We shall begin by quantising the electromagnetic field and demonstrating the different representations of light: quadrature states, Fock states, and coherent states. Once the basic formalism of continuous variable systems has been established, we shall introduce the quasiprobability distributions that best represent quantum states in phase space. We shall also discuss the special class of Gaussian states for which a covariance matrix formalism proves sufficient for most required calculations.

2.1 Introductory quantum optics

Quantisation of the Electromagnetic Field

Maxwell revolutionised science when he introduced his famous equations to describe the behaviour of light. In dielectric media, an electric field $\mathbf{E}$ causes the bound charges in the material to move, inducing a local electric dipole moment. This gives rise to an electric displacement field $\mathbf{D} = \epsilon\epsilon_0\mathbf{E}$ where ϵ_0 is the permittivity of free space and ϵ is the permittivity of the material in question. In free space $\epsilon = 1$. Magnetic fields can be described in terms of the magnetizing field $\mathbf{H}$ and the magnetic induction $\mathbf{B} = \mu\mu_0\mathbf{H}$ where μ_0 is the permeability of free space. The character μ defines the permeability coefficient of the material through which the light travels and in free space is given by $\mu = 1$. Maxwell's equations can be written in differential form as

$$\nabla \cdot \mathbf{D} = 0, \quad \nabla \cdot \mathbf{B} = 0, \quad \nabla \times \mathbf{E} = -\frac{\partial \mathbf{B}}{\partial t}, \quad \nabla \times \mathbf{H} = -\frac{\partial \mathbf{D}}{\partial t} \tag{2.1}$$

and also require the boundary conditions that the fields vanish at infinity.

Maxwell's equations complemented Newtonian mechanics and ushered in the confident age in which it was thought that the universe operated along strictly deterministic lines. With the discoveries of Planck and Einstein at the beginning of the 21^{st} century, quantum uncertainty came to the fore. We can regard the classical fields $\mathbf{E}, \mathbf{D}, \mathbf{B}, \mathbf{H}$ as the expectation values of quantum observables e.g. $\left\langle \hat{\mathbf{E}} \right\rangle = \mathbf{E}$. From this simple yet plausible assumption it follows that

the quantum field strengths must obey Maxwell's equations as well, due to their linearity. By replacing $\mathbf{E}, \mathbf{D}, \mathbf{B}, \mathbf{H}$ in (2.1) with their hatted operator counterparts $\hat{\mathbf{E}}, \hat{\mathbf{D}}, \hat{\mathbf{B}}, \hat{\mathbf{H}}$ we describe the behaviour of the quantum fields.

As in classical electrodynamics, the quantum fields may be expressed in terms of a vector potential $\mathbf{A}$, which can be replaced with an operator $\hat{\mathbf{A}}$.

$$\hat{\mathbf{E}} = -\frac{\partial \hat{\mathbf{A}}}{\partial t}, \quad \hat{\mathbf{B}} = \nabla \times \hat{\mathbf{A}} \tag{2.2}$$

With this, the middle two of Maxwell's equations are automatically satisfied. The electromagnetic field is gauge invariant so for simplicity we introduce the Coulomb gauge

$$\nabla \cdot \hat{\mathbf{A}} = 0. \tag{2.3}$$

This satisfies $\nabla \cdot \hat{\mathbf{D}} = 0$ immediately.

By rewriting the fourth Maxwell equation in terms of $\hat{\mathbf{A}}$ and using the vector identity $\nabla \times \left(\nabla \times \hat{\mathbf{A}}\right) = \nabla\left(\nabla \cdot \hat{\mathbf{A}}\right) - \nabla^2 \hat{\mathbf{A}}$, we arrive at

$$\nabla^2 \hat{\mathbf{A}} - \frac{1}{c^2}\frac{\partial^2 \hat{\mathbf{A}}}{\partial t^2} = 0. \tag{2.4}$$

That is, the vector potential satisfies the wave equation. In deriving the wave equation, the speed of light in a vacuum c emerges as $c = 1/\sqrt{\mu_0 \epsilon_0}$.

The wave nature of light implies that it is subject to the superposition principle: if two light fields interfere their amplitudes add together. This is due to the linearity of Maxwell's equations, which in turn implies that the superposition principle holds in the quantum world. In fact, a quantum field $\hat{\mathbf{A}}(\mathbf{r}, t)$ already contains all possible light fields, waiting to be made into reality by the measurement process.

If we were to consider the classical field $\mathbf{A}(\mathbf{r}, t)$ then we could rewrite it as $\mathbf{A}(\mathbf{r}, t) = \mathbf{A}^{(+)}(\mathbf{r}, t) + \mathbf{A}^{(-)}(\mathbf{r}, t)$ with $\mathbf{A}^{(-)}(\mathbf{r}, t) = \left(\mathbf{A}^{(+)}(\mathbf{r}, t)\right)^{\dagger}$. $\mathbf{A}^{(+)}(\mathbf{r}, t)$ contains all amplitudes which vary as $e^{-i\omega t}, \omega > 0$ and $\mathbf{A}^{(-)}(\mathbf{r}, t)$ contains all amplitudes that vary as $e^{i\omega t}$. Importantly, the complex conjugate is part of the complete set of classical waves because Maxwell's equations are real.

In order to discretise the field variables, it is necessary to assume the field is contained in a finite spatial volume $\mathcal{V}$. The contributions $\mathbf{A}^{(+)}(\mathbf{r}, t)$ can be expanded as

$$\mathbf{A}^{(+)}(\mathbf{r}, t) = \sum_{k=0}^{\infty} \mathcal{A}_k \mathbf{u}_k(\mathbf{r}) e^{-i\omega_k t} \tag{2.5}$$

where the Fourier coefficients $\mathcal{A}_k$ are constant as the field is free. When $\mathcal{V}$ contains no refracting materials all vector mode functions $\mathbf{u}_k(\mathbf{r})$ must independently obey the wave equation (2.4). That is,

$$\left(\nabla^2 + \frac{\omega_k^2}{c^2}\right) \mathbf{u}_k(\mathbf{r}) = 0 \tag{2.6}$$

for all k and the Coulomb gauge implies that $\nabla \cdot \mathbf{u}_k(\mathbf{r}) = 0$. As the modes form a complete, orthonormal set the condition

$$\int_{\mathcal{V}} \mathbf{u}_k^*(\mathbf{r}) \mathbf{u}_{k'}(\mathbf{r}) \, \mathrm{d}\mathcal{V} = \delta_{k,k'} \tag{2.7}$$

also applies.

In theory we could consider any solution to $\mathbf{u}_k(\mathbf{r})$ that satisfied the correct conditions of $\nabla \cdot \mathbf{u}_k(\mathbf{r}) = 0$, equations (2.6) and (2.7). For example, we could consider the plane wave solution appropriate to a cubic volume $\mathcal{V}$ with length of sides given by $\mathcal{L}$:

$$\mathbf{u}_k(\mathbf{r}) = \frac{1}{\mathcal{L}^{3/2}} \mathbf{e}_\sigma e^{i\mathbf{k}\cdot\mathbf{r}}. \tag{2.8}$$

Here, $\mathbf{k}$ is the wave vector, $\mathbf{e}_\sigma$ is the unit polarization vector (which is necessarily orthogonal to $\mathbf{k}$ as $\nabla \cdot \mathbf{u}_k(\mathbf{r}) = 0$, and the dispersion relation $|\mathbf{k}| = \omega_k/c$ is obtained by (2.6). The polarisation index and wave vector are all encompassed in the mode index k.

The quantised vector potential can take the form

$$\begin{aligned}\hat{\mathbf{A}}(\mathbf{r},t) &= \sum_{k=0}^{\infty}\sqrt{\frac{\hbar}{2\omega_k\epsilon_0}}\left[\mathbf{u}_k(\mathbf{r})\,e^{-i\omega_k t}\hat{a}_k + \mathbf{u}_k^*(\mathbf{r})\,e^{i\omega_k t}\hat{a}_k^\dagger\right] \\ &= \sum_{k=0}^{\infty}\sqrt{\frac{\hbar}{2\omega_k\mathcal{V}}}\mathbf{e}_\sigma\left[e^{i(\mathbf{k}\cdot\mathbf{r}-\omega_k t)}\hat{a}_k + e^{-i(\mathbf{k}\cdot\mathbf{r}-\omega_k t)}\hat{a}_k^\dagger\right]. \end{aligned} \tag{2.9}$$

All of the quantumness of field $\hat{\mathbf{A}}(\mathbf{r},t)$ is obtained by replacing the fourier coefficients $\mathcal{A}_k$ with the operators $\hat{a}_k$ and $\hat{a}_k^\dagger$ and imposing that they are mutually adjoint. Maxwell's equations correctly give real values. The normalisation factor renders the operators dimensionless. Equations (2.2) indicate that the electric and magnetic fields can be quantised as

$$\hat{\mathbf{E}}(\mathbf{r},t) = i\sum_{k=0}^{\infty}\sqrt{\frac{\hbar\omega_k}{2\epsilon_0}}\left[\mathbf{u}_k(\mathbf{r})\,e^{-i\omega_k t}\hat{a}_k + \mathbf{u}_k^*(\mathbf{r})\,e^{i\omega_k t}\hat{a}_k^\dagger\right] \tag{2.10}$$

$$\hat{\mathbf{B}}(\mathbf{r},t) = i\sum_{k=0}^{\infty}\sqrt{\frac{\hbar}{2\omega_k\epsilon_0}}\left[(\mathbf{k}\times\mathbf{u}_k(\mathbf{r}))\,e^{-i\omega_k t}\hat{a}_k + (\mathbf{k}\times\mathbf{u}_k^*(\mathbf{r}))\,e^{i\omega_k t}\hat{a}_k^\dagger\right] \tag{2.11}$$

As an ansatz, we consider that the quantum Hamiltonian of an electromagnetic field is given by replacing all field components with operators.

$$H = \frac{1}{2}\int_{\mathcal{V}}(\mathbf{E}\cdot\mathbf{D} + \mathbf{B}\cdot\mathbf{H})\,\mathrm{d}\mathcal{V} \rightarrow \hat{H} = \frac{1}{2}\int_{\mathcal{V}}\left(\epsilon_0\hat{\mathbf{E}}^2 + \frac{\hat{\mathbf{B}}^2}{\mu_0}\right)\mathrm{d}\mathcal{V} \tag{2.12}$$

By inserting (2.10) and (2.11) into (2.12) the Hamiltonian can be written as

$$\hat{H} = \frac{1}{2}\sum_{k=0}^{\infty}\hbar\omega_k\left(\hat{a}_k^\dagger\hat{a}_k + \hat{a}_k\hat{a}_k^\dagger\right). \tag{2.13}$$

By imposing the condition that the field amplitudes $\hat{\mathbf{A}}$ and $\hat{\mathbf{D}}$ at various points in space but at the same point in time are causally disconnected, and observing how the fields transform in time, it is possible to show [13] that the bosonic commutation relation for the introduced mode operators is

$$\left[\hat{a}_k, \hat{a}_{k'}^\dagger\right] = \delta_{k,k'}. \tag{2.14}$$

The Hamiltonian (2.13) can then be rewritten as

$$\hat{H} = \frac{1}{2}\sum_{k=0}^{\infty}\hbar\omega_k\left(\hat{a}_k^\dagger\hat{a}_k + \frac{1}{2}\right). \tag{2.15}$$

The entire electromagnetic field can therefore be described by the tensor product state of all these quantum harmonic oscillators. Each one represents a single electromagnetic mode. The bosonic operators $\hat{a}_k$ and $\hat{a}_k^\dagger$ can be considered as annihilating and creating photons respectively in mode k. The photon number operator, counting the number of photons in mode k is defined as

$$\hat{n}_k = \hat{a}_k^\dagger\hat{a}_k \tag{2.16}$$

An important consequence of the quantisation process is that the vacuum $|0\rangle$ has non-zero energy ($\langle 0|\hat{H}|0\rangle > 0$). Due to Heisenberg's uncertainty principle, the vacuum contains random fluctuations. That is, $|0\rangle$ is a valid quantum state.

With the electromagnetic field quantised and annihilation/creation operators introduced, we can now begin to discuss other representations of continuous variable quantum states. In the remainder of this thesis, $\hbar = 1$ unless otherwise stated.

Quadrature states

In what follows we shall consider representations of a single mode, and for convenience drop the subscript k. We begin by introducing two operators $\hat{x}$ and $\hat{p}$ called the *quadrature operators* and can be considered as the real and imaginary parts of the complex $\hat{a}$ multiplied by a factor[1] of $\sqrt{2}$.

$$\hat{x} = \frac{1}{\sqrt{2}}\left(\hat{a}^\dagger + \hat{a}\right), \quad \hat{p} = \frac{i}{\sqrt{2}}\left(\hat{a}^\dagger - \hat{a}\right) \tag{2.17}$$

The annihilation operator can be written as $\hat{a} = (1/\sqrt{2})(\hat{x} + i\hat{p})$. In quantum optics, the quadratures commonly correspond to the in phase and out of phase components of the electric field amplitude with respect to a reference phase. However, the physical representation of these constructs is not important - they can simply be thought of as conjugate "position" and "momentum" in phase space, satisfying the commutation relation

$$[\hat{x}, \hat{p}] = i \tag{2.18}$$

(where $\hbar = 1$). They have no bearing on the position and momentum of e.g. a photon, which in any case is challenging to define. They can be rotated by a unitary operator $U = \exp[i\phi]$ in phase space and still satisfy the commutation relation (2.18) in their new form

$$\hat{x}_\phi = \hat{x}\cos\phi + \hat{p}\sin\phi, \quad \hat{p}_\phi = -\hat{x}\sin\phi + \hat{p}\cos\phi. \tag{2.19}$$

The phase shift can be thought of, in the quantum optics case, as shifting the reference phase mentioned previously. A phase shift of $\pi/2$ rotates from a position to a momentum representation. The eigenstates of the quadratures, the *quadrature states* satisfy

$$\hat{x}|x\rangle = x|x\rangle, \quad \hat{p}|p\rangle = p|p\rangle \tag{2.20}$$

and are orthogonal and complete:

$$\langle x|x'\rangle = \delta\left(x - x'\right), \quad \langle p|p'\rangle = \delta\left(p - p'\right), \quad \int_{-\infty}^{\infty} |x\rangle\langle x|\mathrm{d}x = \int_{-\infty}^{\infty} |p\rangle\langle p|\mathrm{d}p = \mathbb{1}. \tag{2.21}$$

The quadrature states are not physical as they require an infinite precision to define, but act as a useful mathematical trick. For a wavefunction represented by $|\psi\rangle$ we can define the probability amplitude in the position and momentum bases via

$$\langle x|\psi\rangle = \psi\left(x\right), \quad \langle p|\psi\rangle = \tilde{\psi}\left(p\right). \tag{2.22}$$

The wavefunction $|\psi\rangle$ can be written as e.g.

$$|\psi\rangle = \int_{-\infty}^{\infty} |x\rangle\left\langle x|\psi\right\rangle \mathrm{d}x = \int_{-\infty}^{\infty} \psi\left(x\right)|x\rangle \mathrm{d}x. \tag{2.23}$$

As a final note, position and momentum states are related by Fourier transform:

$$|x\rangle = \frac{1}{2\pi}\int_{-\infty}^{\infty} \mathrm{d}p \exp[-ixp]|p\rangle, \tag{2.24}$$

$$|p\rangle = \frac{1}{2\pi}\int_{-\infty}^{\infty} \mathrm{d}x \exp[+ixp]|x\rangle. \tag{2.25}$$

Fock states

Another useful state representation is the Fock or number state $|n\rangle$, defined as the eigenstate of the number operator $\hat{n}$.

$$\hat{n}|n\rangle = \hat{a}^\dagger\hat{a}|n\rangle = n|n\rangle. \tag{2.26}$$

[1] In the literature, this normalisation factor is not unique and so the quadrature operators may sometimes be defined differently. The most common normalisation factors are 1 and 2 along with the $\sqrt{2}$ used here.

A ket $|n\rangle$ therefore represents a state of n photons (excitations). The annihilation and creation operator respectively lower and raise the number of photons in the mode:

$$\hat{a}|n\rangle = \sqrt{n}|n-1\rangle, \tag{2.27}$$

$$\hat{a}^\dagger|n\rangle = \sqrt{n+1}|n+1\rangle. \tag{2.28}$$

The Fock state $|n\rangle$ can then be thought of as n excitations of the vacuum. That is,

$$|n\rangle = \frac{\left(\hat{a}^\dagger\right)^n}{\sqrt{n}}|0\rangle. \tag{2.29}$$

The Fock states are also orthogonal and complete:

$$\langle n'|n\rangle = \delta_{n,n'}, \quad \sum_{n=0}^{\infty} |n\rangle\langle n| = \mathbb{1}. \tag{2.30}$$

Importantly, equation (2.27) bounds the number of photons from below[2] as $\hat{a}|0\rangle = 0$. One consequence of this is the following. If we express $\hat{a}$ in terms of quadratures but replace the momentum operator $\hat{p}$ with $-i\partial/\partial x$, then it becomes apparent that

$$\hat{a}|0\rangle = \hat{a}\int_{-\infty}^{\infty} \mathrm{d}x\psi_0(x)|x\rangle = \int_{-\infty}^{\infty} \mathrm{d}x\frac{x+(\partial/\partial x)}{\sqrt{2}}\psi_0(x)|x\rangle = 0. \tag{2.31}$$

The solution of this equation is then

$$\psi_0(x) = \frac{1}{\pi^{1/4}}e^{-\frac{x^2}{2}}, \qquad \left(\tilde{\psi}_0(p) = \frac{1}{\pi^{1/4}}e^{-\frac{p^2}{2}}\right). \tag{2.32}$$

That is, the vacuum state can be described by a Gaussian phase space distribution, due to the Heisenberg uncertainty relation. In a similar fashion, the quadrature distributions of the n^{th} Fock state can be expressed as

$$\psi_n(x) = \langle x|n\rangle = \frac{H_n(x)}{\sqrt{2^n n!}\pi^{1/4}}e^{-\frac{x^2}{2}} \tag{2.33}$$

$$\tilde{\psi}_n(p) = \langle p|n\rangle = \frac{H_n(p)}{\sqrt{2^n n!}\pi^{1/4}}e^{-\frac{p^2}{2}} \tag{2.34}$$

where H_n is the n^{th} Hermite polynomial.

Coherent states

As the mode functions $\mathbf{u}_k(\mathbf{r})$ used to define the electric field in (2.10) form an orthonormal set, it logically follows that the eigenstates of the field follow an infinite succession of relations $\hat{a}_k|\alpha_k\rangle = \alpha_k|\alpha_k\rangle$. The coherent state of the field as a whole then is made up of a direct product of the individual states $|\alpha_k\rangle$.

We consider a single mode and drop the mode index k. The oscillator state which satisfies

$$\hat{a}|\alpha\rangle = \alpha|\alpha\rangle \tag{2.35}$$

is known as a coherent state or sometimes as a Glauber state after the Nobel prize winner who first considered them in mathematical detail [21, 22]. In actuality, coherent states were first mentioned by Schrödinger [23] (translated to English in [24]) as a response to criticisms by Lorentz that quantum mechanics did not allow for the emergence of classical behaviour in light. However, the idea is usually credited to Glauber who gave detailed accounts.

---

[2] In actual fact this is not the only possibility. Another solution would be $\hat{a}|0\rangle \neq 0$ but $\hat{a}^\dagger\hat{a}|0\rangle = 0$. This, however, has the unfortunate consequence of leading to a vacuum state wavefunction that cannot be normalised. The resulting wave function is therefore known as the *irregular wave function* of the vacuum.

If we project both sides of (2.35) onto the bra $\langle n|$ and use the adjoint of equation (2.28) then we immediately attain the recursion relation $\sqrt{n+1}\,\langle n+1|\alpha\rangle = \alpha\,\langle n|\alpha\rangle$ from which it can be seen that

$$\langle n|\alpha\rangle = \frac{\alpha^n}{\sqrt{n!}}\,\langle 0|\alpha\rangle\,. \tag{2.36}$$

From the completeness of the Fock states it follows that

$$|\alpha\rangle = \sum_{n=0}^{\infty} |n\rangle\,\langle n|\alpha\rangle = e^{-\frac{|\alpha|^2}{2}} \sum_{n=0}^{\infty} \frac{\alpha^n}{\sqrt{n!}}|n\rangle \tag{2.37}$$

where the normalisation $\langle\alpha|\alpha\rangle = 1$ leads to $\langle 0|\alpha\rangle = e^{-\frac{|\alpha|^2}{2}}$. From (2.36) and (2.37) the photon number distribution is given by a Poissonian distribution as

$$p_n = |\,\langle n|\alpha\rangle\,|^2 = \frac{|\alpha|^{2n}}{n!}e^{-|\alpha|^2}. \tag{2.38}$$

That is, if we repeatedly count the number of photons in a coherent state we obtain n photons with probability p_n. On average we get as many photons as quantified by the mean value $|\alpha|^2$.

A similar situation arises classically, if we were to repeatedly count a number of randomly distributed classical particles. A Poissonian distribution is essentially classical in nature - a light source emitting a coherent state would yield a random spacing between photons and remain unaffected by the detection (annihilation) of a field excitation by definition. Some other photon emitting sources are allowed to have different statistics. For example, a thermal light source gives off "bunches" of photons revealing super-poissonian statistics, and the annihilation of the photon does not leave the thermal state unperturbed. Coherent states thus offer the "most classical" quantum description of light which is to be expected as they are produced, for example, as the output of a laser and so mimic the wave nature of classical light.

It is important to note that the set of coherent states is not orthogonal as they are not eigenstates of a Hermitian operator:

$$\langle\beta|\alpha\rangle = e^{-\frac{|\alpha|^2}{2}-\frac{|\beta|^2}{2}-\beta^*\alpha} \tag{2.39}$$

and so $|\,\langle\beta|\alpha\rangle\,|^2 = \exp[-|\alpha-\beta|^2]$. If $|\alpha\rangle$ and $|\beta\rangle$ differ a lot then the overlap tends to zero asymptotically.

Coherent states can be formulated in another useful way that highlights their properties in phase space. We introduce the unitary *displacement operator*

$$\hat{D}\,(\alpha) = \exp[\alpha\hat{a}^\dagger - \alpha^*\hat{a}] \tag{2.40}$$

which has the properties [25]

$$\mathrm{Tr}\left[\hat{D}\,(\alpha)\right] = \mathrm{Tr}\left[\hat{D}^\dagger\,(\alpha)\right] = \pi\delta\left(\mathcal{R}\,(\alpha)\right)\delta\left(\mathcal{I}\,(\alpha)\right) \tag{2.41}$$

and

$$\hat{D}\,(\alpha_1)\,\hat{D}\,(\alpha_2) = e^{(\alpha_1\alpha_2^* + \alpha_1^*\alpha_2)}\hat{D}\,(\alpha_1+\alpha_2)\,. \tag{2.42}$$

The displacement operator has the effect of adding a complex number α to the annihilation operator:

$$\hat{D}^\dagger\,(\alpha)\,\hat{a}\hat{D}\,(\alpha) = \hat{a} + \alpha. \tag{2.43}$$

We could conceivably apply a negative displacement to a coherent state to see that

$$\hat{a}\hat{D}\,(-\alpha)\,|\alpha\rangle = \hat{D}\,(-\alpha)\,\hat{D}^\dagger\,(-\alpha)\,\hat{a}\hat{D}\,(-\alpha)\,|\alpha\rangle = \hat{D}\,(-\alpha)\,(\hat{a}-\alpha)\,|\alpha\rangle = 0 \tag{2.44}$$

and so $\hat{D}\,(-\alpha)\,|\alpha\rangle = |0\rangle$ which implies that coherent states are simply vacuum states that have been displaced in phase space. Physically, of course, $|\alpha\rangle$ and $|0\rangle$ are quite different, in energy if nothing else. They simply have the same quantum uncertainty as the vacuum, as noticed by Schrödinger in 1926 [23].

However, we can write the complex amplitude α in terms of real and imaginary parts as

$$\alpha = \frac{1}{\sqrt{2}}\,(\bar{x} + i\bar{p})\,. \tag{2.45}$$

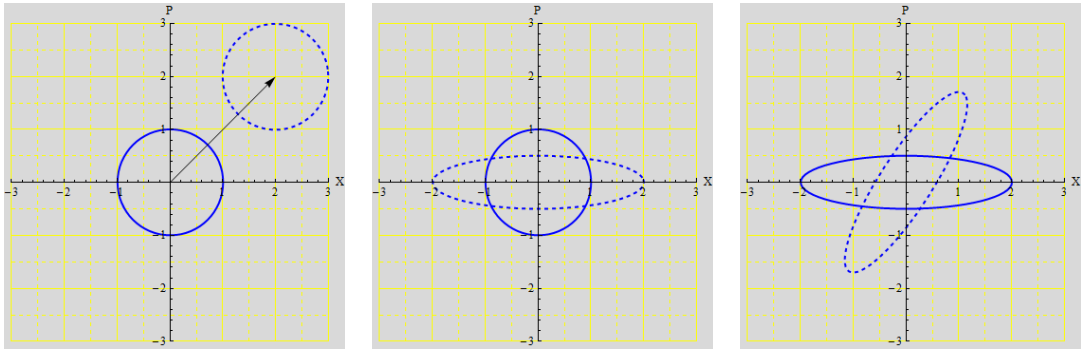

(a) Displacement (b) Squeezing (c) Phase Rotation

Figure 2.1: On a plot of position x and momentum p, a classical system could be represented by a point. In a quantum system there is inherent uncertainty. The effect of the displacement operator is to shift a distribution in phase space (Figure 2.1a). The squeezing operator (Figure 2.1b) reduces the uncertainty in one phase space variable at the expense of the other. The phase operator simply alters the quantum state's orientation (Figure 2.1c).

Replacing (2.45) in the definition of $\hat{D}(\alpha)$ and using the Baker-Hausdorff formula [26]

$$\begin{aligned} e^{\hat{F}+\hat{G}} &= e^{-\frac{1}{2}\left[\hat{F},\hat{G}\right]} e^{\hat{F}} e^{\hat{G}} \\ &= e^{\frac{1}{2}\left[\hat{F},\hat{G}\right]} e^{\hat{G}} e^{\hat{F}} \end{aligned} \tag{2.46}$$

we can write

$$\begin{aligned} \hat{D}(x,p) &= \exp\left[\frac{-i\bar{p}\bar{x}}{2}\right] \exp\left[i\bar{p}\hat{x}\right] \exp\left[-i\bar{x}\hat{p}\right] \\ &= \exp\left[\frac{i\bar{p}\bar{x}}{2}\right] \exp\left[i\bar{x}\hat{p}\right] \exp\left[-i\bar{p}\hat{x}\right] \end{aligned} \tag{2.47}$$

which has the effect of shifting the distributions by $\bar{p}$ and $\bar{x}$ in phase space e.g.

$$\langle x|\alpha\rangle = \frac{1}{\pi^{1/4}} \exp\left[-\frac{(x-\bar{x})^2}{2} + i\bar{p}x - \frac{i\bar{p}\bar{x}}{2}\right]. \tag{2.48}$$

Of course, if $\alpha = 0$ then $\bar{x} = \bar{p} = 0$ and we have the vacuum quadrature distribution. Coherent states have the same level of uncertainty as the vacuum and are minimum uncertainty states i.e. Heisenberg's uncertainty principle

$$\Delta x \Delta p \geq 1/2 \tag{2.49}$$

is saturated for coherent states.

Minimum Uncertainty States and the Squeezing Operator

We could ask what other states saturate the bound (2.49). In fact Pauli [27] (translation [28]) used a beautifully elegant method to show that a minimum uncertainty state $|\phi\rangle$ must satisfy the equation

$$\frac{1}{2}\frac{x}{\Delta^2 x}\phi(x) + \frac{\partial}{\partial x}\phi(x) = 0 \tag{2.50}$$

where $\Delta^2 x$ is the variance of the position distribution. The solution to this is

$$\phi(x) = \frac{1}{(2\Delta^2 x \pi)^{1/4}} \exp\left[-\frac{x^2}{4\Delta^2 x}\right]. \tag{2.51}$$

Up to displacement, minimum uncertainty states are like coherent states. However, there is another beauty to Pauli's solution. Conceivably, the variance $\Delta^2 x$ does not have to equal $1/2$. That is, $\Delta^2 x$ and $\Delta^2 p$ could differ so long as (2.49) is satisfied. The uncertainty in position x of the state could be decreased ("squeezed") at the expense of knowledge of the momentum quadrature.

We parametrise the squeezing by parameter r and so

$$\Delta^2 x = \frac{1}{2}e^{-2r}, \quad \Delta^2 p = \frac{1}{2}e^{2r} \tag{2.52}$$

which can be shown to be the result of applying a unitary squeezing operator [29, 30, 31]

$$\hat{S}(r) = \exp\left[\frac{r}{2}\left(\hat{a}^{\dagger 2} - \hat{a}^2\right)\right] \tag{2.53}$$

to the vacuum $|0\rangle$.

Pauli's proof showed that in fact all minimum uncertainty states are Gaussian and can be thought of as displaced, squeezed, vacuum states in phase space i.e.

$$|\phi\rangle = \hat{D}(\alpha)\,\hat{S}(r)\,|0\rangle, \tag{2.54}$$

which encompasses the vacuum trivially and all coherent states. A minimum uncertainty state would have a position quadrature distribution of

$$\phi(x) = \frac{1}{\pi^{1/4}}e^{r/2}\exp\left[-e^{2r}\frac{(x-\bar{x})^2}{2} + ipx - \frac{i\bar{p}\bar{x}}{2}\right]. \tag{2.55}$$

We can consider the effect of the squeezing operator on the vacuum in more detail by normally ordering it. Define $\hat{K}_+ = \left(\hat{a}^\dagger/2\right)^2$, $\hat{K}_- = \left(\hat{a}/2\right)^2$, $\hat{K}_0 = (\hat{n} + 1/2)$, which have commutation relations

$$\left[\hat{K}_-, \hat{K}_0\right] = 2\hat{K}_-, \quad \left[\hat{K}_+, \hat{K}_0\right] = -2\hat{K}_+, \quad \left[\hat{K}_-, \hat{K}_+\right] = \hat{K}_0. \tag{2.56}$$

The squeezing operator can then be written as

$$\hat{S}(r) = e^{r\hat{K}_+ - r\hat{K}_-} = e^{f(r)\hat{K}_+}e^{g(r)\hat{K}_0}e^{h(r)\hat{K}_-}. \tag{2.57}$$

Following a method demonstrated elsewhere [32, 33, 34], if both sides of (2.57) are differentiated with respect to r and multiplied on the right by $\hat{S}^{-1}(r)$ then the result is

$$\begin{aligned}\hat{K}_+ - \hat{K}_- =& f'(r)\hat{K}_+ + g'(r)e^{f(r)\hat{K}_+}\hat{K}_0 e^{-f(r)\hat{K}_+} \\ &+ h'(r)e^{f(r)\hat{K}_+}e^{g(r)\hat{K}_0}\hat{K}_- e^{-g(r)\hat{K}_0}e^{-f(r)\hat{K}_+}.\end{aligned} \tag{2.58}$$

By applying the operator identity

$$e^{\hat{F}}\hat{G}e^{-\hat{F}} = \hat{G} + \left[\hat{F}, \hat{G}\right] + \frac{1}{2!}\left[\hat{F}, \left[\hat{F}, \hat{G}\right]\right] + \cdots \tag{2.59}$$

and equating operators on each side of the equals sign in (2.58), some differential equations are found. These are

$$f'(r) - 2g'(r)f(r) + h'(r)f^2(r)e^{-2g(r)} = 1, \tag{2.60}$$

$$g'(r) - h'(r)e^{-2g(r)}f(r) = 0, \tag{2.61}$$

$$h'(r)e^{-2g(r)} = -1, \tag{2.62}$$

which have the solutions

$$f(r) = \tanh(r), \quad g(r) = -\ln\left[\cosh(r)\right], \quad h(r) = -\tanh(r). \tag{2.63}$$

The integration constants were found by setting $r = 0$. Thus the squeezing operator in normally ordered form is

$$\hat{S}(r) = e^{\frac{\tanh(r)}{2}\hat{a}^{\dagger 2}}e^{-\ln[\cosh(r)]\left(\hat{n}+\frac{1}{2}\right)}e^{-\frac{\tanh(r)}{2}\hat{a}^2} \tag{2.64}$$

which if applied to the vacuum state yields [35]

$$\hat{S}(r)|0\rangle = \frac{1}{\sqrt{\cosh r}}\sum_{n=0}^{\infty}\left(\frac{\tanh(r)}{2}\right)^n\frac{\sqrt{(2n)!}}{n!}|2n\rangle. \tag{2.65}$$

Consequently, a squeezing operator is not passive. It alters the number of photons in a state. If we consider the energy of a given minimum uncertainty mode $|\phi\rangle$ then

$$\langle\phi|\hat{H}|\phi\rangle = \langle\phi|\hat{a}^\dagger\hat{a} + \frac{1}{2}|\phi\rangle = |\alpha|^2 + \frac{1}{2} + \sinh^2(r). \tag{2.66}$$

In practice, the squeezing of light is accomplished by use of various non-linear crystals. These must be pumped by another laser beam, which amplifies the input parametrically. As both the conjugate position and momentum operators contribute to the energy of the mode, even a squeezed vacuum carries energy beyond the standard vacuum.

2.2 Phase space quasiprobability distributions

Wigner Function

With the essentials of quantum optics now explained, it is possible to consider how to represent a quantum state in phase space. On a plot of conjugate position and conjugate momentum, it would be possible to express a classical system by a single point, but quantum uncertainty renders this impossible in the quantum case as it is infeasible to observe position and momentum simultaneously and precisely. Furthermore, the very notion of a quantum state is hard to define in terms of measurements alone, and it is instead standard to carry out repeated measurements on seemingly identical systems to build up a statistical picture of a quantum object. It is, then, more sensible to consider a phase space distribution, with the singular purpose of being able to calculate observable quantities in a seemingly classical way.

Just as a particular state vector $|\psi\rangle$ admits a quadrature wavefunction $\psi(x) = \langle x|\psi\rangle$, an operator $\hat{O}$ can be described by a phase space function $\mathrm{Tr}\left[\hat{O}\hat{D}\left(\alpha\right)\right]$, where $\hat{D}\left(\alpha\right)$ is the displacement operator of (2.40) and satisfies a completeness relation. With this, it is possible to define a *characteristic function* of a quantum density matrix $\hat{\rho}$ as

$$\chi\left(x,p\right) = \mathrm{Tr}\left[\hat{D}\left(x,p\right)\hat{\rho}\right]. \tag{2.67}$$

The Fourier transform of the characteristic function yields the Wigner function first proposed by Eugene Wigner [36]:

$$\mathcal{W}\left(x,p\right) = \frac{1}{\left(2\pi\right)^2}\int_{-\infty}^{\infty}\chi\left(u,v\right)e^{iux+ivp}\mathrm{d}u\mathrm{d}v. \tag{2.68}$$

The Wigner function can be written in terms of x and p as

$$\mathcal{W}\left(x,p\right) = \frac{1}{2\pi}\int_{-\infty}^{\infty}e^{ipq}\langle x-\frac{q}{2}|\hat{\rho}|x+\frac{q}{2}\rangle\mathrm{d}q. \tag{2.69}$$

Above, for brevity, the Wigner function has been defined for a single mode only, but the extension to an N-mode Wigner function $\mathcal{W}\left(x_1,p_1,\cdots,x_N,p_N\right)$ is not a difficult leap of the imagination.

Here we have an appropriate representation of a quantum state in phase space in the form of a Wigner function. Importantly, $\mathcal{W}\left(x,p\right)$ can become negative in regions or ill-behaved and so is not a true probability distribution. Also, in reality quantum position and momentum cannot be measured simultaneously to form a true probability distribution. It is a *quasiprobability distribution*. The Wigner function satisfies all the desirable properties that a quasiprobability distribution should have [37]. Firstly, the Wigner function has the correct marginal distributions

$$\int_{-\infty}^{\infty}\mathcal{W}\left(x,p\right)\mathrm{d}x = \mathrm{Pr}\left(p\right), \quad \int_{-\infty}^{\infty}\mathcal{W}\left(x,p\right)\mathrm{d}p = \mathrm{Pr}\left(x\right), \tag{2.70}$$

where Pr signifies a probability distribution. If a density matrix $\hat{\rho}$ is rotated in phase space by the unitary operator $U\left(\phi\right) = e^{i\phi}$, then the Wigner function transforms accordingly as

$$\hat{\rho}\rightarrow U(\phi)\hat{\rho}U^{\dagger}(\phi)\Rightarrow\mathcal{W}\left(x,p\right)\rightarrow\mathcal{W}\left(x\cos\phi-p\sin\phi,x\sin\phi+p\cos\phi\right). \tag{2.71}$$

The Wigner function is normalised

$$\int_{-\infty}^{\infty}\mathcal{W}\left(x,p\right)\mathrm{d}x\mathrm{d}p = \mathbb{1} \tag{2.72}$$

and real ($\mathcal{W}(x,p) = \mathcal{W}^{*}(x,p)$) as a representation of Hermitian operators.

By far the most outstanding property of the Wigner function is the overlap formula. For two Hermitian operators e.g. $\hat{\rho}$ and $\hat{O}$

$$\begin{aligned}\mathrm{Tr}\left[\hat{\rho}\hat{O}\right] &= \int_{-\infty}^{\infty}\langle x'|\hat{\rho}\hat{O}|x'\rangle \mathrm{d}x' \\ &= \int_{-\infty}^{\infty}\langle x'|\hat{\rho}|x''\rangle\langle x''|\hat{O}|x'\rangle \mathrm{d}x'\mathrm{d}x'' \\ &= \frac{1}{2\pi}\int_{-\infty}^{\infty} e^{ip(q_1+q_2)}\langle x-\frac{q_1}{2}|\hat{\rho}|x+\frac{q_1}{2}\rangle\langle x-\frac{q_2}{2}|\hat{O}|x+\frac{q_2}{2}\rangle \mathrm{d}q_1\mathrm{d}q_2\mathrm{d}x\mathrm{d}p \\ &= (2\pi)\int_{-\infty}^{\infty}\mathcal{W}_{\rho}(x,p)\,\mathcal{W}_{O}(x,p)\,\mathrm{d}x\mathrm{d}p. \end{aligned} \tag{2.73}$$

That is, one can calculate the expectation value of an operator $\hat{O}$ acting on state $\hat{\rho}$ by looking at the phase space distribution overlap of the two operators. The overlap formula allows for an easy change of basis. For example, if a switch to a basis $|n\rangle\langle n|$ was required, then it would be only necessary to replace $\mathcal{W}_O(x,p)$ in (2.73) with the Fock state Wigner function

$$\mathcal{W}_n(x,p) = \frac{(-1)^n}{\pi}e^{-x^2-p^2}\mathrm{L}_n\left(2x^2+2p^2\right) \tag{2.74}$$

where L_n denotes the n^{th} Laguerre polynomial. The purity of a state can also be described by (2.73)

$$\mathrm{Tr}\left[\hat{\rho}^2\right] = 2\pi\int_{-\infty}^{\infty}\mathcal{W}^2(x,p)\,\mathrm{d}x\mathrm{d}p \tag{2.75}$$

and the von-Neumann entropy of $\hat{\rho}$ is bounded by

$$\mathcal{S}(\hat{\rho}) \geq 1 - 2\pi\int_{-\infty}^{\infty}\mathcal{W}^2(x,p)\,\mathrm{d}x\mathrm{d}p. \tag{2.76}$$

Another property of the Wigner function is that it is bounded from above,

$$|\mathcal{W}(x,p)| \leq \frac{1}{\pi}. \tag{2.77}$$

It is easy to show how a Wigner function transforms with the operators mentioned so far. In addition to the phase shift operation (2.71), the squeezing operator (2.53) and displacement operator (2.47) transform the Wigner function as

$$\mathcal{W}(x,p) \to \mathcal{W}\left(e^{r}x, e^{-r}p\right) \quad \text{and} \quad \mathcal{W}(x,p) \to \mathcal{W}(x-\bar{x}, p-\bar{p}) \tag{2.78}$$

respectively.

Other quasiprobability distributions: s-parametrization

We could consider other quasiprobability distributions that have other useful properties. In particular, we could re-examine equation (2.67), defining the characteristic function as the trace of the displacement operator with the density matrix $\hat{\rho}$:

$$\chi(\alpha) = \mathrm{Tr}\left[\rho\hat{D}(\alpha)\right] = \mathrm{Tr}\left[\rho e^{\alpha\hat{a}^\dagger - \alpha^*\hat{a}}\right]. \tag{2.79}$$

Importantly, the displacement operator in (2.79) is symmetrically ordered - if the exponential was to be expanded, the operators $\hat{a}$ and $\hat{a}^\dagger$ would be combined symmetrically. By treating the characteristic function as a generating function, it is therefore possible to find that

$$\left\langle\left[\hat{a}^{\dagger m}\hat{a}^n\right]_{\mathrm{sym}}\right\rangle = \mathrm{Tr}\left[\hat{\rho}\left[\hat{a}^{\dagger m}\hat{a}^n\right]_{\mathrm{sym}}\right] = \frac{\partial^{(m+n)}}{\partial\alpha^m\partial\alpha^{*n}}\chi(\alpha)\Big|_{\alpha=\alpha^*=0} \tag{2.80}$$

where, for example, $\left[\hat{a}^\dagger\hat{a}^2\right]_{\mathrm{sym}} = \hat{a}\hat{a}\hat{a}^\dagger + \hat{a}\hat{a}^\dagger\hat{a} + \hat{a}^\dagger\hat{a}\hat{a}$.

However, one could instead use the Baker-Hausdorff formula (2.46) to rewrite the characteristic function in two alternative ways:

$$\chi(\alpha) = \mathrm{Tr}\left[\hat{\rho} e^{-\frac{|\alpha|^2}{2}} e^{\alpha \hat{a}^\dagger} e^{-\alpha^* \hat{a}}\right] = e^{-\frac{|\alpha|^2}{2}} \mathrm{Tr}\left[\hat{\rho} e^{\alpha \hat{a}^\dagger} e^{-\alpha^* \hat{a}}\right] = e^{-\frac{|\alpha|^2}{2}} \chi_{\mathcal{N}}(\alpha), \tag{2.81}$$

$$\chi(\alpha) = \mathrm{Tr}\left[\hat{\rho} e^{\frac{|\alpha|^2}{2}} e^{-\alpha^* \hat{a}} e^{\alpha \hat{a}^\dagger}\right] = e^{\frac{|\alpha|^2}{2}} \mathrm{Tr}\left[\hat{\rho} e^{-\alpha^* \hat{a}} e^{\alpha \hat{a}^\dagger}\right] = e^{\frac{|\alpha|^2}{2}} \chi_{\mathcal{A}}(\alpha). \tag{2.82}$$

In the above, the subscripts $\mathcal{N}$ and $\mathcal{A}$ stand for normally and antinormally ordered respectively. That is, if $\chi_{\mathcal{N}}(\alpha)$ and $\chi_{\mathcal{A}}(\alpha)$ were to be treated as generating functions then

$$\left\langle \hat{a}^{\dagger m} \hat{a}^n \right\rangle = \mathrm{Tr}\left[\hat{\rho} \hat{a}^{\dagger m} \hat{a}^n\right] = \frac{\partial^{(m+n)}}{\partial \alpha^m \partial \alpha^{*n}} \chi_{\mathcal{N}}(\alpha)\Big|_{\alpha=\alpha^*=0}, \tag{2.83}$$

$$\left\langle \hat{a}^m \hat{a}^{\dagger n} \right\rangle = \mathrm{Tr}\left[\hat{\rho} \hat{a}^m \hat{a}^{\dagger n}\right] = \frac{\partial^{(m+n)}}{\partial \alpha^m \partial \alpha^{*n}} \chi_{\mathcal{A}}(\alpha)\Big|_{\alpha=\alpha^*=0}. \tag{2.84}$$

The normally ordered and anti-normally ordered characteristic functions play a special role in this thesis, but as can be seen above, one can be turned into the other by multiplying by a suitable exponential. More commonly, one defines an s-parametrised characteristic function as

$$\chi(\alpha; s) = \chi(\alpha) e^{s\frac{|\alpha|^2}{2}} \tag{2.85}$$

which for convenience we shall write in terms of conjugate position and momentum as

$$\chi(x, p; s) = \chi(x, p) e^{\frac{s}{4}\left(x^2+p^2\right)} \tag{2.86}$$

The effect on the Wigner function is to convolve it with Gaussian distributions parametrised by a real parameter s [38, 39]. It is also possible to define quasiprobability distributions parametrised by complex numbers [40] but that is beyond the scope of this thesis. The s-parametrised quasiprobability distributions are given by the Fourier transform of (2.86):

$$\mathcal{W}(x, p; s) = \frac{1}{(2\pi)^2} \int_{-\infty}^{\infty} \chi(u, v; s) e^{iux+ivp} \mathrm{d}u\mathrm{d}v. \tag{2.87}$$

The most important cases for this thesis are $s = 0, 1, -1$. When $s = 0$, the characteristic function (2.86) is unchanged and so (2.87) reduces to the standard Wigner function.

If $s = -1$ then the parametrised characteristic function is the anti-normally ordered $\chi_{\mathcal{A}}$ and the corresponding quasiprobability distribution is known as the *Q function*, denoted $\mathcal{Q}$. The Q function is a simple convolution of the Wigner function with the vacuum distribution $\mathcal{W}_{\mathrm{vac}}(x, p) = (1/\pi)\exp[-x^2 - p^2]$ and the result is a smooth, non-negative, normalized quasiprobability distribution

$$\mathcal{Q}(x, p) \equiv \mathcal{W}(x, p; -1) = \int_{-\infty}^{\infty} \mathcal{W}(x', p') \frac{\exp[-(x - x')^2 - (p - p')^2]}{\pi} \mathrm{d}x'\mathrm{d}p'. \tag{2.88}$$

On comparison with the overlap formula (2.73) it is clear that the Q function simply gives the probability distribution for finding the coherent state $\alpha = (1/\sqrt{2})(x + ip)$.

$$\mathcal{Q}(x, p) = \frac{\langle \alpha | \hat{\rho} | \alpha \rangle}{2\pi} \tag{2.89}$$

Importantly, as will be seen in Chapter 5 the Q function acts as a generating function for density matrix elements.

For $s = 1$ the P function, $\mathcal{P}$ (also known as the Glauber-Sudarshan function [41, 42]) is obtained, and is of importance in Chapter 8. Due to the *optical equivalence theorem* a density matrix $\hat{\rho}$ can be written as

$$\hat{\rho} = \int_{-\infty}^{\infty} \mathcal{P}(x, p) |\alpha\rangle\langle\alpha| \mathrm{d}x\mathrm{d}p \tag{2.90}$$

(where once again $\alpha = (1/\sqrt{2})(x + ip)$). Traditionally, the P function has been used to indicate whether a state exhibits non-classical behaviour. If the Wigner function can be negative, then

the P function can exhibit far worse behaviour. Not much more will be said of the P function here except that it can be very ill-behaved. After all, a pure state $|\psi\rangle\langle\psi|$ cannot be written as a distribution of coherent states unless $|\psi\rangle$ itself is a coherent state. In that case, the P function is simply a delta function. From this observation, the P function of a Fock state $|n\rangle$ must contain derivatives of a two dimensional delta function - very strange behaviour indeed.

The relationship between the s-parametrized formulae and the overlap function is

$$\mathrm{Tr}\left[\hat{\rho}\hat{O}\right] = \frac{1}{2\pi}\int_{-\infty}^{\infty} \mathcal{W}_{\rho}\left(x,p;s\right)\mathcal{W}_{O}\left(x,p;-s\right)\mathrm{d}x\mathrm{d}p. \tag{2.91}$$

2.3 Gaussian States

The primary tools for exploring quantum information theory in the continuous variable setting are the Gaussian states and Gaussian maps. Gaussian states are those states with a Gaussian characteristic function (2.67) (and hence a Gaussian Wigner function) and Gaussian maps are those transformations that turn one Gaussian state into another.

Gaussian states are of great practical relevance. The quantum vacuum, for one, is a Gaussian state, as are the coherent states $|\alpha\rangle$ resulting from a displacement of the vacuum in phase space. Squeezing, phase-shifting and beamsplitter transformations, are all examples of Gaussian maps. Quite often, non-linear operations can also be approximated to a high calibre by Gaussian maps.

In this Section, we shall introduce only the most relevant qualities of bosonic Gaussian states to this thesis. Consequently, a lot of fascinating areas of investigation shall not be delved into. For brilliant reviews of the basic facts of Gaussian quantum information processing, see those by Braunstein and Van Loock [43] and Ferraro [25]. For a particular focus on entanglement in Gaussian states see the PhD thesis of Adesso [44] and the review [45]. For an up-to-date overview of all Gaussian Quantum Information Theory see [46].

Definition of a Gaussian state

An N-mode Gaussian state is a state with a Gaussian Wigner function that can be written in terms of a covariance matrix γ as

$$\mathcal{W}\left(x_1,p_1,\ldots,x_N,p_N\right) = \frac{\exp\left[-\left(\mathbf{R}^T-\mathbf{d}^T\right)\gamma^{-1}\left(\mathbf{R}-\mathbf{d}\right)\right]}{\pi^N\sqrt{\det\gamma}} \tag{2.92}$$

where $\mathbf{R} = \left(x_1,p_1,\ldots,x_N,p_N\right)^T$ and $\mathbf{d} = \left(\langle x_1\rangle,\langle p_1\rangle,\ldots,\langle x_N\rangle,\langle p_N\rangle\right)^T$ is a vector of first moments i.e. displacements. The covariance matrix is defined as

$$\gamma_{lm} = \left\langle \hat{R}_l\hat{R}_m + \hat{R}_m\hat{R}_l \right\rangle - 2d_ld_m. \tag{2.93}$$

It is very important to note that definitions vary throughout the literature. The definition of the covariance matrix given above is compatible with $[\hat{x}_j,\hat{p}_k] = i\delta_{j,k}$. Other possibilities that frequently surface are $[\hat{x}_j,\hat{p}_k] = 2i\delta_{j,k}$ with a factor of $1/2$ appearing in (2.93) (as is used in e.g. [44] and [45]), or $[\hat{x}_j,\hat{p}_k] = i\delta_{j,k}$ with the factor of $1/2$ in (2.93), in which case the Wigner function (2.92) is altered accordingly.

Interestingly, for Gaussian states all of the s-parametrized quasiprobability distributions can be found by replacing γ in (2.92) with γ_s, and γ_s is defined by

$$\gamma_s = \gamma - s\mathbb{1}. \tag{2.94}$$

The quantities that characterise all continuous variable Wigner representations are the statistical moments of the Gaussian state. The first moment is simply the mean value of the observables (e.g. $\mathbf{d}$) and the second characterises the covariance matrix (2.93). One may ask whether there exist continuous variable states that are fully characterised by, for example, their skewness or kurtosis (3^{rd} and 4^{th} moments). In fact, as a result of the Marcinkiewicz Theorem [47, 48, 49], to fully characterise a continuous variable state you either need just the first two moments (for Gaussian states) or you need all of them!

The covariance matrix is a real, $2N \times 2N$, symmetric matrix. To represent a feasible quantum state the only requirement is that a covariance matrix satisfy Heisenberg's Uncertainty Principle [50] which can be expressed conveniently as

$$\gamma + i\Omega \geq 0 \tag{2.95}$$

where $\Omega = \oplus_{j=1}^{N} \omega$ and ω is given by

$$\omega = \begin{pmatrix} 0 & 1 \\ -1 & 0 \end{pmatrix}. \tag{2.96}$$

From the diagonal terms in (2.95) one easily derives the usual expression of Heisenberg's uncertainty principle. From the definition (2.93), the covariance matrix of the vacuum is given by $\gamma_{\text{vac}} = \mathbb{1}$. All other Gaussian states can be seen as the result of Gaussian maps on γ_{vac}.

Gaussian Maps

In general, a quantum state undergoes a *quantum operation* [51] consisting of a linear map $\Xi : \hat{\rho} \to \Xi(\hat{\rho})$ which is completely positive and potentially trace-decreasing. More will be made of this in Chapter 3. A quantum operation is said to be a *quantum channel* if it is trace-preserving, and the simplest of these are reversible and represented by unitary transformations U with $U^\dagger U = \mathbb{1}$. The density matrix $\hat{\rho}$ then transforms as $U\hat{\rho}U^\dagger$. A Gaussian unitary channel therefore consists of those quantum channels that transform Gaussian states to Gaussian states. Usually the unitary can be represented by $U = \exp[-i\hat{H}]$ where $\hat{H}$ is a Hamiltonian which is at most a second-order polynomial in the field operators $\hat{a}$ and $\hat{a}^\dagger$.

As a consequence of the Stone Von-Neumann Theorem, all Gaussian unitaries acting on the Hilbert space level can be represented by a symplectic operation S on the phase space level. That is a Gaussian unitary can be identified with a matrix S that acts on the phase space variables (x,p) and is essentially defined by how the phase space variables tranform i.e.

$$\mathbf{R}' = S\mathbf{R}. \tag{2.97}$$

The matrix S must necessarily satisfy

$$S\Omega S^T = \Omega \tag{2.98}$$

to be symplectic and to preserve Heisenberg's Uncertainty Principle. As a consequence of (2.98), $\det S = 1$. A generic unitary Gaussian map can consist of a symplectic operation and a displacement. For example, if we were to displace a Gaussian state in phase space by $\mathbf{d}'$ and perform a symplectic transformation S the first and second moments would transform as

$$\mathbf{d} \to S\mathbf{d} + \mathbf{d}', \quad \gamma \to S\gamma S^T \tag{2.99}$$

respectively.

Some of the most important transformations that have been introduced so far can be represented by a symplectic operation. The squeezing operation (2.53) can be represented by

$$S_{SQ}(r) = \begin{pmatrix} e^r & 0 \\ 0 & e^{-r} \end{pmatrix} \tag{2.100}$$

and a phase space rotation can be represented by

$$S_{PH}(\theta) = \begin{pmatrix} \cos\theta & \sin\theta \\ -\sin\theta & \cos\theta \end{pmatrix}. \tag{2.101}$$

The most general one mode covariance matrix γ_{one} can be represented as a result of squeezing and rotation of a thermal state in phase space and can be written as

$$\gamma_{\text{one}} = (2\langle n \rangle + 1) S_{PH}(\theta) S_{SQ}(r) \gamma_{\text{vac}} S_{SQ}^T(r) S_{PH}^T(\theta) \tag{2.102}$$

where $\langle n \rangle$ is the average number of photons in the mode and $\gamma_{\text{vac}} = \mathbb{1}$. If $\langle n \rangle = 0$, we have the most general form of a *pure* Gaussian covariance matrix. This corresponds to a rotated

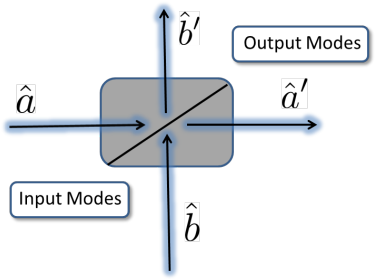

Figure 2.2: A beamsplitter is a four port optical device, taking two modes as input and releasing two modes as output. Both input modes are partially transmitted and partially reflected by the beamsplitter.

and displaced squeezed state $|\alpha,\theta,r\rangle = \hat{D}(\alpha)\hat{U}(\theta)\hat{S}(r)|0\rangle$ although later in this thesis (e.g. Chapter 9) the rotation and squeezing are amalgamated as e.g. $|\alpha, re^{i\theta}\rangle$.

Vitally, some very useful multimode operations are Gaussian in nature. Firstly, we have the lossless beamsplitter which takes two input modes and combines them by either transmitting or reflecting photons proportional to a transmittance coefficient T (see Figure 2.2). In the Heisenberg picture, a beamsplitter transforms the annihilation operators of the two input modes ($\hat{a}$ and $\hat{b}$ respectively) as

$$\begin{pmatrix}\hat{a}'\\ \hat{b}'\end{pmatrix} = \begin{pmatrix}\sqrt{T} & -\sqrt{1-T}\\ \sqrt{1-T} & \sqrt{T}\end{pmatrix}\begin{pmatrix}\hat{a}\\ \hat{b}\end{pmatrix}, \tag{2.103}$$

and so, by taking the adjoint of equation (2.103) and representing two input Fock states $|n_1,n_2\rangle$ using equation (2.29), it can (after a lot of algebra) be shown that a beamsplitter mixes two Fock states as

$$\begin{aligned}|n_1,n_2\rangle \rightarrow & \frac{1}{\sqrt{n_1!n_2!}}\sum_{k_1,k_2}^{n_1,n_2}\frac{\left(\sqrt{T}\right)^{k_1}\left(-\sqrt{1-T}\right)^{n_1-k_1}\left(\sqrt{1-T}\right)^{k_2}\left(\sqrt{T}\right)^{n_2-k_2}}{\sqrt{(k_1+k_2)!(n_1+n_2-k_1-k_2)!}}\\ & \times\binom{n_1}{k_1}\binom{n_2}{k_2}|k_1+k_2,n_1+n_2-k_1-k_2\rangle.\end{aligned} \tag{2.104}$$

The total photon number is conserved, but the photons are distributed between the two output modes proportional to T. Using equation (2.104), one sees that if a single photon in each input mode is incident on a 50/50 beamsplitter, then 2 photons emerge in one output port or the other. This is the famous Hong-Ou-Mandel effect. A beamsplitter interaction between two Gaussian states can be represented by the symplectic operation

$$S_{\mathrm{BS}}(T) = \begin{pmatrix}\sqrt{T} & 0 & \sqrt{1-T} & 0\\ 0 & \sqrt{T} & 0 & \sqrt{1-T}\\ -\sqrt{1-T} & 0 & \sqrt{T} & 0\\ 0 & -\sqrt{1-T} & 0 & \sqrt{T}\end{pmatrix}. \tag{2.105}$$

If we squeeze a vacuum mode in x and another mode in p, and combine both modes on a 50/50 beamsplitter ($T=1/2$) then we arrive at the covariance matrix of the *two mode squeezed vacuum*

$$\begin{aligned}\gamma^{TMSV} &= S_{\mathrm{BS}}(1/2)\left(S_{SQ}(r)\oplus S_{SQ}(-r)\right)\gamma_{\mathrm{vac}}\left(S_{SQ}^{T}(r)\oplus S_{SQ}^{T}(-r)\right)S_{\mathrm{BS}}^{T}(1/2)\\ &= \begin{pmatrix}\cosh(2r) & 0 & \sinh(2r) & 0\\ 0 & \cosh(2r) & 0 & -\sinh(2r)\\ \sinh(2r) & 0 & \cosh(2r) & 0\\ 0 & -\sinh(2r) & 0 & \cosh(2r)\end{pmatrix}.\end{aligned} \tag{2.106}$$

This Gaussian state has zero mean. In the limit of infinite squeezing ($r\rightarrow\infty$) the state approaches the legendary, and yet unphysical, Einstein-Podolsky-Rosen state [52] in which the positions and momenta of two subsystems are maximally entangled. The two mode squeezed

vacuum is a pure state and any two mode pure Gaussian state can be represented by covariance matrix (2.106). The Fock state representation of the two mode squeezed vacuum is

$$|\Psi\rangle = \sqrt{1-\lambda^2}\sum_{n=0}^{\infty}\lambda^n\,|nn\rangle \tag{2.107}$$

with $\lambda = \tanh(r)$.

Another significant Gaussian operation is the Quantum Non-Demolition (QND) interaction. The quantum non-demolition interactions [53, 54] are well-known from quantum metrology. They are decribed by Hamiltonians of the form e.g.

$$\hat{H}_{\text{QND}} = \kappa\hat{P}_S\hat{P}_A \tag{2.108}$$

where κ is the interaction strength and $\hat{P}_{S/A}$ are the quadratures of the system/ancillary mode. The system and ancillary mode interact in such a way as to leave one quadrature component of each subsystem intact whilst phase shifting the conjugate components. In particular, in the Heisenberg picture, where the quadratures evolve via the Heisenberg equations of motion, only the position quadratures of the system and ancillary modes would be affected by equation (2.108) as the momenta quadratures commute with the Hamiltonian. Furthermore, for light it was also shown that it is possible to create a QND Hamiltonian using optical instruments such as biased beamsplitters and squeezers in combination [55].

Importantly for Chapter 5, quantum non-demolition interactions can also be represented by symplectic operations. For an interaction between a system and ancillary mode, given by the interaction Hamiltonian $\hat{H}_{\text{int}} = \kappa\hat{R}_j\hat{R}_k$, the corresponding symplectic operation $S_{\text{QND}}^{(\kappa\hat{R}_j\hat{R}_k)}$ is given by

$$S_{\text{QND}}^{(\kappa\hat{X}\hat{X})} = \begin{pmatrix} 1 & 0 & 0 & 0 \\ 0 & 1 & -\kappa & 0 \\ 0 & 0 & 1 & 0 \\ -\kappa & 0 & 0 & 1 \end{pmatrix}, \qquad S_{\text{QND}}^{(\kappa\hat{X}\hat{P})} = \begin{pmatrix} 1 & 0 & 0 & 0 \\ 0 & 1 & 0 & -\kappa \\ \kappa & 0 & 1 & 0 \\ 0 & 0 & 0 & 1 \end{pmatrix},$$
$$S_{\text{QND}}^{(\kappa\hat{P}\hat{X})} = \begin{pmatrix} 1 & 0 & \kappa & 0 \\ 0 & 1 & 0 & 0 \\ 0 & 0 & 1 & 0 \\ 0 & -\kappa & 0 & 1 \end{pmatrix}, \qquad S_{\text{QND}}^{(\kappa\hat{P}\hat{P})} = \begin{pmatrix} 1 & 0 & 0 & \kappa \\ 0 & 1 & 0 & 0 \\ 0 & \kappa & 1 & 0 \\ 0 & 0 & 0 & 1 \end{pmatrix}. \tag{2.109}$$

Symplectic analysis of Gaussian states

In 1936, Williamson [56] proved that all positive definite real matrices of even dimensions can be diagonalised by symplectic operations. For the N-mode covariance matrix γ, there always exists a symplectic transformation that puts the covariance matrix in symplectic form γ_ν

$$S\gamma S^T = \gamma_\nu = \oplus_{j=1}^{N}\begin{pmatrix} \nu_j & 0 \\ 0 & \nu_j \end{pmatrix}, \tag{2.110}$$

where $\oplus$ denotes the direct sum of matrices. The *symplectic eigenvalues* ν_j can be found as the eigenvalues of $|i\Omega\gamma|$. The determinant of any Gaussian state is easily expressed as $\det(\gamma) = \prod_j \nu_j^2$. Furthermore, for Heisenberg's Uncertainty Principle to hold, and hence for γ to represent a true quantum covariance matrix, $\nu_j \geq 1$ for all j. The symplectic diagonalisation of a covariance matrix corresponds to the decomposition of a Gaussian state into thermal modes. The covariance matrix (2.110) corresponds to the density matrix being expressed as

$$\hat{\rho}^{\otimes} = \otimes_{j=1}^{N}\frac{2}{\nu_j+1}\sum_{n=0}^{\infty}\left(\frac{\nu_j-1}{\nu_j+1}\right)^n |n\rangle_j\langle n|, \tag{2.111}$$

where $\otimes$ denotes the tensor product of density matrices. In this Williamson form, each mode is a Gaussian state in thermal equilibrium at a temperature T_j characterised by the average number of photons $\langle n_j\rangle$ and frequency ω_j. The average number is described by Bose-Einstein statistics

$$\langle n_j\rangle = \frac{\nu_j-1}{2} = \frac{1}{\exp[\frac{\hbar\omega_j}{k_B T_j}]-1}. \tag{2.112}$$

There are other important quantities relating to the symplectic spectrum $\{\nu_j\}$. The seralian [57] is defined as the sum of the determinants of all the 2×2 submatrices of γ and can be calculated from symplectic eigenvalues via

$$\Delta(\gamma) = \sum_{j=1}^{N} \nu_j^2. \tag{2.113}$$

The invariance of Δ for multiple modes [58] follows from the the knowledge that all symplectic operations can be decomposed as products of two-mode transformations [59] and the invariance of Δ in the two-mode case (see [60] for proof).

The von-Neumann entropy of any N-mode Gaussian state can easily be calculated in terms of the symplectic eigenvalues of covariance matrix γ [61]. The entropy is calculated via

$$\mathcal{S}(\rho) = \sum_{j=1}^{N} \mathfrak{F}(\nu_j) \tag{2.114}$$

where

$$\mathfrak{F}(\nu) = \left(\frac{\nu+1}{2}\right) \ln\left(\frac{\nu+1}{2}\right) - \left(\frac{\nu-1}{2}\right) \ln\left(\frac{\nu-1}{2}\right). \tag{2.115}$$

Noticeably, the state is pure (i.e. entropy (2.114) is zero) if and only if $\nu_j = 1$ for all j. The covariance matrix of a *pure* Gaussian state satisfies

$$-\Omega\gamma\Omega\gamma = -\Omega SS^T\Omega SS^T = -\Omega S\Omega S^T = -\Omega\Omega = \mathbb{1} \tag{2.116}$$

where γ can be expressed as SS^T for all pure states.

Bipartite Gaussian States

If we were to consider that two parties, Alice and Bob, possessed a Gaussian state (of m and n modes respectively), the covariance matrix of the system could be expressed as

$$\gamma = \begin{pmatrix} \alpha & \sigma \\ \sigma^T & \beta \end{pmatrix} \tag{2.117}$$

where α is a $2m \times 2m$ matrix, β is a $2n \times 2n$ matrix and σ contains the correlations between Alice and Bob's modes.

It would be most desirable to explore how a bipartite Gaussian state transforms under local Gaussian operations. As Gaussian maps have effects only on the level of covariances, it is possible to formulate the effect of a Gaussian map on a Gaussian state also in terms of covariances. There have been many works ([62],[63] to name a few) showing how a bipartite state transforms under a Gaussian map reducing the number of modes. Ultimately, if we were to project Bob's modes onto a Gaussian state with covariance matrix γ_p, then a Gaussian operation has been performed. The result is that the covariance matrix of Alice's modes, and their displacement in phase space, are transformed as

$$\gamma \to \alpha - \sigma(\beta + \gamma_p)^{-1}\sigma^T, \quad \mathbf{d} \to \frac{1}{2}\sigma(\beta + \gamma_p)^{-1}\mathbf{d}. \tag{2.118}$$

The proofs given in the literature are complicated but the principle behind (2.118) is simple, and just requires the overlap formula (2.73). Consider, as an example, a map where there are no displacements i.e. we are only concerned with the transformation of the covariance matrix. Then we express

$$\begin{aligned} \gamma^{-1} &= \begin{pmatrix} \left(\alpha - \sigma\beta^{-1}\sigma^T\right)^{-1} & -\left(\alpha - \sigma\beta^{-1}\sigma^T\right)^{-1}\sigma\beta^{-1} \\ -\beta^{-1}\sigma^T\left(\alpha - \sigma\beta^{-1}\sigma^T\right)^{-1} & \beta^{-1} + \beta^{-1}\sigma^T\left(\alpha - \sigma\beta^{-1}\sigma^T\right)^{-1}\sigma\beta^{-1} \end{pmatrix} \\ &= \begin{pmatrix} A & C \\ C^T & B \end{pmatrix}. \end{aligned} \tag{2.119}$$

The measurements of Bob's modes (with Gaussian measurement $\hat{G}_B$) can be written using the Wigner overlap formula as

$$\begin{aligned}\mathrm{Tr}\left[\hat{\rho}_{AB}\hat{G}_B\right] &= \frac{(2\pi)^n \exp\left[-\eta_A^T A \eta_A\right]}{\pi^{m+n}\sqrt{\det\gamma}} \int_{-\infty}^{\infty} \exp\left[-\eta_B^T\left(B+\gamma_p^{-1}\right)\eta_B - 2\eta_A^T C\eta_B\right] \mathrm{d}\eta_B \\ &= \frac{(2\pi)^n \pi^n}{\pi^{m+n}\sqrt{\det\gamma}\sqrt{\det\left(B+\gamma_p^{-1}\right)}} \exp\left[-\eta_A^T\left(A - C\left(B+\gamma_p^{-1}\right)^{-1}C^T\right)\eta_A\right] \quad (2.120)\end{aligned}$$

where $\eta_A^T = (x_1, p_1, \cdots, x_m, p_m)$ and $\eta_B^T = (x_{m+1}, p_{m+1}, \cdots, x_{m+n}, p_{m+n})$. This can be thought of as a probability of projecting onto $\hat{G}_B$ multiplied by a Wigner function characterised by the covariance matrix $\gamma' = \left(A - C\left(B+\gamma_p^{-1}\right)^{-1}C^T\right)^{-1}$ which, with repeated and careful use of the binomial inverse theorem

$$(\mathcal{A}+\mathcal{U}\mathcal{B}\mathcal{V})^{-1} = \mathcal{A}^{-1} - \mathcal{A}^{-1}\mathcal{U}\mathcal{B}\left(\mathcal{B}+\mathcal{B}\mathcal{V}\mathcal{A}^{-1}\mathcal{U}\mathcal{B}\right)^{-1}\mathcal{B}\mathcal{V}\mathcal{A}^{-1} \quad (2.121)$$

can be put into the required form (2.118). Homodyne detection of Bob's modes is a projection onto a pure generic state, given for a single mode in (2.102), in the limit of infinite squeezing. Heterodyning too is a Gaussian map.

In a similar way, we can also consider what happens to the covariance matrix of subsystem A if we trace out subsystem B. Using the Wigner Overlap formula and utilising the binomial inverse theorem it is possible to show that the covariance matrix of equation (2.117) reduces to simply α. That is, we simply cut away all other submatrices (β and σ).

Most important for this thesis is the case when Alice and Bob each possess a single mode ($m = n = 1$). If this is the case then there exist local symplectic operations S_1 and S_2, applied as $S = S_1 \oplus S_2$, that transform γ into the *standard form*

$$\gamma = \begin{pmatrix} a & 0 & c_+ & 0 \\ 0 & a & 0 & c_- \\ c_+ & 0 & b & 0 \\ 0 & c_- & 0 & b \end{pmatrix} \quad (2.122)$$

which can be a mixed state in general. The invariants of this standard form can be expressed as

$$\det\gamma = (ab - c_+^2)(ab - c_-^2), \quad (2.123)$$

$$\Delta(\gamma) = a^2 + b^2 + 2c_+c_- \quad (2.124)$$

and the symplectic eigenvalues are given by

$$\nu_\pm = \sqrt{\frac{\Delta(\gamma) \pm \sqrt{\Delta^2(\gamma) - 4\det\gamma}}{2}} \quad (2.125)$$

2.4 Summary of Chapter 2

The standard toolbox for quantum optics has been unpacked in this chapter and proves very useful for describing continuous variable systems in general. The beauty of the language of quantum optics is that it shows, in effect, the boundary between particle and wave-like quantum objects in continuous variables. The Wigner function and other phase space quasiprobability distributions provide, for a single mode, a way to visualise a quantum state.

A particular focus has been applied to Gaussian states, which play a crucial role throughout this thesis. In later chapters, the Gaussian state formalism will be used in the context of entanglement distillation, and analytic formulae for non-classicality measures shall be provided based on the elements of covariance matrices phrased in standard form.

Part II

Quantum Entanglement

Chapter 3

Quantum Entanglement

In 1935, Einstein, Podolsky and Rosen [52] introduced a bipartite quantum state, perfectly correlated in position and momentum, as an example the "incompleteness" of quantum mechanics. This was based on two precepts: "locality" and "reality". "Locality" asserts that there can be no "spooky action at a distance". "Reality" means "If, without in any way disturbing a system, we can predict with certainty (i.e. with probability equal to unity) the value of a physical quantity, then there exists an element of physical reality corresponding to this physical quantity".

For Einstein, Podolsky and Rosen, this example was meant to be a *reductio ad absurdum* showing a fundamental flaw with quantum theory. After all, a measurement on one subsystem of the bipartite state that they considered had the effect of collapsing the wavefunction of the other and yet "since at the time of measurement the two systems no longer interact, no real change can take place in the second system in consequence of anything that may be done to the first system". Einstein thought there must be more to quantum mechanics i.e. hidden variables, and indeed spent the rest of his life looking for another explanation. Although unphysical, this state can be achieved by the two mode squeezed vacuum in the limit of infinite squeezing. This seminal paper galvanised the physics community.

Schrödinger [64] first coined the term entanglement (*Verschränkung*) to describe this phenomenon. The term appeared again later in the second of the triplet of papers in which he introduced the famous Schrödinger cat [65] (translation [66]). Schrödinger placed the phenomenon at the centre of quantum theory but was also troubled. In a letter to Einstein dated 7^{th} June, 1935, he wrote "I was very happy that, in your work that recently appeared in *Phys. Rev.*, you have publicly caught the dogmatic quantum mechanics by the collar, regarding that which we had already discussed so much in Berlin"[1]. Schrödinger went on to say "The point of my foregoing discussion is this: we do not have a quantum mechanics that takes into account relativity theory, that is, among other things, that respects the finite speed of propagation of all effects".

Ultimately, quantum entanglement appeared troublesome, but is now recognised as a genuine signature of quantum theory with bountiful applications. After a long hiatus, broken by John Bell (Section 3.1), there has been a resurgence of interest in recent years. Notably, in the 1990s quantum entanglement was formalised in terms of entropic quantities (see e.g. [67, 68, 69, 70]). Quantum entanglement is now viewed as a potent resource, with applications in quantum cryptography [71], quantum dense coding [72] and quantum teleportation [73, 74]. The quest for quantum cryptography and quantum computing led, in turn, to algorithms [75, 76]. Quantum entanglement went from being a philosopher's toy to an experimentalist's tool!

This chapter aims to give a brief review of the biggest results concerning quantum entanglement, albeit far from exhaustive. For an extensive review see [77]. Only bipartite entanglement shall be considered here. We begin by setting the historical context of quantum entanglement. From there, we aim to capture the properties of entanglement qualitatively and quantitatively. Some of the most vital separability criteria shall be covered, and information on measures of entanglement.

[1] The original letter is in German at the Einstein Archives at the Hebrew University of Jerusalem. This translation is from a copy of the letter held at the Howard Gotlieb Archival Research Center and extracts appear in [3].

3.1 Bell's Inequalities

For a long time, the notion of quantum entanglement was ignored. This altered with John Bell. Bell phrased the EPR idea of a deterministic world in terms of a local hidden variable model (LHVM) by assuming that (1) measurement results are determined by properties the particles carry prior to, and independent of, the measurement (realism), and (2) results obtained at one location are independent of any actions at spacelike separated points (locality) [2]. The third presumption is Free Will i.e. that the setting of the measurement devices is independent of the hidden variables in the state to be measured. Local hidden variables are taken as a working hypothesis to find restrictions. It was Aspect [78, 79, 80] that first performed the most convincing[2] tests of Bell's inequalities after a long struggle. Before that they were seen as controversial.

Imagine the following scenario. Alice and Bob have a pair of particles (A and B respectively) which they have created with a quantum experiment of one form or another. They each have two measuring devices (A_1 & A_2 for Alice, and B_1 & B_2 for Bob) and can independently choose which of these measuring devices they use. They simultaneously observe the two particles A and B by performing a measurement with one of their devices. For simplicity we can assume that each measurement device has two possible outcomes, $+1$ and -1. Bell's inequality then states that for a LHVM

$$\langle A_1 B_1\rangle + \langle A_1 B_2\rangle + \langle A_2 B_1\rangle - \langle A_2 B_2\rangle \leq 2. \tag{3.1}$$

To see this we expand the left hand side of (3.1) as

$$\begin{aligned}\langle A_1 B_1\rangle + \langle A_1 B_2\rangle + \langle A_2 B_1\rangle - \langle A_2 B_2\rangle &= \langle A_1 B_1 + A_1 B_2 + A_2 B_1 - A_2 B_2\rangle \\ &= \langle A_1(B_1 + B_2) + A_2(B_1 - B_2)\rangle\,. \end{aligned}\tag{3.2}$$

As the outcomes are ± 1 we have two possibilities:

- $B_1 = B_2$ in which case we get the expectation value to be $\pm 2A_1$,
- $B_1 = -B_2$ in which case the expectation value is $\pm 2A_2$.

Therefore,

$$\langle A_1 B_1\rangle + \langle A_1 B_2\rangle + \langle A_2 B_1\rangle - \langle A_2 B_2\rangle = \sum_{a_1,a_2,b_1,b_2} p(a_1,a_2,b_1,b_2)(a_1 b_1 + a_1 b_2 + a_2 b_1 - a_2 b_2) \leq 2. \tag{3.3}$$

This clear bound has nothing to do with the experimental apparatus used, and only concerns itself with limits on expectation values. Although Aspect violated the bound, there are still some hidden variable theories that remain popular, but all must now admit a non-local element. The most famous of these is the de-Broglie/Bohm pilot wave theory [84] which Einstein also found appealing.

It is now known that all pure states that are not product states (i.e. separable) must violate a Bell inequality (see [85, 86]). For mixed states, there are states that are allowed to violate Bell's inequalities and which are demonstrably entangled. One example is the Werner state [87]. Acín *et al.* [88] also showed that there are non-maximally entangled states that maximally violate Bell-type inequalities. Since Bell, there have been further developments to the theory, most notably the CHSH inequalities [89]. Also, Greenberger, Horne, and Zeilinger went beyond the Bell inequalities to show that entanglement of more than two particles leads to a contradiction with the LHVM for nonstatistical predictions in quantum theory [90].

3.2 Characterising Bipartite Entanglement

Definition of an entangled state

The definition of quantum entanglement was first put forward in [87]. To be more precise, a separable state was defined, and any quantum state not satisfying this definition must be

[2]The word "convincing" has been used as opposed to "definitive". All experimental Bell tests suffer from loopholes. See e.g.[81, 82, 83]. Usually this is due to detector inefficiencies etc. The problem is that it is almost impossible to say definitively that the LHVM model has been violated (and is categorically impossible if one does not accept Free Will as a valid assumption).

non-separable. A separable state $\hat{\rho}_{AB}$ is a state that can be written as the convex mixture

$$\hat{\rho}_{AB} = \sum_j p_j \hat{\rho}_{A,j} \otimes \hat{\rho}_{B,j} \tag{3.4}$$

and a non-separable state cannot. This negative definition of non-separability is perfectly adequate, but more recently [91] it has been shown that if a state $\hat{\rho}_{AB}$ is non-separable, then there will be another quantum state σ whose teleportation fidelity will be magnified when used in conjunction with $\hat{\rho}_{AB}$. An entangled state could then be positively defined as any state $\hat{\rho}_{AB}$ that can be used in "entanglement activation".

Werner and Wolf [92] showed that for bipartite Gaussian states with covariance matrix γ, equation (3.4) is equivalent to saying that there exist two covariance matrices γ_A and γ_B such that

$$\gamma \geq \begin{pmatrix} \gamma_A & 0 \\ 0 & \gamma_B \end{pmatrix} \tag{3.5}$$

where the $\geq$ sign is understood as a relation amongst all eigenvalues. Keeping the definition of a Gaussian state (2.93) in mind, this means that is is possible to create γ using two covariance matrices in product form centred at the origin in phase space (i.e. defined by $\left\langle \hat{R}_l \hat{R}_m + \hat{R}_m \hat{R}_l \right\rangle$ alone) and adding classically correlated noise such that, in effect,

$$\gamma = \begin{pmatrix} \gamma_A & 0 \\ 0 & \gamma_B \end{pmatrix} + \chi \tag{3.6}$$

where χ is a matrix created by classical noise.

The geometry of quantum states

The set of separable states (i.e. those satisfying (3.4)) form a convex and compact set. For two separable bipartite states $\hat{\rho}^{(1)}_{AB}$ and $\hat{\rho}^{(2)}_{AB}$, we could write a linear mixture of the two as

$$p\hat{\rho}^{(1)}_{AB} + (1-p)\hat{\rho}^{(2)}_{AB} = p\sum_j p_j \hat{\rho}^{(1)}_{A,j} \otimes \hat{\rho}^{(1)}_{B,j} + (1-p)\sum_j q_j \hat{\rho}^{(2)}_{A,j} \otimes \hat{\rho}^{(2)}_{B,j} \tag{3.7}$$

which is also a separable state. As the set of separable states is convex it must be contained *within* the convex set of all quantum states. With this in mind, it should be possible to detect whether a state is entangled by slicing up the space of all density matrices sufficiently to determine whether a given state $\hat{\rho}_{AB}$ is inside or ouside the set of separable states.

As a corollary of the Hahn-Banach theorem, given any convex set and an external point, there exists a plane such that the point lays on one side whilst the convex set resides on the other. If the convex set were taken to be the set of separable states, then the operator defining the plane is known as an *entanglement witness*.

If we were to consider an arbitrary vector space $\mathcal{V}$, then a plane in $\mathcal{V}$ can be defined by finding all the vectors $|u\rangle$ that satisfy

$$\langle u|\psi\rangle = 0 \tag{3.8}$$

where $|u\rangle$ is a unit vector orthogonal to the plane. The plane is then defined by a single vector $|\psi\rangle$ such that all the vectors $\{|u\rangle\}$ in the plane are orthogonal to it. For Hermitian operators this would correspond to

$$\mathrm{Tr}\left[\hat{O}_u \hat{O}_\psi\right] = 0. \tag{3.9}$$

So, we could define a witness $\hat{W}$ to be a Hermitian operator that acts as a plane through the convex set of all quantum states for which an entangled quantum state $\hat{\sigma}$ falls on one side and the convex set of separable states is on the other side. By definition

$$\mathrm{Tr}[\hat{W}\hat{\rho}] = 0 \tag{3.10}$$

defines the plane. Then we define that if a state $\hat{\rho}_{\mathrm{sep}}$ is separable then $\mathrm{Tr}[\hat{W}\hat{\rho}_{\mathrm{sep}}] \geq 0$. Necessarily, state $\hat{\sigma}$ is entangled if and only if there exists an operator $\hat{W}$ such that $\mathrm{Tr}\left[\hat{W}\hat{\sigma}\right] < 0$ whilst $\mathrm{Tr}[\hat{W}\hat{\rho}_{\mathrm{sep}}] \geq 0$ for all separable states $\hat{\rho}_{\mathrm{sep}}$. Terhal [93] pointed out that a violation of a Bell

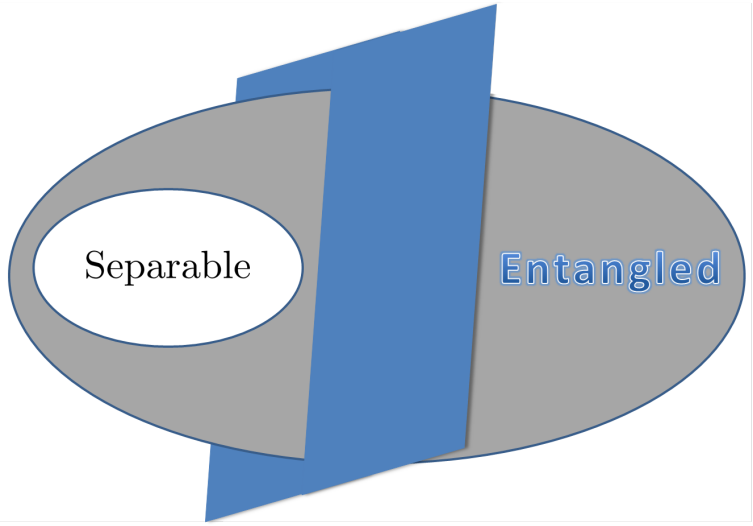

Figure 3.1: The convex set of separable states is a subset of the convex set of all states. Entanglement witnesses, such as the plane above, can bisect the set of quantum states, but not the set of separable states. An optimal entanglement witness would bisect the set of all quantum states right at the boundary of the separable states.

inequality can be expressed as a witness of entanglement, and coined the term *entanglement witness*. Since then lots of work has been carried out.

Needless to say, entanglement witnesses are more of a mathematical tool than anything else. It is more common to use separability criteria (see Section 3.3). Witnesses shall, however, play a role later on in this thesis.

Qualities of entanglement

The geometric ideas of the previous section are useful for the mathematical formulation of entanglement but are not useful for understanding the properties of entanglement. We here outline a more operational interpretation, similar to that found in [94].

In quantum information we can consider a generalised measurement on a state. As is standard in an approach to quantum evolution, one considers a system to evolve either via unitary operations or through the collapse of the wavefunction resulting from a projective measurement. Instead, a more general scenario could be explored, in which interactions occur with ancillary quantum states:

1. Ancillary particles are introduced
2. Joint unitary operations are performed on both the system in question and the ancillae, and
3. Some particles are then discarded based on measurement outcomes.

If the ancillae are originally uncoordinated with the system then we can describe the evolution via the *Kraus operators*. If total knowledge of the measurement outcomes is retained then the state corresponding to measurement outcomes j occurs with probability $p_j = \mathrm{Tr}[\hat{A}_j \hat{\rho} \hat{A}_j^\dagger]$ and is given by

$$\rho_j = \frac{\hat{A}_j \hat{\rho} \hat{A}_j^\dagger}{\mathrm{Tr}[\hat{A}_j \hat{\rho} \hat{A}_j^\dagger]} \tag{3.11}$$

where ρ is the initial state and the $\{\hat{A}_j\}$ are the Kraus Operators. The normalisation condition $\sum_j \hat{A}_j^\dagger \hat{A}_j = \mathbb{1}$ holds.

Sometimes, when a system interacts with an environment, all or part of the knowledge of measurement outcomes is lost. At the extreme end, the only hope for the observer is to average

over all the possible measurement outcomes, that is, to trace out the ancillary particles. Such a map is said to be *trace preserving* and is given by

$$\hat{\rho} \to \hat{\rho}' = \sum_j \hat{A}_j \hat{\rho} \hat{A}_j^\dagger. \tag{3.12}$$

We can now discuss the most important defining aspect of quantum entanglement, the *LOCC constraint*. In any experiment involving quantum communication, it is most desirable to distribute entangled quantum states between distant, separate locations. If the states are perfectly entangled, then it would be feasible to communicate via teleportation, and so the perfect distribution of entanglement is almost synonymous with perfect quantum communication. However, noise will always play a detrimental role to the ability to communicate, and to distribute the entangled states. One favoured option would be to use these imperfect channels and then to battle the noise using local operations and classical communication (LOCC). Loosely speaking, the correlations that can emerge from local operations and classical communication can be considered as classical correlations.

If we then try to use a bipartite quantum state to perform some task that cannot be simulated using these essentially classical correlations, then the only option is that the ability to do so must be due to some inherent quantum correlations that were already present in the state. This is an essential consideration to the study of quantum entanglement. In practice the set of LOCC operations is very large and Alice and Bob may use classical communication before or after any round of local operations. They may perform one round of measurements, communicate these results to each other classically, and then use the measurement outcomes to indicate what their next move should be. There is, consequently, no simple characterisation of LOCC operations, so other classes (with some sense of LOCC) have to be considered. For example we could consider the set of *separable operations* which can be described as all Krauss operators with a product decomposition as

$$\hat{\rho}_j = \frac{\left(\hat{A}_j \otimes \hat{B}_j\right) \hat{\rho} \left(\hat{A}_j^\dagger \otimes \hat{B}_j^\dagger\right)}{\mathrm{Tr}\left[\left(\hat{A}_j \otimes \hat{B}_j\right) \hat{\rho} \left(\hat{A}_j^\dagger \otimes \hat{B}_j^\dagger\right)\right]} \tag{3.13}$$

where $\sum_j \hat{A}_j^\dagger \hat{A}_j \otimes \hat{B}_j^\dagger \hat{B}_j = \mathbb{1}$. All LOCC operations can be formed in terms of separable operations.

Following this idea of LOCC constraints, we can point out the main properties that entanglement has. These are

- Separable states, those given in (3.4), must possess no entanglement. These states can be easily created from LOCC operations and they trivially satisfy local hidden variable models.
- The entanglement of a single quantum state cannot increase deterministically under LOCC operations. More specifically, if we know that a state $\hat{\rho}$ can be turned into another state $\hat{\sigma}$ by LOCC operations then anything that $\hat{\rho}$ can be used for involving LOCC operations can be equally well simulated using $\hat{\sigma}$ and LOCC operations. That is not to say that things cannot be altered by other methods (see Section 3.4).
- As the inverse of a local unitary matrix is another local unitary matrix, then if the entanglement in a quantum state could decrease via a local unitary operation, it would logically follow that the inverse operation would increase the entanglement. This cannot occur due to the reason mentioned previously, and so entanglement must be invariant to local unitary operations.
- There are quantum states in finite dimensional Hilbert spaces that are said to be maximally entangled, e.g. the singlet state $1/\sqrt{2}\left(|01\rangle + |10\rangle\right)$, which by definition yield a maximally mixed thermal state when one subsystem is traced out. In the continuous variable regime this is not the case when finite energy is assumed. A maximally entangled state could only be achieved by taking e.g. the two mode squeezed vacuum in the non-physical limit of infinite squeezing.

With these qualitative ideas expounded, we can now explore theoretical techniques for detecting entanglement.

3.3 Separability and Non-separability Criteria

Now that the idea of an entangled state has been firmly planted, we shall consider how to detect entanglement. The best way is in fact to consider separability and non-separability criteria. These consist of statements of the form "A separable state possesses the quality .... If the state in question does not possess this quality, then it must necessarily be entangled" or a converse statement.

Positive but not completely positive maps

At about the same time as the theory of entanglement witnesses was being developed, there was also research done in the area of positive but not completely positive maps. A positive map is a superoperator that will transform a matrix with positive eigenvalues (such as quantum density matrices) into another positive matrix. That is, a map Λ is positive if, for any positive matrix ρ, we have $\Lambda(\rho) \geq 0$. A map Λ is positive if it preserves hermiticity and the cone of positive elements. From any map Λ another map affecting a larger system, $(\mathbb{1} \otimes \Lambda)$ can be defined with the effect

$$(\mathbb{1} \otimes \Lambda) \left(\sum_j p_j \rho_{A,j} \otimes \rho_{B,j} \right) = \sum_j p_j \rho_{A,j} \otimes \Lambda \left(\rho_{B,j} \right) \tag{3.14}$$

If the RHS of the above equation is also positive, then the map Λ is said to be *completely positive*. All physical evolution of a system is given by completely positive maps. But to test entanglement, we want to find positive but not completely positive maps. A quantum state $\hat{\rho}_{AB}$ is separable if and only if

$$(\mathbb{1} \otimes \Lambda) \left(\hat{\rho}_{AB} \right) \geq 0 \tag{3.15}$$

for all positive but not completely positive maps.

Effectively, a density matrix has to be positive semidefinite and hermitian with $\mathrm{Tr}\left[\hat{\rho}\right] = 1$. If we apply a map Λ to a state ρ that is positive, then $\Lambda(\rho)$ is also a valid quantum state. However, if $(\mathbb{1} \otimes \Lambda) \hat{\rho}_{AB}$ is not positive, then the use of the map on one of the subsystems of a bipartite state does not yield a valid state. As shall be seen, there has been major exploration into finding operations, or some symmetry to be broken, that would transform a single quantum object into another single quantum object, but which does not apply on sub parts of larger systems.

Peres-Horodecki Criterion

One of the most powerful criterion based on positive but not completely positive maps is the positive partial transposition criterion (PPT). For finite dimensional systems this was first shown in [95]. The PPT criterion states that for a separable state $\hat{\rho}_{AB} = \sum_j p_j \hat{\rho}_{A,j} \otimes \hat{\rho}_{B,j}$, the form $\hat{\rho}_{AB}^{T_A} = \sum_j p_j \hat{\rho}_{A,j}^T \otimes \hat{\rho}_{B,j}$ is also a valid density matrix. It also guarantees the positivity of $\hat{\rho}_{AB}^{T_B}$ defined in an analogous way. Horodecki [96] showed that the PPT criterion is necessary and sufficient for quantum states $\hat{\rho}_{AB}$ defined on Hilbert space $\mathcal{H}_{AB} = \mathcal{H}_A \otimes \mathcal{H}_B$ where the dimensions of $\mathcal{H}_A$ and $\mathcal{H}_B$ are $d_A = d_B = 2$ and $d_A = 2, d_B = 3$.

For continuous variables the PPT criterion has also been shown [97] to be valid. There, it was shown that in phase space the PPT criterion can be interpreted as a reflection of the phase space coordinates of one subsystem about the position axis. That is, if a density matrix can be represented by the coordinates (x_A, p_A, x_B, p_B) then $\hat{\rho}_{AB}^{T_B}$ can be represented by $(x_A, p_A, x_B, -p_B)$. This corresponds to a time reversal of one subsystem. For one lone quantum object, time reversal would still lead to a valid quantum state, but when performed on part of a greater quantum state, the result is not in general a positive density matrix.

Reduction and Majorisation criteria

As was noticed by Schrödinger, the whole is more than a sum of its parts. It is known that in quantum mechanics the von-Neumann entropy of a subsystem $\hat{\rho}_A = \mathrm{Tr}_B[\hat{\rho}_{AB}]$ can be greater than the entropy of the global state. That is,

$$\mathcal{S}\left(\hat{\rho}_A\right) > \mathcal{S}\left(\hat{\rho}_{AB}\right). \tag{3.16}$$

If this is true then it is known that the state is more disordered locally than globally and the state must be non-separable. Separable states must satisfy $\mathcal{S}(\hat{\rho}_A) \leq \mathcal{S}(\hat{\rho}_{AB})$. Majorisation theory can be a very useful tool in quantum information and can allow us to see whether (3.16) holds. For two matrices $\mathbf{A}$ and $\mathbf{B}$ of dimensions d_A and d_B we can put their respective eigenvalues into vectors in descending order $a^{\downarrow} = \left(a_1^{\downarrow}, \cdots, a_{d_A}^{\downarrow}\right)$ and $b^{\downarrow} = \left(b_1^{\downarrow}, \cdots, b_{d_B}^{\downarrow}\right)$. If for example $d_A < d_B$ then we put $a_{d_A+1}^{\downarrow} = 0, \cdots, a_{d_B}^{\downarrow} = 0$. Then if

$$\sum_{j=1}^{k} a_j^{\downarrow} \leq \sum_{j=1}^{k} b_j^{\downarrow} \quad k = 1, 2, \cdots \tag{3.17}$$

we say that $\mathbf{A}$ is *majorised by* $\mathbf{B}$ (or $\mathbf{A} \succ \mathbf{B}$)[3]. If $\mathbf{A}$ is majorised by $\mathbf{B}$ then for any Schur concave functional f of $\mathbf{A}$ and $\mathbf{B}$, it is true that $f(\mathbf{A}) \geq f(\mathbf{B})$. Consequently, for two density matrices $\hat{\rho}^{(1)}$ and $\hat{\rho}^{(2)}$ for which $\hat{\rho}^{(1)} \succ \hat{\rho}^{(2)}$, their von-Neumann entropies must satisfy $\mathcal{S}\left(\hat{\rho}^{(1)}\right) \geq \mathcal{S}\left(\hat{\rho}^{(2)}\right)$. With this majorisation tool it is possible to check the entropic relations between the global and local states. Majorisation works in the continuous variable case too [98].

It was shown in [99] that the majorisation criterion follows from the reduction criterion. This is defined [100] by the positive but not completely positive map

$$\Lambda^R(X) = \mathrm{Tr}\left[X\right] \cdot \mathbb{1} - X, \tag{3.18}$$

which is equivalent to stating that for a separable density matrix

$$\hat{\rho}_A \otimes \mathbb{1} - \hat{\rho}_{AB} \geq 0 \tag{3.19}$$

where $\hat{\rho}_A = \mathrm{Tr}_B\left[\hat{\rho}_{AB}\right]$. For two qubits, the reduction criterion also provides a necessary and sufficient condition for separability, although it was shown that in general the reduction criterion is weaker than the PPT criterion. Consequently, the PPT criterion can detect any states that the reduction and majorization criteria detect, but can also detect states beyond the scope of this pair.

Range criterion

One of the first criteria that surfaced able to detect entangled quantum states that the PPT criterion could not was the *range criterion* [101] which operates on finite dimensions.

The range criterion states: For a separable state $\hat{\rho}_{AB}$, there exists a set of product vectors $|a_i b_i\rangle$ such that the set $\{|a_i, b_i\rangle\}$ spans the range of $\hat{\rho}_{AB}$ and also the set $\{|a_i^* b_i\rangle\}$ spans the range of $\hat{\rho}_{AB}^{T_A}$ where $|a^*\rangle$ denotes the vector consisting on the complex conjugated components of $|a\rangle$. The range criterion has detected states for which the PPT criterion has failed [101, 102].

Local Uncertainty Relations

For continuous variable systems, one of the first separability criteria to emerge was the Duan criterion [103]. The Duan criterion is an inseparability criterion based on the variances of two Einstein-Podolsky-Rosen like operators. One defines operators

$$\hat{u} = |s|\hat{x}_1 + \frac{1}{s}\hat{x}_2, \tag{3.20}$$

$$\hat{v} = |s|\hat{p}_1 - \frac{1}{s}\hat{p}_2 \tag{3.21}$$

where s is an arbitrary non-zero real number and $(\hat{x}_j, \hat{p}_j)$ are the quadratures corresponding to system j. Then the Duan criterion states that for any separable state $\hat{\rho}_{AB}$, the total variance

[3] As an interesting but at times distressing quirk, the symbol denoting majorisation has changed. In some older references such as [98] and in my own **[IV]**, the statement $\mathbf{A}$ *is majorised by* $\mathbf{B}$ is denoted as in the main text $\mathbf{A} \succ \mathbf{B}$. However, in many modern references such as [99], the notation has been reversed i.e. $\succ$ is replaced with $\prec$ although the meaning is the same. In this thesis, our notation follows from [98]

of a pair of EPR-like operators defined by equations (3.20) and (3.21) with the commutators $[\hat{q}_j, \hat{p}_{j'}] = i\delta_{jj'}(j, j' = 1, 2)$ satisfies the inequality

$$\left\langle (\Delta\hat{u})^2 \right\rangle_{\rho_{AB}} + \left\langle (\Delta\hat{v})^2 \right\rangle_{\rho_{AB}} \geq s^2 + \frac{1}{s^2}. \tag{3.22}$$

General separability criteria based on uncertainty relations and valid for both discrete and continuous variable systems were introduced by Giovannetti [104] and Hofmann & Takeuchi [105]. It should be noted that Hofmann's criterion was initially designed for discrete variables but is equally valid for continuous variable states. It was also shown that Hofmann's criterion could be used to detect entanglement in quantum states with positive partial transposition [106].

3.4 Entanglement Distillation and Bound Entanglement

In many protocols in quantum information theory, success is dependent on the entanglement content of two quantum objects held by Alice & Bob and spatially separated. If we were to consider that Alice created the bipartite state and then sent Bob his quantum present via a noisy channel, then it stands to reason that the initial entanglement in $\hat{\rho}_{AB}$ will have decreased. Once spatially separated, could Alice and Bob use local operations and classical communication to improve the entanglement between their subsystems once again?

In 1996, Bennett *et al.* [107] responded in the affirmative. In their seminal paper, they established that when two distant parties share n copies of a bipartite mixed state $\hat{\rho}_{AB}$ containing noisy entanglement, they can perform LOCC and obtain some number $k < n$ of a system in a state closer to a singlet state (i.e. closer to a pure entangled state and with more entanglement). Such a sequence of LOCC operations achieving this goal is known as *entanglement purification* or *entanglement distillation*.[4] The ratio $r = k/n$ in the limit of large n when optimised is used to define an entanglement measure, the *distillable entanglement* (see Section 3.5).

Entanglement distillation protocols have been found for qubits. For example, one-way hashing distillation protocols [108] in which only one party can tell the other the results of any local measurements, are closely linked to error correcting codes. Two way recurrence distillation protocols have also been defined [107, 108]. Notably, it has been shown that all two qubit states are distillable [109].

However, for the purposes of this thesis, the most relevant distillation protocols are the so-called *procrustean entanglement distillation* schemes [110], named for the mythical Greek bandit, Procrustes, who would lure weary travellers to rest on his comfortable bed, which could magically fit a person perfectly. He neglected to tell them that this marvel of ergonomic design could only be achieved by removing the legs of anyone too tall or stretching anyone too short.

In a similar way, procrustean entanglement distillation schemes aim to increase the entanglement in a system by altering the coefficients in the Schmidt decomposition whilst retaining the general structure. Such a protocol implies that a state transforms as

$$|\psi\rangle_{\text{in}} = \sum_{k}^{K} s_k |e_k\rangle \otimes |f_k\rangle \rightarrow |\psi\rangle_{\text{out}} = \sum_{k}^{K} t_k |e_k\rangle \otimes |f_k\rangle \tag{3.23}$$

where the output state is necessarily more entangled than the input state and $\{|e_j\rangle\}$ and $\{|f_k\rangle\}$ are orthonormal sets of basis vectors. That is, Alice and Bob use LOCC to conditionally transform the Schmidt coefficients of each entangled input state to obtain a more entangled output state.

Procrustean entanglement concentration schemes can be applied to just a single copy of a state. The trade-off is that procrustean schemes are necessarily probabilistic - just as with Procrustes' victims' legs, the "extra" probabilistic outcomes are chopped off, i.e. the state is altered by a probabilistic post-selection after some transformation to the state. The methods are necessarily probabilistic due to a theorem by Nielsen [111] based on majorisation. Nielsen

[4] Over time, the terminology has altered significantly. Although "purification" of course can only apply to LOCC that transform a mixed state closer to a pure entangled state, the term "distillation" is more commonly used to just denote any set of LOCC that increase entanglement. For example in Chapter 5 we transform an initial pure state to a mixed state with more entanglement. We use the terms "distillation" and "concentration" interchangeably throughout this thesis.

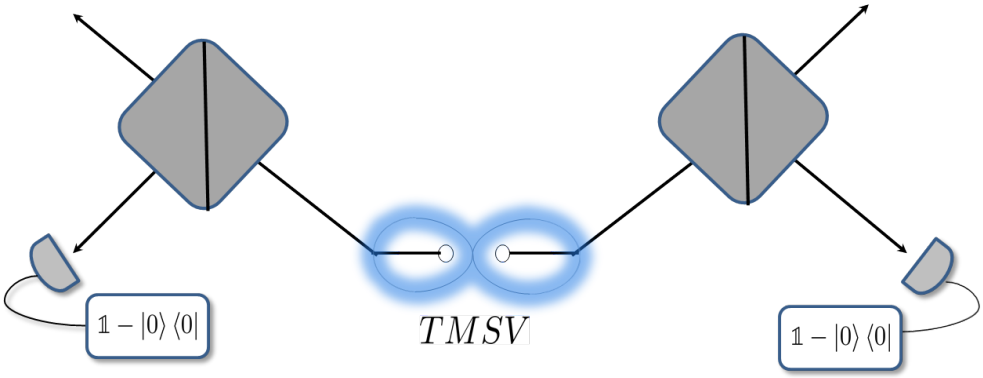

Figure 3.2: An example of a traditional continuous variable distillation scheme. Both arms of a two mode squeezed vacuum are incident on highly transmissive beamsplitters. One or more photons may be siphoned off and, if successfully detected, the (now non-Gaussian) remainder of the two mode squeezed vacuum is more entangled.

showed that one can only transform the pure state $\hat{\rho}_{\text{in}}$ into the pure state $\hat{\rho}_{\text{out}}$ deterministically using LOCC if $\text{Tr}_B[\hat{\rho}_{\text{out}}]$ is majorised by $\text{Tr}_B[\hat{\rho}_{\text{in}}]$. This in turn would imply that one could only turn $\hat{\rho}_{\text{in}}$ into $\hat{\rho}_{\text{out}}$ by deterministic LOCC if $\hat{\rho}_{\text{in}}$ is more entangled than $\hat{\rho}_{\text{out}}$. As this is the polar opposite of what we want, to increase the entanglement necessarily requires a probabilistic action.

In the continuous variable setting, procrustean entanglement concentration schemes have proved most useful. On the theory side, Opartný *et al.* [112] showed how beamsplitters and photon subtraction can be used to increase the entanglement in a two mode squeezed vacuum (TMSV) as part of a teleportation scheme. The distillation aspect of this was seized upon and improved [113, 114, 115] and a rigorous theoretical description was given by Kitagawa *et al.* [116]. Experimentally, there have been some notable successes [117, 118], including with non-Gaussian noise [119]. In a fairly recent proposal [120] a complete CV entanglement "distillery" has been proposed, harnessing limited physical space for storing quantum states and distilling entanglement. There, clever manipulation of an imperfect quantum memory complements a beamsplitter based entanglement concentration scheme. The discovery of more continuous variable entanglement distillation schemes is hampered by a notorious no-go theorem stating that it is impossible to distil entanglement in Gaussian states with Gaussian operations alone [62, 63, 121].

One of the best known of the entanglement distillation schemes aims at increasing the entanglement of a two mode squeezed vacuum by impinging each arm of the TMSV on a highly transmissive beamsplitter. If some photons are subtracted and detected by a waiting photon counter or avalanche photodiode, then the entanglement of the TMSV increases, although the resultant entangled state is mixed (see Figure 3.2). In Chapters 4 and 5 we develop this idea by showing that two QND interactions can be used to simulate a beamsplitter interaction to distil entanglement in two atomic ensembles. We then show that a single QND interaction could be used to the same end.

At first glance it appears that entanglement distillation has met the challenge that opened this section. Alice could create a bipartite, entangled quantum state and send Bob his share of the state via a noisy quantum channel, with any losses that arise being corrected later by local operations and classical communication. Perfect quantum communication would then require sufficient distillation, but any noise distorting the initial state could be corrected for. The spanner in the works came from M. Horodecki *et al.* [122] (for the continuous variable case it was later shown in [123]) who showed that no positive partially transposed (PPT) state can be distilled. Clearly, separable states cannot become entangled from LOCC, but other entangled states with a positive partial transpose can also not be distilled. The states that are known to be entangled but are not distillable are called *bound entangled* states. There is a sense that the entanglement of these mixed states (and it *is* only found in mixed states) is bound to the system.

One big open question in QIT is whether or not there exist non-distillable states that are not

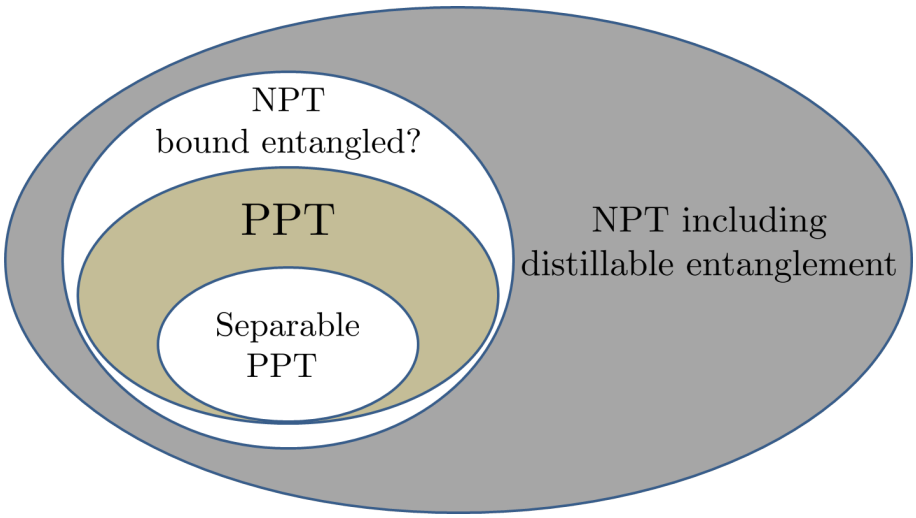

Figure 3.3: The separable states have a positive partial transpose (PPT) and are a subset of a larger set of all density matrices with a positive partial transpose, including bound entangled states. There may then be bound entangled states with a negative partial transpose (NPT), and all quantum states possessing distillable entanglement must have a negative partial transpose.

PPT. Although bound entangled states are known to exist, there has been no characterisation of the set of bound entangled states, but are all NPT states distillable? See [77] and references within for more information on this.

3.5 Entanglement Measures

It is the instinct of the physicist to not simply admire the beauty in nature, but to try to quantify it. So far, we have tried to give an operational characterisation of entanglement and have discussed increasing entanglement by local operations and classical communication. But this begs the question: How can we know that we have truly *increased* the entanglement in the system? By what gauge is it justified to say that the entanglement in a system has increased? In this section, we look at a small and by no means complete survey of entanglement measures that illuminate the attempts made to quantify entanglement. An entanglement measure is simply a mathematical tool which captures the essence of all the properties discussed earlier. In Chapter 6 we define our own potential measure of entanglement in Gaussian states.

In the continuous variable regime, it is possible to define measures so long as the mean energy is bounded (if not, then one may demonstrate that in an arbitrarily small neighbourhood of a pure product state, there are pure states with arbitrarily strong entanglement [124]). However, we here describe some measures that were initially defined for finite dimensional systems, although will also state how well they carry across to the continuous variable setting. A number of measures have been defined for Gaussian states, usually as an extrapolation from the qudit measures.

An axiomatic approach to entanglement measures

One approach to finding entanglement is to propose a list of all the properties that would be desired from a good measure [125]. Then, any functional of a probability density matrix satisfying those properties would be useful as an entanglement measure $\mathfrak{E}$. The most obvious two are

- *For any separable state* $\hat{\rho}_{sep}$

$$\mathfrak{E}\left(\hat{\rho}_{\mathrm{sep}}\right) = 0 \tag{3.24}$$

- $\mathfrak{E}$ *does not increase on average under LOCC*

$$\mathfrak{E}\left(\hat{\rho}_{AB}\right) \geq \sum_j p_j \mathfrak{E}\left(\frac{\hat{A}_j \hat{\rho}_{AB} \hat{A}_j^\dagger}{\mathrm{Tr}\left[\hat{A}_j \hat{\rho}_{AB} \hat{A}_j^\dagger\right]}\right) \tag{3.25}$$

where the A_j *are Krauss operators and* $p_j = Tr\left[\hat{A}_j \hat{\rho}_{AB} \hat{A}_j^\dagger\right]$.

Vidal [126] in fact, argued that monotonicity under LOCC should be the only postulate necessarily required under an entanglement measure. Further to the above two qualities of a measure, below are some more desirable properties.

- *Convexity: Convexity is a useful property that is sometimes justified as capturing the notion of loss of information. This would therefore mean*

$$\mathfrak{E}\left(\sum_j p_j \hat{\rho}_j\right) \leq \sum_j p_j \mathfrak{E}\left(\hat{\rho}_j\right) \tag{3.26}$$

- *Additivity: Given an entanglement measure and a state* $\hat{\rho}_{AB}$*, one may ask that* $\mathfrak{E}\left(\hat{\rho}_{AB}^{\otimes n}\right) = n\mathfrak{E}\left(\hat{\rho}_{AB}\right)$ *where* $\hat{\rho}_{AB}^{\otimes n}$ *denotes* $\hat{\rho}_{AB} \otimes \hat{\rho}_{AB} \otimes \cdots \hat{\rho}_{AB}$ *(n times). If this holds, the measure is said to be additive.*

Some of the measures that are most useful for quantifying entanglement are not additive, but given any non-additive measure we could define an additive measure $\mathfrak{E}'$ as

$$\mathfrak{E}'\left(\hat{\rho}_{AB}\right) := \lim_{n\to\infty} \frac{\mathfrak{E}\left(\hat{\rho}_{AB}^{\otimes n}\right)}{n}. \tag{3.27}$$

A far more scarce property of entanglement measures is *strong additivity*. That is, given two states $\hat{\rho}_1$ and $\hat{\rho}_2$

$$\mathfrak{E}\left(\hat{\rho}_1 \otimes \hat{\rho}_2\right) = \mathfrak{E}\left(\hat{\rho}_1\right) + \mathfrak{E}\left(\hat{\rho}_2\right). \tag{3.28}$$

- *Reduces to entropy of entanglement on pure states*

This is a desirable property in both the discrete and continuous variable regime. It is known that in finite dimensions, any entanglement monotone that is additive on pure states and sufficiently continuous must equal $\mathcal{S}\left(\hat{\rho}_A\right)$ on all pure states [127, 128, 129].

- *Asymptotic Continuity*

Some of the most useful entanglement measures are introduced below, beginning with the entropy of entanglement.

Entropy of Entanglement

The entropy of entanglement captures the essence of what Schrödinger thought most remarkable about quantum mechanics [64]:

> *Another way of expressing the peculiar situation is: the best possible knowledge of a whole does not necessarily include the best possible knowledge of all its parts, even though they may be entirely separated and therefore virtually capable of being "best possibly known", i.e. of possessing, each of them, a representative of its own.*

In particular, the entropy of entanglement is a good measure of entanglement in pure states and is defined as the Von-Neumann entropy of the reduced state. That is, for a bipartite state $\hat{\rho}_{AB}$, the entropy of entanglement is given by

$$\mathcal{E}_{v.N}\left(\hat{\rho}_{AB}\right) = \mathcal{S}\left(\hat{\rho}_A\right) \tag{3.29}$$

where $\hat{\rho}_A = \mathrm{Tr}_B\left[\hat{\rho}_{AB}\right]$. Similarly $\mathcal{E}_{v.N}\left(\hat{\rho}_{AB}\right) = \mathcal{S}\left(\hat{\rho}_B\right)$. For a pure state $\hat{\rho}_{AB}$, as has been seen $\mathcal{S}\left(\hat{\rho}_{AB}\right) = 0$, so the entropy of entanglement simply shows that there is more uncertainty in the parts than in the whole. For Gaussian states, the entropy of entanglement is easily calculated from the symplectic spectrum of Alice's reduced covariance matrix and equation (2.114). It should be noted that the entropy of entanglement is not a good measure of entanglement for bipartite mixed states.

Distillable Entanglement and Entanglement Cost

With regards to distillation, we could ask the following question: If Alice and Bob shared n copies of a state $\hat{\rho}_{AB}$ and carry out LOCC transformations to transform their combined state, as closely as possible, to m copies of a maximally entangled qubit state, then what is the best possible rate $r = m/n$ of distillation? In the limit of large n, the distillable entanglement can be defined [107, 108, 94] as the best possible rate over all possible LOCC schemes Λ to convert n copies of $\hat{\rho}_{AB}$ to m copies of the maximally entangled state $(|\phi_+\rangle\langle\phi_+|^{\otimes m})$ where $|\phi_+\rangle = \frac{1}{\sqrt{2}}(|00\rangle + |11\rangle)$.

$$\mathcal{E}_D(\hat{\rho}_{AB}) := \sup\left\{r : \lim_{n\to\infty}\left[\inf_\Lambda ||\Lambda\left(\hat{\rho}_{AB}^{\otimes n}\right) - \left(|\phi_+\rangle\langle\phi_+|^{\otimes m}\right)||\right] = 0\right\} \tag{3.30}$$

Distillable entanglement tells us the rate at which noisy mixed states can be converted back to good singlet states, having been sent along a noisy channel. Distillable entanglement in the CV regime is difficult to compute, as expected. For Gaussian states, distillation with respect to all possible quantum operations must be considered, due to the no-go theorem [62, 63, 121] stating that it is impossible to distil entanglement with Gaussian operations alone. Consequently, although the concept of distillable entanglement can be envisaged for continuous variables, there is no way to conceivably calculate it, even for a subset of possible states such as Gaussian states.

We could ask the opposite question: What is the maximal rate r at which one can convert blocks of maximally entangled 2 qubit states into output states that approximate many copies of $\hat{\rho}_{AB}$, such that the approximations become vanishingly small in the limit of large block sizes. This is known as *entanglement dilution* and gives rise to the *entanglement cost*:

$$\mathcal{E}_C(\hat{\rho}_{AB}) := \inf\left\{r : \lim_{n\to\infty}\left[\inf_\Lambda ||\hat{\rho}_{AB}^{\otimes n} - \Lambda\left(\left(|\phi_+\rangle\langle\phi_+|^{\otimes m}\right)\right)||\right] = 0\right\} \tag{3.31}$$

If one was to perform a cycle of entanglement dilution and distillation, then often there would be a discrepancy between the input and output states [130] even in the asymptotic limit. In general,

$$\mathcal{E}_D(\hat{\rho}_{AB}) \leq \mathcal{E}_C(\hat{\rho}_{AB}). \tag{3.32}$$

Entanglement of Formation

For a mixed state $\hat{\rho}_{AB}$, the Entanglement of Formation (EoF) is defined as

$$\mathcal{E}_F(\hat{\rho}_{AB}) := \inf\left\{\sum_j p_j \mathcal{E}_{v.N}(|\psi_j\rangle\langle\psi_j|) : \quad \hat{\rho}_{AB} = \sum_j p_j |\psi_j\rangle\langle\psi_j|\right\}. \tag{3.33}$$

The EoF represents the minimal possible average entanglement over all pure state decompositions of $\hat{\rho}_{AB}$, using the entropy of entanglement as a quantifier of the entanglement in the pure states. It can be expected that it is closely related to the entanglement cost of $\hat{\rho}_{AB}$. It should be noted that the entanglement cost is dependent on $\hat{\rho}_{AB}^{\otimes n}$, not $\hat{\rho}_{AB}$, and it is unknown for which states $\mathcal{E}_F$ scales accordingly. It is instead possible to define the *regularised entanglement of formation* as

$$\mathcal{E}_F^\infty(\hat{\rho}_{AB}) := \lim_{n\to\infty}\frac{\mathcal{E}_F\left(\hat{\rho}_{AB}^{\otimes n}\right)}{n} \tag{3.34}$$

which was proven rigorously in [131] to be equal to the entanglement cost $\mathcal{E}_C(\hat{\rho}_{AB})$.

For a long time it was conjectured that the EoF was additive, and there were indeed some indications (e.g. [132, 133, 134]). If true, this would have implied that

$$\mathcal{E}_F = \mathcal{E}_F^\infty = \mathcal{E}_C. \tag{3.35}$$

Recently, however, Hastings [135] showed by counterexample that EoF is not additive on all states.

In the continuous variable regime, Giedke *et al.* [136] found the EoF of two-mode symmetric Gaussian states ($a = b$ in Equation (2.122)). If we define the functions $k_\pm(x) = \left(x^{-1/2} \pm x^{1/2}\right)^2/4$ then symmetric two-mode Gaussian states $\hat{\rho}_G^{\text{sym}}$ have an EoF value of

$$\mathcal{E}_F(\hat{\rho}_G^{\text{sym}}) = k_+(x_{\text{sym}})\log\left[k_+(x_{\text{sym}})\right] - k_-(x_{\text{sym}})\log\left[k_-(x_{\text{sym}})\right] \tag{3.36}$$

where the argument is given by

$$x_{\text{sym}} = \sqrt{(a - c_+)(a + c_-)}. \tag{3.37}$$

The formula for symmetric two-mode Gaussian states was found by a decomposition over Gaussian pure states, and it was conjectured that this would always be true, i.e. that the entanglement of formation would always be found by a decomposition over Gaussian pure states. With this idea in mind Wolf *et al.* defined the Gaussian Entanglement of Formation (GEoF) [137] (denoted $E_f^G(\hat{\rho}_{AB})$) for a bipartite Gaussian state as the optimal decomposition of a Gaussian state over all pure Gaussian states.

Finally, Marian and Marian [138] found the optimal pure state decomposition of an arbitrary two-mode Gaussian state. They also found that for any two-mode Gaussian state, $E_f^G(\hat{\rho}_{AB}) = \mathcal{E}_F(\hat{\rho}_{AB})$. Furthermore, they also showed that on two mode Gaussian states, the Entanglement of Formation is additive!

Relative Entropy of Entanglement

The quantum relative entropy

$$\mathcal{S}(\hat{\rho}||\hat{\sigma}) := \text{Tr}[\hat{\rho}\log\hat{\rho} - \hat{\rho}\log\hat{\sigma}] \tag{3.38}$$

is a very useful gauge for distinguishing between quantum states. It is not, strictly speaking, a measure as $\mathcal{S}(\hat{\rho}||\hat{\sigma}) \neq \mathcal{S}(\hat{\sigma}||\hat{\rho})$ in most cases, but is useful all the same. The *relative entropy of entanglement* can be defined as

$$\mathcal{E}_R^X(\hat{\rho}_{AB}) := \inf_{\sigma\in X}\mathcal{S}(\hat{\rho}_{AB}||\hat{\sigma}) \tag{3.39}$$

with respect to a set X. The set X can be taken to be the set of separable states, PPT states, or non-distillable states (if PPT and non-distillable are not the same). The measure then asks for the distance between $\hat{\rho}_{AB}$ and the closest state $\hat{\sigma}$ within set X. The regularised version, $\mathcal{E}_R^\infty$ acts as an upper bound on the distillable entanglement [128]. Remarkably, it is fully computable for two qubits [139] and Friedland and Gour [140] have shown that an analytic solution should in principle exist for multipartite states in any number of finite dimensions. Within the continuous variable regime, the most successful form of this measure is the *Gaussian Relative Entropy of Entanglement* [141]. In this case, for any Gaussian entangled state this measure is defined as the minimal quantum relative entropy between the state and the set of Gaussian separable states.

Negativity and Logarithmic Negativity

The Negativity of a quantum state $\hat{\rho}_{AB}$ is defined as the sum of the eigenvalues of the partially transposed state and can be written as

$$\mathcal{N}(\hat{\rho}_{AB}) = \frac{1}{2}\text{Tr}\left(\sqrt{(\hat{\rho}_{AB}^{T_A})^2} - \hat{\rho}_{AB}^{T_A}\right) = \frac{\left\|\hat{\rho}_{AB}^{T_A}\right\| - 1}{2}, \tag{3.40}$$

where $\|\cdot\|$ denotes the trace-norm, i.e. $\sqrt{\hat{\rho}_{AB}\hat{\rho}_{AB}^\dagger}$, and $\hat{\rho}_{AB}^{T_A}$ is the partial transpose of the density matrix $\hat{\rho}_{AB}$ with respect to subsystem A. It was introduced by Zyckowski *et al.* [142] and shown to be an entanglement monotone by Vidal and Werner [143].

The negativity is useful as it is easy to compute numerically and works for both discrete and continuous variable states. Sometimes it can be calculated analytically. For example, if we consider the density matrix of the two mode squeezed vacuum (TMSV),

$$\hat{\rho}_{\text{TMSV}} = \left(1 - \lambda^2\right)\sum_{m,n=0}^{\infty}\lambda^{m+n}|mm\rangle\langle nn|, \tag{3.41}$$

and partially transpose with respect to subsystem A, we obtain

$$\hat{\rho}_{\text{TMSV}}^{T_A} = \left(1 - \lambda^2\right)\sum_{m,n=0}^{\infty}\lambda^{m+n}|nm\rangle\langle mn|. \tag{3.42}$$

We next consider the structure of $\hat{\rho}_{\mathrm{TMSV}}^{T_A}$. Whenever $m = n$, the corresponding element $\left(1-\lambda^2\right)\lambda^{2m}$ is an eigenvalue and is positive as $0 \leq \lambda \leq 1$ and so does not contribute to the negativity. Whenever $m \neq n$, the density matrix elements can be written in a block diagonal form where the blocks take the form

$$\begin{pmatrix} 0 & \left(1-\lambda^2\right)\lambda^{m+n} \\ \left(1-\lambda^2\right)\lambda^{m+n} & 0 \end{pmatrix}.$$

The eigenvalues of this matrix are $\pm\left(1-\lambda^2\right)\lambda^{m+n}$ (i.e. one positive and one negative eigenvalue). The sum of the negative eigenvalues is then given by

$$\mathcal{N}\left(\hat{\rho}_{\mathrm{TMSV}}\right) = \frac{1}{2}\left(\sum_{m,n=0}^{\infty}\left(1-\lambda^2\right)\lambda^{m+n} - \left(1-\lambda^2\right)\sum_{m=0}^{\infty}\lambda^{2m}\right) = \frac{\lambda}{1-\lambda} \tag{3.43}$$

where on the left hand side we have expressed the sum over m, n with $m \neq n$ as the sum over all m, n minus the sum over all $m = n$. The factor of $\frac{1}{2}$ is to negate double counting.

More useful is the *logarithmic negativity*

$$\mathcal{E}_{\mathcal{N}}(\hat{\rho}_{AB}) = \log(1 + 2\mathcal{N}(\hat{\rho}_{AB})) = \log(\left\|\hat{\rho}_{AB}^{PT}\right\|) \tag{3.44}$$

as it is additive. The logarithm is taken with different bases throughout the literature, and is commonly taken to be base 2 for qubits. When discussing the logarithmic negativity of continuous variable, we shall use the natural log. The logarithmic negativity of the two mode squeezed vacuum can be calculated from Equations (3.43) and (3.44) to be

$$\mathcal{E}_{\mathcal{N}}(\mathrm{TMSV}) = \ln(1+\lambda) - \ln(1-\lambda). \tag{3.45}$$

Plenio [144] showed that the logarithmic negativity also satisfies the strong monotonicity condition (3.25)

$$\mathcal{E}_{\mathcal{N}}\left(\hat{\rho}_{AB}\right) \geq \sum_j p_j \mathcal{E}_{\mathcal{N}}\left(\frac{\hat{A}_j\hat{\rho}_{AB}\hat{A}_j^{\dagger}}{\mathrm{Tr}\left[\hat{A}_j\hat{\rho}_{AB}\hat{A}_j^{\dagger}\right]}\right) \tag{3.46}$$

although $\mathcal{E}_{\mathcal{N}}$ is *not* convex because the logarithm is not convex. The Negativity and Logarithmic Negativity are of course zero on bound entangled states by definition and are upper bounds to the distillable entanglement.

As has been said previously, partial transposition corresponds to partial time reversal in Gaussian states. To see this effect on a Gaussian state, one simply defines

$$\theta_{A|B} = \mathrm{diag}\left(\underbrace{1,-1,1,-1,\cdots,1,-1}_{\text{Alice's modes}},\underbrace{1,1,1,1,\cdots,1,1}_{\text{Bob's modes}}\right) \tag{3.47}$$

if transposing with respect to A and transforms the covariance matrix as $\gamma \to \theta_{A|B}\gamma\theta_{A|B}$. The logarithmic negativity of the Gaussian state $\hat{\rho}_G$ is then given by

$$\mathcal{E}\left(\hat{\rho}_G\right) = -\sum_{j=1}^{N}\log\left[\min\left(1,\tilde{\mu}_j\right)\right] \tag{3.48}$$

where $\{\tilde{\mu}_j\}$ are the symplectic eigenvalues of $\hat{\rho}_G^{T_A}$. This can be shown by symplectically diagonalising $\theta_{A|B}\gamma\theta_{A|B}$ and examining the thermal decomposition (2.111).

Throughout Chapters 4 and 5 we shall make extensive use of the logarithmic negativity to explore entanglement distillation in non-Gaussian states.

Squashed Entanglement

Squashed entanglement was introduced by Christandl and Winter [145] and was inspired by the intrinsic information (see Chapter 6). For a tripartite state $\hat{\rho}_{ABE}$ satisfying $\mathrm{Tr}_E\left[\hat{\rho}_{ABE}\right] = \hat{\rho}_{AB}$ we define the squashed entanglement between subsystems A and B as

$$\mathcal{E}_{sq}\left(\hat{\rho}_{AB}\right) = \inf_{\hat{\rho}_{ABE}}\frac{1}{2}\mathcal{I}_q\left(\hat{\rho}_{AB|E}\right) \tag{3.49}$$

where $\mathcal{I}_q\left(\hat{\rho}_{AB|E}\right) = \mathcal{S}\left(\hat{\rho}_{AE}\right)+\mathcal{S}\left(\hat{\rho}_{BE}\right)-\mathcal{S}\left(\hat{\rho}_{ABE}\right)-\mathcal{S}\left(\hat{\rho}_{E}\right)$ is the conditional mutual information. The squashed entanglement has a lot of delightful properties. It is additive on the tensor product

$$\mathcal{E}_{sq}\left(\hat{\rho}_1 \otimes \hat{\rho}_2\right) = \mathcal{E}_{sq}\left(\hat{\rho}_1\right) + \mathcal{E}_{sq}\left(\hat{\rho}_2\right) \tag{3.50}$$

and superadditive

$$\mathcal{E}_{sq}\left(\hat{\rho}_{AA'BB'}\right) \geq \mathcal{E}_{sq}\left(\hat{\rho}_{AB}\right) + \mathcal{E}_{sq}\left(\hat{\rho}_{A'B'}\right). \tag{3.51}$$

The squashed entanglement is convex and equal to $\mathcal{S}\left(\hat{\rho}_A\right)$ on pure states. It provides a lower bound to $\mathcal{E}_F$ and $\mathcal{E}_C$, an upper bound to $\mathcal{E}_D$, and was proven to be continuous [146]. It is not known whether $\mathcal{E}_{sq}\left(\hat{\rho}_{AB}\right) = 0$ if and only if $\hat{\rho}_{AB}$ is separable. Unfortunately, it is rarely easy to calculate the squashed entanglement.

3.6 Summary of Chapter 3

Quantum entanglement provides a tantalising resource for quantum information processing. In this chapter we have attempted to qualify and quantify entanglement whilst highlighting the aspects relevant to continuous variables. Entanglement distillation has been discussed and will be of paramount importance to the next two chapters.

Chapter 4

Entanglement Distillation in Macroscopic Atomic Ensembles using effective beamsplitter approximation

4.1 Motivation

In the previous chapter, the concept of quantum entanglement was introduced, along with the notion of distillation. In this chapter, a theoretical proposal shall be introduced for putting this knowledge into practice.

In quantum communication, the direct distribution of quantum states is limited by untameable losses in transmission and the no-cloning theorem. For channels such as optical fibres, the probability for both absorption and depolarisation of a photon increases exponentially with the length of a fibre. Accordingly, the number of attempts required to transmit a photon without absorption must increase with the distance between the sender and receiver, and even when a photon arrives, it barely resembles what it was when sent. In short, the delicate superpositions required for quantum information processing prove untenably evanescent when being communicated.

Briegel *et al.* [147] proposed the use of quantum repeaters to overcome this problem, and the idea is remarkably reminiscent of using signal amplifiers in classical communication. Briegel's proposal was as follows. If Alice wanted to send to Bob some quantum information, they would need to enlist the aid of Charlie1, Charlie2,$\cdots$,CharlieN[1]. Then Alice could share a set of weakly entangled pairs with Charlie1. Charlie1 in turn could separately share some weakly entangled pairs with Charlie2 and so on. CharlieN shares some weakly entangled pairs with Bob. Between each couple, the weakly entangled pairs can be distilled into one strongly entangled pair. Importantly, Charlie1 can perform a global measurement on his bipartition of the entangled state he shares with Alice and the entangled state he shares with Charlie2. Charlie2 can do likewise as can his brothers until eventually there exists a long chain running between Alice and Bob.

Briegel *et al.* showed that such an approach would prove advantageous for Alice to communicate with Bob. Evidently, some form of entanglement distillation is required, but importantly, so is quantum memory.

For a review on quantum memory see [148, 11] but for the purposes of this thesis we are only concerned with one setup in particular. Whereas for the transport of quantum signals, light as a medium has no immediate rivals, for the storage of quantum states, one must look to atoms. Atoms provide a good candidate for quantum memory devices due to the relatively long lifetimes of atomic excitations. More interesting is the prospect of using light-atom interactions to transfer quantum information between the two.

Duan *et al.* [149] published a theoretical method for entangling two atomic ensembles. By installing a cloud of identical atoms in a biased magnetic field, and sending in heavily polarised light, it was thought that the quantum state of the light would be written onto the macroscopic spin states of the atoms. If the light then interacted with a second cloud, the macroscopic spin states of the two atomic ensembles would become entangled.

[1] Their parents were not particularly imaginative

This was impressively demonstrated by Julsgaard *et al.* [9] and has been improved upon since. However, to gauge the entanglement between the two ensembles, the fidelity of a teleported pulse was measured. Although above the classical threshold, the entanglement remained weak. This begs the question: can one increase the entanglement between two atomic ensembles?

In Section 4.2 the experimental setup will be described. Thereafter, a procrustean distillation scheme for the ensembles will be put forward, analogous to that of Eisert *et al.* [114] (and illustrated in Figure 3.2). An approximate "beamsplitter" interaction between a mode of light and an atomic ensemble will be described in Section 4.3 and in Section 4.4 this will be used for distillation.

The work of this chapter has been published in **[I]** and **[III]**.

4.2 The system and interactions

The setup of Julsgaard *et al.* involved sending heavily polarised light through atomic ensembles held in magnetic fields. It shall be described in a simplified format below but for a detailed description, see [150].

Consider a pulse of light, or collection of photons, propagating in the $z-$direction. The polarization state is well described by the Stokes Operators

$$\hat{S}_x = \frac{1}{2}\left(\hat{a}_x^\dagger \hat{a}_x - \hat{a}_y^\dagger \hat{a}_y\right) \tag{4.1}$$

$$\hat{S}_y = \frac{1}{2}\left(\hat{a}_x^\dagger \hat{a}_y + \hat{a}_y^\dagger \hat{a}_x\right) \tag{4.2}$$

$$\hat{S}_z = \frac{1}{2i}\left(\hat{a}_x^\dagger \hat{a}_y - \hat{a}_y^\dagger \hat{a}_x\right) \tag{4.3}$$

where $\hat{a}_x$ and $\hat{a}_y$ are annihilation operators for photons polarised in the x and y directions respectively as described in Chapter 2. The Stokes operators, to all intents and purposes, describe the differences between the number of photons polarised in different directions. That is, $\hat{S}_x$ counts the difference between the number of photons polarised in the x direction and the y direction, $\hat{S}_y$ refers to the difference in numbers at polarisations of 45°, and $\hat{S}_z$ looks at circularly polarised photons. The Stokes operators satisfy the commutation relation

$$\left[\hat{S}_k, \hat{S}_l\right] = i\epsilon_{klm}\hat{S}_m \tag{4.4}$$

where ϵ_{klm} is the Levi-Civita symbol. The Stokes operators are dimensionless.

By heavily polarising the light in the x direction, the operator $\hat{S}_x$ can be approximated by its expectation value $\left\langle \hat{S}_x \right\rangle$. That is, we treat $\hat{S}_x$ as essentially classical. Significantly, the commutation relation (4.4) between $\hat{S}_y$ and $\hat{S}_z$ now satisfies

$$\left[\hat{S}_y, \hat{S}_z\right] = i\left\langle \hat{S}_x \right\rangle. \tag{4.5}$$

On examination of the commutation relations for quadrature operators (2.18), the Stokes operators can be used to represent quadrature operators of the light pulse.

$$\hat{X}_L = \frac{\hat{S}_y}{\sqrt{\left\langle \hat{S}_x \right\rangle}}, \quad \hat{P}_L = \frac{\hat{S}_z}{\sqrt{\left\langle \hat{S}_x \right\rangle}}, \tag{4.6}$$

$$\left[\hat{X}_L, \hat{P}_L\right] = i. \tag{4.7}$$

These quadrature operators have expectation values of zero, as a pulse of x polarised photons would be found by measurement to have polarisation in the $\pm 45°$ directions or circular directions with equal probability. It is worth pointing out that if the polarisation of the pulse shifted by a small angle out of alignment with the x axis, then the expectation value of $\hat{S}_y$ would be non-zero, and $\left\langle \hat{X}_L \right\rangle$ would be non-zero. The quadratures themselves would be ill-defined if the angle was

large. With that, we are satisfied that if the number of photons in the pulse was large, then the conjugate position and momentum quadratures would become well-defined.

The choice of atomic gas was Caesium 133. Two macroscopic ensembles of $N_a \approx 10^{12}$ caesium atoms at room temperature and with a ground state degeneracy were placed in a homogeneous magnetic field. There, the caesium atoms were pumped into the $|F = 4, m_F = 4\rangle$ state in the first cell and $|F = 4, m_F = -4\rangle$ in the second cell to form coherent spin states oriented in the $+x$ and $-x$ directions respectively. If the total angular momentum of a single atom (defined by nuclear spin and total electronic angular momentum) is denoted by the vector $\hat{\mathbf{j}}$, then the collective angular momentum $\hat{\mathbf{J}}$, defined as the sum of all the angular momenta of the atoms can be described by its components

$$\hat{J}_x = \frac{N_a}{2} \sum_{m_F} m_F \hat{\sigma}_{m_F, m_F}, \tag{4.8}$$

$$\hat{J}_y = \frac{N_a}{2} \sum_{m_F} C\left(F, m_F\right) \left(\hat{\sigma}_{m_F+1, m_F} + \hat{\sigma}_{m_F, m_F+1}\right), \tag{4.9}$$

$$\hat{J}_z = \frac{N_a}{2i} \sum_{m_F} C\left(F, m_F\right) \left(\hat{\sigma}_{m_F+1, m_F} + \hat{\sigma}_{m_F, m_F+1}\right) \tag{4.10}$$

where $\hat{\sigma}_{\mu,\nu} = \frac{1}{N_a} \sum_{k=1}^{N_a} |\mu\rangle\langle\nu|_k$ and

$$C\left(F, m_F\right) = \sqrt{F(F+1) - m_F(m_F+1)}. \tag{4.11}$$

By pumping the atoms in each ensemble into a coherent spin state, as with the Stokes operators the components of the total angular momentum spin operators $\hat{J}_{x_1}$ and $\hat{J}_{x_2}$ can be replaced by their expectation values. The different directions of the magnetic fields ensure that $\left\langle \hat{J}_{x_1} \right\rangle = -\left\langle \hat{J}_{x_2} \right\rangle$. As with the light mode, the replacement of the $\hat{J}_x$ operators with their expectation values allowed for the definition of "atomic" spin quadratures

$$\hat{X}_A = \frac{\hat{J}_y}{\sqrt{\left\langle \hat{J}_x \right\rangle}}, \quad \hat{P}_A = \frac{\hat{J}_z}{\sqrt{\left\langle \hat{J}_x \right\rangle}}. \tag{4.12}$$

The caesium vapour samples were placed inside paraffin coated cells to ensure that the spin decoherence time when the atoms collided with the walls would be large. By performing the experiment at room temperature, the jostling of the atoms ensured that all atoms travelled through any light pulses applied.

The interaction between light and the atoms was a linearised dipole interaction with far off-resonant detuning,

$$\hat{H} = \sum_j -\mathbf{d}_j \cdot \mathbf{E}(\mathbf{R}_j) \tag{4.13}$$

where $\mathbf{d}_j = -e\mathbf{r}_j$ is the dipole operator for the jth atom and $\mathbf{R}_j$ is the location of the jth atom. If, for example, the polarized light propagates in the z-direction through an atomic ensemble, the linearised interaction Hamiltonian can be written as

$$\hat{H} = a \int_0^T \hat{S}_z(t) \hat{J}_z(t) dt \approx \kappa \hat{P}_L \hat{P}_A \tag{4.14}$$

where a is a coupling constant, renormalised to κ on the RHS. The full derivation of this QND Hamiltonian from the off-resonant dipole interaction can be found in [150]. Physically, the QND Hamiltonian (4.14) causes the polarisation of the light to rotate about the axis of propagation, dependant on the quadrature distribution of the atoms. The back action effect on the atoms is to rotate the macroscopic spin state.

By sending the polarised light through both atomic ensembles and taking a homodyne measurement, it is possible to collapse the atomic states into an entangled "two mode squeezed vacuum" with variance $\Delta^2 \left(\hat{X}_{A_1} - \hat{X}_{A_2}\right) = \Delta^2 \left(\hat{P}_{A_1} + \hat{P}_{A_2}\right) = e^{-2r}$, where r is dependent on κ and given by

$$r = \frac{1}{2} \ln\left[1 + 2\kappa^2\right]. \tag{4.15}$$

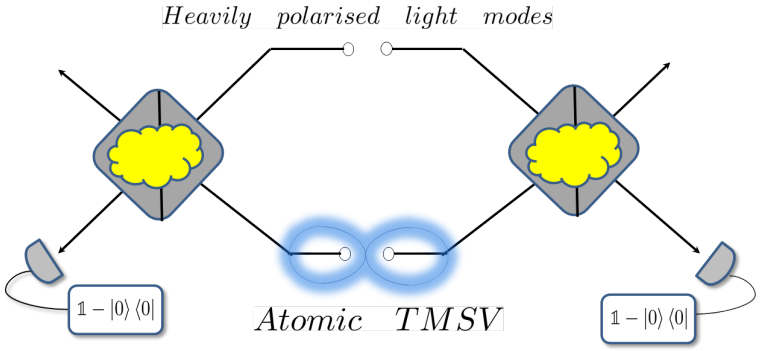

Figure 4.1: The principle behind the entanglement concentration scheme for atomic ensembles. The entanglement concentration protocol works similar to the light scheme [114, 151]. The coherent spin states of two atomic ensembles are initially entangled as a two mode squeezed vacuum (TMSV). Then x-polarised light (number basis $|0\rangle$) interacts with the atoms in a way that approximates the beamsplitter interaction of the light scheme. Following the interaction, non-Gaussian measurements of the number of y-polarised photons are performed. A positive response from both detectors heralds an increase in entanglement between the atomic ensembles.

It is assumed that any displacement of the joint atomic quadrature distributions from the centre in phase space caused by the entanglement process itself is so small as to be negligible.

Julsgaard *et al.* achieved a teleportation fidelity of 55% when testing how entangled they could get their caesium atoms. The quest is on to find a way of increasing the entanglement in the caesium gas samples.

One possible method, considered here, is analogous to the protocol of [114], mentioned in Chapter 3. In that procrustean distillation scheme for light, both arms of a TMSV had photons subtracted to increase their entanglement. Would it be possible to create something similar for atomic ensembles? A beamsplitter-like interaction and non-Gausssian element would be paramount (see Figure 4.1).

4.3 A beamsplitter interaction between light and an atomic ensemble

The first step to consider in Figure 4.1 is how to accomplish a "beamsplitter" interaction between light and the atoms. The solution put forward in this section takes advantage of two passes of the light pulse through the sample.

Whereas a single pass of a light pulse through an atomic ensemble corresponds to the simple QND interaction (4.14), multiple passes open up the possibility for a larger design freedom of the effective Hamiltonian, as for each pass a particular form of the underlying QND interaction can be adjusted (see e.g. [152]). For example, a double pass scheme [153] has been shown to be useful for the generation of polarisation squeezed light by optical Faraday rotation. Another double pass scheme was suggested and thoroughly studied by Muschik *et al.* [154] that also used atomic ensembles and light in order to enact quantum memories. There the light-atom interaction was shown to include two main parts, one equivalent to the beamsplitter interaction, and the other to two-mode squeezing. Depending on the geometry of the set-up, either of the two underlying dynamics could be selected.

Here we take a different approach. The actual double-pass interaction of the light mode with the atomic ensemble is used to approximate a beamsplitter interaction. The light mode is initially prepared in the state $|\psi_l\rangle_L$, which can be written in the quadrature bases

$$|\psi_l(x)\rangle_L = \int_{-\infty}^{\infty} \mathrm{d}x_l \psi_l(x_l) |x_l\rangle_L \tag{4.16}$$

$$|\tilde{\psi}_l(p)\rangle_L = \int_{-\infty}^{\infty} \mathrm{d}p_l \tilde{\psi}(p_l) |p_l\rangle_L \tag{4.17}$$

with the eigenbases $|x_l\rangle_L$ and $|p_l\rangle_L$ as the respective eigenvectors of the quadrature operators $\hat{X}_L$ and $\hat{P}_L$ defined in Equation (4.6). Similarly the atomic ensemble can be described by the distributions $\psi_a(x_a)$ and $\tilde{\psi}_a(p_a)$.

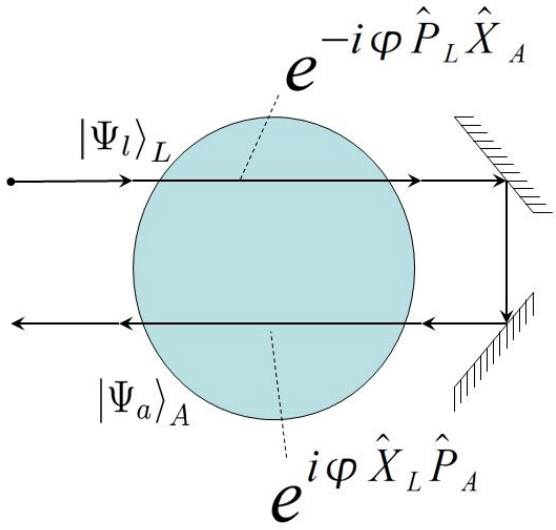

Figure 4.2: To approximate a beamsplitter type interaction between the atomic ensemble and a field mode requires one QND interaction of $e^{-i\varphi \hat{P}_L \hat{X}_A}$ followed by another different QND interaction of $e^{i\varphi \hat{X}_L \hat{P}_A}$. The coupling phase constant ϕ should be weak compared to the initial entangling coupling strength. Taken from **[I]**.

In this configuration the light mode first interacts via the QND interaction $\hat{H}_1 = \phi \hat{P}_L \hat{X}_A$ (see Figure 4.2). The tunable parameter ϕ, dependent on the detuning and other parameters, is assumed to be weaker than the coupling κ initially used to entangle the atomic ensembles. The emerging light field is then reflected back into the atomic ensembles for a further QND interaction $\hat{H}_2 = -\phi \hat{X}_L \hat{P}_A$. The second QND interaction can be implemented by performing local operations on the light field and atomic ensembles.

The free Hamiltonians of the field and ensemble are assumed to be vanishing here for clarity so that the results are unique up to a suitable unitary transformation. Each QND interaction generates an associated evolution operator

$$\hat{U}_1 = e^{-i\phi \hat{P}_L \hat{X}_A}, \tag{4.18}$$

$$\hat{U}_2 = e^{i\phi \hat{X}_L \hat{P}_A}, \tag{4.19}$$

which takes the initial input state $|\psi_I\rangle_{LA} = |\psi_l\rangle_L |\psi_a\rangle_A$ and transforms it to

$$|\psi_I\rangle_{LA} \to e^{i\phi \hat{X}_L \hat{P}_A} e^{-i\phi \hat{P}_L \hat{X}_L} |\psi_l\rangle_L |\psi_a\rangle_A. \tag{4.20}$$

In the position basis it is clear that the two interactions have the effect

$$\hat{U}_2 \hat{U}_1 |x_l\rangle_L |x_a\rangle_A = |x_l + \phi x_a\rangle_L |x_a - \phi(x_l + x_a)\rangle_A. \tag{4.21}$$

At this stage a number of approximations are introduced. Firstly, the interaction strength ϕ is assumed to be small. This is in direct contrast to the initial requirement for entanglement that κ be strong, and is the primary reason why the letter ϕ has been used in place of κ. The interaction strength ϕ is dependent on a number of tunable parameters such as the cross-sectional area of the laser beam and the detuning from the transition frequencies of the caesium atoms and so this poses no problems. In fact, it is far harder to make the interaction strong.

With this approximation, we can make the further approximations that $x_l \approx \sqrt{1-\phi^2} x_l$ and $(1-\phi^2) x_a \approx \sqrt{1-\phi^2} x_a$. However, the validity of these approximations contains further constraints. The approximations are only good when $\phi << 1$ and x_l, x_a are small. However, x_l and x_a can assume values over the entire real line, making this approximation worthless unless we restrict to input states with quadrature distributions $\psi_l(x_l)$ and $\psi_a(x_a)$ that are large in the regions where the approximations hold well and negligible otherwise.

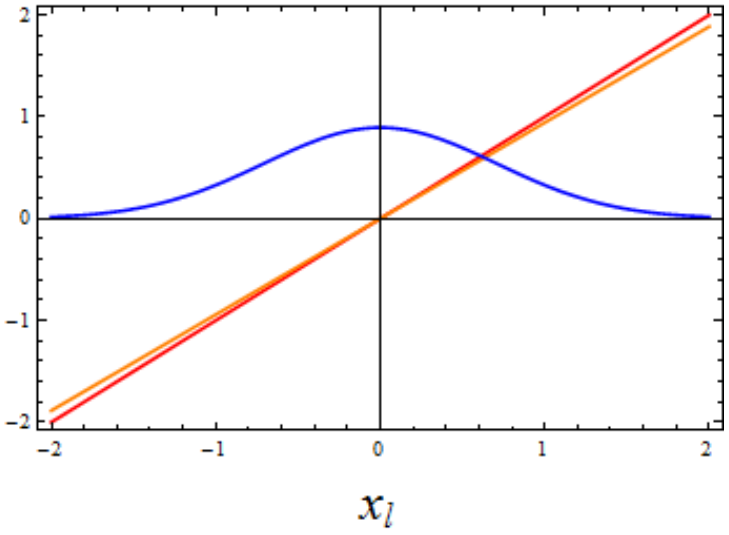

Figure 4.3: Graphical representation of the joint approximation required to allow multiple QND passes to behave like a beamsplitter for the example of x_l. The quadrature distribution $\psi_l(x_l)$ (blue) needs to be small where the approximation $x_l = \sqrt{1-\phi^2}x_l$ (red, orange respectively) is not a good approximation. Therefore there are restrictions on both the coupling strength ϕ and on the wavefunctions of the light and atoms for which the approximation would be applicable. A similar restriction exists for the momentum quadrature of the light mode.

Narrow Gaussian states that are centred in phase space and peak around the origin are good for this approximation, and consequently the squeezed atomic spin distributions of the ensembles are well suited. The joint constraint on the input states and the coupling (graphically illustrated in Figure 4.3) is reminiscent of the approximations in the weak measurement formalism of Aharanov *et al.* [155].

Assuming that the conditions are satisfied, the final output of the interaction $\hat{U}_2\hat{U}_1$ is given by

$$\begin{aligned} |\Psi_F\rangle &= \int_{-\infty}^{\infty} \mathrm{d}x_l \mathrm{d}x_a \psi_l(x_l)\,\psi_a(x_a)\,|x_l+\phi x_a\rangle_L \left|\left(1-\phi^2\right)x_a-\phi x_l\right\rangle_A \\ &\approx \int_{-\infty}^{\infty} \mathrm{d}x_l \mathrm{d}x_a \psi_l(x_l)\,\psi_a(x_a) \left|\sqrt{1-\phi^2}x_l+\phi x_a\right\rangle_L \left|\sqrt{1-\phi^2}x_a-\phi x_l\right\rangle_A . \end{aligned}$$

These reasonable approximations, when satisfied, cause the double pass of the heavily polarised light mode through a caesium gas sample to mimic a beamsplitter operation. For this to behave like a proper beamsplitter, of course, similar conditions apply to the conjugate momenta distributions of the light and atoms, namely $\left(1-\phi^2\right)p_l \approx \sqrt{1-\phi^2}p_l$ and $p_a \approx \sqrt{1-\phi^2}p_a$.

To examine how well these approximations hold for different states, the fidelity of the output state $|\Psi_F\rangle_{LA}$ with the output state of a true beamsplitter interaction $|\Psi_F\rangle_{BS}$ can be considered. This is the overlap of the Wigner function for the idealised case with the Wigner function of the output of the approximation (see Equation (2.73)). In all cases, the atomic state is assumed to be a centred Gaussian - a very reasonable assumption based on the methods of Julsgaard *et al.* [9, 10].

Figure 4.4 shows how the approximation holds up when the light is assumed to be in a "vacuum" state[2]. As expected the approximation holds well. Figure 4.5 shows that the approximation does not hold when the light is strongly squeezed, except when ϕ is very small. This is intuitively correct - if the light is squeezed in position, then the momentum distribution is antisqueezed. Consequently, although the approximation $\sqrt{1-\phi^2}x_l \approx x_l$ holds well, the conjugate momentum distribution for the light mode has support where $\left(1-\phi^2\right)p_l \approx \sqrt{1-\phi^2}p_l$ does not hold well.

[2]The term "vacuum" here means simply that no y-polarised photons exist in the mode, as the photons have to be x-polarised regardless in order for $\hat{X}_L$ and $\hat{P}_L$ to be well defined.

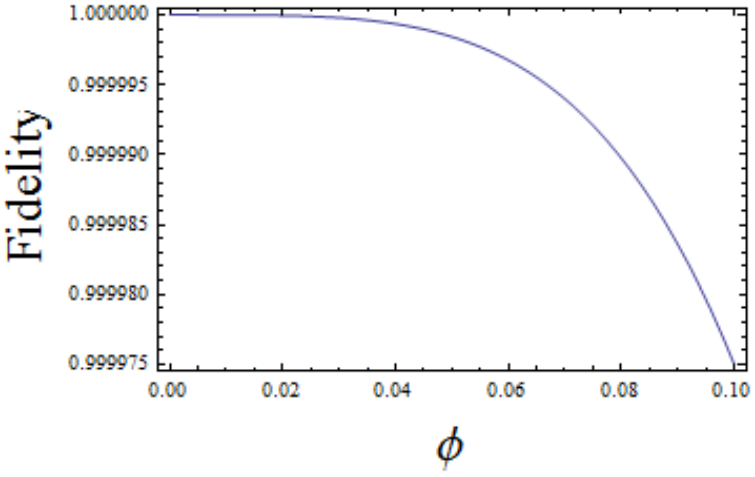

Figure 4.4: The fidelity of the system on the interval $0 \leq \phi \leq 0.1$ when only centred Gaussian modes are used in the interaction. The fidelity stays at almost unity when the interaction strength is low. Taken from **[I]**.

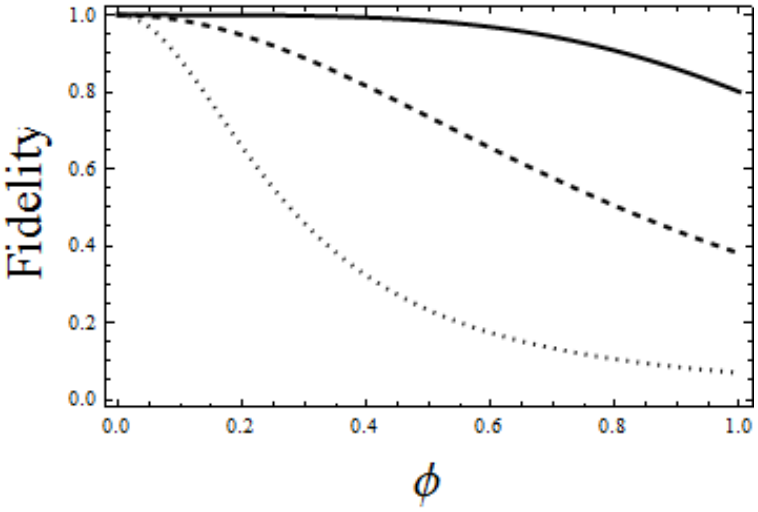

Figure 4.5: Fidelity is plotted against ϕ for squeezed light interacting with the atoms with squeezing parameter $r = 0$ (solid), $r = 1$ (dashed) and $r = 2$ (dotted). Taken from **[I]**.

For coherent and coherent squeezed states, the fidelity drops down substantially as the displacement in phase space increases. This, too, is to be expected. This behaviour does not prove problematic for the light and atoms described above, as the very definition of the quadratures relies on the distributions being approximately centred at the origin in phase space, by virtue of the physical limits of the system. The concept of "displacing" the light or atom phase space quadratures defined in the previous section seems absurd.

A successful approximate beamsplitter interaction between a light mode and atomic ensemble has been characterised. We shall now proceed to discuss the remainder of the concept shown in Figure 4.1 - non-Gaussian measurements and distillation.

4.4 Entanglement distillation of two atomic ensembles

With the "beamsplitter" interaction between a light mode and an atomic ensemble now described, it is possible to consider the distillation as follows. The caesium gas samples of Julsgaard's experiment [9] were successfully entangled as an atomic "two mode squeezed vacuum",

written in the number basis as

$$|TMSV\rangle = \sqrt{1-\lambda^2}\sum_{n=0}^{\infty}\lambda^n|n\rangle_1|n\rangle_2 \tag{4.22}$$

where n is the photon number and $\lambda = \tanh(r)$ quantifies the reduction (squeezing) of the quantum uncertainty of the global state, with r as in Equation (4.15). For ease of calculation, the atomic state shall be represented as in Equation (4.22). The number basis does have a true meaning here. On consideration of an "annihilation" operator for the atoms $\hat{a}_A = \frac{1}{\sqrt{2}}\left(\hat{X}_A + i\hat{P}_A\right)$, then the number n represents (up to normalisation) the number of atoms in the upper excited spin state of the basis of the $\hat{J}_x$ operator. That is, $n = 1$ corresponds to the superposition of all possible combinations of atomic spins of the atoms in the ensemble for which a single atom is excited.

A light mode, prepared as previously, can be considered as a vacuum state in phase space. That is, there are no photons polarised in the y direction despite a steady base stream of linearly x-polarised photons, so that $\left\langle \hat{S}_y \right\rangle = \left\langle \hat{S}_z \right\rangle = 0$. The interpretation of the number basis for the light mode is easier to comprehend. By polarising the light heavily in the x direction, the assumption is made that $\hat{a}_x \to \langle \hat{a}_x \rangle$ and $\hat{a}_x^\dagger \to \langle \hat{a}_x^\dagger \rangle$ and $\langle \hat{a}_x \rangle = \langle \hat{a}_x^\dagger \rangle = A_x$. The Stokes operators can then be written as

$$\left\langle \hat{S}_x \right\rangle \approx \frac{A_x^2}{2} \tag{4.23}$$

$$\hat{S}_y \approx \frac{A_x}{2}\left(\hat{a}_y + \hat{a}_y^\dagger\right) \tag{4.24}$$

$$\hat{S}_z \approx \frac{A_x}{2i}\left(\hat{a}_y - \hat{a}_y^\dagger\right) \tag{4.25}$$

and with this in mind, an annihilation operator for the light mode $\hat{a}_L$ can be defined as

$$\hat{a}_L = \frac{1}{\sqrt{2}}\left(\hat{X}_L + i\hat{P}_L\right) = \frac{1}{\sqrt{2}}\frac{\hat{S}_y + i\hat{S}_z}{\sqrt{\left\langle \hat{S}_x \right\rangle}} = \hat{a}_y. \tag{4.26}$$

The number operator $\hat{n}_L = \hat{a}_L^\dagger \hat{a}_L$ simply counts the number of photons polarised in the y direction, initially $\langle \hat{n}_L \rangle = 0$. The initial state of the light and atoms together is given by

$$|\Psi_I\rangle_{LA} = \sqrt{1-\lambda^2}\sum_{n=0}^{\infty}\lambda^n|n\rangle_1|n\rangle_2|0\rangle_3|0\rangle_4 \tag{4.27}$$

where the subscripts 1 and 2 denote the first and second atomic modes respectively, and 3 and 4 denote the light vacuum modes. The light modes 3 and 4 are sent through the atomic ensembles 1 and 2 respectively in the double pass scenario described in the previous section. This double pass scheme then performs the role of a beamsplitter transformation and is treated accordingly in what follows (see Chapter 2). The quantum state after the beamsplitter interaction can be described by

$$\begin{aligned}|\Psi_F\rangle_{LA} = \quad & \textstyle\sum_{n=0}^{\infty}\sqrt{1-\lambda^2}\lambda^n\sum_{k_1,k_2=0}^{n}\sqrt{\binom{n}{k_1}\binom{n}{k_2}}\phi^{k_1+k_2}\left(1-\phi^2\right)^{2n-k_1-k_2} \\ & \times|n-k_1\rangle_1|n-k_2\rangle_2|k_1\rangle_3|k_2\rangle_4\end{aligned} \tag{4.28}$$

where ϕ represents the strength of the interaction.

The outgoing light modes must then be passed through a polarised filter to remove the base stream of x polarised photons, and allowing only photons whose polarisations have been rotated by the interaction until y polarised to proceed (Figure 4.6). A detector must then register whether y polarised photons are present.

The likelihood of completing a double-pass scheme and rotating the polarisation of a single photon to be aligned with the y axis is negligible. To try to rectify this somewhat, it is noticed that modern day detectors are unable to distinguish the number of photons present. It is instead assumed that the detectors used can, to a high degree of efficiency, detect simply the presence

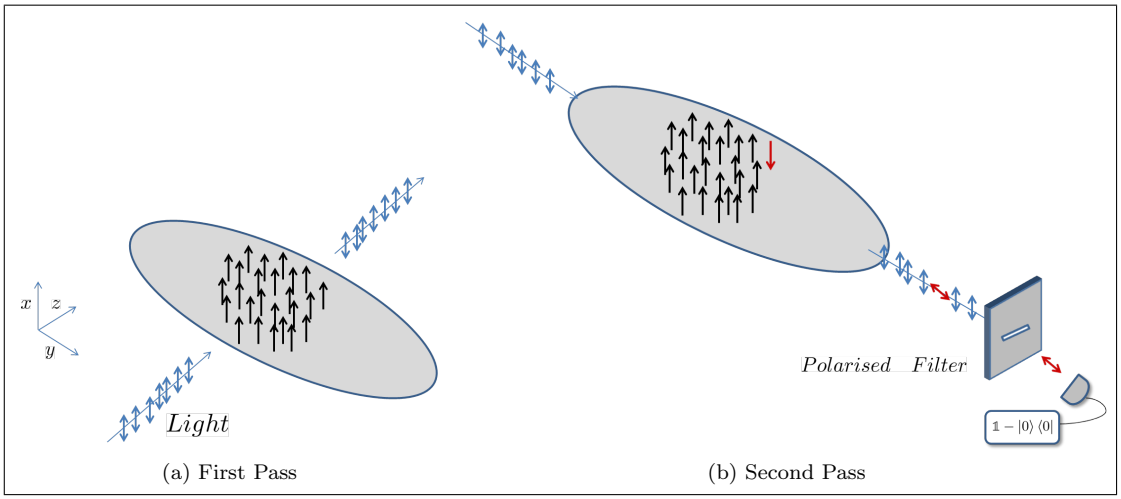

(a) First Pass (b) Second Pass

Figure 4.6: The light mode is initially strongly polarised in the x-direction. By interacting twice with the spin-polarised atomic ensemble, one or more of the spins is probabilisticalloy flipped. This is heralded by the detection of y-polarised photons by the photodetector.

of one or more photons (on-off detectors). Such a measurement can be performed, for example, by avalanche photodiodes. The state in this case becomes

$$|\Psi_A\rangle_{\text{out}} = \sqrt{\frac{1-\lambda^2}{S}} \sum_{n=0}^{\infty} \sum_{u,v=1}^{\infty} \lambda^n \sqrt{\binom{n}{u}\binom{n}{v}} \times \phi^{u+v} \left(1-\phi^2\right)^{2n-u-v} |n-u\rangle_1 |n-v\rangle_2 \tag{4.29}$$

where S is the probability of getting an affirmative measurement at both detectors

$$S = \frac{1-\lambda^2}{1-\lambda^2\left(\phi^2+(1-\phi^2)^2\right)^2} - \frac{2\left(1-\lambda^2\right)}{1-\lambda^2\left(1-\phi^2\right)^2\left(\phi^2+(1-\phi^2)^2\right)} + \frac{1-\lambda^2}{1-\lambda^2\left(1-\phi^2\right)^4}. \tag{4.30}$$

The amount of entanglement in the two ensembles is quantified by the negativity and logarithmic negativity of the state, defined in Chapter 3 and rewritten here.

$$\mathcal{N}(\hat{\rho}_{AB}) = \tfrac{1}{2}\text{Tr}\left(\sqrt{(\hat{\rho}_{AB}^{T_A})^2} - \hat{\rho}_{AB}^{T_A}\right) = \frac{\left\|\hat{\rho}_{AB}^{T_A}\right\|-1}{2}$$
$$\mathcal{E}_{\mathcal{N}}(\hat{\rho}_{AB}) = \log(1+2\mathcal{N}(\hat{\rho}_{AB})) = \log(\left\|\hat{\rho}_{AB}^{PT}\right\|) \tag{4.31}$$

For projections onto an exact photon state (i.e. single photon detection), the negativity and logarithmic negativity can be calculated analytically. However, for on-off type measurements the entanglement measures must be calculated numerically due to the infinite sums over u and v. Fortunately these sums appear to converge quickly and so a reliable truncation point can be set.

The calculation of the negativity and logarithmic negativity for the mixed state resulting from on-off detections can be carried out in a similar manner to Kitagawa *et al.* [116]. Firstly, the density matrix of the state is expanded as

$$|\psi_A\rangle_{\text{out}}\langle\psi_A| = \sum_{a,b,c,d=0}^{\infty} \rho_{abcd} |a\rangle_1\langle c| \otimes |b\rangle_2\langle d|, \tag{4.32}$$

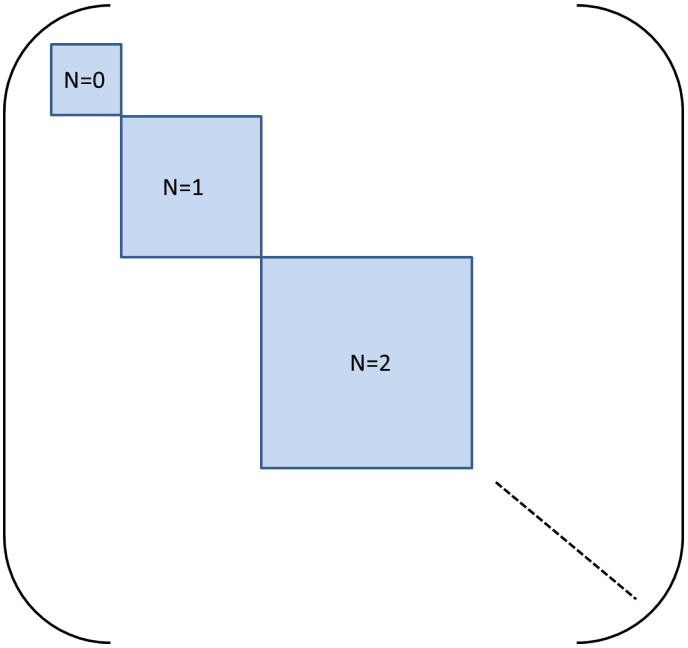

Figure 4.7: The density matrix elements of the partially transposed state can be arranged into block diagonal form where each block is of dimensions $(N+1)\times(N+1)$, for $N = 0 \cdots N_{\max}$. For details, see text.

where

$$\begin{aligned}\rho_{abcd} &= \left({}_1\langle a|_2\langle b|\right)|\Psi_A\rangle_{\text{out}}\langle\Psi_A|\left(|c\rangle_1|d\rangle_2\right)\\ &= \frac{(1-\lambda^2)}{S}\sum_{u,v=1}^{\infty}\lambda^{a+u}\lambda^{c+u}\\ &\quad\times\sqrt{\binom{a+u}{u}\binom{a+u}{v}\binom{c+u}{u}\binom{c+u}{v}}\\ &\quad\times(\phi)^{2(u+v)}\left(1-\phi^2\right)^{2(a+c+u-v)}\delta_{a-b,v-u}\delta_{c-d,v-u}.\end{aligned} \tag{4.33}$$

The partial transpose of this state is given by

$$\left(|\Psi_A\rangle_{\text{out}}\langle\Psi_A|\right)^{PT} = \sum_{a,b,c,d}^{\infty}\rho_{adcb}|a\rangle_1\langle c|\otimes|b\rangle_2\langle d| \tag{4.34}$$

and the elements are zero unless the total number of y polarised photons detected in both modes $N = a+b = c+d$ is non-zero. This follows logically from the delta functions in ρ_{adcb}.

Operator (4.34) can be put into block diagonal form (Figure 4.7). For each value of N, the corresponding elements of ρ_{adcb} can be harvested and put into an $(N+1)\times(N+1)$ block matrix $\left(|\Psi_A\rangle_{\text{out}}\langle\Psi_A|\right)^{PT}_{(N)}$. With this, the matrix $\left(|\Psi_A\rangle_{\text{out}}\langle\Psi_A|\right)^{PT}$ can be written as the direct sum of all the block matrices.

$$\left(|\Psi_A\rangle_{\text{out}}\langle\Psi_A|\right)^{PT} = \oplus_{N=0}^{\infty}\left(|\Psi_A\rangle_{\text{out}}\langle\Psi_A|\right)^{PT}(N) \tag{4.35}$$

The negativity of the partially transposed state is then computed by numerically diagonalising each block matrix individually, and adding up the absolute value of all negative eigenvalues. A cut-off, $N_{\max}$, is introduced that is large enough compared with the mean number of excited spins. There is, of course, a trade-off between $N_{\max}$ and the length of time required to perform the calculation. For the purpose of this calculation, a value of $N_{\max} = 100$ was used as this was deemed sufficient for the logarithmic negativity (calculated from the negativity) to converge to

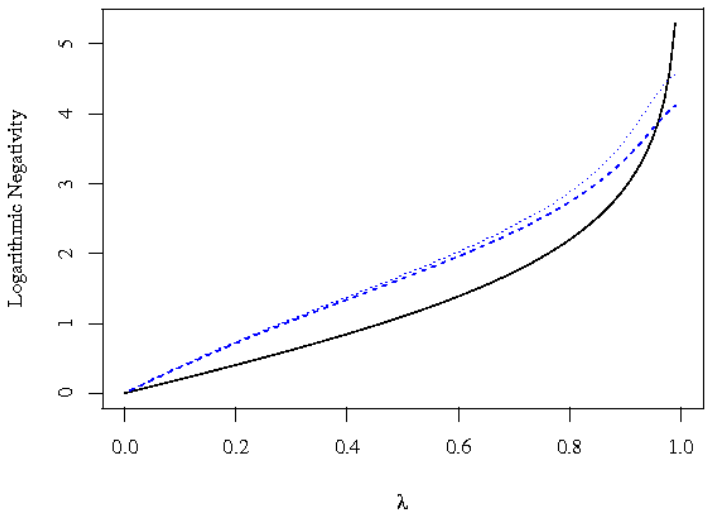

Figure 4.8: A plot of the logarithmic negativity against λ for (i) standard two mode squeezed state (solid) and for the output of the photon subtracted scheme for the beamsplitter like interaction between light and atomic ensemble when (ii) $\phi = 0.1$ (dashed) and (iii) $\phi = 0.01$ (dotted). See text for discussion. Taken from **[III]**.

approximately seven significant figures. To increase $N_{\max}$ beyond this was not beneficial. The results can be seen in Figure 4.8

The entanglement between the two atomic ensembles is increased for all values of initial squeezing except for very high λ. The increase in the logarithmic negativity is not very large but comparable with the traditional protocol, in which light is used in place of atomic ensembles. As can be seen, a trade-off is required between the interaction strength and the probability of success (Figure 4.9). As the interaction strength increases, so does the probability of success, but the validity of the beamsplitter approximation decreases. It is worth noting, however, that the beamsplitter approximation has a very high fidelity of approximately 0.99 even when the interaction strength is as high as $\phi \approx 0.35$.

As λ approaches approximately 0.95, the concentration procedure ceases to bring further benefit. This may be misleading, however, as the numerical precision is less when λ is very high due to lack of convergence. It is conjectured that for all λ, the entanglement would increase.

4.5 Modelling Detector Inefficiencies

The largest contribution to loss in the photon subtraction scheme for light modes comes from detector inefficiencies, in particular the detector erroneously not sensing the presence of a photon. For the atomic ensemble scheme, the efficiency of the detectors will also play a crucial role. The detectors here have a reduced number of photons to detect due to the polarisation filter used to hold off the base stream of x polarised photons. The inefficiency can be modelled as an ideal detector behind a beamsplitter of transmittivity η. The light mode is combined with a vacuum on the beamsplitter and the vacuum is traced out before the measurement is performed. For a Fock state combining with a vacuum mode, this amounts to the transformation

$$|k,0\rangle \rightarrow \sum_{s=0}^{k} \sqrt{\binom{k}{s}} (\sqrt{\eta})^s \left(\sqrt{1-\eta}\right)^{k-s} |s, k-s\rangle. \tag{4.36}$$

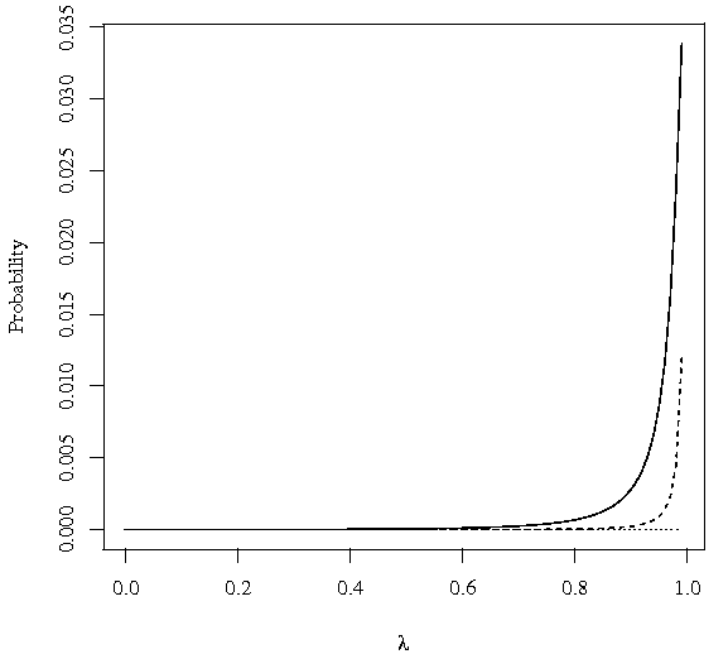

Figure 4.9: Probability of success against λ for (i) interaction strength $\phi = 0.1$ (solid) (ii) $\phi = 0.05$ (dashed) and (iii) $\phi = 0.01$ (dotted). The probabilities of success are small but comparable with the light scheme. Taken from **[III]**.

Directly before detection is performed, the density matrix is given by

$$\begin{aligned}\rho = &\left(1-\lambda^2\right)\sum_{m,n=0}^{\infty}\lambda^{m+n}\sum_{k_1,k_2=0}^{n}\sum_{j_1,j_2=0}^{m}\sqrt{\binom{n}{k_1}\binom{m}{j_1}\binom{n}{k_2}\binom{m}{j_2}}\\ &\times\phi^{j_1+k_1+j_2+k_2}\left(1-\phi^2\right)^{2n+2m-j_1-k_1-j_2-k_2}\sum_{s=0}^{k_1}\sum_{t=0}^{j_1}\sum_{y=0}^{k_2}\sum_{z=0}^{j_2}N_{s,y,t,z}^{k_1,k_2,j_1,j_2}\\ &\times|n-k_1\rangle_1\langle m-j_1|\otimes|n-k_2\rangle_2\langle m-j_2|\otimes|s\rangle_3\langle t|\otimes|y\rangle_4\langle z| \end{aligned} \tag{4.37}$$

where

$$\begin{aligned}N_{s,y,t,z}^{k_1,k_2,j_1,j_2} =&\sqrt{\binom{k_1}{s}\binom{j_1}{t}\binom{k_2}{y}\binom{j_2}{z}}\left(\sqrt{1-\nu^2}\right)^{j_1+k_1+j_2+k_2-s-t-y-z}\\ &\times\nu^{s+t+y+z}\delta_{k_1-s,j_1-t}\delta_{k_2-y,j_2-z}.\end{aligned} \tag{4.38}$$

Light modes 3 and 4 are subsequently measured for the presence or absence of photons using the operator $(\mathbb{1}-|0\rangle\langle 0|)$ and traced out. The density matrix of the two remaining atomic modes can then be described by

$$\begin{aligned}\rho_{\text{out},\eta} = &\sum_{m,n=0}^{\infty}\left(1-\lambda^2\right)\lambda^{m+n}\sum_{k_1,k_2=0}^{\min(m,n)}\sqrt{\binom{n}{k_1}\binom{m}{k_1}\binom{n}{k_2}\binom{m}{k_2}}\phi^{2(k_1+k_2)}\\ &\times\left(1-\phi^2\right)^{2n+2m-2k_1-2j_1}\left[1-(1-\eta)^{k_1}-(1-\eta)^{k_2}+(1-\eta)^{k_1+k_2}\right]\\ &\times|n-k_1\rangle_1\langle m-k_1|\otimes|n-k_2\rangle_2\langle m-k_2|\end{aligned} \tag{4.39}$$

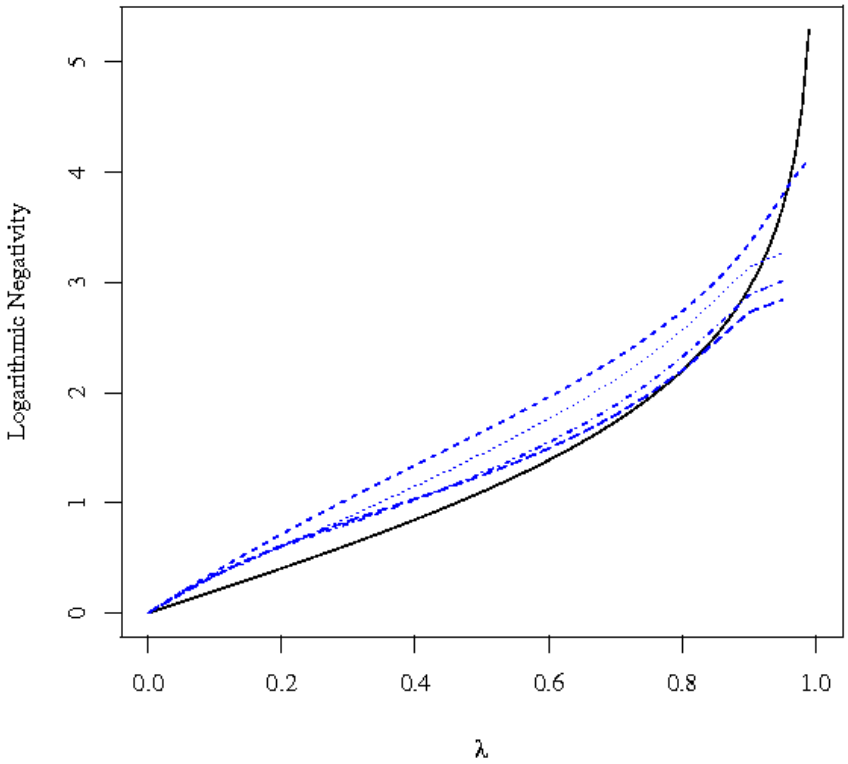

Figure 4.10: Dependence of the logarithmic negativity on the efficiency of the detectors. The solid line depicts the initial two mode squeezed state of the entangled atomic ensembles. Then the logarithmic negativity is shown for $\eta = 1$ (dashed line), $\eta = 0.8$ (dotted line), $\eta = 0.5$ (dash-dot), and $\eta = 0.2$ (long dash). The interaction strength is $\phi = 0.1$. Taken from **[III]**.

and the probability of success, taking into account detector losses, is given by

$$S_\eta = \frac{1-\lambda^2}{1-\lambda^2\left[\phi^2+(1-\phi^2)^2\right]^2} + \frac{1-\lambda^2}{1-\lambda^2\left[\phi^2(1-\eta)+(1-\phi^2)^2\right]^2} - \frac{2\left(1-\lambda^2\right)}{1-\lambda^2\left[\phi^2(1-\eta)+(1-\phi^2)^2\right]\left[\phi^2+(1-\phi^2)^2\right]}. \tag{4.40}$$

The effect that detector inefficiency has on the logarithmic negativity of the atomic ensembles can be shown in Figure 4.10.

As expected, the entanglement concentration becomes less pronounced for low detector efficiency. The positive message is that even for efficiencies as low as $\eta = 0.2$ there is still a range of λ values for which entanglement is increased (although the probability of success is quite low in this case). This range is experimentally accessible and so it is good news that the entanglement concentration protocol is more robust against imperfections.

4.6 Summary of Chapter 4

The tools and language of quantum optical entanglement distillation have been applied to a collection of entangled atomic gas samples. Similar to the scheme of Eisert *et al.* [114], in the attempt made in this chapter, on-off detector clicks herald the successful "photon subtraction"

(spin flip in the atomic ensembles) and thus successful entanglement distillation. The significant ingredients for this recipe were

- a double-pass QND interaction between heavily polarised light modes and the atomic ensembles.
- a non-Gaussian element in the form of a photodetector.

The obvious question to ask is this: why use a double pass? Would a single pass suffice? Is it really necessary to use an approximation? These questions shall be answered in Chapter 5.

Chapter 5

Entanglement Distillation with QND Hamiltonians

5.1 Motivation

As has been shown in the previous chapter, it is possible to distil entanglement in two atomic ensembles using two QND interactions to mimic a beamsplitter interaction followed by a non-Gaussian measurement. However, it would prove rather difficult experimentally to fire a pulse through an atomic ensemble and reflect it back, suitably phase-shifted, for a second interaction, all without losing coherence or significantly altering the base polarisation of the photons, and thereby leading to the light quadratures becoming ill-defined. Not to mention the fact that in the experimental set-up of Julsgaard *et al.* [9] the length of the pulse is long and so the laboratory would have to be a shining example of ergonomic design in order to perform the double pass.

Although the "beamsplitter" approximation showed that QND interactions do indeed prove useful, it would be far more desirable (and easier on the poor experimentalists) if a single pass QND interaction could be used. It would be of great benefit to show that a QND interaction could be used for entanglement distillation as it would increase drastically the amount of options open to choose from. With the rich history of QND interactions in, for example, the search for gravity waves, it would be most intriguing to see what other uses they could be put to. The success of the beamsplitter approximation approach certainly justifies an examination of this. However, in the previous chapter, the beamsplitter approximation was implicitly used to calculate the logarithmic negativity of the output state in the Fock basis, desirable from a programming perspective. The QND interaction's effect on the Fock basis is far harder to work with than a beamsplitter interaction. Moreover, direct calculation in the Fock basis for a given distillation scheme is cumbersome and unwieldy from a theoretical physicist's take on life, and is not easy to adapt to changes (i.e. to quickly see the effects of further interactions).

In what follows, an elegant method is presented for directly calculating the density matrix elements of a mixed state resulting from a Gaussian state undergoing an entanglement distillation process in the number basis. This approach is not groundbreaking, but does knit together the threads that have appeared in various works to efficiently calculate density matrix elements. It is also incredibly versatile, making additional interactions as simple as multiplying small, finite matrices. In short, we amalgamate ideas on using the well-known formalism of Gaussian states to represent non-Gaussian states [156, 157] and calculate density matrix elements using multivariate Hermite polynomials [158, 159, 160].

Two protocols are presented here as examples and, inspired by the problem put forward in the previous chapter, QND interactions are used. Although in this chapter, protocols are not bound to any particular physical system, (although, indeed, the word "photon" is often used to describe a number state), the observant reader will notice that the first protocol could easily describe the elements of the previous chapter, but with a single QND pass.

In Section 5.2 the first example scheme will be presented; a procrustean entanglement concentration protocol replacing the conventional beamsplitter interaction with the QND interaction between a Gaussian ancilla and a Gaussian entangled state. In Section 5.3 an alternative scheme is put forward, where an auxiliary mode is non-Gaussian and a post-measurement is Gaussian. In both cases the logarithmic negativity of the state is shown to increase, demonstrating a

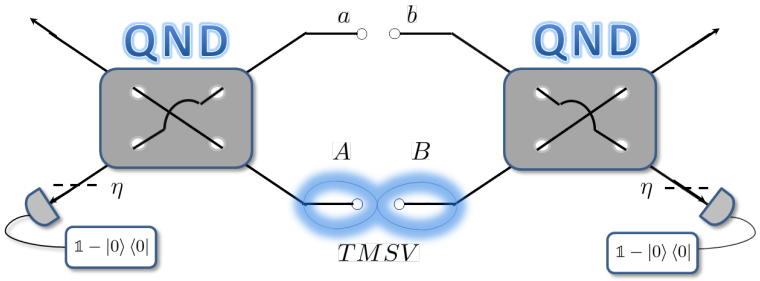

Figure 5.1: The two modes of a two mode squeezed vacuum interact with two vacuum modes which are subsequently measured for the presence or absence of photons. If successful, the entanglement of the two mode squeezed state increases. Taken from [**V**].

successful continuous variable entanglement distillation based on the QND Hamiltonian.

5.2 Protocol I

The first entanglement concentration scheme is depicted in Figure 5.1. A two mode squeezed vacuum interacts with two auxiliary modes via QND interaction. The ancillary modes are subsequently detected for the presence or absence of photons. If successful, detector clicks herald entanglement concentration and the two mode squeezed vacuum has transformed into a non-Gaussian mixed state possessing a higher entanglement content.

The key to calculating the density matrix elements of the mixed state output is to notice that all the quantum states involved are initially Gaussian and the QND interaction is a Gaussian map. Indeed, the protocol can, up to and including the QND operation between TMSV and ancillae, be dealt with on the level of covariance matrices and symplectic transformations. The TMSV (modes A and B) can initially be described by Equation (2.106) and the vacuum modes (a and b) by $\gamma_{\text{vac}} = \mathbb{1}$. The initial covariance matrix of all four modes before any interaction is simply given by

$$\gamma_{\text{init}} = \gamma_{AB}^{\text{TMSV}} \oplus \gamma_{\text{vac},a} \oplus \gamma_{\text{vac},b}. \tag{5.1}$$

Mode A interacts with mode a and mode B interacts with mode b via QND interaction (see Equation (2.109)). As an example we consider interactions of the form $\hat{H}_{\text{int}} = \kappa \hat{X}_A \hat{P}_a$ and $\hat{H}_{\text{int}} = \kappa \hat{X}_B \hat{P}_b$. Throughout this chapter, the scheme is always symmetric with all operations on mode A being the same as on mode B although there is no requirement that this be the case. Due to this symmetry, we will simply refer to a $\kappa \hat{X}\hat{P}$ interaction (without subscripts) implying that the interaction happens to both arms of the TMSV. The symplectic operation $S_{\text{QND}}^{(\kappa \hat{X}\hat{P})}$, written in Equation (2.109), must be expanded to incorporate all 4 modes, i.e. rewritten as

$$S_{\text{QND}}^{(\kappa \hat{X}\hat{P})} = \begin{pmatrix} 1 & 0 & 0 & 0 & 0 & 0 & 0 & 0 \\ 0 & 1 & 0 & 0 & 0 & -\kappa & 0 & 0 \\ 0 & 0 & 1 & 0 & 0 & 0 & 0 & 0 \\ 0 & 0 & 0 & 1 & 0 & 0 & 0 & -\kappa \\ \kappa & 0 & 0 & 0 & 1 & 0 & 0 & 0 \\ 0 & 0 & 0 & 0 & 0 & 1 & 0 & 0 \\ 0 & 0 & \kappa & 0 & 0 & 0 & 1 & 0 \\ 0 & 0 & 0 & 0 & 0 & 0 & 0 & 1 \end{pmatrix} \tag{5.2}$$

and applied as $S_{\text{QND}}^{(\kappa \hat{X}\hat{P})} \gamma_{\text{init}} S_{\text{QND}}^{(\kappa \hat{X}\hat{P})T}$ in the usual way. Conceivably, other schemes could be considered simply by further multiplying symplectic matrices, e.g. double passes.

With this, the interaction is performed. The non-Gaussian measurement can be considered as a perfect detector behind a beamsplitter of transmittance η (see e.g. [161, 114]). Such an operation is a simple Gaussian channel, characterised by the symplectic transformation $S_{\text{loss}}(\eta) = \sqrt{\eta}\mathbb{1}$ and the addition of $(1-\eta)\mathbb{1}$ [162]. Immediately prior to the measurement, the covariance matrix of the 4 mode state is given by

$$\gamma = (\mathbb{1}_{AB} \oplus S_{\text{loss},ab})\, S_{\text{QND}}^{(\kappa \hat{X}\hat{P})} \gamma_{\text{init}} S_{\text{QND}}^{(\kappa \hat{X}\hat{P})T} (\mathbb{1}_{AB} \oplus S_{\text{loss},ab}) + (\mathbb{0} \oplus (1-\eta)\mathbb{1}_{ab}) \tag{5.3}$$

where $\mathbb{0}$ is a four by four matrix of zeroes. With this, the efficiency of the detector is immediately taken into account. At this time, the state has a Gaussian Wigner Function $\mathcal{W}_\gamma$.

Importantly, the measurement $\hat{\Pi} = \mathbb{1} - |0\rangle\langle 0|$ provides the vital non-Gaussian element, but itself consists of the sum of two Gaussian operations, namely $\mathbb{1}$ (tracing out the mode in question) and $|0\rangle\langle 0|$ (projection onto the vacuum). The Wigner function $\mathcal{W}_{AB} \equiv \mathcal{W}_{AB}(x_A, p_A, x_B, p_B)$ of modes A and B after the measurement is given by

$$\mathcal{W}_{AB} = M \sum_{i,j=0}^{1} (-1)^{i+j} P^{(ij)} \mathcal{W}_{AB}^{(ij)}. \tag{5.4}$$

That is, the total Wigner function $\mathcal{W}_{AB}$ is given by a superposition of normalised Gaussian Wigner functions $\mathcal{W}_{AB}^{(ij)} \equiv \mathcal{W}_{AB}^{(ij)}(x_A, p_A, x_B, p_B)$ with $i = 0$ implying that mode a has been projected onto $|0\rangle\langle 0|$ and $i = 1$ indicating that a has been traced out. The index j tells the story of mode b. The constants $P^{(ij)}$ are the probabilities associated with $\mathcal{W}_{AB}^{(ij)}$ and M is a global normalisation constant given as $M = \left(\sum_{i,j} (-1)^{i+j} P^{(ij)}\right)^{-1}$.

Each Gaussian Wigner function $\mathcal{W}_{AB}^{(ij)}$ is described by

$$\mathcal{W}_{AB}^{(ij)} = \frac{1}{\pi^2 \sqrt{\det \gamma_{AB}^{(ij)}}} \exp\left[-\mathbf{R}^T \gamma_{AB}^{(ij)-1} \mathbf{R}\right] \tag{5.5}$$

with $\mathbf{R} = (x_A, p_A, x_B, p_B)^T$. The 4×4 covariance matrices $\gamma_{AB}^{(ij)}$ that make up the Gaussian Wigner functions $\mathcal{W}_{AB}^{(ij)}$ and the normalisation constants $P^{(ij)}$ are calculated from γ by considering the Wigner overlap formula (2.73). Tracing out a mode corresponds to an overlap with $\mathcal{W}_{\mathbb{1}} = 1/2\pi$ and a projection onto the vacuum corresponds to an overlap with $\mathcal{W}_0 = \pi^{-1} \exp\left[-x^2 - p^2\right]$.

To see this we define

$$\Gamma = \gamma^{-1} = \begin{pmatrix} \Gamma_{AB} & \sigma \\ \sigma^T & \Gamma_{ab} \end{pmatrix} \tag{5.6}$$

where γ is an 8×8 matrix as in Equation (5.3). In the exponent of the corresponding Wigner function $\mathcal{W}_\gamma$, the 4×4 matrix Γ_{AB} describes the entangled modes A and B and Γ_{ab} describes the auxiliary modes a and b with σ capturing the cross-correlations. The Wigner overlap with $\mathcal{W}_{\mathbb{1}}$ or $\mathcal{W}_0$ becomes a Gaussian integral from which the $\gamma_{AB}^{(ij)}$ matrices can be derived. Then $\gamma_{AB}^{(ij)} = \left(\Gamma_{AB}^{(ij)}\right)^{-1}$ where

$$\Gamma_{AB}^{(ij)} = \Gamma_{AB} - \sigma \left(\Gamma_{ab}^{(ij)}\right)^{-1} \sigma^T; \tag{5.7}$$

$$\Gamma_{ab}^{(ij)} = \Gamma_{ab} + (1-i)\,\mathbb{1} \oplus (1-j)\,\mathbb{1}. \tag{5.8}$$

The normalisation constants $P^{(ij)}$ can be calculated by integrating what remains over x_A, p_A, x_B and p_B. Consequently,

$$P^{(ij)} = \frac{2^{2-i-j} \sqrt{\det \Gamma}}{\sqrt{\det \Gamma_{AB}^{(ij)}} \sqrt{\det \Gamma_{ab}^{(ij)}}}. \tag{5.9}$$

With the example of $S_{\mathrm{QND}}^{(\kappa\hat{X}\hat{P})}$ being used in Equation (5.3), the matrices currently take the form

$$\gamma_{AB}^{(11)} = \begin{pmatrix} \cosh(2r) & 0 & \sinh(2r) & 0 \\ 0 & \kappa^2+\cosh(2r) & 0 & -\sinh(2r) \\ \sinh(2r) & 0 & \cosh(2r) & 0 \\ 0 & -\sinh(2r) & 0 & \kappa^2+\cosh(2r) \end{pmatrix}$$

$$\gamma_{AB}^{(10)} = \begin{pmatrix} \frac{\eta\kappa^2+2\cosh(2r)}{2+\eta\kappa^2\cosh(2r)} & 0 & \frac{2\sinh(2r)}{2+\eta\kappa^2\cosh(2r)} & 0 \\ 0 & \kappa^2+\cosh(2r) & 0 & -\sinh(2r) \\ \frac{2\sinh(2r)}{2+\eta\kappa^2\cosh(2r)} & 0 & \frac{2\cosh(2r)}{2+\eta\kappa^2\cosh(2r)} & 0 \\ 0 & -\sinh(2r) & 0 & \frac{1}{2}(2-\eta)\kappa^2+\cosh(2r) \end{pmatrix}$$

$$\gamma_{AB}^{(01)} = \begin{pmatrix} \frac{2\cosh(2r)}{2+\eta\kappa^2\cosh(2r)} & 0 & \frac{2\sinh(2r)}{2+\eta\kappa^2\cosh(2r)} & 0 \\ 0 & \frac{1}{2}(2-\eta)\kappa^2+\cosh(2r) & 0 & -\sinh(2r) \\ \frac{2\sinh(2r)}{2+\eta\kappa^2\cosh(2r)} & 0 & \frac{\eta\kappa^2+2\cosh(2r)}{2+\eta\kappa^2\cosh(2r)} & 0 \\ 0 & -\sinh(2r) & 0 & \kappa^2+\cosh(2r) \end{pmatrix}$$

$$\gamma_{AB}^{(00)} = \begin{pmatrix} \frac{2\left(\eta\kappa^2+2\cosh(2r)\right)}{4+\eta^2\kappa^4+4\eta\kappa^2\cosh(2r)} & 0 & \frac{4\sinh(2r)}{4+\eta^2\kappa^4+4\eta\kappa^2\cosh(2r)} & 0 \\ 0 & \frac{1}{2}(2-\eta)\kappa^2+\cosh(2r) & 0 & -\sinh(2r) \\ \frac{4\sinh(2r)}{4+\eta^2\kappa^4+4\eta\kappa^2\cosh(2r)} & 0 & \frac{2\left(\eta\kappa^2+2\cosh(2r)\right)}{4+\eta^2\kappa^4+4\eta\kappa^2\cosh(2r)} & 0 \\ 0 & -\sinh(2r) & 0 & \frac{1}{2}(2-\eta)\kappa^2+\cosh(2r) \end{pmatrix} \tag{5.10}$$

with coefficients

$$\begin{aligned} P^{(11)} &= 1, \\ P^{(10)} &= P^{(01)} = \sqrt{\frac{1}{1+\frac{1}{2}\eta\kappa^2\cosh(2r)}}, \\ P^{(00)} &= \sqrt{\frac{4}{4+\eta^2\kappa^4+4\eta\kappa^2\cosh(2r)}}. \end{aligned} \tag{5.11}$$

At this point, all of the quantities in Equation (5.4) have been defined for the Wigner function of the non-Gaussian mixed state resulting from the protocol in Figure 5.1. However, to show that the entanglement in the two modes has increased, we require the density matrix elements of the state. These can be calculated with the help of the Q function and multidimensional Hermite polynomials [158, 159, 160].

The Q function is described by a convolution of the Wigner function with the vacuum [13] and so

$$\mathcal{Q}_{AB}^{(ij)}(\alpha,\beta) = \frac{\exp\left[-\mathcal{R}^\dagger\left(\mathbf{U}\gamma^{(ij)}\mathbf{U}^\dagger+\mathbb{1}\right)^{-1}\mathcal{R}\right]}{\pi^2\sqrt{\det\left(\gamma^{(ij)}+\mathbb{1}\right)}} \tag{5.12}$$

where $\mathcal{R} = \left(\alpha,\alpha^\dagger,\beta,\beta^\dagger\right)$ and $\mathbf{U}$ is the unitary transformation between $(\hat{x}_A,\hat{p}_A,\hat{x}_B,\hat{p}_B)^T \rightarrow \left(\hat{a},\hat{a}^\dagger,\hat{b},\hat{b}^\dagger\right)^T$:

$$\mathbf{U} = \frac{1}{\sqrt{2}}\begin{pmatrix} 1 & i & 0 & 0 \\ 1 & -i & 0 & 0 \\ 0 & 0 & 1 & i \\ 0 & 0 & 1 & -i \end{pmatrix}. \tag{5.13}$$

The Q function, as pointed out in section 2.2 can also be written as

$$\mathcal{Q}^{(ij)}(\alpha,\beta) = \frac{1}{(2\pi)^2}\langle\alpha|\langle\beta|\hat{\rho}^{(ij)}|\alpha\rangle|\beta\rangle \tag{5.14}$$

which can be used to find the density matrix elements in the Fock basis. By rewriting (5.14) using the Fock state representations of the coherent states (2.37) and rearranging one finds

$$(2\pi)^2 \mathcal{Q}^{(ij)}(\alpha,\beta) = \sum_{l,m,n,p=0}^{\infty} \frac{(\alpha^*)^l}{\sqrt{l!}} \frac{(\beta^*)^m}{\sqrt{m!}} \frac{(\alpha)^n}{\sqrt{n!}} \frac{(\beta)^p}{\sqrt{p!}} \rho_{lmnp} \tag{5.15}$$

where $\rho_{lmnp} = \langle l|\langle m|\hat{\rho}|n\rangle|p\rangle$. If one considers the differentiation of the right hand side of (5.15) with respect to $\alpha^*, \beta^*, \alpha, \beta$ a total of l, m, n and p times respectively, and evaluates at $\alpha = \beta = 0$ then one finds

$$\left(\frac{\partial}{\partial\alpha^*}\right)^l \left(\frac{\partial}{\partial\beta^*}\right)^m \left(\frac{\partial}{\partial\alpha}\right)^n \left(\frac{\partial}{\partial\beta}\right)^p \left(\sum_{l,m,n,p} \frac{(\alpha^*)^l}{\sqrt{l!}} \frac{(\beta^*)^m}{\sqrt{m!}} \frac{(\alpha)^n}{\sqrt{n!}} \frac{(\beta)^p}{\sqrt{p!}} \rho_{lmnp} \right)\Bigg|_{\alpha=\beta=0} = \sum_{l,m,n,p} \sqrt{l!m!n!p!}\rho_{lmnp} \tag{5.16}$$

and consequently

$$\begin{aligned} \rho_{lmnp}^{(ij)} &= \langle l|\langle m|\hat{\rho}^{(ij)}|n\rangle|p\rangle \\ &= \frac{(2\pi)^2}{\sqrt{l!m!n!p!}} \left(\frac{\partial^{l+n}}{\partial\alpha^{*l}\partial\alpha^n}\right) \left(\frac{\partial^{m+p}}{\partial\beta^{*m}\partial\beta^p}\right) \left[\mathcal{Q}_{AB}^{(ij)}(\alpha,\beta)\, e^{|\alpha|^2+|\beta|^2}\right]\Big|_{\alpha=\beta=0}. \end{aligned} \tag{5.17}$$

As the Q functions $\mathcal{Q}_{AB}^{(ij)}(\alpha,\beta)$ are Gaussian, the matrix element is most conveniently expressed in terms of the multivariate Hermite polynomials H_{lmnp} (see Appendix A). After successful detection, the total matrix is given by $\hat{\rho}$ with matrix elements

$$\rho_{lmnp} = \frac{4M(-1)^{l+m+n+p}}{\sqrt{l!m!n!p!}} \sum_{i,j=0}^{1} \frac{(-1)^{i+j} P^{(ij)} H_{lmnp}^{\{\mathbf{C}^{(ij)},0\}}}{\sqrt{\det\left(\gamma^{(ij)}+\mathbb{1}\right)}}. \tag{5.18}$$

where for brevity $H_{lmnp}^{\{\mathbf{C}^{(ij)},0\}} \equiv H_{lmnp}^{\{\mathbf{C}^{(ij)},0\}}(0,0,0,0)$. The matrices $\mathbf{C}^{(ij)}$ are defined from the matrix equation

$$\mathbf{C}^{(ij)} = \mathbf{B}\left[\left(\mathbf{U}\gamma^{(ij)}\mathbf{U}^\dagger + \mathbb{1}\right)^{-1} - \frac{1}{2}\mathbb{1}\right]\mathbf{D} \tag{5.19}$$

with

$$\mathbf{B} = \begin{pmatrix} 1 & 0 & 0 & 0 \\ 0 & 0 & 1 & 0 \\ 0 & 1 & 0 & 0 \\ 0 & 0 & 0 & 1 \end{pmatrix}, \quad \mathbf{D} = \begin{pmatrix} 0 & 0 & 1 & 0 \\ 1 & 0 & 0 & 0 \\ 0 & 0 & 0 & 1 \\ 0 & 1 & 0 & 0 \end{pmatrix}. \tag{5.20}$$

The purpose of $\mathbf{B}$ and $\mathbf{D}$ is simply to rearrange the elements of the matrix in such a way as to make the matrix compatible with the form given in (A.2) and to make ρ_{lmnp} proportional to $H_{lmnp}^{\{\mathbf{C}^{(ij)},0\}}$. As demonstrated in Appendix A, there is a recursion relation for the Hermite polynomials, and so a computer program can calculate the density matrix elements of each $\hat{\rho}^{(ij)}$ quickly and efficiently to a very high precision, subject to a truncation point limiting how high l, m, n and p can roam.

With this, as previously, the partially transposed matrix

$$\sum_{l,m,n,p=0}^{N_{\max}} \rho_{nmlp}|l\rangle\langle n| \otimes |m\rangle\langle p|$$

can be used to calculate the negativity and logarithmic negativity.

The logarithmic negativity of the mixed state resulting from this protocol is shown in Figure 5.2. The graph demonstrates the performance of the protocol dependent on the initial squeezing parameter r and the interaction strength κ (see caption). Entanglement concentration is successful if κ is in the range of weak to medium values i.e. for a moderate QND interaction between the TMSV and auxiliary modes, for a wide range of the initial squeezing in the TMSV.

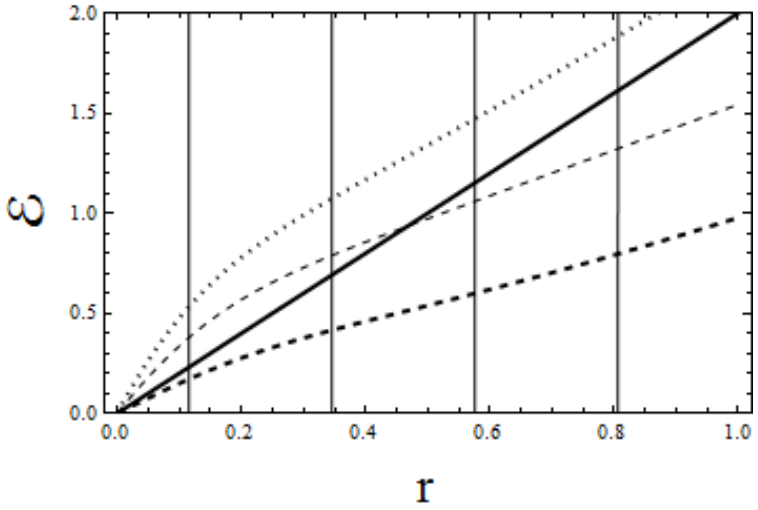

Figure 5.2: Logarithmic Negativity of TMSV (solid line), and after a QND interaction of the form $\kappa\hat{X}\hat{P}$ with strength 0.1 (dotted), 0.5 (dashed), and 1 (thick dashed). The scheme used is that depicted in Figure 5.1. The entanglement increase is best when weak interactions are used. Strong interactions can decrease the entanglement in the initial TMSV. The vertical lines from left to right indicate where the initial squeezing r is 1dB, 3dB, 5dB, and 7dB. Taken from **[V]**.

If the interaction strength is too strong (e.g. $\kappa = 1$) then the effect of the QND interaction on the entanglement content is negative. As the interaction strength decreases, the logarithmic negativity of the resultant state increases and the performed QND operation is beneficial, at least when the initial squeezing of the TMSV is weak. That is, as the interaction strength decreases, it becomes more likely that just a single photon is subtracted from each arm of the TMSV and these photons are detected. As expected, this compares well to the traditional protocol in which beamsplitters are used in place of QND interactions, investigated numerically in [116].

After all, if the pure state resulting from a single photon subtraction in both modes of the entangled state is more entangled than the initial state, then it should not matter which interaction exactly is used to subtract the photons. It is no surprise then that a QND interaction would work, as possibly would any other type of Gaussian interaction that only weakly perturbs the input state.

5.3 Protocol II

Whereas Protocol I relies on a Gaussian ancillary mode interacting with the Gaussian TMSV via QND interaction, and a subsequent non-Gaussian measurement, one could also consider a protocol which uses a non-Gaussian ancilla and a Gaussian measurement after a QND interaction (Figure 5.3).

The key advantage to the protocol depicted in Figure 5.3 is that the unreliable photon detections that provide the non-Gaussianity can be performed off-line to a certain extent. It would be quite plausible to carry out photon subtractions from a squeezed vacuum, and only using the mode as an auxillary mode if the detectors click. Also, the post-interaction detection of the light mode, homodyne detection, is far more reliable and highly efficient. Once the density matrix elements of the final mixed state are found, the negativity and logarithmic negativity can be calculated as previously.

Preparatory step

In the protocol of Figure 5.3, the ancillary modes a and b are in a quantum state with a non-Gaussian Wigner function. Specifically, they are prepared as a photon subtracted squeezed vacuum state. That is, they begin as Gaussian states with covariance matrix $\gamma_{SQ,a}(s) \oplus \gamma_{SQ,b}(s)$ where $\gamma_{SQ}(s) = S_{SQ}(s)\,\gamma_{\text{vac}} S_{SQ}^{T}(s)$ and S_{SQ} is as in equation (2.100). The modes then pass

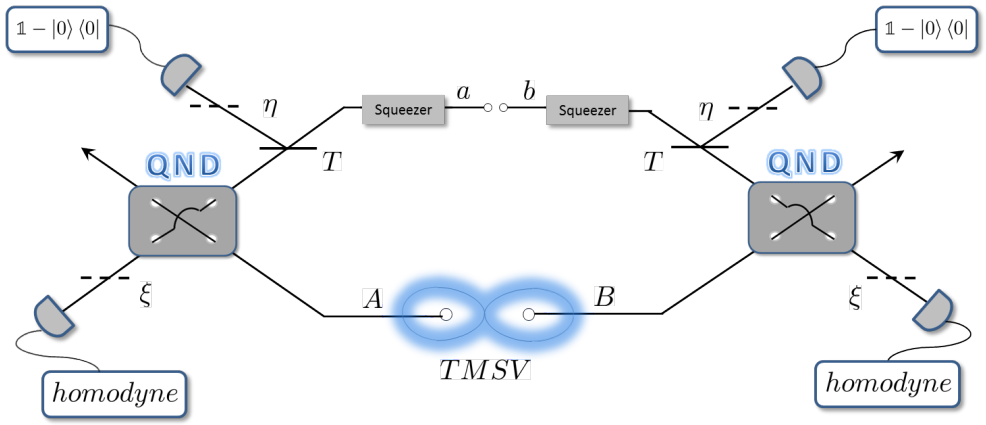

Figure 5.3: A non-Gaussian ancillary state is first created in a preparatory step by subtracting photons from a squeezed vacuum. The ancilla then interacts with the TMSV via QND interactions and is measured by homodyne detection. Taken from **[V]**.

through beamsplitters of transmittance T with any subtracted photons subsequently being detected with efficiency η. As the transmittance T increases, the model approaches the limit of just a single photon being deducted from the mode. Throughout the remainder of this chapter, $T = 0.95$ whenever numerical calculations are performed.

The Wigner function of the non-Gaussian state can be calculated by introducing two further modes described by covariance matrices $\gamma_{\mathrm{vac},c}$ and $\gamma_{\mathrm{vac},d}$ that coincide with $\gamma_{SQ,a}(s)$ and $\gamma_{SQ,b}(s)$ respectively on the beamsplitters and are subsequently acted on with $\hat{\Pi} = \mathbb{1} - |0\rangle\langle 0|$. If the photon subtraction is successful, then the Wigner function $\mathcal{W}_{ab} = M_{ab} \sum_{ij} (-1)^{i+j} P^{(ij)} \mathcal{W}_{ab}^{(ij)}$ where this time index i tells whether mode c was traced out ($i = 1$) or projected onto the vacuum ($i = 0$), with j providing the details of mode d. The probability of success is given by $M_{ab} = \left(\sum_{i,j} (-1)^{i+j} P^{(ij)}\right)^{-1}$.

The Gaussian Wigner functions are provided by the covariance matrices $\gamma_{ab}^{(ij)} = \gamma_{\mathrm{prep}}^{(i)} \oplus \gamma_{\mathrm{prep}}^{(j)}$ where

$$\gamma_{\mathrm{prep}}^{(k)} = \begin{pmatrix} \vartheta_+(k) & 0 \\ 0 & \vartheta_-(k) \end{pmatrix} \tag{5.21}$$

and

$$\vartheta_\pm(k) = 1 + \frac{(2-k)\left(e^{\pm 2s} - 1\right) T}{1 + (1-k)\left(1 + \eta\left(e^{\pm 2s} - 1\right)(1-T)\right)}. \tag{5.22}$$

The coefficients $P^{(ij)}$ are calculated as

$$P^{(ij)} = \frac{2^{2-i-j}\sqrt{\vartheta_+(i)\vartheta_-(i)\vartheta_+(j)\vartheta_-(j)}}{\sqrt{\tau_+(i)\tau_-(i)\tau_+(j)\tau_-(j)}} \tag{5.23}$$

with

$$\tau_\pm(k) = 1 - k - \frac{1 + \left(e^{\pm 2s} - 1\right) T}{(1-\eta)\left(e^{\pm 2s} - 1\right)(1-T) - e^{\pm 2s}} \tag{5.24}$$

At this point we have a non-Gaussian state $\mathcal{W}_{ab}$, consisting of a superposition of Gaussian states. If the preparatory step could be performed independently and only passed to the interaction and homodyne measurement if successful then we could consider $\eta = 1$.

Interaction and Detection

A non-Gaussian state produced in the preparatory step further interacts with the TMSV via QND coupling and the ancilla is subsequently passed on for homodyning on a detector of efficiency ξ. An angle θ describes the phase of the homodyne measurement, that is the angle at which homodyning is performed in phase space. An angle of $\theta = 0$ corresponds to a measurement of position quadrature $x_{\theta=0} = x$ (the x marginal distribution) whereas an angle of

$\pi/2$ describes the momentum quadrature measurement $x_{\theta=\pi/2} = p$ (the p-distribution). Thus the homodyne measurement is characterised by the generalized quadratures $x_{\theta,a}, x_{\theta,b}$. Directly before measurement, we can calculate the covariance matrices to be

$$\begin{aligned}\gamma_{ABab}^{(ij)} = \quad & \left(\mathbb{1}_{AB} \oplus S_{PH}\left(\theta\right)\right) \gamma_{int}^{(ij)} \left(\mathbb{1} \oplus \xi\mathbb{1}\right) \left(\mathbb{1}_{AB} \oplus S_{PH}^{T}\left(\theta\right)\right) \\ & + \left(\mathbb{0}_{AB} \oplus \left(1-\xi\right)\mathbb{1}_{ab}\right)\end{aligned} \tag{5.25}$$

with

$$\gamma_{int}^{(ij)} = S_{\mathrm{QND}} \left[\gamma_{AB}^{TMSS} \oplus \gamma_{ab}^{(ij)}\right] S_{\mathrm{QND}}^{T}. \tag{5.26}$$

To see what happens after the homodyne detection we project the quadratures $x_{\theta,a}$ and $x_{\theta,b}$ onto an outcome z. We also trace out the conjugate quadratures ($x_{\theta+\pi/2,a}$ and $x_{\theta+\pi/2,b}$).

At this point the remaining covariance matrix for A and B and the correlations due to the z measurements can be described by a 6×6 matrix $\mu^{(ij)}$ such that

$$\left(\mu^{(ij)}\right)^{-1} = \begin{pmatrix} \mathcal{A}^{(ij)} & \mathcal{C}^{(ij)} \\ \mathcal{C}^{T(ij)} & \mathcal{B}^{(ij)} \end{pmatrix} \tag{5.27}$$

where $\mathcal{A}^{(ij)}$ is a 4×4 matrix (modes A and B), $\mathcal{B}^{(ij)}$ is a 2×2 matrix descibing the z correlations, and $\mathcal{C}^{(ij)}$ contains the cross correlations. The probability of projection of modes a and b is given by

$$q_z^{(ij)} = \frac{\sqrt{\det\left(\mathcal{B}^{(ij)} - \mathcal{C}^{T(ij)}\mathcal{A}^{(ij)-1}\mathcal{C}^{(ij)}\right)}}{\pi} \exp\left[-\left(z,z\right)\left[\mathcal{B}^{(ij)} - \mathcal{C}^{T(ij)}\mathcal{A}^{(ij)-1}\mathcal{C}^{(ij)}\right]\left(z,z\right)^{T}\right] \tag{5.28}$$

and the Q function describing modes A and B reads

$$Q_{AB}^{(ij)}\left(\alpha,\beta\right) = \frac{\sqrt{\det\Phi^{(ij)}}}{\pi^2} \exp\left[-\frac{-\Lambda^{(ij)}\Phi^{(ij)-1}\Lambda^{(ij)\dagger}}{4}\right] \exp\left[-\mathcal{R}^{T}\Phi^{(ij)}\mathcal{R} - \Lambda^{(ij)}\mathcal{R}\right] \tag{5.29}$$

where

$$\Phi^{(ij)} = \mathbf{U}\left(\mathcal{A}^{(ij)-1} + \mathbb{1}\right)^{-1}\mathbf{U}^{\dagger}, \tag{5.30}$$

and

$$\Lambda^{(ij)} = 2\left(z,z\right)\mathcal{C}^{(ij)T}\mathcal{A}^{(ij)-1}\left(\mathcal{A}^{(ij)-1} + \mathbb{1}\right)^{-1}\mathbf{U}^{\dagger}. \tag{5.31}$$

By defining $\Phi'^{(ij)} = \mathbf{B}\left[\Phi^{(ij)} - (1/2)\,\mathbb{1}\right]\mathbf{D}$ and $\Lambda' = \Lambda\mathbf{D}$ we can write the density matrix elements as

$$\rho_{lmnp} = \frac{4M_{\mathrm{hom}}}{\sqrt{l!m!n!p!}} \sum_{i,j=0}^{1} \left(-1\right)^{i+j} P^{(ij)} q_z^{(ij)} \sqrt{\det\Phi^{(ij)}} \exp\left[-\frac{-\Lambda^{(ij)}\Phi^{(ij)-1}\Lambda^{(ij)\dagger}}{4}\right] H_{lmnp}^{\{\Phi'^{(ij)},\Lambda'^{(ij)}\}} \tag{5.32}$$

with

$$M_{\mathrm{hom}} = \left(\sum_{i,j=0}^{1} \left(-1\right)^{i+j} P^{(ij)} q_z^{(ij)}\right)^{-1}. \tag{5.33}$$

From this, the logarithmic negativity of modes A and B can be calculated as before.

In contrast to the first protocol, the second protocol is sensitive to which interactions are used. The position and momentum correlations in the TMSV are not mixed by the QND interactions and so the effects induced by interaction Hamiltonians e.g. $H_{\mathrm{int}}^{(\kappa XP)}$ and $H_{\mathrm{int}}^{(\kappa PP)}$ are equivalent. Correspondingly, the choice of measurement on the ancillary modes is important. If, for example, the interaction $H_{\mathrm{int}}^{(\kappa XP)}$ is used, then the momentum quadratures of the ancillary modes are, by definition, unaffected but information about the TMSV is imprinted on the position quadrature distribution. If homodyne measurements on the ancillas are performed on p ($\theta = \pi/2$) then the resulting outcome can reveal nothing about the state of the TMSV and the probabilities $q_z^{(ij)}$ (5.28) are independent of κ and r. As nothing can be learned probabilistically about modes A and B, procrustean entanglement concentration cannot occur. The effects on the TMSV can be transformed away by local Gaussian operations and ancillary modes and so

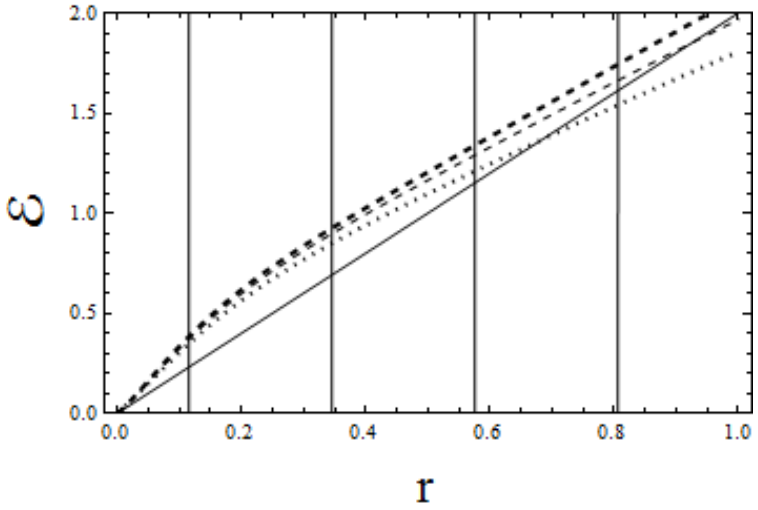

Figure 5.4: Performance of protocol II (Fig. 5.3): Logarithmic Negativity of TMSV before (solid line), and after a QND interaction for different initial squeezing of the ancilla modes. The QND interaction is of the form $\kappa\hat{X}\hat{P}$ and has strength $\kappa = 0.5$; homodyne outcome $z \approx 0$. The ancillary modes are squeezed by $s = 0.1$ (0.87dB) (black dotted), $s = 0.5$ (4.34dB) (black dashed) and $s = 1$ (8.69dB) (thick black dashed). The improvements of entanglement in the TMSV gained by increasing the squeezing of the ancillary modes is small when the initial squeezing of the TMSV r is small. The vertical lines from left to right indicate where the initial squeezing of the TMSV r is 1dB, 3dB, 5dB, and 7dB. $\eta = \xi = 1$. Taken from **[V]**.

the entanglement of the TMSV is unchanged. The above is true irrespective of whether the ancillary modes are initially squeezed in position or momentum.

If homodyne measurements were taken of the position quadratures ($\theta = 0$) then information about the TMSV will have been probabilistically imprinted on this measured distribution. If $H_{\text{int}}^{(\kappa XP)}$ is used then the momentum quadratures of the TMSV contain information about the momentum quadratures of the ancillary modes. That is, some noise has been added to modes A and B which can assist or disrupt entanglement concentration. If the ancillary modes are squeezed in momentum, then only a little noise is added to the p quadratures of the TMSV. The result is an increase in entanglement dependent on s and κ (Figure 5.4). If the ancillary modes are squeezed in position then the momentum quadratures are anti-squeezed and so a lot of noise is added to the TMSV, having a detrimental effect on the entanglement.

As can be seen in Figures 5.4 and 5.5, successful entanglement concentration is achieved if the ancillary modes are squeezed in p-quadrature, the QND interaction is of the form $H_{\text{int}}^{(\kappa XP)}$, and homodyne measurement is performed in x-quadratures. The protocol is noticeably insensitive to ancillary mode squeezing - the logarithmic negativity of the resulting state is largely unaffected for low levels of TMSV initial squeezing.

Unlike Protocol I a weak interaction strength ruins the entanglement in the system. Similarly, if the strength is too strong then the entanglement decreases. If $\kappa \approx 0.5$ then concentration successfully occurs.

5.4 Summary of Chapter 5

We have presented here two procrustean entanglement concentration schemes utilizing Quantum non-Demolition (QND) interactions and photon detectors. The first scheme relied upon QND interactions between Gaussian ancillary modes and a TMSV to successfully subtract photons from the TMSV as heralded by on/off detectors. We have shown how to efficiently calculate the density matrix elements of the resulting quantum state, which can then be used to calculate the logarithmic negativity of the state. This is a non-trivial task. In the asymptotic limit of the QND interaction strength $\kappa \to 0$, one would find that a single photon is subtracted from each arm of the TMSV, although the probability of heralding entanglement concentration

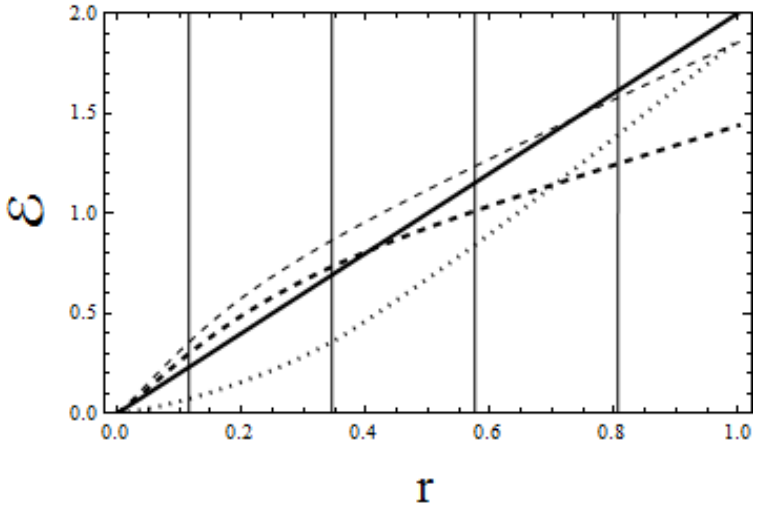

Figure 5.5: Performance of protocol II (Fig. 5.3): Logarithmic Negativity of TMSV before (solid line), and after a QND interaction for different QND interaction strengths. The QND interaction is of the form $\kappa\hat{X}\hat{P}$. The non-Gaussian ancillary modes are initially squeezed by $s = 0.2$ (1.74dB) and it is assumed that the homodyne measurement outcome is $z \approx 0$. The interaction strengths are $\kappa = 0.1$ (black dotted), $\kappa = 0.5$ (black dashed) and $\kappa = 1$ (thick black dashed). An intermediate interaction strength is preferable. The vertical lines from left to right indicate where the initial squeezing of the TMSV r is 1dB, 3dB, 5dB, and 7dB. $\eta = \xi = 1$. Taken from [**V**].

approaches zero. This is intuitively correct as the behavior mimics the protocol of [114] in which highly transmissive beamsplitters are used in place of weak QND interactions. There, as the transmittance approaches 1, one finds that a single photon is subtracted from each arm, which is the optimal outcome for entanglement concentration. The results of [114] can be revisited by replacing $S_{\rm QND}$ with $S_{\rm BS}(T)$ in equation (5.3) where $S_{\rm BS}(T)$ is the symplectic operation corresponding to a beamsplitter transformation, given in Chapter 2, equation (2.105). We find that the method we have used for calculating density matrix elements for this protocol offers an improvement in numerical speed and efficiency over calculations in the Fock basis directly.

Double pass schemes, i.e., letting the ancillae interact with the TMSV twice, do not give any advantage in protocol I. For example $S_{\rm QND}^{(\kappa_2\hat{X}\hat{P})}S_{\rm QND}^{(\kappa_1\hat{X}\hat{P})} = S_{\rm QND}^{((\kappa_1+\kappa_2)\hat{X}\hat{P})}$ but the logarithmic negativity is highest for weak interaction strength. By altering the interaction between passes e.g. $S_{\rm QND}^{(\kappa_2\hat{P}\hat{X})}S_{\rm QND}^{(\kappa_1\hat{X}\hat{P})}$ there is some advantage over a double pass scheme using the same interaction twice but this is still eclipsed by the single pass schemes.

As to detector efficiencies, at low levels of initial TMSV squeezing r, there can still be an increase in entanglement for weak interactions such as $\kappa = 0.1$ when the detector efficiency exceeds approximately 50%, $\eta > 0.5$.

The second protocol relied on QND interactions to mix a TMSV with photon subtracted squeezed vacuum modes, that is with a non-Gaussian ancillae. The non-Gaussian ancillary modes are then detected after the interaction using homodyne detectors. As was stated in the previous section, the success of this scheme is dependent on the initial squeezing of the ancillary modes, the choice of interaction, and the angle θ of homodyning. It is most likely that a homodyne measurement yields a result $z = 0$, and the logarithmic negativity shows an improvement so long as the measurement outcome does not stray too far from this.

The benefit of the second protocol is that the probabilistic non-Gaussian state preparation could be performed off-line and therefore the efficiency η of the on/off detectors could be assumed to be good. Then only the homodyne detector efficiency needs to be taken into account.

Let us now consider the feasibility of the implementation of the protocols presented here in a laboratory setting. In a purely optical setup in which the TMSV is created by parametric down conversion and the QND operations are performed with beamsplitters and squeezers, protocol I is probably the easiest to implement, although other effects such as a nonzero dark count rate of the detectors would need consideration. However, in the atomic systems of [9] where

the entangled macroscopic spin states of two caesium gas samples represent the TMSV and off-resonant dipole interactions with strongly polarized light form the QND interactions, the vacuum ancillary modes are not true vacuum modes. They are instead modes of heavily polarized light. The heralding of the entanglement concentration comes from detecting photons for which the interaction has altered the polarization, but this requires heavy filtering, a problem that is most likely insurmountable with current technology. Protocol II does not suffer this problem and so is the best choice in the atomic case. The probabilities of success in both cases are comparable with those for the beamsplitter-based light schemes, already demonstrated [117] in the laboratory. The possibility of distilling entanglement in atomic ensembles represents the main motivation for using a general QND Hamiltonian for entanglement concentration.

Chapter 6

Gaussian Intrinsic Information

This chapter is concerned with a new potential measure of quantum entanglement in continuous variable bipartite Gaussian states. Such measures are still sought after if they have an operational interpretation. As has been seen from Chapter 3, the logarithmic negativity is easily computable on Gaussian states. However, it is operationally unclear what such a measure means. The Gaussian entanglement of formation is known in some cases but is difficult to calculate in general and also provides no clear operational interpretation on mixed states.

In this self-contained chapter, an attempt is made at establishing a new entanglement measure for bipartite Gaussian states. This task has not yet been completed but looks promising. Work is ongoing in collaboration with Dr Ladislav Mišta at Palacký University. The measure is based on a well-known problem from cryptography that has been partially translated into the finite dimensional Hilbert space setting for use in quantum information theory.

In Section 6.1 we explain the motivation in classical cryptography for which the Intrinsic Information was defined. In Section 6.2 we explain briefly what this means for qudits.

From Section 6.3 onwards, we try to translate this to Gaussian states. As has been said, this is only a partial result but appears promising.

6.1 Motivation

One of the ever fundamental problems in quantum cryptography is the task of establishing a secret key between Alice (who wants to send a message) and Bob (receiver) in a real environment. Traditionally in a symmetric cipher, regardless of the exact form the cipher takes, Alice would encrypt her message, or *plaintext*, with a secret key. The resulting *ciphertext* would be sent to Bob who would then use the same key to decrypt and obtain the original message.

However, suppose that the courier Alice uses is not to be trusted. The courier gives a facsimile of the ciphertext to an eavesdropper, Eve, who using centuries old techniques can find the key and thereby crack the code. The techniques at her disposal include frequency analysis. If the length of the key is shorter than the length of the message, then to encode one message the key will be used over and over again. Repetition is the root of all evil and Eve can spot patterns in the ciphertext to establish what the key must be. The ciphertext can therefore be used to crack the current message and all future messages using the same key. In [163], Shannon proved the disheartening theorem that a ciphertext C can only be perfectly, information-theoretically secure if the (classical) mutual information between the message M and ciphertext, $\mathcal{I}(M:C)$ is zero.

First described by Frank Miller in 1882, the one-time pad, or *Vernam cipher*, was reinvented in 1917 and gave an added security. The solution was clear - if the key was the same length as the plaintext then there would be no repetitive loopholes for Eve to exploit. If a different key was used for every message (i.e. no repetition across multiple messages) then the ciphertext cannot give up the key.

However, an obvious problem arose. How could Alice send the key to Bob in the first place? Public key cryptography introduced by Diffie and Hellman [164] solves this problem under two assumptions. Firstly, Eve is unable to solve a very hard computational problem in a

feasible amount of time[1] and secondly, Eve only has passive access to the communication between Alice and Bob. Thus public key cryptography is computationally secure but not information-theoretically secure.

Theorists in classical information theory have given this problem a lot of thought. Ignoring the technicalities of individual methods for key distribution, the overall idea is the same [165]. Communication occurs between Alice and Bob with Eve having an active or passive role and consequently, after this round of communication all three parties share a classical distribution[2] P_{XYZ}. The part of this that Alice and Bob share is usually termed the *raw key* and they must try to produce a secret key by postprocessing, error checking etc.

Alice and Bob aim to turn their distribution into a perfectly correlated list of symbols about which Eve knows nothing, and to do so they can perform local operations on their individual distributions and communicate over a public channel. This is known as an LOPC protocol. To get unconditional security, it is important to show in information-theoretic terms that there is no correlation between Eve's distribution and Alice and Bob's after the LOPC protocol, at least in the asymptotic limit.

The *secret key rate* of X and Y with respect to Z, denoted by $\mathcal{K}(X:Y||Z)$, is the maximum rate at which Alice and Bob can agree on a secret key K in such a way that the amount of information Eve is privy to is negligible. This could be phrased in an alternative way [166]. The secret key rate $\mathcal{K}$ is the maximal R such that for every $\epsilon > 0$ and for all sufficiently large N there exists a protocol, using public discussion over an insecure but authenticated channel, such that Alice and Bob who receive $X^N = \{X_1, \cdots, X_N\}$ and $Y^N = \{Y_1, \cdots, Y_N\}$, respectively, compute the same key K with probability at least $1 - \epsilon$ satisfying

$$\mathcal{I}\left(\mathcal{K} : CZ^N\right) \leq \epsilon \tag{6.1}$$

$$\mathcal{H}(\mathcal{K}) \geq \log[\mathcal{K}] - \epsilon \tag{6.2}$$

$$\frac{1}{N}\mathcal{H}(K) \geq R - \epsilon \tag{6.3}$$

where C denotes the communication channel (i.e. the complete collection of all the messages sent over the channel), $\mathcal{H}$ is the Shannon entropy $\mathcal{H}(p_{\mathcal{X}}) = -\sum_x p_{\mathcal{X}=x} \log[p_{\mathcal{X}=x}]$, and the classical mutual information is given by

$$\mathcal{I}(X:Y) = \mathcal{H}(p_X) + \mathcal{H}(p_Y) - \mathcal{H}(p_{XY}). \tag{6.4}$$

Note, the logarithm of equation (6.2) is usually taken to be to base 2 when discussing bits but this is unimportant.

From the definition above, it is clear that the secret key rate is not something that is easy to find. Bounds must be found. It is intuitive that the secret key rate can never be less than Alice and Bob's shared information reduced by the correlations between Eve and one party. That is, there is a lower bound on the secret key rate of the form

$$\max[\mathcal{I}(X:Y) - \mathcal{I}(X:Z), \mathcal{I}(X:Y) - \mathcal{I}(Y:Z)] \leq \mathcal{K}(X:Y||Z) \tag{6.5}$$

with the bound being saturated if the communication between Alice and Bob only flows one way [167]. As the left hand side of the inequality may be negative but the secret key rate may not, it makes more sense to write

$$\max[\mathcal{I}(X:Y) - \mathcal{I}(X:Z), \mathcal{I}(X:Y) - \mathcal{I}(Y:Z), 0] \leq \mathcal{K}(X:Y||Z). \tag{6.6}$$

Upper bounds also exist. The secret key rate can certainly never exceed the mutual information between Alice and Bob. The secret key rate can also never exceed their mutual information conditioned on what Eve knows, so

$$\mathcal{K}(X:Y||Z) \leq \min[\mathcal{I}(X:Y), \mathcal{I}(X:Y|Z)] \tag{6.7}$$

[1] All bank codes are based on the famous RSA cipher which is dependent on the unproven rule that a very large number cannot be factorised in a reasonable amount of time. If implemented correctly, it would on average take all of the computers on the planet longer than the age of the universe to crack a single code by brute force. This is by far one of the biggest inspirations for creating quantum computers.

[2] X, Y, Z have been used in place of A, B, E to avoid any confusion later on. X corresponds to Alice's part of the distribution, Y to Bob, and Z to Eve.

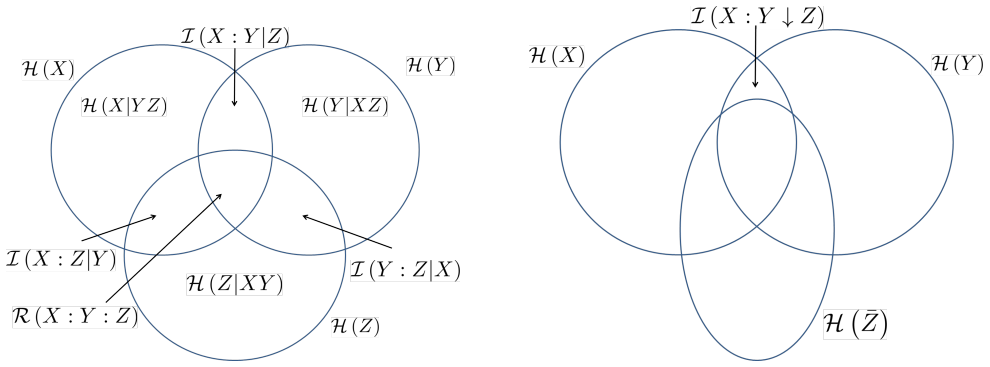

(a) Entropies of three random variables

(b) The role of intrinsic information

Figure 6.1: The relationship between different classical entropic quantities is shown in Figure 6.1a. In the centre is the fully symmetric quantity $\mathcal{R}(X:Y:Z) = \mathcal{I}(X:Y) - \mathcal{I}(X:Y|Z)$, although this may be negative. In Figure 6.1b, the role of Eve's post-processing is shown. She is able to decrease the amount of secret correlations that Alice and Bob share. We have used $\mathcal{H}(X)$ in place of $\mathcal{H}(p_X)$ etc. for ease of notation. Adapted from [168].

where the second term is given by

$$\mathcal{I}(X:Y|Z) = \mathcal{H}(p_{XZ}) + \mathcal{H}(p_{YZ}) - \mathcal{H}(p_{XYZ}) - \mathcal{H}(p_Z) \tag{6.8}$$

and $\mathcal{H}$ is the Shannon entropy. Equation (6.8) can be thought of as a classical analogue to the conditional quantum mutual information in the definition of squashed entanglement (3.49).

But let us consider this term further. After the initial round of communication yielding P_{XYZ}, Eve may choose to do some form of post-processing which would change $\mathcal{I}(X:Y|Z)$. This conditional mutual information could be decreased, forming a tighter bound on the secret key rate $\mathcal{K}(X:Y||Z)$. We can now define the intrinsic information (intrinsic conditional mutual information).

Given a distribution P_{XYZ} the intrinsic information is defined as

$$\mathcal{I}(X:Y\downarrow Z) = \inf_{P_{\bar{Z}|Z}} \left\{ \mathcal{I}\left(X:Y|\bar{Z}\right) : \quad P_{XY\bar{Z}} = \sum_Z P_{XYZ} P_{\bar{Z}|Z} \right\} \tag{6.9}$$

where the infimum is taken over all discrete random variables $\bar{Z}$ such that $XY \to Z \to \bar{Z}$ is a Markov chain. That is, the transformation to $\bar{Z}$ from Z has no dependence on XY - it is Eve's local operation only. So the secret key rate is bounded from above as

$$\mathcal{K}(X:Y||Z) \leq \mathcal{I}(X:Y\downarrow Z). \tag{6.10}$$

The intrinsic information then satisfies the following inequalities:

$$0 \leq \quad \mathcal{I}(X:Y\downarrow Z) \leq \mathcal{I}(X:Y) \tag{6.11}$$

$$\mathcal{I}(X:Y\downarrow Z) \leq \mathcal{I}(X:Y|Z). \tag{6.12}$$

In [168], it was also conjectured that if $\mathcal{I}(X:Y\downarrow Z) > 0$ then $\mathcal{K}(X:Y||Z) > 0$.

On a significant sidenote, it is possible to define another quantity, the Information of Formation $\mathcal{I}_{\text{form}}(X:Y|Z)$ that, loosely speaking, quantifies how able Alice and Bob are to create their joint probability distribution using local operations and public communication (LOPC). It is discovered by finding the infimum over all LOPC channels able to do that. It acts as an upper bound on the intrinsic information, and therefore on the secret key rate

$$\mathcal{I}(X:Y\downarrow Z) \leq \mathcal{I}_{\text{form}}(X:Y|Z). \tag{6.13}$$

An examination of $\mathcal{I}_{\text{form}}$ in conjunction with $\mathcal{K}(X:Y||Z)$ can yield some very interesting results and has led to one of the few examples of ideas from quantum information theory directly inspiring advances in classical information theory, as opposed to the other way round. For

a long time, it was wondered whether there was a classical analogue to bound entanglement [169, 170]. The answer is yes, the *bound information*, and a probability distribution P_{XYZ} possesses bound information when

$$\mathcal{K}(X:Y||Z)=0, \quad \mathcal{I}_{\text{form}}(X:Y|Z)>0. \tag{6.14}$$

That is, bound information is when a distribution can be formed with correlations from which no secret key can be distilled. Such distributions can be found for qubits [171] and continuous variables [172].

6.2 Intrinsic Information in qudit systems

Gisin, Renner and Wolf [169] considered the problem of distilling a secret key from a probability distribution resulting from measurements on a quantum state. If Alice were to try communicating a pure state to Bob over a noisy quantum channel, they would only ever end up sharing a mixed state as information would leak away.

A mixed state, then, is not a true fundamental object, it is a sign of the researchers' ignorance. For the full knowledge of the initial system, we would need to gather everything that was ever lost. We can assume that Eve has done this so that overall, Alice, Bob & Eve share a pure state $|\psi\rangle_{ABE}$ which reduces to the mixed state shared by Alice and Bob when Eve is traced out.

When Alice and Bob share many independent systems $\hat{\rho}_{AB}$ there are basically two possibilities for generating a secret key. They either first measure their respective subsystems and perform a classical protocol secure against all measurements (POVMs) that Eve can perform (i.e. against all possible distributions P_{XYZ} that can result after Eve's measurements). Or they could run a protocol on $\hat{\rho}_{AB}$ in the quantum domain with local operations and classical communication. Such a protocol would simply be a purification scheme (see Section 3.4) with the aim of eliminating Eve from the scenario. The process of using quantum processing to obtain a pure state, followed by measurements, is known as *quantum privacy amplification*. For the purposes of this chapter, we are instead concerned with the first of these scenarios in which classical processing is performed on the outcome of measurements.

When given a state $|\psi\rangle_{ABE}$ between Alice, Bob and Eve, the classical distribution $P_{XYZ}={}_A\langle x|\ {}_B\langle y|\ {}_E\langle z|\ \psi\rangle_{ABE}$ resulting from local POVM measurements by all parties, possesses intrinsic information $\mathcal{I}(X:Y\downarrow Z)$ between Alice and Bob (conditioned on E) if and only if $\hat{\rho}_{AB}=\text{Tr}_E\left[|\psi\rangle_{ABE}\right]$ is entangled [169]. However, this correspondence clearly depends on the measurement bases used by Alice, Bob and Eve. That is, if Alice and Bob share an entangled $\hat{\rho}_{AB}$ but perform the wrong local measurements then the intrinsic information may disappear. If, on the other hand, $\hat{\rho}_{AB}$ is separable but Eve performs bad measurements, the intrinsic information may become positive despite the fact that $\hat{\rho}_{AB}$ could have been manufactured by local operations and classical communication (LOCC). Consequently, the correspondence between intrinsic information and entanglement must involve some optimisation over all possible measurements on all sides.

A similar correspondence is seen within protocols and is supported by many examples - the distribution P_{XYZ} allows for classical key agreement if and only if quantum key agreement is possible from the state $\hat{\rho}_{AB}$.

Gisin and Wolf [170] introduced the following measure of entanglement on a state $\hat{\rho}_{AB}$ in finite dimensional Hilbert spaces:

$$\mu(\hat{\rho}_{AB})=\min_{\{|z\rangle\}}\left(\max_{\{|x\rangle,|y\rangle\}}\left(\mathcal{I}(X:Y\downarrow Z)\right)\right) \tag{6.15}$$

That is, Alice and Bob share a state $\hat{\rho}_{AB}$. Eve holds a subsystem such that as a whole $|\psi\rangle_{ABE}$ is pure. Alice, Bob and Eve each perform local POVMs on the pure global state, yielding P_{XYZ}, except that Alice and Bob perform measurements chosen to maximise their classical correlations whilst Eve works against them.

For finite dimensional systems, it was shown that

$$\mu(\hat{\rho}_{AB})=0 \quad \text{if } \hat{\rho}_{AB} \text{ is separable} \tag{6.16}$$

meaning that Eve can choose a measurement basis forcing the classical correlations between Alice and Bob to disappear. On pure states

$$\mu\left(\hat{\rho}_{AB}\right) = \mathcal{E}_{v.N.}\left(\hat{\rho}_{AB}\right) \tag{6.17}$$

as Eve can do nothing to interfere with the communication between Alice and Bob. Also, $\mu\left(\hat{\rho}_{AB}\right)$ is in general convex so

$$\mu\left(p\hat{\rho}_1 + (1-p)\hat{\rho}_2\right) \leq p\mu\left(\hat{\rho}_1\right) + (1-p)\mu\left(\hat{\rho}_2\right). \tag{6.18}$$

It is this measure of entanglement that we attempt to translate to the continuous variable regime.

6.3 Introducing Gaussian Intrinsic Information

Defining the Gaussian Intrinsic Information

We now consider what form a measure such as (6.15) may take in the continuous variable regime. For ease we consider the case where everything is Gaussian - the state $\hat{\rho}_{AB}$ is Gaussian, the measurements performed on all subsystems are Gaussian POVMs and the post processing that Eve performs is limited to Gaussian channels. The Gaussian intrinsic information is then given by

$$\mu_G\left(\hat{\rho}_{AB}\right) = \min_{\hat{\Pi}_E^G}\left(\max_{\{\hat{\Pi}_A^G,\hat{\Pi}_B^G\}}\left(\mathcal{I}\left(A:B\downarrow E\right)\right)\right) \tag{6.19}$$

where $\hat{\Pi}_A^G$, $\hat{\Pi}_B^G$ and $\hat{\Pi}_E^G$ are Gaussian POVMS on Alice's, Bob's and Eve's subsystems respectively and now $\mathcal{I}\left(A:B\downarrow E\right)$ is used to denote a minimisation over *Gaussian* post-processing on Eve's subsystem.

To demonstrate this measure, we first consider only a two mode Gaussian state $\hat{\rho}_{AB}$ of modes A and B with zero first moments and the covariance matrix γ and without loss of generality can say that it is in standard form. This last assumption, that the covariance matrix can be written in standard form without loss of generality, implicitly assumes that (6.19) is invariant under local symplectic operations. We go some way to show this shortly. For any such state, there is a symplectic matrix S that transforms the state to the normal form, i.e. $S\gamma S^T = \mathrm{diag}\left(\nu_A,\nu_A,\nu_B,\nu_B\right)$, where $\nu_{A,B} \geq 1$ are the symplectic eigenvalues that we can assume to be arranged in descending order. The symplectic matrices S for performing this transformation are detailed in Appendix B. To find the purification of $\hat{\rho}_{AB}$ requires two steps. Firstly, we diagonalise γ and attach two modes E_1 and E_2 such that E_1 appears to form a pure two mode squeezed vacuum with A, and E_2 with B, i.e.

$$\begin{pmatrix} \nu_A\mathbb{1} & 0 & \sqrt{\nu_A^2-1}\sigma_z & 0 \\ 0 & \nu_B\mathbb{1} & 0 & \sqrt{\nu_B^2-1}\sigma_z \\ \sqrt{\nu_A^2-1}\sigma_z & 0 & \nu_A\mathbb{1} & 0 \\ 0 & \sqrt{\nu_B^2-1}\sigma_z & 0 & \nu_B\mathbb{1} \end{pmatrix}$$

expressed in 2×2 blocks with $\sigma_z = \mathrm{diag}\left(1,-1\right)$ being the Pauli z-matrix. However, the operation S usually required to get to this form is generally a global measurement and so may have distorted the amount of entanglement in the system, or even created it. For this reason we must reverse this operation using $S^{-1}\oplus\mathbb{1}_{E_1,E_2}$. With respect to $AB|E_1E_2$ splitting the covariance matrix of the purification of the state, $|\Psi\rangle_{ABE}$ attains the form:

$$\gamma_\pi = \begin{pmatrix} \gamma & \beta \\ \beta^T & \nu_A\mathbb{1}_{E_1}\oplus\nu_B\mathbb{1}_{E_2} \end{pmatrix}, \tag{6.20}$$

where $\beta \equiv S^{-1}\left[\oplus_{j=A,B}\sqrt{\nu_j^2-1}\sigma_z^{(j)}\right]$. We have then restricted ourselves to minimisation over all Gaussian purifications $|\Psi\left(R\right)\rangle_{ABE} = U_E\left(R\right)|\Psi\rangle_{ABE}$. We further assume that Alice, Bob and Eve perform a Gaussian POVM of the form

$$\Pi_j^G\left(d_j\right) = \frac{1}{2\pi}\hat{D}_j\left(d_j\right)\Pi_j^G\hat{D}_j^\dagger\left(d_j\right), \quad j = A,B,E. \tag{6.21}$$

Here the seed element Π_j^G is a normalised density matrix of a generally mixed Gaussian state (which is single mode in the cases of Alice and Bob but two-mode for Eve) with covariance matrix Γ_j and zero displacements. The operator $\hat{D}\left(d_j\right) = \exp\left[-i\mathbf{d}_j^T \Omega \hat{\mathbf{R}}_j\right]$ is the displacement operator (discussed in detail in Chapter 2), where $\hat{\mathbf{R}}_j = \left(\hat{x}_j, \hat{p}_j\right)^T$ and $\mathbf{d}_j^T = \left(d_j^{(x)}, d_j^{(p)}\right)$ is a vector of measurement outcomes. The POVM (6.21) satisfies the completeness condition

$$\frac{1}{2\pi}\int \hat{D}_j\left(d_j\right)\Pi_j^G \hat{D}_j^\dagger\left(d_j\right)\mathrm{d}^2 d_j = \mathbb{1}_j, \tag{6.22}$$

where $\mathrm{d}^2 d_j = \mathrm{d}d_j^{(x)}\mathrm{d}d_j^{(p)}$, following from Schur's lemma [173] and the normalisation condition $\mathrm{Tr}\left[\Pi_j^G\right] = \mathbb{1}$.

After the measurements Π_j^G with $j = A, B, E$, characterised by covariance matrices Γ_A, Γ_B and Γ_E on the purification $\left|\Psi\left(R\right)\right\rangle_{ABE}$ we get a Gaussian probability density of eight real variables. Two of these variables are for Alice (for notational convenience grouped under d_A), two for Bob (d_B) and four for Eve (d_E) and the distribution is given by

$$\begin{aligned}\mathcal{P}\left(d_A, d_B, d_E\right) &= \mathrm{Tr}\left[\Psi\left(R\right)\otimes_{j=A,B,E}\Pi_j^G\left(d_j\right)\right] \\ &= \mathrm{Tr}\left[\Psi\otimes_{j=A,B}\Pi_j\left(d_j\right)\otimes\Pi_E^{G'}\left(d'_E\right)\right] \\ &= P\left(d_A, d_B, d'_E\right)\end{aligned} \tag{6.23}$$

where $\Psi \equiv \left|\Psi\right\rangle_{ABE}\left\langle\Psi\right|$, $\Psi\left(R\right) \equiv \left|\Psi\left(R\right)\right\rangle_{ABE}\left\langle\Psi\left(R\right)\right|$, and

$$\Pi_E^{G'}\left(d'_E\right) = \frac{1}{\left(2\pi\right)^2}\hat{D}\left(d'_E\right)\Pi_E^{G'}\hat{D}^\dagger\left(d_E^{'}\right), \tag{6.24}$$

where $d_E^{'} = R^{-1}d_E$ and the seed element $\Pi_E^{G'}$ has the covariance matrix $\Gamma'_E = R^{-1}\Gamma_E\left(R^{-1}\right)^T$. After some algebra we obtain the probability density (6.23) in the form

$$P\left(d\right) = \frac{e^{-d^T\Sigma^{-1}d}}{\pi^4\sqrt{\det\gamma}} \tag{6.25}$$

with $d = \left(d_A, d_B, d'_E\right)^T$ and the classical correlation matrix (CCM)

$$\Sigma = \gamma_\pi + \Gamma_A \oplus \Gamma_B \oplus \Gamma'_E = \begin{pmatrix} \alpha & \beta \\ \beta^T & \delta \end{pmatrix}. \tag{6.26}$$

Eve then processes her measurement outcome d'_E using the Gaussian conditional density

$$P\left(d_{\bar{E}}|d'_E\right) = \frac{P\left(d'_E, d_{\bar{E}}\right)}{P\left(d'_E\right)} \tag{6.27}$$

where we have assumed that the Gaussian joint probability distribution $P\left(d_{\bar{E}}, d'_E\right)$ has the classical covariance matrix[3]

$$\chi = \begin{pmatrix} \delta & C \\ C^T & \zeta \end{pmatrix}, \tag{6.28}$$

and $P\left(d'_E\right)$ is the marginal density of the variable d'_E. The conditional density (6.27) is simply discovered to be

$$P\left(d_{\bar{E}}|d'_E\right) = \frac{e^{-\left(d_{\bar{E}} - C^T\delta^{-1}d'_E\right)\left(\zeta - C\delta^{-1}C^T\right)^{-1}\left(d_{\bar{E}} - C^T\delta^{-1}d'_E\right)}}{\pi^2\sqrt{\det\left(\zeta - C^T\delta^{-1}C\right)}}. \tag{6.29}$$

[3]In principle, the random vector $d_{\bar{E}}$ can be of a larger size than the original random vector d'_E. In view of the fact that for discrete channels the minimum in equation (6.15) can be a channel with the range of the output variable $\bar{E}$ no larger than the range of the input variable E [174], we here assume that this is true too for the continuous variable systems. That is, we here assume that the dimensions of matrix B are no longer than the dimensions of δ. This is an entirely unproven assumption and further work should be carried out to clarify this, but it seems reasonable. Regardless, if it can be shown that using this assumption $\mu_G\left(\hat{\rho}_{AB}\right)$ satisfies all the properties of an entanglement measure, then it is a moot point.

After the channel, we have the full distribution given by

$$P\left(d_A, d_B, d_{\bar{E}}\right) = \int P\left(d_A, d_B, d'_E\right) P\left(d_{\bar{E}}|d'_E\right) \mathrm{d}d'_E \tag{6.30}$$

which is in itself another Gaussian function characterised by the classical covariance matrix

$$\bar{\Sigma} = \begin{pmatrix} \alpha & \beta\delta^{-1}C \\ C^T\delta^{-1}\beta^T & \zeta \end{pmatrix}. \tag{6.31}$$

Note that if Eve performs no processing, then the channel (6.28) is given by

$$\chi = \begin{pmatrix} \delta & \delta \\ \delta & \delta \end{pmatrix} \tag{6.32}$$

and $\bar{\Sigma} = \Sigma$.

Simplifying the Gaussian Entanglement Measure

We shall first focus on the evaluation of the Gaussian intrinsic information. Making use of the Shannon formula [175] for the entropy of an N-dimensional random vector distributed according to a Gaussian distribution P with covariance matrix λ,

$$\mathcal{H}\left(P\right) = \ln\left[(2\pi e)^{\frac{N}{2}}\sqrt{\det\lambda}\right], \tag{6.33}$$

we obtain using equation (6.8) the formula

$$\mathcal{I}\left(A:B|\bar{E}\right) = \frac{1}{2}\ln\left[\frac{\det\bar{\Sigma}_{AE}\det\bar{\Sigma}_{BE}}{\det\bar{\Sigma}\det\bar{\Sigma}_E}\right]. \tag{6.34}$$

The submatrices $\bar{\Sigma}_{AE}$, $\bar{\Sigma}_{BE}$ are defined as

$$\bar{\Sigma}_{AE} = \begin{pmatrix} \sigma_A & \sigma_{AE} \\ \sigma_{AE}^T & \sigma_E \end{pmatrix}, \quad \bar{\Sigma}_{BE} = \begin{pmatrix} \sigma_B & \sigma_{BE} \\ \sigma_{BE}^T & \sigma_E \end{pmatrix}, \tag{6.35}$$

and $\bar{\Sigma}_E = \sigma_E$, where the matrices σ are subblocks of the CCM (6.31) with respect to the $A|B|E$ splitting

$$\bar{\Sigma} = \begin{pmatrix} \sigma_A & \sigma_{AB} & \sigma_{AE} \\ \sigma_{AB}^T & \sigma_B & \sigma_{BE} \\ \sigma_{AE}^T & \sigma_{BE}^T & \sigma_E \end{pmatrix}. \tag{6.36}$$

In order to optimise over the postprocessing, it is convenient to express the conditional mutual information (6.8) through the determinants of smaller matrices. Specifically, for the Gaussian distributions here one has $\mathcal{I}\left(A:B|\bar{E}\right) = \mathcal{I}\left(A:B|\bar{E}=\bar{e}\right)$ where on the right hand side is the mutual information between A and B conditioned on the variable $\bar{E}$ equal to a certain value $\bar{e}$ which coincides with the mutual information of the conditional distribution $P\left(d_A, d_B|d_{\bar{E}}\right)$. This then gives

$$\mathcal{I}\left(A:B|\bar{E}\right) = \frac{1}{2}\ln\left[\frac{\det\sigma_A^{\mathrm{cond}}\det\sigma_B^{\mathrm{cond}}}{\det\sigma_{AB}^{\mathrm{cond}}}\right] \equiv \mathcal{I}_{\mathrm{cond}}\left(A:B\right), \tag{6.37}$$

where we have defined

$$\sigma_{AB}^{\mathrm{cond}} = \begin{pmatrix} \sigma_A & \sigma_{AB} \\ \sigma_{AB}^T & \sigma_B \end{pmatrix} - \begin{pmatrix} \sigma_{AE} \\ \sigma_{BE} \end{pmatrix}\sigma_E^{-1}\begin{pmatrix} \sigma_{AE}^T & \sigma_{BE}^T \end{pmatrix} \tag{6.38}$$

and the other classical covariance matrices $\det\sigma_A^{\mathrm{cond}}$ and $\det\sigma_B^{\mathrm{cond}}$ are derived by tracing over the other subsystem.

If we express the covariance matrix (6.20) with respect to $A|B|E$ splitting as

$$\gamma_\pi = \begin{pmatrix} \gamma_A & \gamma_{AB} & \gamma_{AE} \\ \gamma_{AB}^T & \gamma_B & \gamma_{BE} \\ \gamma_{AE}^T & \gamma_{BE}^T & \gamma_E \end{pmatrix}, \tag{6.39}$$

and use equation (6.31), we obtain from equation (6.38)

$$\sigma_{AB}^{\text{cond}} = \begin{pmatrix} \gamma_A & \gamma_{AB} \\ \gamma_{AB}^T & \gamma_B \end{pmatrix} + (\Gamma_A \oplus \Gamma_B) - \begin{pmatrix} \gamma_{AE} \\ \gamma_{BE} \end{pmatrix} (\gamma_E + \Gamma'_E)^{-1} C\zeta^{-1} C^T (\gamma_E + \gamma'_E)^{-1} \begin{pmatrix} \gamma_{AE} \\ \gamma_{BE} \end{pmatrix}^T, \tag{6.40}$$

$$\sigma_A^{\text{cond}} = \gamma_A + \Gamma_A - \gamma_{AE} (\gamma_E + \Gamma'_E)^{-1} C\zeta^{-1} C^T (\gamma_E + \Gamma'_E)^{-1} \gamma_{AE}^T, \tag{6.41}$$

$$\sigma_B^{\text{cond}} = \gamma_B + \Gamma_B - \gamma_{BE} (\gamma_E + \Gamma'_E)^{-1} C\zeta^{-1} C^T (\gamma_E + \Gamma'_E)^{-1} \gamma_{BE}^T, \tag{6.42}$$

where the last two classical covariance matrices are derived from the first.

One could view this from a different perspective. The conditional mutual information described in equation (6.37) is simply the mutual information of a joint Gaussian distribution arrived at by performing Gaussian measurements on A and B (characterised by Γ_A and Γ_B respectively) on a two mode Gaussian state with the covariance matrix

$$\tau_{AB} = \begin{pmatrix} \gamma_A & \gamma_{AB} \\ \gamma_{AB}^T & \gamma_B \end{pmatrix} - \begin{pmatrix} \gamma_{AE} \\ \gamma_{BE} \end{pmatrix} (\gamma_E + \Gamma'_E)^{-1} C\zeta^{-1} C^T (\gamma_E + \gamma'_E)^{-1} \begin{pmatrix} \gamma_{AE} \\ \gamma_{BE} \end{pmatrix}^T. \tag{6.43}$$

In other words, it is the classical mutual information of the classical Gaussian probability density characterised by CCM $\tau_{AB} + \Gamma_A \oplus \Gamma_B$.

6.4 Properties

In this section we shall attempt to flesh out some of the characteristics of the Gaussian intrinsic information.

Pure States

In the case of pure states, the purification takes the form $|\Psi\rangle_{ABE} = |\psi\rangle_{AB}|\psi\rangle_E$. All of the symplectic eigenvalues of γ are equal to 1 and so $\beta = 0$ in equations (6.20), (6.26) and (6.31). That is, $\bar{\Sigma} = \alpha \oplus \zeta$ and $P(d_A, d_B, d_{\bar{E}}) = P(d_A, d_B)$. This then ensures that $\mathcal{I}\left(A : B|\bar{E}\right) = \mathcal{I}(A : B)$.

As shall be seen in Chapter 8 and can be found in [**II**], the optimal measurement that Alice and Bob can perform (at least in the two mode case) is homodyning. The measure reduces to

$$\mu_G\left(\rho_{AB}^{(\text{pure})}\right) = \ln\left[\sqrt{\det \gamma_A}\right] \tag{6.44}$$

where γ_A is the covariance matrix of mode A. Note that this is not equal to the von-Neumann entropy of the reduced state - that would be given by $\mathfrak{F}\left(\sqrt{\det \gamma_A}\right)$. In fact, as shall be seen in Chapter 8, the best possible measurement that Alice and Bob could perform to maximise their post-measurement mutual information $\mathcal{I}(A : B)$ would be photon counting, but this is beyond the Gaussian regime that we have restricted ourselves to.

Separable States

As has been stated previously, if γ is the covariance matrix of a separable bipartite Gaussian state, then it holds that

$$\gamma \geq \begin{pmatrix} \gamma_A & 0 \\ 0 & \gamma_B \end{pmatrix}. \tag{6.45}$$

Thus γ can be created by taking a two mode Gaussian product state and adding classical noise in the form of a matrix χ:

$$\gamma = \begin{pmatrix} \gamma_A & 0 \\ 0 & \gamma_B \end{pmatrix} + \chi. \tag{6.46}$$

Regardless of what the purification of γ looks like when Eve's mode has been included, it is always possible for Eve to find a measurement (such as a projection onto an infinitely hot thermal state) to return the Gaussian state shared by Alice and Bob to the form (6.46). The classical noise matrix cannot increase the classical mutual information of Alice's and Bob's shared classical probability distribution after they perform local measurements on this state, and so they can only ever achieve the levels of communication that they would acquire from a Gaussian product state. Therefore, the measure yields zero on separable states.

Invariance under local symplectic operations

At present we cannot show that the Gaussian Intrinsic Information is non-increasing under Gaussian local operations and classical communication (GLOCC) in general but we can show the non-trivial result that the Gaussian Intrinsic Information μ_G is invariant under local symplectic operations. This is equivalent to saying that μ_G neither increases nor decreases under the influence of local Gaussian unitary operations. To show this, we begin with the covariance matrix γ' of a Gaussian state that is *not* in standard form. γ' can be put into standard form γ by local symplectic operations, so

$$\gamma = \begin{pmatrix} t_A & 0 \\ 0 & t_B \end{pmatrix} \gamma' \begin{pmatrix} t_A^T & 0 \\ 0 & t_B^T \end{pmatrix} \tag{6.47}$$

where $t_j \Omega t_j^T = \Omega$, $j = A, B$. The purification of the state takes the form

$$\gamma'_\pi = \begin{pmatrix} \left(t_A^{-1} \oplus t_B^{-1}\right) \gamma \left(\left(t_A^T\right)^{-1} \oplus \left(t_B^T\right)^{-1}\right) & \left(t_A^{-1} \oplus t_B^{-1}\right) \beta \\ \beta^T \left(\left(t_A^T\right)^{-1} \oplus \left(t_B^T\right)^{-1}\right) & \nu_A \mathbb{1} \oplus \nu_B \mathbb{1} \end{pmatrix} \tag{6.48}$$

(c.f. equation (6.20)) where we have used the inversion of (6.47) to replace γ' in γ'_π. The measurements performed by Alice and Bob, Γ'_A and Γ'_B, can be chosen as

$$\Gamma'_A = t_A^{-1} \Gamma_A \left(t_A^T\right)^{-1}, \quad \Gamma'_B = t_B^{-1} \Gamma_B \left(t_B^T\right)^{-1}, \tag{6.49}$$

where Γ_A and Γ_B are the measurements they would have performed if the covariance matrix had been in standard form. That is the shift from γ to γ' is corrected for in the choice of measurements. The above modification to the purification γ'_π and the modification to the choice of measurements performed by Alice and Bob are then carried through as in Section 6.3 until we can define

$$\bar{\Sigma}' = \begin{pmatrix} \sigma'_A & \sigma'_{AB} & \sigma'_{AE} \\ \sigma'^{T'}_{AB} & \sigma'_B & \sigma'_{BE} \\ \sigma'^{T'}_{AE} & \sigma'^{T'}_{BE} & \sigma'_E \end{pmatrix} \tag{6.50}$$

in place of equation (6.36). In order to show the invariance of μ_G under local symplectic operations, we must show that

$$\frac{1}{2} \ln \left[\frac{\det \bar{\Sigma}'_{AE} \det \bar{\Sigma}'_{BE}}{\det \bar{\Sigma}' \det \bar{\Sigma}'_E} \right] = \frac{1}{2} \ln \left[\frac{\det \bar{\Sigma}_{AE} \det \bar{\Sigma}_{BE}}{\det \bar{\Sigma} \det \bar{\Sigma}_E} \right]. \tag{6.51}$$

To do this, we first note that $\sigma'_E = \sigma_E$ and so $\det \bar{\Sigma}'_E = \det \bar{\Sigma}_E$. We then note that $\sigma'_{AE} = t_A^{-1} \sigma_{AE}$ and $\sigma'_A = t_A^{-1} \sigma \left(t_A^T\right)^{-1}$. As a consequence,

$$\begin{aligned} \det \bar{\Sigma}'_{AE} &= \det \sigma'_A \det \left[\sigma'_E - \sigma'^{T'}_{AE} \left(\sigma'_A\right)^{-1} \sigma'_{AE} \right] \\ &= \det \sigma'_A \det \left[\sigma_E - \sigma_{AE}^T \left(t_A^{-1}\right)^T t_A^T \sigma_A^{-1} t_A t_A^{-1} \sigma_{AE} \right] \\ &= \det \sigma_A \det \left[\sigma_E - \sigma_{AE}^T \sigma_A^{-1} \sigma_{AE} \right] \\ &= \det \bar{\Sigma}_{AE}, \end{aligned} \tag{6.52}$$

where in the second and third lines we have used the fact that $\sigma'_A = t_A^{-1} \sigma_A \left(t_A^T\right)^{-1}$ and that $\det t_A = \det t_A^{-1} = 1$ as t_A is a symplectic matrix. Exactly the same argument can be used to show that $\det \bar{\Sigma}'_{BE} = \det \bar{\Sigma}_{BE}$ and a similar argument can be used to show that $\det \bar{\Sigma}' = \det \bar{\Sigma}$. Thus equation (6.51) holds and the measure is invariant under local symplectic operations. We are therefore justified in assuming that the covariance matrix of the Gaussian state under examination is provided in standard form.

Comments on optimisation of the measure

It is unknown at this time whether it is possible to commute the order of maximisation and minimisation in equation (6.19). In the definition of Gaussian Intrinsic Information, it is necessary to first optimise over Eve's post-processing, as in the definition of intrinsic information

in (6.9). One then must maximise over the measurements that Alice and Bob perform, and finally minimise over the measurement that Eve performs in the first place. It certainly seems as though the minimisation and maximisation should be commuted as this is in the spirit of what the measure means in quantum cryptography. Eve first does everything in her power to distort the quantum state shared by Alice and Bob so as to minimise the correlations they share. Alice and Bob then wish to perform measurements to make the best of what they are left with.

If we assume that the minimisation and maximisation in the definition (6.19) can be reversed, that is $\tilde{\mu}_G(\hat{\rho}_{AB}) = \mu_G(\hat{\rho}_{AB})$ where

$$\tilde{\mu}_G(\hat{\rho}_{AB}) = \max_{\{\hat{\Pi}_A^G, \hat{\Pi}_B^G\}} \left(\min_{\hat{\Pi}_E^G} \left(\mathcal{I}(A:B \downarrow E) \right) \right), \tag{6.53}$$

then we can say a lot more about the optimisation. Significantly, as far as Alice and Bob's measurements are concerned we can restrict to pure covariance matrices in Γ_A and Γ_B (see Appendix C). When optimising over Eve's measurement with covariance matrix Γ'_E followed by the Gaussian post-processing $E \to \bar{E}$ with classical covariance matrix χ as in (6.28), we must distinguish between three different cases.

Case 1: C is regular

In this case, C^{-1} exists. The measurement Γ'_E and post-processing is equivalent to another measurement with covariance matrix

$$\tilde{\Gamma}_E = \Gamma'_E + \delta \left(C^T\right)^{-1} \zeta C^{-1} \delta - \delta. \tag{6.54}$$

That means that the post-processing is incorporated into the measurement itself. We can then simply perform minimisation over $\tilde{\Gamma}_E$ of the CCM

$$\tilde{\sigma}_{AB}^{\text{cond}} = \Gamma_A \oplus \Gamma_B + \tilde{\tau}_{AB}, \tag{6.55}$$

where

$$\tilde{\tau}_{AB} = \begin{pmatrix} \gamma_A & \gamma_{AB} \\ \gamma_{AB}^T & \gamma_B \end{pmatrix} - \begin{pmatrix} \gamma_{AE} \\ \gamma_{BE} \end{pmatrix} \left(\gamma_E + \tilde{\Gamma_E}\right)^{-1} \begin{pmatrix} \gamma_{AE} \\ \gamma_{BE} \end{pmatrix}^T, \tag{6.56}$$

and then maximise with respect to Γ_A and Γ_B. The measure would then read

$$\tilde{\mu}_G(\hat{\rho}_{AB}) = \max_{\{\hat{\Pi}_A^G, \hat{\Pi}_B^G\}} \left(\min_{\hat{\Pi}_E^G} \frac{1}{2} \ln \left[\frac{\det \tilde{\sigma}_A^{\text{cond}} \det \tilde{\sigma}_B^{\text{cond}}}{\det \tilde{\sigma}_{AB}^{\text{cond}}} \right] \right) \tag{6.57}$$

where $\tilde{\sigma}_A^{\text{cond}}$ and $\tilde{\sigma}_B^{\text{cond}}$ are the reduced covariance matrices of $\tilde{\sigma}_{AB}^{\text{cond}}$. Due to the monotonicity of the logarithm, we can optimise over just the argument

$$g = \frac{\det \tilde{\sigma}_A^{\text{cond}} \det \tilde{\sigma}_B^{\text{cond}}}{\det \tilde{\sigma}_{AB}^{\text{cond}}}, \tag{6.58}$$

and then

$$\tilde{\mu}_G(\hat{\rho}_{AB}) = \frac{1}{2} \ln [g_{\text{opt}}] \tag{6.59}$$

where, of course, $g_{\text{opt}} = \max_{\{\hat{\Pi}_A^G, \hat{\Pi}_B^G\}} \left(\min_{\hat{\Pi}_E^G} g \right)$.

Case 2: The matrix $C = 0$

In this case the final classical distribution, characterised by $\bar{\Sigma}$, takes the same form as it does for the pure states and $P(d_A, d_B | d_{\bar{E}}) = P(d_A, d_B)$. Consequently, this implies that $\mathcal{I}\left(A:B|\bar{E}\right) = \mathcal{I}(A:B)$.

Case 2 is in fact fully incorporated into Case 1 already. If Eve performed a measurement onto a mixed state $\tilde{\Gamma}_E = (1 + 2\langle \hat{n} \rangle)\mathbb{1}$, which corresponds to the product of two identical thermal states, but it was infinitely hot ($\langle \hat{n} \rangle \to \infty$) then the measurement has the same effect as if she had never performed a measurement in the first place. That is, no knowledge is gained from

$\tilde{\Gamma}_E$ and consequently the conditional probability distributions of Alice and Bob are unaffected, which is what happens when $C = 0$.

Case 3: $C \neq 0$ is singular

The most complicated case is when C is singular but not given by a matrix of zeros. If γ is a covariance matrix for a two mode Gaussian state then C must be a 4×4 matrix in the most general case. It is not known how to treat this at this time.

However, in the case of GLEMS, which can be purified by adding a single mode, we can find a reasonable expression for g in equation (6.58). This shall be explored in the next subsection.

Gaussian Least Entangled Mixed States for given local and global purities (GLEMS)

Two mode Gaussian Least Entangled Mixed States for given local and global purities (GLEMS) have two symplectic eigenvalues, one of which is equal to 1. That is $\nu_A > \nu_B = 1$ and $\nu_A = \sqrt{\det \gamma}$. GLEMS can be purified by a single Gaussian mode, and could always be transformed by symplectic operations to a form in which mode B is a vacuum and modes A and E form a two mode squeezed vacuum [176]. The matrix χ in equation (6.28) is a 4×4 positive semidefinite matrix that can be transformed by local symplectic operations into the standard form with $\delta = d\mathbb{1}$, $\zeta = b\mathbb{1}$ and $C = \mathrm{diag}\,(c_1, c_2)$ where $c_1 \geq |c_2| \geq 0$. For singular C we thus have $c_1 > 0$ and $c_2 = 0$, which gives

$$(\gamma_E + \Gamma'_E)^{-1} C\zeta C^T (\gamma_E + \Gamma'_E)^{-1} = U \begin{pmatrix} \bar{\nu} & 0 \\ 0 & 0 \end{pmatrix} U^T \tag{6.60}$$

where we have used the fact that $\gamma_E = \nu_A \mathbb{1}$ and U denotes the matrix diagonalising Γ'_E (and therefore also $\gamma_E + \Gamma'_E$). If $\Gamma'_E = \tau U \mathrm{diag}\left(e^{2r}, e^{-2r}\right) U^T$, where τ is the symplectic eigenvalue of Γ'_E then

$$\bar{\nu} = \frac{c_1^2}{bd^2} \sqrt{\frac{\nu_A + \tau e^{-2r}}{\nu_A + \tau e^{2r}}} \tag{6.61}$$

where $d = \sqrt{(\nu_A + \tau e^{2r})(\nu_A + \tau e^{-2r})}$.

We would like to know whether in this case the post-measurement processing could conceivably be swallowed up by the measurement itself. We can see this by assuming that Eve's subsystem is sent to a balanced beamsplitter and combined with a mixed Gaussian state with covariance matrix

$$\tilde{\Gamma}^t_E = U \begin{pmatrix} e^{-2t} + \bar{\nu} - \nu_A & 0 \\ 0 & e^{2t} \end{pmatrix} U^T \tag{6.62}$$

where $\bar{\nu} - \nu_A$ is a non-negative number necessarily greater than or equal to τ from (6.61). The distribution $\tilde{\Gamma}^t_E$ can be viewed as a rotated squeezed vacuum with noise added onto one of the quadratures. If Eve then performs homodyne measurements on the resulting state then we find that

$$\left(\gamma_E + \tilde{\Gamma}^t_E\right)^{-1} \to U \begin{pmatrix} \bar{\nu} & 0 \\ 0 & 0 \end{pmatrix} U^T$$

in the limit of $t \to \infty$ and so the action of the channel χ can be incorporated into the measurement process.

With this knowledge we can derive a different formula for g_{opt} for GLEMS, at least in the case where in the definition of γ we have $bc_+ + ac_- \neq 0$. In this case we can incorporate Eve's post measurement processing with her measurement into the POVM $\tilde{\Gamma}_E = \tau U(\phi) V(r) U^T(\phi)$, where $\tau \geq 1$ is the symplectic eigenvalue of $\tilde{\Gamma}_E$, and

$$U(\phi) = \begin{pmatrix} \cos\phi & -\sin\phi \\ \sin\phi & \cos\phi \end{pmatrix}, \quad V(r) = \begin{pmatrix} e^{2r} & 0 \\ 0 & e^{-2r} \end{pmatrix} \tag{6.63}$$

where $\phi \in [0, \pi)$ and $r \in [0, \infty)$. This collapses mode A into the Gaussian state with covariance matrix

$$\gamma_A^{\mathrm{cond}} = U^T(\phi) \begin{pmatrix} \frac{\nu_A \tau e^{2r} + 1}{\nu_A + \tau e^{2r}} & 0 \\ 0 & \frac{\nu_A \tau e^{-2r} + 1}{\nu_A + \tau e^{-2r}} \end{pmatrix} U(\phi) \tag{6.64}$$

and $\tilde{\sigma}_{AB}^{\text{cond}}$ in equation (6.55) becomes

$$\tilde{\sigma}_{AB}^{\text{cond}} = S^{-1}\left(\gamma_A^{\text{cond}} \oplus \mathbb{1}\right)\left(S^{-1}\right)^T \tag{6.65}$$

where the matrix S can be found using the recipe in Appendix B. If we express the inverse of the symplectic matrix with respect to $A|B$ splitting as

$$S^{-1} = \begin{pmatrix} s_{AA} & s_{AB} \\ s_{BA} & s_{BB} \end{pmatrix} \tag{6.66}$$

then we obtain the quantity $g \equiv g_{GLEMS}$ as

$$g_{GLEMS} = \frac{\left(\det s_{AA}\right)^2 \left(\det s_{BA}\right)^2 \det X \det Y}{\det Z} \tag{6.67}$$

where

$$\begin{aligned} X = &\quad \gamma_A^{\text{cond}} + s_{AA}^{-1}\left(s_{AB}s_{AB}^T + \Gamma_A\right)\left(s_{AA}^T\right)^{-1} \\ Y = &\quad \gamma_A^{\text{cond}} + s_{BA}^{-1}\left(s_{BB}s_{BB}^T + \Gamma_B\right)\left(s_{BA}^T\right)^{-1} \\ Z = &\quad \left(\gamma_A^{\text{cond}} \oplus \mathbb{1}\right) + S\left(\Gamma_A + \Gamma_B\right)S^T. \end{aligned} \tag{6.68}$$

The optimal argument, g_{opt} is then obtained by minimising this function with respect to τ, r and ϕ and then maximising with respect to pure covariance matrices Γ_A and Γ_B.

6.5 Summary of Chapter 6

We have introduced a potential entanglement measure for Gaussian states. Importantly, it is still vital that we prove that μ_G is non-increasing under GLOCC operations, although it is invariant with respect to local symplectic operations. The quantity is zero on separable states and reduces to a simple expression on pure states. Some simplifications to the expression can be found and it is thought that equation (6.53) holds in general.

It also has an operational interpretation borrowed from the realm of quantum cryptography. Alice, Bob and Eve possess a pure state from which Alice and Bob wish to create a classical probability distribution about which Eve knows nothing, in order to create a secret key. Eve wishes to minimise the amount of secret correlations that Alice and Bob can share by performing a special measurement on her subsystem and locally processing the result classically. The measure is then an upper bound on the secret key rate $\mathcal{K}\left(A:B|E\right)$, and thus in a sense gives a limit on how much classical secrecy Alice and Bob can achieve from the shared quantum state.

This is an ongoing work but looks very promising.

Part III

Beyond Entanglement

Chapter 7

Non-classicality Indicators

When the foundations of modern quantum theory were laid, there were many competing schools of thought on how best to interpret the differences between observations on a classical and quantum level. The apparent victor was Niels Bohr with the Copenhagen Interpretation, which argues that a quantum system may be completely described by a wavefunction representing the state of the system, which may vary gradually in time but collapses suddenly upon measurement of an observable. That is, the measurement of some observable quantity of a physical system causes an instantaneous change in the state of the system, unless the state prior to the measurement is an eigenstate of the observable.

Attempting to challenge Bohr, Einstein *et al.* [52] introduced the notion of quantum entanglement, with the aim of showing the incompleteness of quantum mechanics. As has been seen in previous chapters, they failed. Overwhelming evidence of quantum entanglement has been seen in the lab, and it is now a vital piece of kit for the quantum information toolbox. Non-classical correlations exist.

It is perhaps unsurprising that an information theoretic approach was opted as a surefire way to explore entanglement, and as has been seen in previous chapters, has had a lot of success. Interestingly, with these information quantities, signatures of correlations having no classical counterpart can be traced even in separable states, but their nature is very different from entanglement. In fact, while entanglement can be seen as a consequence of the superposition principle, more general forms of non-classical correlations arise essentially from the non-commutativity of quantum observables. When speaking about composite systems, separable states are often perceived as essentially classical. However, *truly* classical states represent just a small subset of separable states [177]. Moreover, it is also possible to show that almost all separable states possess a finite amount of non-classical correlations. This has fuelled a still unsettled debate, and an active stream of research, to decide whether separable states containing non-classical correlations can also be directly useful for quantum information tasks.

These non-classical correlations beyond entanglement are thought to assist in some protocols. For instance, the DQC1 protocol [178, 179] allows for a computation that gives an exponential speedup for the computation of the normalised trace of a unitary operator $2^{-n}\mathrm{Tr}\left[U_n\right]$. It is also conjectured that nonclassicality measures could account for the distribution of entanglement between two spatially separated quantum systems via an ancillary state that is separable at all times [180, 181, 182, 183] (the state is tripartite entangled but separable with respect to the bipartition of the ancilla).

More recently, a zoology of indicators of non-classical correlations have been introduced, and in the following chapters we play an active role in this field by examining the strength and legitimacy of these measures. At the forefront of these is the Quantum Discord, which shall be discussed in some detail in Section 7.1. The primary position of quantum discord is essentially due to it being the chronological leader, but other measures have also been defined. The properties of these shall be discussed in Section 7.5.

Researchers have also come to inquire about the relationship between these non-classicality measures and quantum entanglement. Are they perhaps two sides of the same coin? This trail of thought shall be followed, although it is still very much an open question.

In what follows, the quantum discord shall be introduced. A feverish attempt has been made by researchers trying to establish its credentials in the case of finite dimensional systems,

and some interesting results have been found. An introduction will be presented here in order to give a flavour of the parallels that can be drawn between discord and entanglement. Other non-classicality measures will also be introduced. The extension to continuous variable systems is not straightforward, due an inherent optimization problem. It is a primary aim of this thesis to advance into this unknown realm, as will be seen in Chapters 8 and 9.

7.1 Quantum Discord

Definition

Let us first consider the classical scenario with two distinct random variables A and B with well defined probability distributions p_A and p_B respectively. The joint probability distribution p_{AB} is related to the other two as $p_B = \sum_a p_{A=a,B}$ and $p_A = \sum_b p_{A,B=b}$. Shannon [184] introduced the classical mutual information

$$\mathcal{I}(A:B) = \mathcal{H}(p_A) + \mathcal{H}(p_B) - \mathcal{H}(p_{AB}) \tag{7.1}$$

with $\mathcal{H}(p_{\mathcal{X}}) = -\sum_x p_{\mathcal{X}=x} \log[p_{\mathcal{X}=x}]$ being the Shannon entropy. The base of the logarithm is often taken to be base 2 when discussing bits. When discussing continuous variables the natural log will be used.

The Shannon entropy represents the uncertainty of a single random event. Loosely speaking, we could consider how many decimal digits are required to communicate a given number e.g. 8520. The number of digits is roughly the logarithm of the number (base 10 for decimal digits) of the number we wish to communicate. With this thought in mind, the meaning of the Shannon entropy is the expectation value of the number of decimal digits (if log is taken to base 10) required to communicate distribution $p_{\mathcal{X}}$. The classical mutual information $\mathcal{I}(A:B)$ then tells the reduction in uncertainty of one random variable, given the knowledge of the other.

In actual fact, the Shannon entropy can be thought of as the classical equivalent of the von-Neumann entropy, which was put forward almost 20 years earlier [6]. However, Shannon is usually credited as being the father of information theory.

In the continuous variable setting, one can define similar quantities. For a probability density function $f(x)$, the differential entropy (which shall also be denoted $\mathcal{H}$ as they have almost the same properties) can be defined as [185]

$$\mathcal{H}(\mathcal{X}) = \int f(x) \log[f(x)]\, dx. \tag{7.2}$$

This allows the classical mutual information to be defined in the same way as before. Returning to the discrete case, one can use Bayes rule,

$$p_{A|B=b} = \frac{p_{A,B=b}}{p_{B=b}} \tag{7.3}$$

which identifies the probability distribution of one random variable outcome given a measurement of the other, to rewrite the quantum mutual information as

$$\mathcal{J}_c(A:B) = \mathcal{H}(p_A) - \mathcal{H}(A|B) \tag{7.4}$$

where $\mathcal{H}(A|B) = \sum_b p_{B=b} \mathcal{H}\left(p_{A|B=b}\right)$ is the *conditional entropy* of A given B. A different symbol $\mathcal{J}_c$ has been used for reasons that will shortly become apparent. Due to the symmetry of $\mathcal{I}(A:B)$, we can also equivalently write

$$\mathcal{J}_c(A:B) = \mathcal{H}(p_B) - \mathcal{H}(B|A). \tag{7.5}$$

This holds for the differential entropy case as in general $f(x|y) = f(x,y)/f(y)$.

Ollivier and Zurek [7] examined what happens when one generalises the concept of mutual information to quantum systems. Naturally one chooses to do this by replacing the classical Shannon entropy with the von-Neumann entropy $\mathcal{S}$ and the probability distribution $p_{\mathcal{X}}$ with the probability density matrix $\hat{\rho}_{\mathcal{X}}$. The quantum mutual information is then written as

$$\mathcal{I}_q(\hat{\rho}_{AB}) = \mathcal{S}(\hat{\rho}_A) + \mathcal{S}(\hat{\rho}_B) - \mathcal{S}(\hat{\rho}_{AB}) \tag{7.6}$$

where $\hat{\rho}_A = \mathrm{Tr}_B[\hat{\rho}_{AB}]$ etc. The quantum version $\mathcal{I}_q$ was initially used to study entanglement [186] and rediscovered a few years later [187]. While the definition (7.6) is formally simple, an operational interpretation for the quantity itself was missing until 2005 when Groisman, Popescu and Winter [188] showed it could be interpreted as the total correlations in a bipartite state $\hat{\rho}_{AB}$, as measured by the asymptotically minimal amount of local noise one has to add to turn it into a product state.

The translation to the quantum world of $\mathcal{J}_c(A:B)$ is not such a trivial task. The conditional entropy term in (7.5) requires us to specify the state of A given a measurement on B. Such a statement is ambiguous in quantum theory until the to-be-measured set of states B is selected.

For any bipartite state $\hat{\rho}_{AB}$ whose correlations are purely classical, the mutual information can be equivalently expressed as

$$\begin{aligned} \mathcal{J}^{\leftarrow}(\hat{\rho}_{AB}) &= \mathcal{S}(\hat{\rho}_A) - \inf_{\{\hat{\Pi}_i\}} \mathcal{H}_{\{\hat{\Pi}_i\}}(A|B)\,, \\ \mathcal{J}^{\rightarrow}(\hat{\rho}_{AB}) &= \mathcal{S}(\hat{\rho}_B) - \inf_{\{\hat{\Pi}_i\}} \mathcal{H}_{\{\hat{\Pi}_i\}}(B|A)\,, \end{aligned} \tag{7.7}$$

with $\mathcal{H}_{\{\hat{\Pi}_i\}}(A|B) \equiv \sum_i p_i \mathcal{S}(\hat{\rho}^i_{A|B})$ being the quantum conditional entropy[1] associated with the post-measurement density matrix $\hat{\rho}^i_{A|B} = \mathrm{Tr}_B[\hat{\Pi}_i\hat{\rho}_{AB}]/p_i$, obtained upon performing the POVM $\{\hat{\Pi}_i\}$ on system B (p_i=Tr$[\hat{\Pi}_i\hat{\rho}_{AB}]$). The optimization over POVMs is necessary to single out the least disturbing measurement to be performed on one subsystem, so that the change of entropy on the other subsystem yields a quantifier of the correlations between the two parts. Notice that the subscript c of (7.5) has been dropped, and arrows have been introduced to denote on which subsystem the measurement has been performed. In general $\mathcal{I}_q \geq \mathcal{J}^{\leftarrow}, \mathcal{J}^{\rightarrow}$ and $\mathcal{J}$ shall be referred to as *one way classical correlation* from now on.

Such a discrepancy is now recognised as a signature of non-classicality of the correlations of $\hat{\rho}_{AB}$ and the difference between the total correlations $\mathcal{I}_q$ and one way classical correlations defines what Ollivier and Zurek baptized as the[2] *quantum discord*,

$$\begin{aligned} \mathcal{D}^{\leftarrow}(\hat{\rho}_{AB}) &= \mathcal{I}_q(\hat{\rho}_{AB}) - \mathcal{J}^{\leftarrow}(\hat{\rho}_{AB}) \qquad (7.8) \\ &= \mathcal{S}(\hat{\rho}_B) - \mathcal{S}(\hat{\rho}_{AB}) + \inf_{\{\hat{\Pi}_i\}} \mathcal{H}_{\{\hat{\Pi}_i\}}(A|B)\,; \\ \mathcal{D}^{\rightarrow}(\hat{\rho}_{AB}) &= \mathcal{I}_q(\hat{\rho}_{AB}) - \mathcal{J}^{\rightarrow}(\hat{\rho}_{AB}) \qquad (7.9) \\ &= \mathcal{S}(\hat{\rho}_A) - \mathcal{S}(\hat{\rho}_{AB}) + \inf_{\{\hat{\Pi}_i\}} \mathcal{H}_{\{\hat{\Pi}_i\}}(B|A)\,.. \end{aligned}$$

The quantum discord as defined above is necessarily asymmetric. A symmetrised version, or "two-way quantum discord" can be defined as

$$\mathcal{D}^{\leftrightarrow}(\hat{\rho}_{AB}) = \max\left\{\mathcal{D}^{\leftarrow}(\hat{\rho}_{AB}), \mathcal{D}^{\rightarrow}(\hat{\rho}_{AB})\right\} \tag{7.10}$$

and in this form becomes vanishing if and only if a state is purely classically correlated [192].

The introduction of the quantum discord was little recognised at its advent. In fact Henderson and Vedral [193] independently advocated the one way classical correlation (7.7) as a gauge of non-classicality.

Key Properties of Quantum Discord

With the suggestion that discord was responsible for the speedup of DQC1 [8] over classical algorithms, a flurry of activity was initiated into the properties of discord. Dakic, Vedral &

[1] As can be seen by different approaches (e.g. [189, 190]) the concept of one way classical correlation, and in turn, the quantum discord, is dependent on a particular idea of how to translate the classical conditional entropy in (7.5), $\mathcal{H}(A|B)$ into the quantum regime. If instead we made the leap $\mathcal{H}(A|B) = \mathcal{H}(p_{AB}) - \mathcal{H}(p_B) \rightarrow \mathcal{S}(\hat{\rho}_{A|B}) = \mathcal{S}(\hat{\rho}_{AB}) - \mathcal{S}(\hat{\rho}_A)$ then things would be different. This possible definition of quantum conditional entropy also has an interpretation in quantum information theory [191]. This quantity is troubling as it can be negative on entangled states, in stark contrast to the classical conditional entropy. The negative of this quantity is known as *coherent information*. O the road not taken!

[2] In the original paper by Ollivier and Zurek [7], concerning qubit systems, only projective measurements were performed, and there was no optimisation over measurement bases in the definition. However the form (7.8) has now evolved into the standard definition of quantum discord.

Brukner [194], and independently Datta [195] found necessary and sufficient conditions on a finite dimensional state $\hat{\rho}_{AB}$ for the discord to be zero. They arrived at these by different considerations. As a result, for a state $\hat{\rho}_{AB}$,

$$\mathcal{D}^{\leftarrow}(\hat{\rho}_{AB}) = 0 \quad \text{if} \quad \hat{\rho}_{AB} = \sum_i p_i |i\rangle\langle i| \otimes \hat{\rho}_{B,i} \quad \text{in basis diagonalising} \quad \hat{\rho}_A \tag{7.11}$$

$$\mathcal{D}^{\rightarrow}(\hat{\rho}_{AB}) = 0 \quad \text{if} \quad \hat{\rho}_{AB} = \sum_j p_j \hat{\rho}_{A,j} \otimes |j\rangle\langle j| \quad \text{in basis diagonalising} \quad \hat{\rho}_B \tag{7.12}$$

for some bases $\{|i\rangle\}$ and $\{|j\rangle\}$. Datta showed that $\hat{\rho}_{AB}$ has zero two-way discord if and only if the eigenvectors of the joint state are separable, which also gives a mathematical definition of pointer states - they are those with zero discord. Interestingly, the closed set of purely classically correlated states ($\mathcal{D} = 0$) have measure zero [177].

The quest is on to find upper bounds on the quantum discord [196]. A simple upper bound is given by

$$\mathcal{D}^{\leftarrow}(\hat{\rho}_{AB}) \leq \mathcal{S}(\hat{\rho}_B) \tag{7.13}$$

and recently, Xi *et al.* [197] found a sufficient and necessary condition on finite $\hat{\rho}_{AB}$ for this upper bound to be saturated. They showed that for two-qubit systems it could only ever be saturated by pure states. Some non-trivial bounds have been found for other classes of finite dimensional quantum states [198, 199].

In practice it is very difficult to compute the quantum discord of a generic quantum state due to the optimization over POVMs required. Analytic solutions have only ever been found for highly symmetric states in the qudit case [200, 201, 202, 203, 204]. There is currently no surefire way of finding the optimal measurement for an arbitrary two qubit state, although some progress has been made [205].

The effect of local operations and classical communication on quantum correlations beyond entanglement is an emerging area. Streltsov *et al.* [206] showed that in a mixed state with no quantum correlations, a local (non-unitary) operation could be performed on one of the subsystems and induce quantum correlations in the global state.

7.2 The Koashi-Winter Relation

Since the notion of quantum correlations beyond entanglement was put forward [7], the relations between non-classicality and entanglement have been a focal point of research. Parallels have been drawn between the properties of entanglement and the properties of discord.

Whilst classical correlations can be shared freely between many parties, quantum ones cannot. If a quantum system A is entangled to a quantum system B then there is a strict limit on the amount of entanglement that A or B can share with a third party C. If, in a finite dimensional system, A and B are maximally entangled, then neither A nor B can be entangled to C at all! This property was wryly given the sardonic title of *monogamy of entanglement*. However, if A and B are maximally entangled, then neither can even be classically correlated with C. Similarly, if A and B were perfectly classically correlated then both would be forbidden from being entangled to other systems.

In an impressive publication, Koashi and Winter [207] showed an extraordinary property relating the one way classical correlation (7.7) $\mathcal{J}^{\leftarrow}$ to the Entanglement of Formation, $\mathcal{E}_F$ (see Section 3.5). Consider a *pure* tripartite state $\hat{\rho}_{ABC}$ where as usual $\hat{\rho}_{AB} = \mathrm{Tr}_C[\hat{\rho}_{ABC}]$. Then visualise an ensemble $\{p_j, |\psi_j\rangle\}$ achieving the optimal decomposition required in the definition of $\mathcal{E}_F$ (Equation (3.33)). Then there must exist some measurement on subsystem C of $\hat{\rho}_{ABC}$ such that $\hat{\rho}_{AB} = \sum_j p_j |\psi_j\rangle\langle\psi_j|$.

By tracing out subsystem B this implies that there is a measurement on C applied to $\mathrm{Tr}_B[\hat{\rho}_{ABC}]$ that leaves state A in $\mathrm{Tr}_B[|\psi_j\rangle\langle\psi_j|]$. From the definition of the one way classical communication (7.7)

$$\begin{aligned} \mathcal{J}^{\leftarrow}(\hat{\rho}_{AC}) &\geq \mathcal{S}(\hat{\rho}_A) - \sum_j p_j \mathcal{E}_{v.N}(|\psi_j\rangle\langle\psi_j|) \\ &= \mathcal{S}(\hat{\rho}_A) - \mathcal{E}_F(\hat{\rho}_{AB}). \end{aligned} \tag{7.14}$$

Conversely, perform a measurement on C that minimises, in the definition of $\mathcal{J}^{\leftarrow}(\hat{\rho}_{AC})$, the conditional entropy term $\mathcal{H}_{\{\hat{\Pi}_i\}}(A|C)$. By careful consideration of the properties of the measurement, namely decomposing the measurements $\{\hat{\Pi}_i\}$ into rank one projectors $|\phi_j\rangle\langle\phi_j|$, it can be seen that

$$\mathcal{E}_F(\hat{\rho}_{AB}) \leq \mathcal{S}(\hat{\rho}_A) - \mathcal{J}^{\leftarrow}(\hat{\rho}_{AC}). \tag{7.15}$$

Putting (7.14) and (7.15) together yields the Koashi Winter relation

$$\mathcal{E}_F(\hat{\rho}_{AB}) + \mathcal{J}^{\leftarrow}(\hat{\rho}_{AC}) = \mathcal{S}(\hat{\rho}_A). \tag{7.16}$$

If we were to design a regularised version of the one way classical communication, termed usually the *distillable common randomness*

$$\mathcal{J}^{\leftarrow,\infty}(\hat{\rho}_{AC}) = \lim_{n\to\infty} \frac{\mathcal{J}^{\leftarrow}\left(\hat{\rho}_{AC}^{\otimes n}\right)}{n} \tag{7.17}$$

then a similar formula explains the monogamy relation in terms of the entanglement cost

$$\mathcal{E}_C(\hat{\rho}_{AB}) + \mathcal{J}^{\leftarrow,\infty}(\hat{\rho}_{AC}) = \mathcal{S}(\hat{\rho}_A). \tag{7.18}$$

The Koashi-Winter relation[3] also shows that the quantum discord's additivity is related to the additivity of the entanglement of formation i.e. it isn't additive [135]. Furthermore, Fanchini *et al.* [208] used this relation to show what they dubbed the "quantum conservation law" in a tripartite pure state:

$$\mathcal{E}_F(\hat{\rho}_{AB}) + \mathcal{E}_F(\hat{\rho}_{AC}) = \mathcal{D}^{\leftarrow}(\hat{\rho}_{AB}) + \mathcal{D}^{\leftarrow}(\hat{\rho}_{AC}) \tag{7.19}$$

Similarly, if one was to perform optimal measurements on subsystem C, the difference in discord with respect to the other subsystems can be expressed as

$$\mathcal{D}^{\leftarrow}(\hat{\rho}_{AC}) - \mathcal{D}^{\leftarrow}(\hat{\rho}_{BC}) = \mathcal{S}(\hat{\rho}_A) - \mathcal{S}(\hat{\rho}_B) \tag{7.20}$$

and there is also a chain rule [209] relating the discord of the three systems, given by

$$\mathcal{E}_F(\hat{\rho}_{AB}) = \mathcal{D}^{\leftarrow}(\hat{\rho}_{AB}) + \mathcal{D}^{\leftarrow}(\hat{\rho}_{BC}) - \mathcal{D}^{\rightarrow}(\hat{\rho}_{BC}). \tag{7.21}$$

It is worth noting that the Koashi-Winter relation is valid for continuous variable systems.

7.3 Physical Interpretation of the Quantum Discord

For a long time the quantum discord was an answer to a question that nobody knew. There was no physical interpretation of the functional. To this end, there have been two main approaches, firstly in terms of an analogy to thermodynamics and secondly from a purely information theoretic perspective. We shall begin with the latter.

Quantum State Merging and Quantum Discord

One operational interpretation of quantum discord emerged simultaneously and independently from two sources [210, 211], based on the quantum state merging protocol [212, 213]. A brief description shall be given of quantum state merging. A basic brick in classical information theory is the notion of partial information, which is a generalisation of the noisy coding theorem. One can ask: How many bits does the sender (Alice) need to send to transmit a message from the source, provided that the receiver (Bob) already has some prior information about the source. This amount of bits is called the *partial information*. Slepian and Wolf [214] showed that the partial information is equal to the entropy of the source reduced by the mutual information, which is equal to the classical conditional entropy $\mathcal{H}(A|B) = \mathcal{H}(p_{AB}) - \mathcal{H}(p_B)$.

[3]Remarkably, in the same article this relation was used to show that $\mathcal{E}(\hat{\rho}_{AB}) + \mathcal{E}(\hat{\rho}_{AC}) \leq \mathcal{E}\left(\hat{\rho}_{A,(BC)}\right)$ for entanglement measures $\mathcal{E}$ including the distillable entanglement $\mathcal{E}_D$, the squashed entanglement $\mathcal{E}_{sq}$ and the distillable secret key.

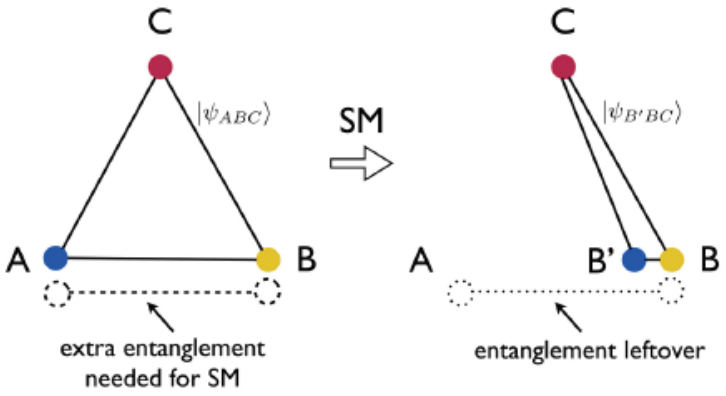

Figure 7.1: Pure state $|\psi\rangle_{ABC}$ is shared by Alice, Bob and Charlie. Alice attempts to transfer her state to Bob using LOCC and extra entanglement if necessary. Extended state merging takes into account the initial resources required in building the initial states between A and B also. Figure reproduced from [211]. Copyright (2011) by The American Physical Society.

Horodecki *et al.* [212] asked a similar question for the quantum case. Consider a source, emitting unknown pure bipartite states $\{|\psi_1\rangle_{AB}, |\psi_2\rangle_{AB}, \cdots\}$ from a distribution with average density matrix $\hat{\rho}_{AB}$. The density matrix $\hat{\rho}_{AB}$ is known to Alice and Bob but they do not know the constituents - for any given state they possess, the state is unknown, but the statistics of the source are. How much quantum communication is required for Alice to transfer her part of the unknown sequence of states $\{|\psi_1\rangle_{AB}, |\psi_2\rangle_{AB}, \cdots\}$ to Bob's location?

It can more elegantly be examined in a different way. Given a source $|\psi\rangle_{ABC}$, the purification of $\hat{\rho}_{AB}$ (i.e. $\hat{\rho}_{AB} = \mathrm{Tr}_C\left[|\psi\rangle_{ABC}\langle\psi|\right]$), how much quantum information is required for Alice to transfer her part of the state to Bob whilst maintaining coherence with Charlie?

By acting on n copies of $|\psi\rangle_{ABC}$, they aim to end up in a state close to $|\psi\rangle^{\otimes n}_{B'BC}$ which is exactly the same as n copies of $|\psi\rangle_{ABC}$ except that what was initially Alice's part of the state is now well and truly in Bob's capable hands. Moreover, errors are allowed but must vanish in the asymptotic limit $n \to \infty$.

Alice and Bob may use extra, pre-established two-qubit maximally entangled pairs (ebits), but these constitute a valuable resource and if consumed must be paid for. Local operations and classical communication are for free. The answer is that the optimal amount of information is

$$\mathcal{S}\left(A|B\right) = \mathcal{S}\left(\hat{\rho}_{AB}\right) - \mathcal{S}\left(\hat{\rho}_{B}\right), \tag{7.22}$$

per copy of the state, of ebits spent in the process. This quantity may then be positive or negative with the following implications:

- A positive value means that the entanglement must be consumed (and Alice transfers her part of the global state to Bob via teleportation).
- A negative value means that not only is no extra entanglement required, but also Alice and Bob retain $-\mathcal{S}\left(A|B\right)$ ebits per copy merged, which can be saved up for future use[4].

Cavalcanti *et al.* considered the following: Although Alice and Bob may get extra entangled resources to put away for a rainy day if $\mathcal{S}\left(A|B\right)$ is negative, they no longer share the starting entangled states. They defined the *total entanglement consumption*

$$\Gamma\left(A > B\right) := \mathcal{E}_F\left(\hat{\rho}_{AB}\right) + \mathcal{S}\left(A|B\right) \tag{7.23}$$

where $\mathcal{E}_F$ is the entanglement of formation of $\hat{\rho}_{AB}$. $\Gamma\left(A > B\right)$ quantifies the total entanglement consumed in state merging by taking into account the amount of entanglement Alice and Bob

[4]Quantum state merging has also been used to identify another entanglement measure, known as the *conditional entanglement of mutual information* [215]

would have needed to prepare $\hat{\rho}_{AB}$ by LOCC and "lost" during quantum state merging. That is, Equation (7.23) characterises the process of "extended state merging" in which firstly the state $\hat{\rho}_{AB}$ is created from maximally entangled states by LOCC, and then Alice's part is merged to Bob.

So how does this relate to discord? Rather trivially in fact. On examination, the discord of Alice's state, given a measurement by Charlie can be rewritten as

$$\mathcal{D}^{\leftarrow}\left(\hat{\rho}_{AC}\right) = \mathcal{J}^{\leftarrow}\left(\hat{\rho}_{AC}\right) - \mathcal{S}\left(A|C\right) \tag{7.24}$$

where $\mathcal{S}\left(A|C\right) = \mathcal{S}\left(\hat{\rho}_{AC}\right) - \mathcal{S}\left(\hat{\rho}_{C}\right)$. Next consider the Koashi-Winter relation for a pure tripartite system (7.16) relation for a tripartite pure state system, rewritten here

$$\mathcal{S}\left(\hat{\rho}_{B}\right) = \mathcal{E}_{F}\left(\hat{\rho}_{AB}\right) + \mathcal{J}^{\leftarrow}\left(\hat{\rho}_{BC}\right). \tag{7.25}$$

By substituting there the definition of $\mathcal{J}^{\leftarrow}\left(\hat{\rho}_{BC}\right)$ it is found that

$$\mathcal{E}_{F}\left(\hat{\rho}_{AB}\right) = \inf_{\{\hat{\Pi}_i\}} \mathcal{H}_{\{\hat{\Pi}_i\}}(B|C) = \inf_{\{\hat{\Pi}_i\}} \mathcal{H}_{\{\hat{\Pi}_i\}}(A|C). \tag{7.26}$$

Substituting this into the definition of quantum discord (Equation (7.8)) and noting that as $\hat{\rho}_{ABC}$ is pure, $\mathcal{S}\left(\hat{\rho}_{AC}\right) = \mathcal{S}\left(\hat{\rho}_{B}\right)$ and $\mathcal{S}\left(\hat{\rho}_{C}\right) = \mathcal{S}\left(\hat{\rho}_{AB}\right)$ we obtain

$$\mathcal{D}^{\leftarrow}\left(\hat{\rho}_{AC}\right) = \mathcal{E}_{F}\left(\hat{\rho}_{AB}\right) + \mathcal{S}\left(\hat{\rho}_{AB}\right) - \mathcal{S}\left(\hat{\rho}_{B}\right) = \Gamma\left(A > B\right). \tag{7.27}$$

That is, the discord between Alice and Charlie (measurement on C) is equal to the total entanglement consumption in an extended state merging protocol from Alice to Bob. The asymmetry of the discord can be interpreted as the different resources required for Charlie to merge his state to Bob from what Alice required.

To be more consistent with the concept of state merging, it is beneficial to use Equation (7.17) to define a regularised quantum discord

$$\mathcal{D}^{\leftarrow,\infty}\left(\hat{\rho}_{AB}\right) = \lim_{n\to\infty} \frac{\mathcal{D}^{\leftarrow}\left(\hat{\rho}_{AB}^{\otimes n}\right)}{n} \tag{7.28}$$

and it follows that

$$\mathcal{D}^{\leftarrow,\infty}\left(\hat{\rho}_{AB}\right) = \Gamma^{\infty}\left(A > B\right) \tag{7.29}$$

where $\Gamma^{\infty}\left(A > B\right)$ is a regularised version of the total entanglement consumption, defined in the usual way.

Madhok and Datta [210] took a slightly different approach. For a tripartite system

$$\mathcal{S}\left(A|BC\right) \leq \mathcal{S}\left(A|B\right). \tag{7.30}$$

Simply put, from the point of view of the state merging protocol, having more prior information makes state merging cheaper. If Bob does not acknowledge Charlie's system, then state merging is more expensive. Madhok and Datta assumed that initially Charlie's state is $|0\rangle$ (pure). As $|\psi\rangle_{ABC}$ is pure globally, $\mathcal{S}\left(\hat{\rho}_{AB}\right) = \mathcal{S}\left(\hat{\rho}_{ABC}\right)$. A unitary interaction then occurs between B and C. After the interaction the global state is still pure and denoted $|\psi\rangle_{ABC}$ Similarly, $\mathcal{I}_{q}\left(\hat{\rho}_{A,BC}\right) = \mathcal{I}_{q}\left(\hat{\rho}_{A',B'C'}\right)$ and $\mathcal{I}_{q}\left(\hat{\rho}_{A',B'}\right) \leq \mathcal{I}_{q}\left(\hat{\rho}_{A',B'C'}\right)$. Then

$$\mathcal{S}\left(A|B\right) = \mathcal{S}\left(\hat{\rho}_{A}\right) - \mathcal{I}_{q}\left(\hat{\rho}_{AB}\right) = \mathcal{S}\left(\hat{\rho}_{A}\right) - \mathcal{I}_{q}\left(\hat{\rho}_{A,BC}\right) = \mathcal{S}\left(A|BC\right). \tag{7.31}$$

Thus one could always view the cost of merging Alice's state to Bob's as the cost of merging A with B & C together. If Charlie's system is then discarded,

$$\mathcal{I}_{q}\left(\hat{\rho}_{A'B'}\right) \leq \mathcal{I}_{q}\left(\hat{\rho}_{A',B'C'}\right) = \mathcal{I}_{q}\left(\hat{\rho}_{A,BC}\right) = \mathcal{I}_{q}\left(\hat{\rho}_{AB}\right). \tag{7.32}$$

The difference $\mathcal{I}_{q}\left(\hat{\rho}_{AB}\right) - \mathcal{I}_{q}\left(\hat{\rho}_{A'B'}\right)$ reduces to the quantum discord when optimized. Discord, then, is the minimum possible increase in the cost of quantum communication in order to perform state merging, when a measurement is performed on the party receiving the final state.

Quantum discord and Maxwell's Demon

In an attempt to understand the limitations of thermodynamics, Maxwell introduced a character (today named Maxwell's demon) that has been summoned regularly in many areas of physics. Maxwell's demon was initially invoked to demonstrate that the second "law" of thermodynamics was in fact a statistical principle that holds most of the time but is not is an absolute law.

The simplified version of the thought experiment [216], put forward by Szilárd [217] is as follows: Imagine a molecule in a box, freely able to move in a volume $\mathcal{V}$. A partition is inserted and Maxwell's demon observes whether the molecule is in the left half or right half. On the side of the box in which the molecule sits, the demon inserts a piston coupled to a load in place of the partition. The box is then put in contact with a thermal reservoir and the one molecule gas expands isothermally until, once again, the volume in which it can travel is the original $\mathcal{V}$. The expansion has lifted the load and the demon can continuously repeat this process, turning heat from the reservoir into pure work in clear violation of the second law.

Landauer's principle "exorcised" Maxwell's demon with his erasure principle. Szilárd's engine is not a complete cycle until the knowledge of which side of the partition the molecule was on is erased. The answer to the paradox then becomes clear: the missing work resides in the demon's memory, and the demon must clear his head for the cycle to be complete. The cost of erasing is proportional to the entropy of the probability distribution resulting from the demon's measurements.

Zurek [218] considered the quantum version with Szilárd's engine S in contact with a thermal reservoir at constant temperature ($k_B T = 1$), expanding through a Hilbert space of volume d_S. The demon's observations are performed on apparatus A and the combined state is $\hat{\rho}_{SA}$ (dimension $d_S d_A$). Zurek showed that a "classical" demon, only able to perform local measurements and gain information about the apparatus, would only be able to retrieve a maximum net work of

$$W^C = \log\left[d_S d_A\right] - \mathcal{S}\left(\hat{\rho}_A\right) + \inf_{\{\hat{\Pi}_i\}} \mathcal{H}_{\{\hat{\Pi}_i\}}(S|A) \tag{7.33}$$

after erasure. That is, the demon would have to choose optimal local measurements on the apparatus, only giving him access to part knowledge of the state of the system. However, if the demon could carry out non-local measurements in the global space, he could extract work amounting to

$$W^Q = \log\left[d_S d_A\right] - \mathcal{S}\left(\hat{\rho}_{SA}\right). \tag{7.34}$$

The difference between the work that can be extracted by a global and a local demon from the system is equivalent to the quantum discord.

The dilution/distillation gap

Cornelio *et al.* [219] explored the difference between entanglement cost $\mathcal{E}_C\left(\hat{\rho}_{AB}\right)$ and the distillable entanglement $\mathcal{E}_D$ in a cycle of dilution and distillation of a large number of copies of a quantum state (see Figure 7.2). They were able to show that in all cycles where $\mathcal{E}_C > \mathcal{E}_D$, the regularised discord (Equation (7.28)) is a measure of the amount of entanglement lost in each dilution/distillation cycle. As expected, if $\mathcal{E}_C = \mathcal{E}_D$ for some particular state $\hat{\rho}_{AB}$ then the cycle is reversible and the discord in state $\hat{\rho}_{AB}$ is zero. For the irreversible processes, some information is lost to the environment.

Further to the main result, Cornelio *et al.* were able to find a closed expression for the discord of a class of quantum states. Interestingly, it could conceivably be possible that the discord in a single copy of $\hat{\rho}_{AB}$ could be non-zero, whereas in the asymptotic limit of many copies, the regularised discord may be zero (and therefore the deficit in entanglement in the cycle) could be zero. Such a result would be as a consequence of the non-additivity of the entanglement of formation.

7.4 Extension to Gaussian states

The discussion so far has centred on non-classical correlations in finite-dimensional systems, as this is the playing field on which most research into non-classicality has been carried out. What has been included so far has served to express how intricate and useful non-classicality measures can be, and to give a flavour of the open problems that are left to solve for continuous variables.

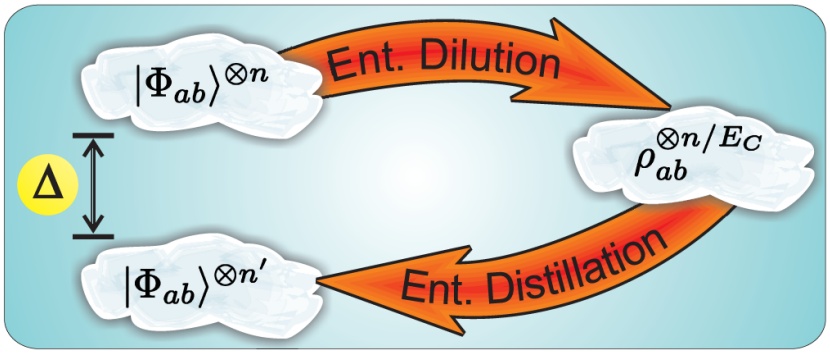

Figure 7.2: In a cycle of entanglement dilution and distillation with many copies, the deficit Δ is given by the regularised discord (7.28). For a reversible process the deficit (and regularised discord) is zero. Figure reproduced from [219]. Copyright (2011) by The American Physical Society.

The optimisation process necessary for quantum discord makes it an intractable problem in the continuous variable regime. After all, how does one define a general, non-Gaussian, continuous variable measurement on a subsystem of a generic continuous variable state? One would need to examine the Wigner function overlap of the subject state with all possible one mode Wigner functions. Discord, then, is well-defined in the continuous variable regime, but almost impossible to calculate explicitly except with good guess-work, or finding measurements that render the conditional entropy to be zero (as $\inf_{\{\hat{\Pi}_i\}} \mathcal{H}_{\{\hat{\Pi}_i\}}(A|B) \geq 0$).

So far, discord has only been examined for Gaussian states. As discord is invariant under local unitary transformations [220], it is possible to focus analysis on Gaussian states whose covariance matrices are in the standard form (Equation (2.122)). It is possible to define a Gaussian version of quantum discord [220, 221] in which the optimisation of the conditional entropy is taken over all generalised Gaussian POVMs on subsystem B. Gaussian states do not form a convex set, yet every Gaussian state admits a decomposition into pure Gaussian states. Therefore it is sufficient to limit the measurement to pure Gaussian states. Giorda and Paris found the optimal measurement for squeezed thermal states [220] and Adesso and Datta [221] found the Gaussian discord for all two mode Gaussian states.

The two mode Gaussian state is first put into standard form as

$$\gamma = \begin{pmatrix} a & 0 & c_+ & 0 \\ 0 & a & 0 & c_- \\ c_+ & 0 & b & 0 \\ 0 & c_- & 0 & b \end{pmatrix}. \tag{7.35}$$

Taking advantage of the formula for the entropy of a Gaussian state (2.114), the Gaussian discord is given by

$$\mathcal{D}_G^{\leftarrow}(\hat{\rho}_{AB}) = \mathfrak{F}(b) - \mathfrak{F}(\nu_-) - \mathfrak{F}(\nu_+) + \inf_{\sigma_0} \mathfrak{F}\left(\sqrt{\det \epsilon}\right) \tag{7.36}$$

where σ_0 is the covariance matrix of the Gaussian measurement on subsystem B and

$$\epsilon = a\mathbb{1} - \begin{pmatrix} c_+ & 0 \\ 0 & c_- \end{pmatrix} (b\mathbb{1} + \sigma_0)^{-1} \begin{pmatrix} c_+ & 0 \\ 0 & c_- \end{pmatrix} \tag{7.37}$$

is the state of subsystem A after the measurement. The optimal value of $\det \epsilon$ is found by

$$\inf_{\sigma_0} \det \epsilon = \begin{cases} \frac{2c_+^2 c_-^2 + \left(b^2-1\right)\left(\det\gamma - a^2\right) + 2|c_+ c_-|\sqrt{c_+^2 c_-^2 + (b^2-1)(\det\gamma - a^2)}}{\left(b^2-1\right)^2} \\ \text{if } \left(\det\gamma - a^2 b^2\right)^2 \leq \left(b^2+1\right) c_+^2 c_-^2 \left(\det\gamma + a^2\right); \\ \frac{a^2 b^2 - c_+^2 c_-^2 + \det\gamma - \sqrt{c_+^4 c_-^4 + (\det\gamma - a^2 b^2)^2 - 2c_+^2 c_-^2 (a^2 b^2 + \det\gamma)}}{2b^2} \\ \text{otherwise.} \end{cases} \tag{7.38}$$

For states falling into the second category, the optimal measurement strategy is homodyning. The first case is a more general measurement. As before $\mathcal{D}_G^{\rightarrow}(\hat{\rho}_{AB})$ and $\mathcal{D}_G^{\leftrightarrow}(\hat{\rho}_{AB})$ can also be

defined accordingly. As the Gaussian discord is defined using only an optimisation over Gaussian POVMs,

$$\mathcal{D}^{\leftarrow}\left(\hat{\rho}_{AB}\right) \leq \mathcal{D}_{G}^{\leftarrow}\left(\hat{\rho}_{AB}\right). \tag{7.39}$$

For a general two-mode Gaussian state, it is an open question as to whether non-Gaussian measurements (e.g. photon detection) can lead to further minimisation of the discord, or whether the Gaussian discord and discord are one and the same. Numerical evidence supports the latter statement.

It was also shown that the only two mode Gaussian states with zero discord are product states of the form $\gamma = \gamma_A \oplus \gamma_B$. All correlated two-mode Gaussian states have non-classical correlations. For all separable two mode Gaussian states, $\hat{\rho}_{AB}^{\text{sep}}$

$$\mathcal{D}_{G}^{\leftarrow}\left(\hat{\rho}_{AB}^{\text{sep}}\right) \leq \frac{(b-1)}{2}\log\left[\frac{(b+1)}{(b-1)}\right] \leq 1. \tag{7.40}$$

This implies further that if $\mathcal{D}_{G}^{\leftarrow}\left(\hat{\rho}_{AB}\right) \geq 1$ the $\hat{\rho}_{AB}$ is entangled.

The Koashi-Winter relation can also be used in the Gaussian setting. Consider a state $\hat{\rho}_{AB}$. The purification of $\hat{\rho}_{AB}$ usually requires the addition of two more modes (S and T), such that $\hat{\rho}_{AB} = \text{Tr}_{ST}\left[\hat{\rho}_{ABST}\right]$. In the Gaussian setting,

$$\mathcal{J}_{G}^{\leftarrow}\left(\hat{\rho}_{AB}\right) + E_{f}^{G}\left(\hat{\rho}_{A,ST}\right) = \mathcal{S}\left(\hat{\rho}_{A}\right) \tag{7.41}$$

where E_{f}^{G} is the Gaussian entanglement of formation, and $\mathcal{J}_{G}^{\leftarrow}\left(\hat{\rho}_{AB}\right)$ is the one way classical information when optimised over Gaussian POVMs. From the definition of $\mathcal{J}_{G}^{\leftarrow}$, we get the rather simple relation $E_{f}^{G}\left(\hat{\rho}_{A,ST}\right) = \inf_{\sigma_0} \mathfrak{F}\left(\sqrt{\det \epsilon}\right)$.

Furthermore, in the case of two mode Gaussian states where one of the symplectic eigenvalues $\nu_{-} = 1$, the purification requires a single extra mode. It is known [138] that $E_{f}^{G}\left(\hat{\rho}_{AS}\right) = \mathcal{E}_{F}\left(\hat{\rho}_{AS}\right)$ (as $\hat{\rho}_{AS}$ is a two mode Gaussian state), which in turn implies that $\mathcal{J}_{G}^{\leftarrow}\left(\hat{\rho}_{AB}\right) = \mathcal{J}^{\leftarrow}\left(\hat{\rho}_{AB}\right)$. So, for two mode Gaussian states where one symplectic eigenvalue is $\nu_{-} = 1$, we have the relation $\mathcal{D}^{\leftarrow}\left(\hat{\rho}_{AB}\right) = \mathcal{D}_{G}^{\leftarrow}\left(\hat{\rho}_{AB}\right)$.

7.5 Alternative non-classicality indicators

Although the quantum discord has been the most researched of the non-classicality measures, there are rivals. In fact, one of the main goals of this thesis is to extend the analysis of non-classicality measures to infinite dimensions. We here introduce some alternatives. This list is far from exhaustive.

Measurement Induced Disturbance

In order to overcome the difficulties involved in the evaluation of quantum discord, Luo introduced the 'measurement-induced disturbance' (MID) as an alternative nonclassicality indicator for bipartite quantum states [222]. Just as with quantum discord, MID is motivated by the observation that in classical systems, local measurements do not induce disturbance. Any bipartite quantum state containing no quantum correlations is left invariant by the action of any bi-local complete measurement. On the other hand, even when a state $\hat{\rho}_{AB}$ is a priori nonclassical, any complete bi-local measurement makes it classical as a result of a decoherence-by-measurement process [222]. Luo's approach was thus to restrict the measurements to the bi-local complete projective measurement $\hat{\mathcal{E}}_A \otimes \hat{\mathcal{E}}_B$ determined by the eigen-projectors $\hat{\mathcal{E}}_j(k)$ of the marginal states $\hat{\rho}_j = \sum_k \lambda_k \hat{\mathcal{E}}_j(k)$ $(j = A, B)$, where λ_k are corresponding eigenvalues, and reads [222]

$$\mathcal{M}(\hat{\rho}_{AB}) = \mathcal{I}_q(\hat{\rho}_{AB}) - \mathcal{I}_q[\hat{\mathcal{E}}(\hat{\rho}_{AB})], \tag{7.42}$$

where

$$\hat{\mathcal{E}}(\hat{\rho}_{AB}) = \sum_{k,l} p_{AB}(k,l)\hat{\mathcal{E}}_A(k) \otimes \hat{\mathcal{E}}_B(l) \tag{7.43}$$

is the post-measurement state after local measurements $\hat{\mathcal{E}}_A$ and $\hat{\mathcal{E}}_B$ and

$$p_{AB}(k,l) = \text{Tr}[\hat{\rho}_{AB}\hat{\mathcal{E}}_A(k) \otimes \hat{\mathcal{E}}_B(l)] \tag{7.44}$$

is the probability of obtaining the outcome (kl). The post-measurement state is obviously fully classical and consequently any correlations contained within can be described sufficiently by the classical mutual information of the distribution p_{AB} (Eq. (7.1)). Hence we can rephrase MID as

$$\mathcal{M}(\hat{\rho}_{AB}) = \mathcal{I}_q(\hat{\rho}_{AB}) - \mathcal{I}(A:B)\,. \tag{7.45}$$

Two important observations distinguish the MID from the quantum discord:

- Both subsystems are locally probed;
- There is no optimization over the local measurements, which are chosen to be the marginal eigen-projectors for every quantum state [5].

The Measurement Induced Disturbance is easily computable for a quantum state in a Hilbert space of any dimensions, and has found widespread applications in several investigations [224]. However, a number of studies have revealed that MID is an unfaithful and unrefined measure of non-classical correlations [223, 192], being non-zero and even maximal for states approaching the classical limit. That is, MID severely overestimates the non-classical correlations in a bipartite state. In Chapter 8 we show how to calculate the MID for any two mode Gaussian state and compare the results to those of other non-classicality measures.

The perhaps obvious remedy to this major drawback is to define an *ameliorated measurement induced disturbance* (AMID) which incorporates into (7.45) a minimisation over the joint bi-local POVM measurements $\hat{\Pi}_A \otimes \hat{\Pi}_B$ on subsystems A and B [192]. Arguably, this puts all of the difficulty back in. The AMID can then be defined as [192, 223, 225]

$$\begin{aligned} \mathcal{A}(\hat{\rho}_{AB}) &= \inf_{\hat{\Pi}_A \otimes \hat{\Pi}_B} \{\mathcal{I}_q(\hat{\rho}_{AB}) - \mathcal{I}(A:B)\} \\ &= \mathcal{I}_q(\hat{\rho}_{AB}) - \mathcal{I}_c(\hat{\rho}_{AB})\,, \end{aligned} \tag{7.46}$$

where

$$\mathcal{I}_c(\hat{\rho}_{AB}) = \sup_{\hat{\Pi}_A \otimes \hat{\Pi}_B} \mathcal{I}(A:B) \tag{7.47}$$

is the classical mutual information of a quantum state $\hat{\rho}_{AB}$, and $\mathcal{I}(A:B)$ is the classical mutual information of the joint probability distribution $p_{AB}(k,l) = \mathrm{Tr}[\hat{\rho}_{AB}\hat{\Pi}_A(k) \otimes \hat{\Pi}_B(l)]$ of outcomes of local measurements $\hat{\Pi}_A$ and $\hat{\Pi}_B$ on $\hat{\rho}_{AB}$. The AMID captures the quantumness of bipartite correlations as signaled by the minimal state disturbance after optimized local measurements. It is a symmetric, strongly faithful nonclassicality measure [192] that vanishes if and only if a bipartite state $\hat{\rho}_{AB}$ is genuinely classically correlated [225, 223], and it is operationally interpreted as the quantum complement to the classical mutual information [Eq. (7.47)], while the latter is in turn a *bona fide* measure of classical correlations in general bipartite quantum states. The AMID thus incorporates the nice properties of discord and MID without showing their respective weaknesses [192, 226]. The evaluation and properties of AMID have been investigated[6] for two–qubit systems [192].

The MID and AMID form a hierarchy with the measures so far defined:

$$\{\mathcal{D}^{\leftarrow}(\hat{\rho}_{AB}), \mathcal{D}^{\rightarrow}(\hat{\rho}_{AB})\} \leq \mathcal{D}^{\leftrightarrow}(\hat{\rho}_{AB}) \leq \mathcal{D}_G^{\leftrightarrow}(\hat{\rho}_{AB}) \leq \mathcal{A}(\hat{\rho}_{AB}) \leq \mathcal{M}(\hat{\rho}_{AB})\,. \tag{7.48}$$

In Chapter 8 we shall extend the analysis of these measures to the continuous variable regime, particularly focussing on Gaussian states. In Chapter 9 we extend this analysis to a simple class of non-Gaussian states.

---

[5] Notice also that this choice of measurements makes MID not uniquely defined on bipartite states whose reduced density matrices have a degenerate spectrum [223], as it is the case for states with maximally mixed marginals.

[6] In Ref. [192] the AMID is defined via an optimization over local projective measurements, rather than more general local POVMs. Both versions of AMID have also been studied in Ref. [223], albeit without naming the considered measures explicitly.

Relative Entropy of Quantumness

Another measure of non-classicality is the Relative Entropy of Quantumness (REQ) [222, 227, 228, 229] defined as the minimum distance (as measured by the quantum relative entropy in Equation (3.38), which is not technically a distance measure - it is asymmetric for a start) from a state $\hat{\rho}_{AB}$ to the nearest classically correlated state $\hat{\sigma}$,

$$Q\left(\hat{\rho}_{AB}\right) = \min_{\hat{\sigma}} \mathcal{S}\left(\hat{\rho}_{AB} || \hat{\sigma}\right). \tag{7.49}$$

The appeal of REQ lies in the parallels that can be drawn with e.g. the relative entropy of entanglement. In [227] a unified view of quantum and classical correlations is advanced using measures of this kind.

As an important sidenote, in [227], the Quantum Dissonance is defined as the relative entropy between the closest separable state $\hat{\chi}_\rho$ to $\hat{\rho}_{AB}$ and the closest classically correlated state $\hat{\sigma}_{\chi_\rho}$ to $\hat{\chi}_\rho$ i.e.

$$Q_{\text{diss}}\left(\hat{\rho}_{AB}\right) = \min_{\hat{\sigma}_{\chi_\rho}} \mathcal{S}\left(\hat{\chi}_\rho || \hat{\sigma}_{\chi_\rho}\right) \tag{7.50}$$

where $\hat{\chi}_\rho$ is the state minimising the relative entropy of entanglement of $\hat{\rho}_{AB}$. The sole purpose of $Q_{\text{diss}}\left(\hat{\rho}_{AB}\right)$ is to define a measure of non-classicality that does not include entanglement.

Returning to REQ (7.49), the measure is faithful (i.e. reaches 0 when the state is classically correlated only), symmetric under permutations of the subsystems, and has an operational interpretation [230]. The definition of REQ transports easily to continuous variables but proves very difficult to evaluate.

Most interestingly, REQ also defines a measure of non-classicality that carries over into the multipartite setting. It is this property that makes one willing to overlook the fact that relative entropy is not a true distance measure, as it puts quantum correlations in $N-$partite states on an equal footing.

Operationally, Piani *et al.* [230] showed that the REQ is interpreted as the resource power of non-classical correlations for the task of generating distillable entanglement (as measured by $\mathcal{E}_D$). In this thesis, the REQ will not play a pivotal role. It has been included as it is another favourite amongst those studying non-classical correlations.

7.6 Summary of Chapter 7

In this chapter, the quantum discord has been introduced as a rudimentary way of quantifying those non-classical correlations that a bipartite quantum state may possess in and beyond entanglement. These correlations have a deep, yet so far unclarified connection to complementarity. Discord, in particular, has been the subject of intensive investigations in recent years and was shown by the Koashi-Winter relation to be intrinsically related to quantum entanglement in a pure tripartite state. It is endowed with operational interpretations via the quantum state merging protocol and quantum Maxwell's demon.

Despite this, other non-classicality measures have been introduced, such as the Measurement Induced Disturbance, which have appealing properties such as symmetry. In the following two chapters, we shall attempt to extend the analysis of these measures into the realm of infinite dimensional systems.

Chapter 8

Extension of MID and AMID to continuous variables

As has been testified to in the previous chapter, research into non-classicality measures has generally been restricted to bipartite qudit systems. The notable exception so far has been the extension of the quantum discord to the Gaussian setting with the Gaussian Discord [220, 221], in which the optimisation of the measurement on one subsystem is restricted to Gaussian POVMs. The Gaussian discord has been readily computed analytically for all two mode Gaussian states.

In this chapter, based on **[II]**, the study of quantum correlations beyond entanglement in two mode Gaussian states is expanded using the instruments of Measurement Induced Disturbance (MID) (7.42) and its ameliorated version. In the spirit of recent studies of Gaussian discord, the Gaussian AMID (GAMID) is introduced and is used to probe non-classical correlations in two mode Gaussian states.

In Section 8.1 the measures used in this chapter shall be reintroduced and the GAMID shall be defined. In Section 8.2, the measurement induced disturbance shall be calculated for two mode Gaussian states, with its Gaussian counterpart explored in Section 8.3. In Sections 8.4 and 8.5 the relationship between the different non-classicality measures, and the entanglement of the Gaussian states, shall be probed.

8.1 Measures of quantum correlations in Gaussian states

The covariance matrix γ contains complete information about all correlations in a Gaussian state, and any symplectic operations leave all correlations and entropic quantities invariant. All two mode Gaussian states can be put into the form

$$\gamma = \begin{pmatrix} a & 0 & c_+ & 0 \\ 0 & a & 0 & c_- \\ c_+ & 0 & b & 0 \\ 0 & c_- & 0 & b \end{pmatrix} \tag{8.1}$$

by local symplectic operations, and without loss of generality we assume throughout this chapter that $c_+ \geq |c_-| \geq 0$. Gaussian states can be readily produced and manipulated in the lab with a high degree of control. Gaussian measurements are those that map Gaussian states into Gaussian states and coincide with the standard toolbox of linear optics (e.g. balanced homodyne detection). Any such measurement is described by a positive operator valued measurement [176]

$$\hat{\Pi}_j^G(d_j) = \frac{1}{2\pi}\hat{D}_j(d_j)\hat{\Pi}_j^G\hat{D}_j^\dagger(d_j), \quad j = A, B. \tag{8.2}$$

The seed element $\hat{\Pi}_j^G$ is a normalised density matrix of a generally mixed single mode Gaussian state with covariance matrix γ_j and zero displacements. The operator $\hat{D}(d_j) = \exp\left[-i\mathbf{d}_j^T\Omega\hat{\mathbf{R}}_j\right]$ is the displacement operator (discussed in detail in Chapter 2), where $\hat{\mathbf{R}}_j = (\hat{x}_j, \hat{p}_j)^T$ and $\mathbf{d}_j^T = \left(d_j^{(x)}, d_j^{(p)}\right)$ is a vector of real numbers describing the shift in phase space. The POVM

satisfies the completeness relation

$$\frac{1}{2\pi}\int_{-\infty}^{\infty}\hat{D}\left(d_j\right)\hat{\Pi}_j^G\hat{D}_j^{\dagger}(d_j)\mathrm{d}d_j^{(x)}\mathrm{d}d_j^{(p)}=\mathbb{1}_j \tag{8.3}$$

following from Schur's lemma and the normalisation condition $\mathrm{Tr}\left[\hat{\Pi}_j\right]=\mathbb{1}$.

The quantum discord $\mathcal{D}^{\leftarrow}\left(\hat{\rho}_{AB}\right)$, introduced in the previous chapter, shall play no part in this discussion directly. When dealing with continuous variables, an optimisation of the measurement over the full Hilbert space is seemingly impossible without an educated guess. In its stead we shall consider the Gaussian discord $\mathcal{D}_G^{\leftarrow}\left(\hat{\rho}_{AB}\right)$, which was also mentioned in the previous chapter. In reality, we can only know that $\mathcal{D}_G^{\leftarrow}\left(\hat{\rho}_{AB}\right)=\mathcal{D}^{\leftarrow}\left(\hat{\rho}_{AB}\right)$ in the cases where $\inf_{\{\hat{\Pi}_j^G\}}\mathcal{H}_{\{\hat{\Pi}_j^G\}}(A|B)=0$, although it was conjectured in [221] that an optimal Gaussian measurement $\hat{\Pi}_j^G$ would be better than any non-Gaussian measurement. The measurement induced disturbance $\mathcal{M}\left(\hat{\rho}_{AB}\right)$ shall also be used.

For pure bipartite states $|\psi\rangle_{AB}$, all the measures of non-classical correlations introduced above (discord, MID, and AMID) reduce to the entropy of entanglement, showing that quantum correlations are faithfully identified with just entanglement in the special case of pure states of composite quantum systems. In order to explore the complicated relationship between entanglement and non-classicality in two mode Gaussian states, the Gaussian entanglement of formation $E_f^G\left(\hat{\rho}_{AB}\right)$ shall be used.

Although, for the same reason as the discord, the AMID $\mathcal{A}\left(\hat{\rho}_{AB}\right)$ is all but impossible to calculate, we can borrow the trick of Gaussian discord and optimise the classical mutual information in the probability distribution of a bi-local Gaussian POVM measurement on the state. With this, the Gaussian Ameliorated Measurement Induced Disturbance (GAMID) is defined as

$$\mathcal{A}^G(\hat{\rho}_{AB})=\mathcal{I}_q(\hat{\rho}_{AB})-\mathcal{I}_c^G(\hat{\rho}_{AB}), \tag{8.4}$$

where

$$\mathcal{I}_c^G(\hat{\rho}_{AB})=\sup_{\hat{\Pi}_A^G\otimes\hat{\Pi}_B^G}\mathcal{I}(A:B) \tag{8.5}$$

is the Gaussian classical mutual information of the quantum state $\hat{\rho}_{AB}$. The true AMID, optimised over general local measurements is then bounded from above as

$$\mathcal{A}(\hat{\rho}_{AB})\leq\min\{\mathcal{A}^G(\hat{\rho}_{AB}),\mathcal{M}(\hat{\rho}_{AB})\}. \tag{8.6}$$

Naturally, one ponders whether $\mathcal{A}\left(\hat{\rho}_{AB}\right)=\mathcal{A}^G\left(\hat{\rho}_{AB}\right)$ on all two mode Gaussian states. After all, the numerical evidence (although, as yet, no proof) indicates that $\mathcal{D}_G^{\leftarrow}\left(\hat{\rho}_{AB}\right)=\mathcal{D}^{\leftarrow}\left(\hat{\rho}_{AB}\right)$ on Gaussian states, and so why should the same not be the case when two local measurements are made? It shall in fact be shown that for some classes of Gaussian states, the best possible Gaussian measurements cannot outperform a non-optimised non-Gaussian measurement (photon counting). This jolting result proves that Gaussian joint measurements may not be the least disturbing measurements on general two mode Gaussian states.

8.2 Measurement Induced Disturbance of two mode Gaussian states

In this section it is shown how to calculate the MID of a two mode Gaussian state $\hat{\rho}_{AB}$ whose covariance matrix γ is in standard form (8.1). The expressions derived here could be straightforwardly recast in terms of a set of four local symplectic invariants for general two mode states that uniquely define the standard form covariances.

As with the Gaussian discord, the quantum mutual information (Eq. (7.6)) of the two mode Gaussian state is required. This is easily shown to be

$$\mathcal{I}_q\left(\hat{\rho}_{AB}\right)=\mathfrak{F}\left(a\right)+\mathfrak{F}\left(b\right)-\mathfrak{F}\left(\nu_+\right)-\mathfrak{F}\left(\nu_-\right) \tag{8.7}$$

where $2\nu_{\pm}^2=\Delta\pm\sqrt{\Delta^2-4\det\gamma}$, $\Delta=a^2+b^2+2c_+c_-$, and $\mathfrak{F}$ is defined in equation (2.115). Only the formulation of the classical mutual information after local projections onto the eigenstates of the marginal density matrices need be derived.

For a generic two mode Gaussian state in standard form, the reduced states are simply thermal states $\hat{\rho}_{th,a}$ and $\hat{\rho}_{th,b}$ with mean number of photons $\langle \hat{n}_A \rangle = (a-1)/2$ and $\langle \hat{n}_B \rangle = (b-1)/2$ respectively. The local measurements $\left(\hat{\mathcal{E}}_A \otimes \hat{\mathcal{E}}_B\right)$ required in the expression for MID must necessarily be projections onto Fock states (joint photon counting),

$$\hat{\mathcal{E}}_j(n) = |n\rangle_j\langle n|, \quad j = A, B, \tag{8.8}$$

and the post-measurement state reads as

$$\hat{\mathcal{E}}(\hat{\rho}_{AB}) = \sum_{m,n=0}^{\infty} p(m,n)|m\rangle_A\langle m| \otimes |n\rangle_B\langle n|, \tag{8.9}$$

where $p(m,n) = {}_A\langle m|{}_B\langle n|\hat{\rho}_{AB}|m\rangle_A|n\rangle_B$ is the joint probability distribution of finding m photons in mode A and n photons in mode B.

In order to calculate the classical mutual information after the measurement, three components are required as

$$\mathcal{I}(A:B) = \mathcal{I}_q\left[\hat{\mathcal{E}}\left(\hat{\rho}_{AB}\right)\right] = \mathcal{H}\left(p(m)\right) + \mathcal{H}\left(p(n)\right) - \mathcal{H}\left(p(m,n)\right) \tag{8.10}$$

where $p(m,n)$ is the joint post-measurement probability distribution and $p(m)$ and $p(n)$ are the marginal distributions. The reduced states $\hat{\rho}^{\hat{\mathcal{E}}}_{A,B} = \mathrm{Tr}_{B,A}\left[\hat{\mathcal{E}}\left(\hat{\rho}_{AB}\right)\right]$ are just equal to the local thermal states and so $\mathcal{H}\left(p(m)\right) = \mathcal{S}\left(\hat{\rho}^{\hat{\mathcal{E}}}_A\right) = \mathfrak{F}\left(a\right)$ and $\mathcal{H}\left(p(n)\right) = \mathcal{S}\left(\hat{\rho}^{\hat{\mathcal{E}}}_B\right) = \mathfrak{F}\left(b\right)$. Consequently, the measurement induced disturbance is simplified to

$$\begin{aligned} \mathcal{M}(\hat{\rho}_{AB}) &= \mathcal{S}[\hat{\mathcal{E}}(\hat{\rho}_{AB})] - \mathcal{S}(\hat{\rho}_{AB}) \\ &= -\sum_{m,n=0}^{\infty} p(m,n)\ln p(m,n) - \mathfrak{F}(\nu_+) - \mathfrak{F}(\nu_-)\,. \end{aligned} \tag{8.11}$$

All that remains, then, is to find the probability distribution $p(m,n)$. This could, in principle, be done quickly by deploying the multivariate Hermite polynomials (Appendix A) as in Chapter 5 although this does in fact require all density matrix elements to be computed, which is an unnecessary waste of memory. Instead, here $p(m,n)$ is derived using the generating function for the distribution in the spirit of references [231, 232, 233].

Any two mode quantum state can be written in terms of its complex normal quantum characteristic function defined as

$$\chi(\beta_1,\beta_2) = \mathrm{Tr}[\hat{\rho}_{AB}e^{\beta_1\hat{a}^\dagger + \beta_2\hat{b}^\dagger}e^{-\beta_1^*\hat{a} - \beta_2^*\hat{b}}], \tag{8.12}$$

where $\hat{a}$ ($\hat{a}^\dagger$) and $\hat{b}$ ($\hat{b}^\dagger$) are annihilation (creation) operators of modes A and B, and β_1, β_2 are complex parameters of the characteristic function.

For a Gaussian state in the standard form with zero means ($\langle a\rangle = \langle b\rangle = 0$) the characteristic function takes the form [232]

$$\begin{aligned} \chi(\beta_1,\beta_2) &= \exp\left[-(B_1|\beta_1|^2 + B_2|\beta_2|^2) + (D\beta_1^*\beta_2^* \right. \\ &\quad \left. + \bar{D}\beta_1\beta_2^* + \text{c.c.})\right], \end{aligned} \tag{8.13}$$

where

$$\begin{aligned} B_1 &= \langle \Delta\hat{a}^\dagger\Delta\hat{a}\rangle = \frac{(a-1)}{2}, \quad B_2 = \langle \Delta\hat{b}^\dagger\Delta\hat{b}\rangle = \frac{(b-1)}{2} \\ D &= \langle \Delta\hat{a}\Delta\hat{b}\rangle = \frac{(c_1-c_2)}{4}, \quad \bar{D} = -\langle \Delta\hat{a}^\dagger\Delta\hat{b}\rangle = -\frac{(c_1+c_2)}{4} \end{aligned} \tag{8.14}$$

and $\Delta\hat{A} = \hat{A} - \left\langle \hat{A} \right\rangle$. The generating function for the distribution $p(m,n)$ is then described by [234]

$$G\left(\lambda_1,\lambda_2\right) = \frac{1}{\pi^2\lambda_1\lambda_2}\int\int \exp\left(-\frac{|\beta_1|^2}{\lambda_1} - \frac{|\beta_2|^2}{\lambda_2}\right)\chi(\beta_1,\beta_2)\mathrm{d}^2\beta_1\mathrm{d}^2\beta_2, \tag{8.15}$$

where λ_1 and λ_2 are real parameters to be used in the generation of the probability distribution. Inserting the characteristic function (8.13) into the integral (8.15) and performing the Gaussian integration yields

$$G(\lambda_1, \lambda_2) = F_+(\lambda_1, \lambda_2) F_-(\lambda_1, \lambda_2) \tag{8.16}$$

with

$$F_j = \frac{1}{\sqrt{1 + B_1\lambda_1 + B_2\lambda_2 + K_j\lambda_1\lambda_2}} \tag{8.17}$$

where

$$K_j = \frac{1}{4}\left[(a-1)(b-1) - c_j^2\right], \quad j = +, -. \tag{8.18}$$

From this, the photon number distribution is found by differentiating the generating function as

$$p(m,n) = \frac{(-1)^{m+n}}{m!n!} \frac{\partial^{m+n} G(\lambda_1, \lambda_2)}{\partial\lambda_1^m \partial\lambda_2^n}\bigg|_{\lambda_1=\lambda_2=1}. \tag{8.19}$$

The derivation of the final solution to this is long and tedious but can be outlined here. After a lot of calculations,

$$\begin{aligned}\left(\frac{\partial}{\partial\lambda_1}\right)^\alpha \left(\frac{\partial}{\partial\lambda_2}\right)^\beta F_j\bigg|_{\lambda_1=\lambda_2=1} &= (-1)^{\alpha+\beta} \frac{(B_1+K_j)^\alpha (B_2+K_2)^\beta}{4^{\alpha+\beta}(1+B_1+B_2+K_j)^{\alpha+\beta+\frac{1}{2}}} \\ &\times \sum_{l=0}^{\min(\alpha,\beta)} l! \binom{\alpha}{l}\binom{\beta}{l} \frac{[2(\alpha+\beta-l)]!}{(\alpha+\beta-l)!} \\ &\times \left[-4K_j \frac{1+B_1+B_2+K_j}{(B_1+K_j)(B_2+K_j)}\right]^l \end{aligned} \tag{8.20}$$

and a function, $Q^{(j)}(\alpha, \beta)$, can be defined as

$$Q^{(j)}(\alpha,\beta) = (-1)\left(\frac{\partial}{\partial\lambda_1}\right)^\alpha \left(\frac{\partial}{\partial\lambda_2}\right)^\beta F_j\bigg|_{\lambda_1=\lambda_2=1}. \tag{8.21}$$

By virtue of Leibniz's product rule, the photon number distribution is explicitly given by

$$\begin{aligned} p(m,n) &= \frac{(-1)^{m+n}}{m!n!} \sum_{\nu_1=0}^{m}\sum_{\nu_2=0}^{n} \binom{m}{\nu_1}\binom{n}{\nu_2} \left(\frac{\partial}{\partial\lambda_1}\right)^{\nu_1} \left(\frac{\partial}{\partial\lambda_2}\right)^{\nu_2} F_1(\lambda_1,\lambda_2) \\ &\times \left(\frac{\partial}{\partial\lambda_1}\right)^{m-\nu_1} \left(\frac{\partial}{\partial\lambda_2}\right)^{n-\nu_2} F_2(\lambda_1,\lambda_2) \\ &= \frac{1}{m!n!} \sum_{\nu_1=0}^{m}\sum_{\nu_2=0}^{n} \binom{m}{\nu_1}\binom{n}{\nu_2} Q^{(1)}(\nu_1,\nu_2) Q^{(2)}(m-\nu_1, n-\nu_2). \end{aligned} \tag{8.22}$$

This formidable formula can be calculated numerically and used to complete the required knowledge for $\mathcal{M}(\hat{\rho}_{AB})$ (Eq. (7.42)). In the case where $c_+ = \pm c_- = c$, we have $K_1 = K_2 = K = \frac{1}{4}\left[(a-1)(b-1) - c^2\right]$ and the distribution (8.22) is simplified to

$$\begin{aligned} p(m,n) &= \frac{(B_1+K)^m (B_2+K)^n}{m!n!(1+B_1+B_2+K)^{m+n+1}} \\ &\times \sum_{j=0}^{\min(m,n)} \binom{m}{j}\binom{n}{j} j!(m+n-j)! \left[-K\frac{1+B_1+B_2+K}{(B_1+K)(B_2+K)}\right]^j. \end{aligned} \tag{8.23}$$

The two mode squeezed vacuum is particularly interesting, and its MID can be calculated directly in the Fock state representation. The two mode squeezed vacuum is given by

$$|\psi(r)\rangle_{AB} = \sqrt{1-q^2} \sum_{n=0}^{\infty} q^n |nn\rangle_{AB} \tag{8.24}$$

where $q = \tanh(r)$. This is already in its Schmidt decomposition with Schmidt coefficients $\mu_m = \sqrt{1-q^2}q^m$. As it is a pure state, $\mathcal{S}\left(\hat{\rho}_{AB}\right) = 0$ and so

$$\mathcal{M}\left(|\psi\left(r\right)\rangle_{AB}\right) = \mathcal{S}\left(\hat{\mathcal{E}}\left[|\psi\left(r\right)\rangle_{AB}\right]\right). \tag{8.25}$$

The post measurement state reads

$$\hat{\mathcal{E}}\left(|\psi\left(r\right)\rangle_{AB}\right) = \left(1-q^2\right)\sum_{n=0}^{\infty} q^{2n}|n\rangle\langle n| \otimes |n\rangle\langle n| \tag{8.26}$$

and its entropy $\mathcal{S}\left(\hat{\mathcal{E}}\left[|\psi\left(r\right)\rangle_{AB}\right]\right) = \mathfrak{F}\left(\cosh(2r)\right)$ which is precisely the entropy of entanglement of the pure two mode Gaussian state. Therefore,

$$\mathcal{M}\left(|\psi\left(r\right)\rangle_{AB}\right) = \mathcal{E}_{v.N}\left(|\psi\left(r\right)\rangle_{AB}\right) = \cosh^2(r)\ln\left[\cosh^2(r)\right] - \sinh^2(r)\ln\left[\sinh^2(r)\right] \tag{8.27}$$

as expected from the definition of MID. Of particular interest, the correct value of MID on a pure two mode squeezed vacuum means that non-Gaussian Fock state measurements produced the optimal value of AMID. $\mathcal{M}\left(|\psi\left(r\right)\rangle_{AB}\right)$ has not overestimated the quantum correlations at all. The interesting question to ask is, can the best possible Gaussian POVMs, in place of Fock state measurements, be used to gain the same result for GAMID? Intriguingly the answer is no, as shall be seen.

8.3 Gaussian AMID of two mode Gaussian states

We now turn our attention to the Gaussian Ameliorated Measurement Induced Disturbance, which replaces the projection onto eigenprojectors required for $\mathcal{M}$ with bi-local Gaussian POVMs. The challenge is to see if optimal local Gaussian measurements can achieve a lower value than the unoptimised Fock state projections.

We hereby develop the framework for the determination of the Gaussian AMID on general two–mode Gaussian states, and provide closed formulas for it in some special cases. As in the previous section, the quantum mutual information is easily calculated by equation (8.7). The nontrivial part in the determination of the quantity (8.4) is the calculation of the classical mutual information $\mathcal{I}_c^G(\hat{\rho}_{AB})$ requiring maximization of the Shannon mutual information $\mathcal{I}(A:B)$ over local Gaussian POVMs $\hat{\Pi}_A$ and $\hat{\Pi}_B$ of the form (8.2).

One important result is proved in Appendix D - we can restrict the measurements to covariant Gaussian POVMs (8.2), projecting onto pure states (rank one POVMS), as in the discrete-variable scenarios [223]. That is, we can focus on POVMs of the form (8.2) where the seed element $\hat{\Pi}_j$ is a pure single mode Gaussian state with covariance matrix γ_j. As discussed in Chapter 2, any pure, one mode covariance matrices can be expressed as $\gamma_j = U\left(\theta_j\right)V\left(r_j\right)U^{\dagger}\left(\theta_j\right)$, where

$$U(\theta_j) = \begin{pmatrix} \cos\theta_j & \sin\theta_j \\ -\sin\theta_j & \cos\theta_j \end{pmatrix}, \quad V(r_j) = \begin{pmatrix} e^{2r_j} & 0 \\ 0 & e^{-2r_j} \end{pmatrix}, \tag{8.28}$$

with $\theta_j \in \langle 0, \pi)$ and $r_j \geq 0$. In this picture, homodyne detection on mode j is recovered in the limit of an infinitely squeezed pure state $\hat{\Pi}_j$, i.e., $r_j \to \infty$. On the other hand, heterodyne detection on mode j corresponds to $r_j = 0$.

Now we want to maximize the Shannon mutual information $\mathcal{I}(A:B)$ of the distribution (D.3),

$$P(d) = \mathrm{Tr}[\left(\hat{\Pi}_A(d_A) \otimes \hat{\Pi}_B(d_B)\right)\hat{\rho}_{AB}],$$

over all single–mode pure-state CMs $\gamma_{A,B}$. Expressing the two–mode state CM γ in block form as in (8.1), and using the formula for the Shannon entropy of a Gaussian distribution P of N variables with classical correlation matrix Σ, $\mathcal{H}(P) = \ln[(2\pi e)^{\frac{N}{2}}\sqrt{\det\Sigma}]$ [175], the sought mutual information can be obtained in the form [235]:

$$\mathcal{I}(A:B) = \frac{1}{2}\ln\left[\frac{\det\left(\gamma_A + A\right)\det\left(\gamma_B + B\right)}{\det\left(\gamma_A \oplus \gamma_B + \gamma\right)}\right]. \tag{8.29}$$

As the determinant is invariant with respect to symplectic transformations we can assume the covariance matrix γ to be in standard form (8.1). As the logarithm is a monotonic function, in order to maximise $\mathcal{I}(A:B)$ it is necessary to find the maximum of the logarithm's argument. Due to the invariance of the determinant under orthogonal transformations, we can then express $\gamma' = \gamma + \gamma_A \oplus \gamma_B$ as

$$\gamma' = \begin{pmatrix} A' & C' \\ C'^T & B' \end{pmatrix} \tag{8.30}$$

where each two by two block is defined by

$$\begin{aligned} A' &= a\mathbb{1} + V(r_A)\,, \quad B' = b\mathbb{1} + V(r_B)\,, \\ C' &= U^T(\theta_A)\mathrm{diag}(c_+, c_-)U(\theta_B)\,. \end{aligned} \tag{8.31}$$

That is, all of the phase dependence has been shifted to the blocks not on the diagonal. The function to be maximised is then

$$f(r_A, r_B, \theta_A, \theta_B) = \frac{\det A' \det B'}{\det \gamma'}, \tag{8.32}$$

and the classical mutual information that we require is given by

$$\mathcal{I}_c^G(\hat{\rho}_{AB}) = \frac{1}{2}\ln\left[\sup_{\{r_{A,B},\theta_{A,B}\}} f(r_A, r_B, \theta_A, \theta_B)\right]. \tag{8.33}$$

The numerator in (8.32) notably does not contain the phase parameters θ_A and θ_B. However, they do feature in the denominator. The denominator can be expressed [97] in terms of symplectic invariants:

$$\begin{aligned} I_1 &= \det A', \quad I_2 = \det B' \\ I_3 &= \det C', \quad I_4 = \mathrm{Tr}\left[A'\Omega C'\Omega B'\Omega C'^T\Omega\right]. \end{aligned} \tag{8.34}$$

The determinant of γ' is then given by $I_1 + I_2 + I_3^2 - I_4$. The denominator in (8.32) then only depends on the phases θ_A and θ_B through the invariant I_4, so we can optimise over the phases by maximising I_4. Thus, in order to find the optimal measurements, it is pragmatic to optimise over the phases first, before turning one's attention to the squeezing parameters r_A and r_B.

Three different cases must be distinguished at this point, depending on the eigenvalues c_+ and c_- of C'.

Case 1: $c_+ = c_- = 0$
In this case, the phases play no role in (8.32) and $I_3 = I_4 = 0$. Equation (8.32) then reduces to 1 so $\mathcal{I}(A:B) = 0$. The quantum mutual information (8.7) is also zero and so $\mathcal{A}^G(\hat{\rho}_{AB}) = 0$. This is intuitively correct. The state $\hat{\rho}_{AB}$ is a Gaussian product state and have neither quantum nor classical correlations. Actually, from the analysis of Gaussian discord, it is known that any non-product two mode Gaussian states have non-zero quantum correlations. In all the other cases, we expect a non-zero $\mathcal{A}^G$.

Case 2: $c_+ > 0$ *and* $c_- = 0$
In this case, for any non-zero r_A and r_B the optimal phases in I_4 are given by $\theta_{A,B,\mathrm{opt}} = \pi/2$ and for these phases the invariant I_4 takes the value

$$I_{4,\mathrm{opt}} = c_+^2\left(a + e^{2r_A}\right)\left(b + e^{2r_B}\right). \tag{8.35}$$

From this we can move to optimise r_A and r_B. We define

$$\begin{aligned} \frac{1}{1 - h(r_A, r_B)} &\equiv g(r_A, r_B) \\ &\equiv f(r_A, r_B, \theta_{A,\mathrm{opt}}, \theta_{B,\mathrm{opt}}). \end{aligned} \tag{8.36}$$

We have $h = I_{4,\mathrm{opt}}/(I_1 I_2)$ and the function h (and consequently g) is obviously maximized in the limits $r_{A,B} \to \infty$ (doubly homodyne detection) when we get

$$g_{\mathrm{hom}} = \frac{ab}{ab - c_+^2}. \tag{8.37}$$

A quick check reveals that $g_{\rm hom}$ is larger than the value of the function g on the boundaries $r_A = 0$ or $r_B = 0$ and so $g_{\rm hom}$ is the optimal values of (8.32) when $c_- = 0$.

Case 3: $c_+, c_- \neq 0$
The general case is far trickier to calculate. We begin by expressing the invariant I_4 as $I_4 = c_+ c_- \,\mathrm{Tr}\,[XB']$ where

$$X = U^T(\theta_B)\,\mathrm{diag}(c_+^{-1}, c_-^{-1})U(\theta_A)\,A'U^T(\theta_A)\,\mathrm{diag}(c_+^{-1}, c_-^{-1})U(\theta_B)\,. \tag{8.38}$$

Next we express the matrix X through the eigenvalue decomposition

$$X = W(\phi)\mathrm{diag}\left[x_A(\theta_A), x_B(\theta_B)\right]W^T(\phi)\,, \tag{8.39}$$

where W is an orthogonal matrix diagonalizing X and $x_1(\theta_A) \geq x_2(\theta_A)$ are the eigenvalues of X depending on the angle θ_A. We can maximize I_4 over the phase ϕ. Further, if we substitute into the obtained formula the explicit forms of eigenvalues $x_{1,2}(\theta_A)$, we can perform also the maximization over the angle θ_A, which finally yields the invariant I_4 maximized over the phases $\theta_{A,B}$ of local measurements of the form:

$$\begin{aligned} I_4' \;=\; & \{[a + \cosh(2r_A)]\,[b + \cosh(2r_B)] \\ & + \sinh(2r_A)\sinh(2r_B)\}\left(c_1^2 + c_2^2\right) \\ & + \{[a + \cosh(2r_A)]\sinh(2r_B) \\ & + [b + \cosh(2r_B)]\sinh(2r_A)\}\left(c_1^2 - c_2^2\right). \end{aligned} \tag{8.40}$$

The corresponding value of f is denoted by $g(r_A, r_B)$. For a generic two–mode mixed Gaussian state it is again convenient to express the function $g(r_A, r_B)$ in terms of $h(r_A, r_B)$ as in Eq. (8.36), being

$$h(r_A, r_B) = (I_4' - I_3^2)/(I_1 I_2)\,, \tag{8.41}$$

where

$$I_1 = (a + e^{2r_A})(a + e^{-2r_A}), \tag{8.42}$$

$$I_2 = (b + e^{2r_B})(b + e^{-2r_B}), \tag{8.43}$$

$$I_3 = c_1 c_2. \tag{8.44}$$

As $\mathcal{I}(A:B) \geq 0$ always, it follows that $h(r_A, r_B) \geq 0$ and the game is on to maximise h. By introducing two new variables $\lambda = e^{2r_A}$ and $\mu = e^{2r_B}$ the extremal points of h can be found by solving the stationary conditions $\partial h/\partial\lambda = 0$ and $\partial h/\partial\mu = 0$, respectively, leading to a set of coupled polynomial equations of the form:

$$\begin{aligned} & c_+^2(a+\lambda)^2\mu^2 + [c_+^2 b(a+\lambda)^2 - c_-^2 b(a\lambda+1)^2 \\ & \quad + c_+^2 c_-^2 a(\lambda^2-1)]\mu - c_-^2(a\lambda+1)^2 = 0, \\ & c_+^2(b+\mu)^2\lambda^2 + [c_+^2 a(b+\mu)^2 - c_-^2 a(b\mu+1)^2 \\ & \quad + c_+^2 c_-^2 b(\mu^2-1)]\lambda - c_-^2(b\mu+1)^2 = 0. \end{aligned} \tag{8.45}$$

Upon solving one equation for μ and inputting the solution into the other, a complicated $12^{\rm th}$ order polynomial in λ emerges, that for the general case can be solved numerically. By taking its real roots calculated numerically together with stationary points on the boundary and picking the one for which h is maximized, we can finally get the optimal squeezing parameters $r_{A,B}$ of the seed elements $\hat{\Pi}_{A,B}$ of optimal local POVMs Eq. (8.2) maximizing the classical mutual information and thus attaining the Gaussian AMID, Eq. (8.4), of a generic two–mode Gaussian state.

Reassuringly, some analytical results can be found for non-trivial cases.

Case 4: Symmetric states
On symmetric Gaussian states, where $a = b$ only one stationary equation $\partial h/\partial\lambda = 0$ need be solved as $\mu = \lambda$. After some algebra the stationarity condition boils down to the following fourth-order polynomial equation

$$a_4\lambda^4 + a_3\lambda^3 + a_2\lambda^2 + a_1\lambda + a_0 = 0, \tag{8.46}$$

where

$$\begin{aligned} a_0 &= -c_-^2, \quad a_1 = -a\left(c_+^2 c_-^2 + 3c_-^2 - a^2 c_+^2\right), \\ a_4 &= c_+^2, \quad a_2 = 3a^2(c_+^2 - c_-^2), \\ a_3 &= a\left(c_+^2 c_-^2 + 3c_+^2 - a^2 c_-^2\right). \end{aligned} \tag{8.47}$$

The equation (8.46) can be solved analytically using the Cardan formulae but the obtained solutions are rather cumbersome and therefore we do not give them here explicitly. Calculating the values of the function $h(\lambda)$ in the admissible real solutions of Eq. (8.46) and also in the stationary points on the boundary, the point in which the function is maximal gives us the sought optimal squeezing.

Case 5: Squeezed Thermal States
Squeezed thermal states are generally asymmetric with $c_+ = c_- = c$. the optimal Gaussian POVMs can be derived in a simple closed form by performing the maximization of h in Eq. (8.41). We find the following results. If the state parameters a, b and c satisfy the inequality $(a+b+1)^2 \geq ab(ab-c^2)$, then the optimality is obtained by homodyne detection ($r_{A,B} \to \infty$) on both modes giving Eq. (8.37); conversely, if $(a+b+1)^2 < ab(ab-c^2)$, then the optimality is obtained by heterodyne detection ($r_A = r_B = 0$, projection onto coherent states) on both modes giving

$$g_{\text{het}} = \left[\frac{(a+1)(b+1)}{(a+1)(b+1)-c^2}\right]^2. \tag{8.48}$$

Summarizing, the Gaussian AMID of two–mode squeezed thermal states is given by Eq. (8.33) with

$$f = \begin{cases} g_{\text{hom}} \text{ [Eq. (8.37)]}, & (a+b+1)^2 \geq ab(ab-c^2); \\ g_{\text{het}} \text{ [Eq. (8.48)]}, & \text{otherwise.} \end{cases} \tag{8.49}$$

Case 6: Pure states
Within the class of the previous section lay the pure states, which must always have the form $a = b = \cosh(2r)$ and $c_+ = -c_- = \sinh(2r)$. In this case, the inequality in equation (8.49) is always satisfied and so double homodyning measurements are always optimal for the calculation of the Gaussian AMID. Although this result is quite intuitive (one could guess that in the pure-state case the optimal local Gaussian measurements possessing maximum Shannon mutual information for distribution of their outcomes would be homodyne detections), the corresponding value of $\mathcal{A}^G$ is strictly bigger than the entropy of entanglement, Eq. (3.29), which corresponds to the true AMID $\mathcal{A}$ globally optimized over joint, possibly non-Gaussian local POVMs as in the definition (7.46); and we know from Eq. (8.27) that the latter is indeed attained by local photon counting: $\mathcal{A}^G(|\psi(r)\rangle_{AB}) > \mathcal{A}(|\psi(r)\rangle_{AB}) = \mathcal{M}(|\psi(r)\rangle_{AB}) = \mathcal{E}_{v.N.}(|\psi(r)\rangle_{AB})$. Namely,

$$\mathcal{A}^G(|\psi(r)\rangle_{AB})) = 2\mathcal{M}(|\psi(r)\rangle_{AB}) - \ln[\cosh(2r)], \tag{8.50}$$

which is strictly bigger than the expression in equation (8.27).

This is particularly interesting as it answers already the question we previously posed - although it appears that when a single measurement is performed on one subsystem (a la discord) the optimal POVM is Gaussian, when we consider the symmetric version this is no longer true. Non-Gaussian measurements can beat the best Gaussian bi-local POVMS.

Naively, one might expect this result to be attributed to how the two mode squeezed vacuum is represented. After all, in the Fock state representation there is a perfect correlation between the number of photons in each subsystem whereas in the position/momentum basis perfect correlation can only be seen in the unphysical limit of $r \to \infty$. This property could then be characterised by the Einstein-Podolsky-Rosen variance $\langle(\hat{x}_A - \hat{x}_B)^2\rangle = e^{-2r}$ which, indeed, tends to zero as $r \to \infty$. However, by taking the difference between $\mathcal{A}^G\left(|\psi(r)\rangle_{AB}\right)$ and $\mathcal{M}\left(|\psi(r)\rangle_{AB}\right)$ and finding the limit as r tends to infinity, one sees that

$$\lim_{r\to\infty}\left[\mathcal{A}^G\left(|\psi(r)\rangle_{AB}\right) - \mathcal{M}\left(|\psi(r)\rangle_{AB}\right)\right] = 1 - \ln[2] \approx 0.3 \tag{8.51}$$

A full numerical comparison between Gaussian AMID, MID and Gaussian discord for two–mode Gaussian states will be provided in the next section.

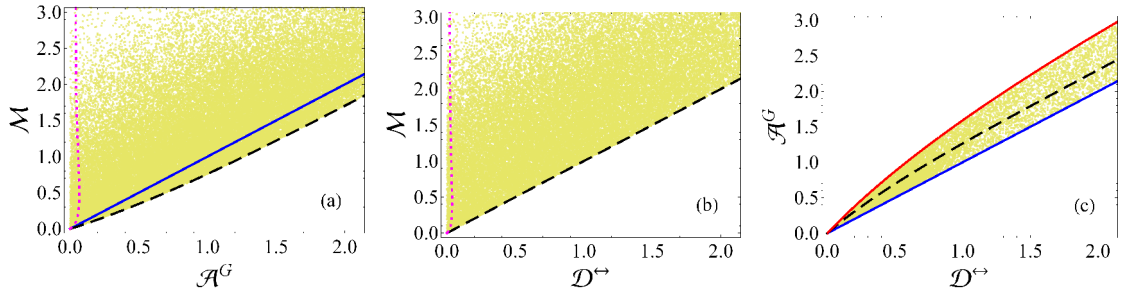

(a) MID vs GAMID (b) MID vs G. Discord (c) GAMID vs G. Discord

Figure 8.1: Comparison between (a) MID versus Gaussian AMID, (b) MID versus two-way Gaussian discord, and (c) Gaussian AMID versus two-way Gaussian discord, for 10^5 randomly generated mixed two–mode Gaussian states. The random Gaussian states were generated by choosing random symplectic matrices and applying them to a diagonal covariance matrix with symplectic eigenvalues chosen from a uniform distribution, as in [236]. Further restrictions were applied to single out e.g. the pure two mode squeezed states. Pure two–mode squeezed states are represented by the dashed black curve in all the plots. See text for details of the other boundaries. All the quantities plotted are dimensionless. Taken from **[II]**. Copyright (2011) by The American Physical Society.

8.4 Comparison between nonclassicality measures for Gaussian states

In this section, we aim to provide an extensive comparative analysis of MID ($\mathcal{M}$), Gaussian AMID ($\mathcal{A}^G$) and the two way Gaussian quantum discord ($\mathcal{D}_G^{\leftrightarrow}$) as tools to quantify the quantumness of correlations in arbitrary two mode Gaussian states via entropic descriptions of the state disturbance following suitable local measurements on one or both local parties. The results of the previous sections show that in Eq. (8.6), either quantity on the right hand side can be the smallest on particular instances of two–mode Gaussian states, suggesting that the subset of two–mode Gaussian states whose true AMID $\mathcal{A}$, Eq. (7.46), is necessarily optimized by non-Gaussian measurements, might have a finite volume in the space of general two–mode Gaussian states.

To confirm this interesting feature, we have generated a large number of random two–mode Gaussian states (up to 10^6), and for each of them we have evaluated the three symmetric nonclassicality indicators $\mathcal{D}_G^{\leftrightarrow}$, $\mathcal{A}^G$, and $\mathcal{M}$, following the prescriptions of the preceding Sections. The resulting analysis is illustrated in Figure 8.1. Panel (a) shows that, while the MID can be arbitrarily larger than the Gaussian AMID in principle, there is nonetheless a finite region in the ($\mathcal{A}^G$, $\mathcal{M}$) diagram that allocates two–mode Gaussian states for which even non-optimized non-Gaussian measurements (specifically, photon counting) result in a larger classical mutual information, hence minimise the quantum correlations in the definition of the AMID, compared to the optimal Gaussian POVMs. In this study the only non-Gaussian measurements considered were photon counting (that emerges in the definition of MID because Gaussian mixed states are essentially thermal states). Therefore, we can expect that the region in which general non-Gaussian measurements are optimal for the AMID can be in principle much larger than the one highlighted by the present study (that is located between the solid straight line and the dashed line in Figure 8.1a). Still, our finding is perhaps one of the most striking instances of an operational quantum informational measure for Gaussian states that can gain a significant optimization by the use of suitable non-Gaussian operations. Non-Gaussian operations can sometimes reveal quantumness more accurately, thus unleashing more precisely the available nonclassical resources, than the best Gaussian measurements, on certain two–mode Gaussian states, including quite remarkably all two–mode pure Gaussian states. Notice however that the rigidity in choosing the non-Gaussian measurements for the evaluation of MID, excluding any optimization procedure, results in most of the cases into a very loose overestimation of the quantum correlations, as testified by the unbounded region above the straight blue line, filled by states where certainly joint photon counting is not optimal for the AMID.

Interestingly, pure states embody the lower bound (dashed black curve) in Figure 8.1a: they are therefore the states where the Gaussian AMID realizes the most dramatic overestimation of the true AMID, that nonetheless can never exceed ≈ 0.3 as computed in the previous section.

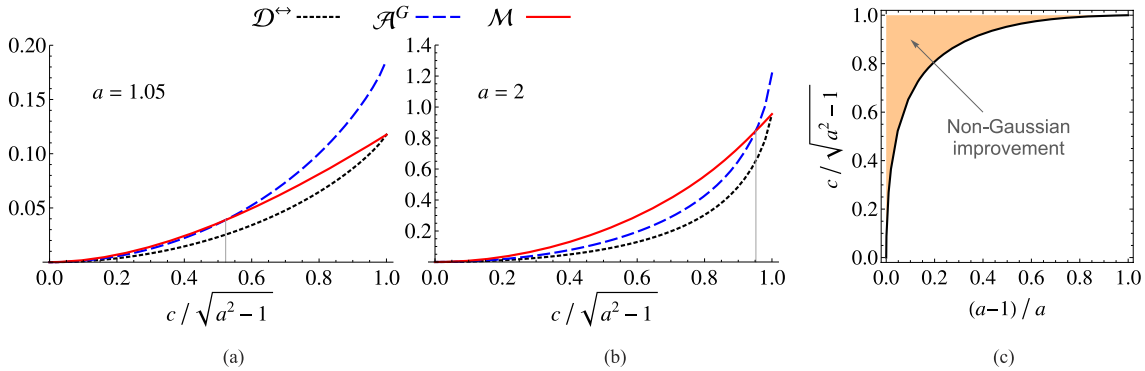

Figure 8.2: Comparison of different measures of quantum correlations for two–mode symmetric squeezed thermal Gaussian states ($b = a, c_1 = -c_2 = c$). Panels (a)-(b): Two-way Gaussian quantum discord $\mathcal{D}_G^{\leftrightarrow} = \max\{\mathcal{D}_G^{\leftarrow}, \mathcal{D}_G^{\rightarrow}\}$ (dotted black line), Gaussian AMID $\mathcal{A}^G$ associated to optimal bi-local Gaussian POVMs (dashed blue line), and unoptimized MID $\mathcal{M}$ associated to joint photon counting (solid red line), plotted versus the normalized state covariance parameter $c/\sqrt{a^2-1}$, for (a) $a = 1.05$ and (b) $a = 2$. The AMID $\mathcal{A}$ optimized over all possible (Gaussian and non-Gaussian) measurements is certainly $\mathcal{A} \leq \min\{\mathcal{M}, \mathcal{A}^G\}$. Both MID and Gaussian AMID majorize the Gaussian discord, but for c bigger than a certain threshold value $c^\star(a)$ (ticked by a vertical gray line in the plots) one has $\mathcal{M} < \mathcal{A}^G$, meaning that non-Gaussian measurements become necessarily optimal for the AMID. Panel (c) depicts the threshold curve $c^\star(a)$ (solid black line), defined by the condition $\mathcal{M} = \mathcal{A}^G$, in the normalized parameter space $\{(a-1)/a, c/\sqrt{a^2-1}\}$. The shaded (orange) region above the threshold line allocates instances of the considered family of states, lying in the neighbourhood of pure two–mode squeezed states, where certainly Gaussian POVMs are not globally optimal for the AMID, since photon counting results in a lower figure of merit. Below the threshold, either Gaussian measurements are optimal or there may exist some more general non-Gaussian measurement that achieves the absolute minimum in $\mathcal{A}$: our analysis cannot rule out this possibility. All the quantities plotted are dimensionless. Taken from **[II]**. Copyright (2011) by The American Physical Society.

A family of states sitting on the blue line in Figure 8.1a will be characterized shortly.

Before that, let us comment on the other panels of Figure 8.1. Panel (b) shows as expected, and in full analogy with the case of two qubits [192], that in general the unoptimized MID based on photon counting is a very loose upper bound to quantum discord for two–mode Gaussian states (reducing to it on pure states, depicted as dashed black again), unbounded from above and relentlessly approaching arbitrarily large values even for states with nearly vanishing quantum correlations as quantified by the (Gaussian) discord. This should discourage the usage of MID in general as it almost always provides overestimations, rather than reliable quantifications, of nonclassicality of bipartite correlations.

The last panel shows also a somehow analogous situation to the two–qubit case [192]: the Gaussian AMID is intimately related to discord, and admits upper and lower bounds at a given value of the two-way Gaussian discord. The lower (blue) boundary in panel (c) accommodates states for which the two quantifiers give identical prescriptions for measuring quantum correlations. These are states with CM in standard form, (8.1), given by

$$\begin{aligned} &a = \cosh(2s),\ b = \cosh^2(r)\cosh(2s) + \sinh^2(r), \\ &c_+ = -c_- = \cosh r \sinh(2s)\,, \end{aligned} \tag{8.52}$$

in the limit $r \to \infty$. They are characterized by $\mathcal{A}^G = \mathcal{D}_G^{\leftrightarrow} = 2\sinh^2 s \ln(\coth s)$. Pure states fill once more the dashed black curve, for which $\mathcal{D}_G^{\leftrightarrow} = \mathcal{E}$, Eq. (8.27), but $\mathcal{A}^G$ is strictly bigger, Eq. (8.50). The upper (red) boundary in Fig. 8.1c can be spanned for instance by symmetric squeezed thermal states ($b = a$, $c_+ = -c_- = c$), with $a \gg 1$ and $c \in [0, \sqrt{a^2-1})$. Upper and lower boundaries ideally conjoin asymptotically for diverging discord and Gaussian AMID.

We can now analyse in detail the competition between the MID associated to photon counting (typically very loose, but optimal on pure states) and the Gaussian AMID (very accurate for mixed and strongly correlated Gaussian states) to maximize the classical mutual information, hence minimizing the AMID, (8.6), on two–mode Gaussian states. We believe it is relevant to focus on the class of two–mode symmetric squeezed thermal Gaussian states

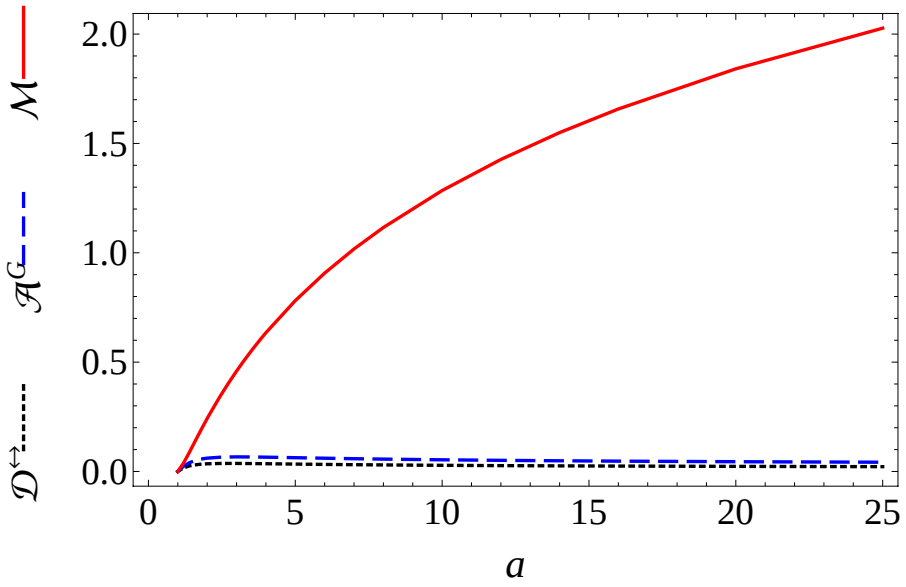

Figure 8.3: Plot of MID (solid red line), Gaussian AMID (dashed blue line) and Gaussian two-way quantum discord (dotted black line) as a function of the parameter a for the two–mode Gaussian states of Eq. (8.53). These curves give origin to the dotted magenta lines in Figure 8.1(a),(b). All the quantities plotted are dimensionless. Taken from **[II]**. Copyright (2011) by The American Physical Society.

($b = a, c_+ = -c_- = c$), for which the involved measures can be simply evaluated [1]. We plot in Figure 8.2 [(a),(b)] a comparison of the three measures studied here as a function of the rescaled state parameters a and c. We see that there is a certain threshold value $c^\star(a)$ beyond which the Gaussian POVMs are no longer optimal for the AMID, and non-Gaussian measurements such as photon counting (via MID) provide a more accurate result, culminating in the extreme case of pure states where those specific measurements are globally optimal. Panel (c) depicts the threshold in the parameter space, highlighting the region where our analysis conclusively reveals the necessity of non-Gaussian measurements for the global optimization of AMID and classical mutual information of the considered class of two–mode Gaussian states. As previously remarked, this region can be in principle (and is likely to be so) much larger. Yet, it certainly occupies a finite volume in the space of general two–mode Gaussian states. Notice that for all the Gaussian states in such a region, non-Gaussian measurements allow one to extract stronger correlated measurement records compared to any bi-local Gaussian measurement, as the classical mutual information is maximized by non-Gaussian detections. The states attaining the threshold identified in this analysis, are an instance of states filling up the blue line in Figure 8.1a.

Finally, we exhibit an example family of two–mode Gaussian states where, on the opposite end, the MID based on non-Gaussian detections is a highly inaccurate measure of quantum correlations. These states sit on the quasi-vertical dashed curves in Figure 8.1(a) and (b). They are symmetric states with

$$b = a,\ c_- = 0,\ \text{and}\ c_+ = (a^2 - 1 - \ln a)/a. \tag{8.53}$$

As apparent from Figure 8.3, their Gaussian discord and Gaussian AMID stay limited (smaller than ≈ 0.06) and rigorously vanish in the asymptotic limit $a \to \infty$. On the other hand, their MID arising from Fock projections increases arbitrarily and diverges for $a \to \infty$, embodying an extreme overestimation of some vanishing quantum correlations. Clearly there will be many more families of Gaussian states where such a behavior will arise.

[1] For squeezed thermal states, the Gaussian discord is optimized by a local heterodyne detection [220, 221].

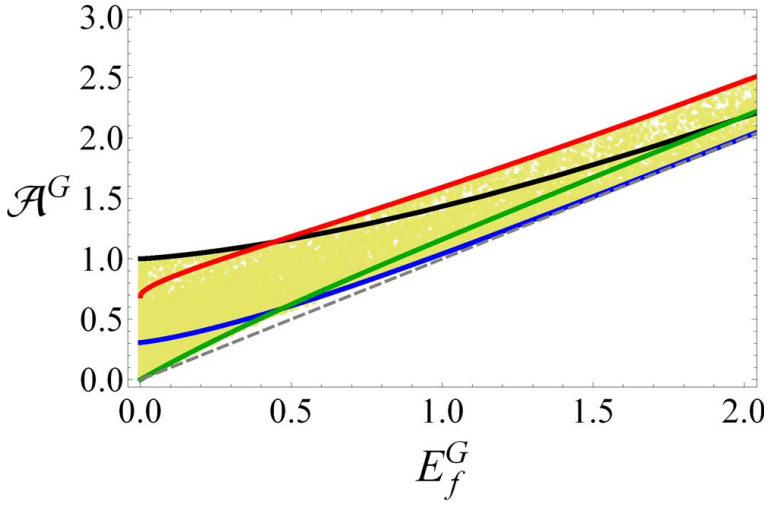

Figure 8.4: Plot of Gaussian AMID $\mathcal{A}^G$ versus Gaussian EoF E_f^G for 10^5 random two–mode Gaussian states. The dashed line of equation $\mathcal{A}^G = E_f^G$ stands as a lower bound for the physically admitted region. Refer to the main text for details of the other curves. All the quantities plotted are dimensionless. Taken from **[II]**. Copyright (2011) by The American Physical Society.

8.5 Nonclassicality versus entanglement

Here we present a numerical comparison between nonclassicality of correlations, measured by means of the Gaussian AMID [Eq. (8.4)], and entanglement, quantified by the Gaussian EoF [137], for generally mixed two–mode Gaussian states. A similar analysis was performed in Ref. [221], with (Gaussian) discord used as a nonclassicality indicator.

Figure 8.4 shows the distribution of Gaussian AMID versus Gaussian EoF for a sample of 10^5 randomly generated two–mode Gaussian states. In analogy with the case of Gaussian discord vs Gaussian EoF, it is possible to identify upper and lower bounds on the Gaussian AMID $\mathcal{A}^G$ at fixed entanglement E_f^G. Interestingly, our numerical exploration shows that for all two–mode Gaussian states $\hat{\rho}_{AB}$, it is

$$\mathcal{A}^G(\hat{\rho}_{AB}) \geq E_f^G(\hat{\rho}_{AB})\,. \tag{8.54}$$

This provides a novel hierarchical relationship between different types of nonclassical resources, entanglement E_f^G, and more general measurement-induced quantum correlations $\mathcal{A}^G$: On the basis of the hereby employed measures (both symmetric by construction and restricted to a fully Gaussian scenario), the latters appear to always encompass and exceed entanglement itself for two–mode generally mixed Gaussian states. A similar relationship does not hold for discord, which can be smaller as well as larger than entanglement of formation, even in a Gaussian scenario [221, 237].

We can provide two families of two–mode Gaussian states for which Eq. (8.54) becomes asymptotically tight. One such class is provided, e.g., by symmetric squeezed thermal states, whose standard form CM is as in Eq. (8.1) with

$$b = a\,, \quad c_+ = -c_- = a - \tilde{\nu}\,, \tag{8.55}$$

where

$$\tilde{\nu} > 0\,, \quad a \geq \max\{\tilde{\nu},\, (1+\tilde{\nu}^2)/(2\tilde{\nu})\}\,. \tag{8.56}$$

The Gaussian EoF of these states (equal to the true EoF minimized over all possible pure-state decompositions, by virtue of the symmetry of the states [136]) is a simple monotonically decreasing function of the positive parameter $\tilde{\nu}$,

$$E_f^G(\tilde{\nu}) = \frac{(1+\tilde{\nu})^2 \ln\left[\frac{(1+\tilde{\nu})^2}{4\tilde{\nu}}\right] - (1-\tilde{\nu})^2 \ln\left[\frac{(1-\tilde{\nu})^2}{4\tilde{\nu}}\right]}{4\tilde{\nu}}\,, \tag{8.57}$$

if $\tilde{\nu} < 1$, and $E_f^G(\tilde{\nu}) = 0$ otherwise. The Gaussian AMID can be computed analytically according to the prescription of Section 8.3, and for any fixed $\tilde{\nu}$ (i.e., fixed Gaussian EoF) one can find the optimal value of the parameter a, in the range defined by (8.56), that minimizes $\mathcal{A}^G$. The resulting $\mathcal{A}^G$ as a function of E_f^G is plotted in Figure 8.4 as a green curve: For this family of states, the Gaussian AMID approaches the Gaussian EoF as the latter tends to zero, tending to saturate inequality (8.54) asymptotically in the regime of infinitesimal correlations.

Furthermore, let us consider another class of symmetric two–mode states, whose standard form CM is as in Eq. (8.1) with

$$b = a,\, c_+ = a - (1+\tilde{\nu}^2)/(2a),\, c_- = a - (2a)/(1+\tilde{\nu}^2)\,, \tag{8.58}$$

where the parameter range is the same as in Eq. (8.56). The Gaussian EoF of these states is still given by Eq. (8.57), while in the limit $a \to \infty$ one can show that their Gaussian AMID is attained by homodyne detections on both modes, yielding $\mathcal{A}^G(\tilde{\nu}) = 1 - \ln(4\tilde{\nu}) + \ln(1+\tilde{\nu}^2)$. The corresponding Gaussian AMID vs Gaussian EoF curve for these states is depicted in Figure 8.4 as a blue curve: In this case, the Gaussian AMID approaches the Gaussian EoF as the latter tends to infinity, also saturating inequality (8.54) asymptotically.

It has to be underlined that the two presented Gaussian families are just examples to show that the bound in Eq. (8.54) can be asymptotically tight, and we remark that the combination of the two presented curves does not provide a strict lower bound to Gaussian AMID against Gaussian EoF for all two–mode Gaussian states, as it is evident from the presence of some random points below the intersection of the two (green and blue) curves – however above the dashed line corresponding to the bound of Eq. (8.54) [see Figure 8.4].

On the other hand, a tight upper bound on the Gaussian AMID at fixed Gaussian EOF can be identified. We found it numerically to be constituted by the maximum of two branches,

$$\mathcal{A}^G(\hat{\rho}_{AB}) \leq \begin{cases} 1 + 2\ln(1+\tilde{\nu}) - \ln(4\tilde{\nu}), \\ \quad 4/\mathrm{e} - 1 \leq \tilde{\nu} \leq 1; \\ \\ \ln(1+\tilde{\nu}) - \ln(\tilde{\nu}), \\ \quad 0 < \tilde{\nu} < 4/\mathrm{e} - 1; \end{cases} \tag{8.59}$$

where $E_f^G(\hat{\rho}_{AB})$ is given by Eq. (8.57).

The first expression in Eq. (8.59) corresponds to the Gaussian AMID of the states of Eq. (8.52) with $s \to \infty$ and $r = 2\tanh^{-1}(\sqrt{\tilde{\nu}})$, and is depicted as a black curve in Fig. 8.4. It provides an upper bound for all two–mode Gaussian states distributed in the $\{E_f^G, \mathcal{A}^G\}$ plane, in the region of moderate entanglement; such a bound converges to 1 in the separability limit ($\tilde{\nu} = 1$). We can thus conclude that the degree of nonclassicality of correlations in separable Gaussian states is always nonzero (apart from the trivial case of uncorrelated, product states) but stays nevertheless limited: It can at most reach unity, whether measured by the discord [220, 221] or by the Gaussian AMID.

The second expression in Eq. (8.59) corresponds instead to the Gaussian AMID of the states of Eq. (8.55) in the limit $a \to \infty$. It bounds from above the value of $\mathcal{A}^G$ for all two–mode Gaussian states with fixed $E_f^G \gtrapprox 0.441$ [where this number is obtained by setting $\tilde{\nu} = 4/\mathrm{e} - 1$ in Eq. (8.57)]. In the limit of infinite entanglement ($\tilde{\nu} \to 0$), the upper bound on the Gaussian AMID converges to $E_f^G + \ln 4 - 1$. Combining this observation with the lower bound (8.54), we have that, interestingly, the following sandwich relation holds for all two–mode Gaussian states with $E_f^G \gg 0$,

$$E_f^G(\hat{\rho}_{AB}) \leq \mathcal{A}^G(\hat{\rho}_{AB}) \leq E_f^G(\hat{\rho}_{AB}) + \ln 4 - 1\,. \tag{8.60}$$

In the previous analysis, we have identified some similarities as well as some key differences in the quantification of nonclassical correlations versus entanglement of Gaussian states when Gaussian AMID rather than quantum discord are employed. In order to have a visual comparison between the two nonclassicality indicators and the Gaussian EoF, we focus on the relevant two-parameter class of symmetric squeezed thermal states $\hat{\rho}_{AB}^{sts}$, with CM as in Eq. (8.55). For these states, the entanglement is given by (8.57) (independently of a), while the discord can be written

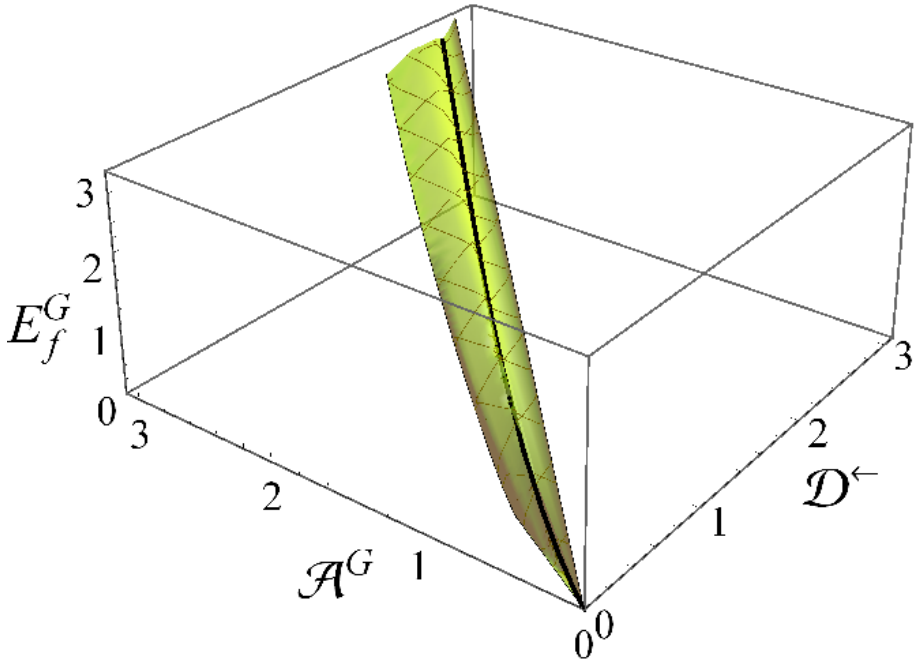

Figure 8.5: 3D Plot of Gaussian EoF E_f^G [Eq. (8.57)] versus Gaussian discord $\mathcal{D}_G^{\leftarrow}$ [Eq. (8.61)] and Gaussian AMID $\mathcal{A}^G$ [Eq. (8.62)] for two–mode symmetric squeezed thermal Gaussian states, characterized by their covariance parameters a and $\tilde{\nu}$ [see Eq. (8.55)]. The solid black line accommodates pure states ($\tilde{\nu} = a - \sqrt{a^2-1}$). All the quantities plotted are dimensionless. Taken from **[II]**. Copyright (2011) by The American Physical Society.

as [220, 221]

$$\begin{aligned}\mathcal{D}_G^{\leftarrow}(\hat{\rho}_{AB}^{sts}) =& \frac{1}{2(1+a)}\Bigg\{\left(4a(\tilde{\nu}+1)-2\tilde{\nu}^2\right)\tanh^{-1}\left(\frac{a+1}{2a\tilde{\nu}+a-\tilde{\nu}^2}\right)\\ &-4(a+1)\sqrt{\tilde{\nu}(2a-\tilde{\nu})}\tanh^{-1}\left(\frac{1}{\sqrt{\tilde{\nu}(2a-\tilde{\nu})}}\right)\\ &+a^2\ln\left[\frac{a+1}{a-1}\right]-\ln\left[\frac{(a+1)\left(2a\tilde{\nu}-\tilde{\nu}^2-1\right)}{(a-1)(\tilde{\nu}+1)(2a-\tilde{\nu}+1)}\right]\Bigg\},\end{aligned} \tag{8.61}$$

and the Gaussian AMID reads

$$\begin{aligned}\mathcal{A}^G(\hat{\rho}_{AB}^{sts}) =& -\ln\left[\frac{2a\tilde{\nu}-\tilde{\nu}^2-1}{a^2-1}\right]+2a\coth^{-1}(a)\\ &-2\sqrt{\tilde{\nu}(2a-\tilde{\nu})}\tanh^{-1}\left(\frac{1}{\sqrt{\tilde{\nu}(2a-\tilde{\nu})}}\right)\\ &-\ln\begin{cases}\frac{a}{\sqrt{a^2-(a-\tilde{\nu})^2}}, & 1+a\left(4+a\left(4-2a\tilde{\nu}+\tilde{\nu}^2\right)\right)\geq 0;\\ \frac{(a+1)^2}{(a+1)^2-(a-\tilde{\nu})^2}, & \text{otherwise.}\end{cases}\end{aligned} \tag{8.62}$$

Figure 8.5 shows E_f^G plotted versus $\mathcal{D}_G^{\leftarrow}$ and $\mathcal{A}^G$ for this particular class of Gaussian states, spanned by a and $\tilde{\nu}$. All two–mode symmetric squeezed thermal states sit on a two-dimensional surface in the space of the three entropic nonclassicality indicators, providing a direct evidence of the intimate yet intricate relationship between the different aspects of quantumness in Gaussian states. One can notice the branch of separable states, in the plane $E_f^G = 0$ with generally nonzero discord and Gaussian AMID; while for all entangled squeezed thermal states, E_f^G can be exactly recast as a function of $\mathcal{D}_G^{\leftrightarrow}$ and $\mathcal{A}^G$: Knowledge of two nonclassicality quantifiers fixes the third one univocally. We remark that such a strict result does not extend to more

general two–mode Gaussian states, which distribute filling a more complex, finite-volume three-dimensional region in the space $\{\mathcal{D}_G^{\leftarrow}, \mathcal{A}^G, E_f^G\}$. Figures 8.1c and 8.4 of this paper, and Figure 1(right) of Ref. [221], represent the two-dimensional projections of such a region onto the planes $\{\mathcal{D}_G^{\leftarrow}, \mathcal{A}^G\}$, $\{E_f^G, \mathcal{A}^G\}$, and $\{E_f^G, \mathcal{D}_G^{\leftarrow}\}$, respectively.

8.6 Summary of Chapter 8

In this chapter we have performed an exhaustive study of nonclassical correlations in generic two mode Gaussian states using information-theoretic non-classicality quantifiers. We have shown how to calculate the Measurement Induced Disturbance $\mathcal{M}$ of a two mode Gaussian state in standard form. The projection onto the eigenvectors of the marginal states corresponds to photon counting, and so the MID quantifies the gap between a state's quantum mutual information and the classical mutual information after local Fock state detections. We then introduced the Gaussian Ameliorated Measurement Induced Disturbance $\mathcal{A}^G$, which looks at the gap between the quantum mutual information and the classical mutual information after local Gaussian measurements. An analytic form of $\mathcal{A}^G$ can be found for important subclasses of two mode Gaussian states. Namely, symmetric states and squeezed thermal states, including pure states. Unfortunately, for more general states one has to find the roots of a 12th order polynomial although this can be done numerically.

Furthermore, we have compared the MID and Gaussian AMID and seen some interesting results. Firstly, for a fixed value of $\mathcal{A}^G$, it is possible to find Gaussian states for which the Measurement Induced Disturbance gives an arbitrarily high reading, even if the Gaussian AMID is infinitesimally small. On the other hand, there also exists a volume of Gaussian states for which the MID gives a lower value than the Gaussian AMID. This is one of the most remarkable finds of this chapter. Contrary to the hypothesis that for quantum discord, Gaussian measurements are optimal on Gaussian states, for the symmetric AMID non-Gaussian measurements have a serious role to play. However, although counter-intuitive, it is known that in some protocols involving Gaussian states a non-Gaussian element is required. This is most obviously demonstrated by the necessity of a non-Gaussian element in the distillation of entanglement in Gaussian states.

We have also compared both the MID and the Gaussian AMID with the two-way Gaussian discord. Once again, we found that for a given value of $\mathcal{D}_G^{\leftrightarrow}$, there are Gaussian states for which the reading given by MID has no upper bound. However, upper and lower bounds exist for the value of Gaussian AMID. Finally, we compared the Gaussian AMID with the Gaussian Entanglement of Formation, identifying lower and upper bounds for the former as a function of the latter. The GAMID always exceeds the Gaussian Entanglement of Formation for all two mode Gaussian states, thus enforcing a hierarchy between two different forms of nonclassicality. Exact relations between Gaussian AMID, Gaussian discord, and Gaussian entanglement of formation can be formulated for special families of Gaussian states such as the symmetric squeezed thermal states.

In the next chapter we shall use these tools to forge ahead and see how these measures act on a simple family of non-Gaussian states.

Chapter 9

Non-classical correlations in the continuous variable Werner state

Non-classical correlations, including and beyond entanglement, have been examined thoroughly in two mode Gaussian states. Measures that aim at capturing the signatures of quantum behaviour in continuous variable systems have been defined that include the Gaussian discord, the Measurement Induced Disturbance (MID), and the Gaussian Ameliorated Measurement Induced Disturbance (GAMID), introduced in the previous chapter. The preceding study caused some interesting behaviour to surface and it is clear that there are some two mode Gaussian states for which the optimal measurement is non-Gaussian when comparing MID and GAMID.

Curiosity drives us to examine how the measures used previously behave on non-Gaussian states. It is probably impossible to evaluate these measures on all non-Gaussian quantum states, just as it is probably impossible to optimise the measures over all possible POVMs, Gaussian and non-Gaussian. The Hilbert space is just a bit too large. We can, however, look at how these measures behave on small families of non-Gaussian states.

In this chapter, based on **[IV]**, we consider a family of two mode states that are the continuous variable counterparts of two-qubit Werner states [87]. They are non-Gaussian states obtained as mixtures of two Gaussian states [238], namely a two mode squeezed vacuum and a two mode thermal product state, and find applications in continuous variable quantum cryptography [239]. These states are defined in Section 9.1. Studying their nonclassicality beyond entanglement is particularly interesting from a fundamental point of view, as they offer a unique test bed to compare the role of Gaussian versus non-Gaussian measurements to extract correlations with minimum disturbance from general two mode continuous variable states.

We show that the states analysed here carry *genuine* non-classical continuous variable correlations. That is, the optimisation in the quantum discord requires an infinite dimensional component[1].

In some families of the CV Werner states considered the quantum discord can be computed analytically. In particular, if we mix the pure two mode squeezed vacuum with a pure vacuum to create a non-Gaussian mixture as in Section 9.2, the optimal measurement in the definition of quantum discord is achieved by the non-Gaussian photon counting. We analyse the gap between the optimal Gaussian measurements (homodyning) and the true discord. In this special case, the quantum discord can also be shown to be equal to other non-classicality measures.

It is possible to find formulae for evaluating these non-classicality measures for the most general continuous variable Werner state, ideally complementing the analysis of the two qubit Werner state performed originally in [7]. We show in Section 9.3 that photon counting provides an upper bound on the quantum discord that coincides with the MID. We also derive a non-trivial lower bound on the discord. In Section 9.4 we introduce an example of a continuous variable PPT state and show that it carries "weak" non-classical correlations, signalled by analytically computable upper and lower bounds on discord which are close and stay small and finite even

[1] If this were not the case then one could argue that any qudit state (e.g. a two qubit state) is an example of a non-Gaussian continuous variable state. They are certainly non-Gaussian as they are mixtures of a few photons, but they span only a finite dimensional space, which is a truncation of the infinite dimensional Hilbert space. In contrast, the continuous variable Werner states require measurements spanning the entire infinite dimensional Hilbert space.

under infinite squeezing.

In this chapter, our results provide insights into the relation between non-classical correlations, entanglement distillability and separability in CV systems outside the Gaussian scenario. From a practical perspective, our results identify the key role of non-Gaussian measurements such as photon counting to access and extract all non-classical correlations in general CV states, even in the particular case of non-Gaussian states with a positive-everywhere Wigner function, such as those studied here.

Before we begin, we note that there has been a notation change throughout this chapter. As the continuous variable Werner state is symmetric under exchange of it's parties, we have

$$\mathcal{D}^{\leftarrow}(\hat{\rho}_{AB}) = \mathcal{D}^{\rightarrow}(\hat{\rho}_{AB}) = \mathcal{D}^{\leftrightarrow}(\hat{\rho}_{AB}) \tag{9.1}$$

and we choose to drop the superscript and refer to all three quantities as $\mathcal{D}$. Also, in this chapter, we drop the hats from all of the density operators for ease of notation. There is no need to refer to individual density matrix elements as there was in e.g. Chapter 5 and so no confusion should arise.

9.1 The continuous variable Werner state

The continuous variable Werner state was first introduced in [238] and is defined as

$$\rho = p\,|\psi(\lambda)\rangle\langle\psi(\lambda)| + (1-p)\,\rho_A^{\text{th}}(\mu) \otimes \rho_B^{\text{th}}(\mu), \tag{9.2}$$

where $0 \leq p \leq 1$,

$$|\psi(\lambda)\rangle = \sqrt{1-\lambda^2}\sum_{n=0}^{\infty}\lambda^n|n,n\rangle_{AB}. \tag{9.3}$$

is the two-mode squeezed vacuum state with $\lambda = \tanh r$ (r is the squeezing parameter) and

$$\rho_j^{\text{th}}(\mu) = (1-\mu^2)\sum_{n=0}^{\infty}\mu^{2n}|n\rangle_j\langle n|, \quad j = A, B \tag{9.4}$$

is the thermal state with $\mu^2 = \langle n_j\rangle/(1+\langle n_j\rangle)$, where $\langle n_j\rangle$ is the mean number of thermal photons in mode j. As with the $d-$ dimensional qudit Werner states, the continuous variable Werner states possess the same structure as those shown to be invariant under the maximal commutative subgroup of $U(d)$ introduced in [240].

9.2 Two mode squeezed vacuum and pure vacuum mixture: $\mu = 0$

First, let us consider the simplest special case of a Werner state with $\mu = 0$ which gives using Eq. (9.2)

$$\rho_0 = p\,|\psi(\lambda)\rangle\langle\psi(\lambda)| + (1-p)\,|00\rangle\langle 00|\,, \tag{9.5}$$

representing just a mixture of a two-mode squeezed vacuum state with the vacuum. For $p > 0$ the partially transposed matrix $\rho_0^{T_A}$ (obtained by transposing ρ_0 with respect to the degrees of freedom of subsystem A only) has negative eigenvalues [238] and therefore, according to the PPT criterion [95, 96], the state (9.5) is entangled. Note that the state (9.5) has been further studied in [239, 241] from the point of view of its entanglement properties, as measured by the negativity, highlighting its applications for quantum key distribution.

Exact calculation of quantum discord

In order to calculate the entropies arising in the expression of quantum discord we need to determine the eigenvalues of the reduced state $\rho_{0,B}$, the global state (9.5) and the conditional state $\rho_{A|i} = \text{Tr}_B[\Pi_B(i)\rho_0]/p_B(i)$. The latter two states attain the form

$$\sigma = \zeta_1\,|\phi_1\rangle\langle\phi_1| + \zeta_2\,|\phi_2\rangle\langle\phi_2|, \tag{9.6}$$

where $\zeta_1 + \zeta_2 = 1$ and $|\phi_{1,2}\rangle$ are generally nonorthogonal normalized pure state vectors. The state (9.6) has at most two-dimensional support spanned by vectors $|\phi_{1,2}\rangle$ corresponding to eigenvalues $\nu_{1,2}$ that read as

$$\nu_{1,2} = \frac{1 \pm \sqrt{1 - 4\zeta_1\zeta_2\left(1 - |\langle\phi_1|\phi_2\rangle|^2\right)}}{2}. \tag{9.7}$$

On inserting the eigenvalues (9.7) into the formula for the von Neumann entropy

$$\mathcal{S}(\sigma) = -\sum_{i=1}^{2} \nu_i \ln \nu_i \tag{9.8}$$

we get analytically the entropy of the state (9.6).

Returning back to the state (9.5) we get, in particular, $|\phi_1\rangle = |\psi(\lambda)\rangle, |\phi_2\rangle = |00\rangle, \zeta_1 = p$ and $\zeta_2 = 1 - p$. The eigenvalues thus amount to

$$\nu_{1,2} = \frac{1 \pm \sqrt{1 - 4p(1-p)\lambda^2}}{2}. \tag{9.9}$$

Hence, we can immediately calculate the entropy $\mathcal{S}(\rho_0)$ using formula (9.8),

$$\begin{aligned}\mathcal{S}(\rho_0) = \quad & -\left(\tfrac{1+\sqrt{1-4p(1-p)\lambda^2}}{2}\right)\ln\left(\tfrac{1+\sqrt{1-4p(1-p)\lambda^2}}{2}\right) \\ & -\left(\tfrac{1-\sqrt{1-4p(1-p)\lambda^2}}{2}\right)\ln\left(\tfrac{1-\sqrt{1-4p(1-p)\lambda^2}}{2}\right).\end{aligned} \tag{9.10}$$

We can next find the entropy of the partial state. Tracing over mode A yields the diagonal reduced state

$$\rho_{0,B} = p\rho_B^{\text{th}}(\lambda) + (1-p)|0\rangle_B\langle 0|, \tag{9.11}$$

with ρ_B^{th} given in Eq. (9.4), possessing the eigenvalues

$$\tilde{\nu}_0 = 1 - p\lambda^2, \quad \tilde{\nu}_{n>0} = p(1-\lambda^2)\lambda^{2n}, \tag{9.12}$$

for $n \in \mathbb{N}$. Making use of the definition (9.8) we get also the entropy of the reduced state in the form

$$\mathcal{S}(\rho_{0,B}) = -\left(\ln(1-p\lambda^2) + p\lambda^2 \ln\left[\frac{p(1-\lambda^2)}{1-p\lambda^2}\right] + \frac{2p\lambda^2\ln\lambda}{1-\lambda^2}\right). \tag{9.13}$$

By far the hardest part is the minimisation of the conditional entropy $\mathcal{H}_{\hat{\Pi}_i}(A|B)$ over all POVMs. State (9.5) has been constructed in such a way as to make it possible to guess at a solution without needing to solve this difficult task explicitly. A closer look at the state reveals that the optimal measurement on mode B is simply photon counting, with the set of projectors $\hat{\Pi}_B(m) = |m\rangle\langle m|$ where $|m\rangle$ is a Fock state. In this case, if we detect the m photons in mode B then the conditional state $\rho_{A|m}$ is simply a *pure* Fock state $|m\rangle\langle m|$ which implies immediately that $\mathcal{H}_{\hat{\Pi}(m)}(A|B) = 0$. As the conditional entropy can never be less than zero, it is clear that we have found the optimal measurement. The discord of state ρ_0 is then equal to

$$\mathcal{D}(\rho_0) = \mathcal{S}(\rho_{0,B}) - \mathcal{S}(\rho_0) \tag{9.14}$$

where the involved entropies are defined in equations (9.10) and (9.13). The discord is an increasing function of both λ and p and is plotted in Figure 9.1. Note, that the considered Werner state (8) belongs to the class of maximally correlated states for which Eq. (9.14) can be proved alternatively [219] using the duality relation between classical correlations and entanglement of formation [207].

Discord versus Gaussian discord and the non-Gaussianity of the state

A rather pertinent question arises: Is there another measurement besides photon counting that realises the minimum of the conditional entropy? With this in mind we explore whether there is any Gaussian measurement that could also give $\mathcal{H}_{\hat{\Pi}(m)}(A|B) = 0$. The answer, as we argue

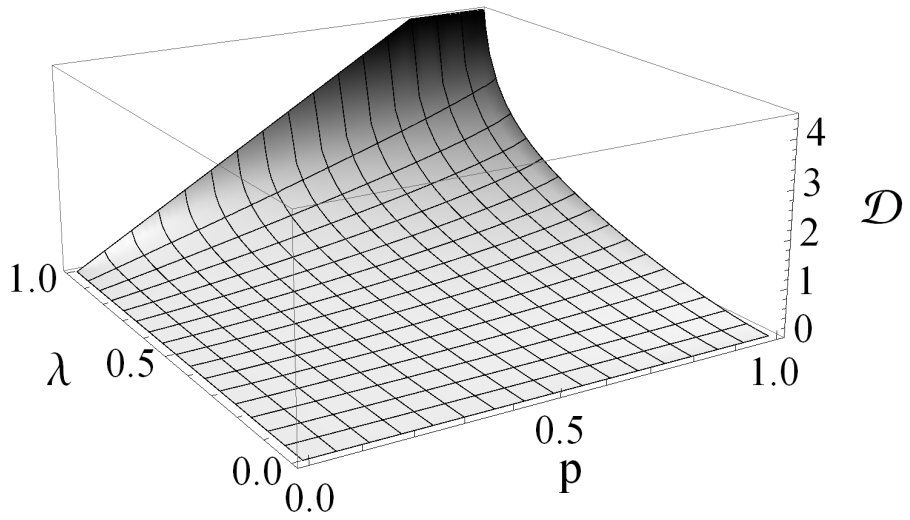

Figure 9.1: Quantum discord $\mathcal{D}$ (Equation (9.14) versus the probability p and the squeezing factor λ for the CV Werner state ρ_0 (Equation (9.5)). All the quantities plotted are dimensionless. Taken from **[IV]**. Copyright (2012) by The American Physical Society.

in the following, is that nonclassical correlations in the state (9.5) captured by discord (9.14) cannot be extracted equally well by any Gaussian measurement. In contrast to the case of two mode Gaussian states, where it is believed that Gaussian measurements are always optimal, in this simple non-Gaussian state, we will show that non-Gaussian measurements are required and the best Gaussian measurement can only ever provide an upper bound to the discord. To show this, consider the following Gaussian POVM [176] consisting of elements

$$\Pi(\alpha) = \frac{1}{\pi}|\alpha,\xi\rangle\langle\alpha,\xi|, \tag{9.15}$$

where

$$|\alpha,\xi\rangle \equiv \hat{D}(\alpha)S(\xi)|0\rangle, \tag{9.16}$$

with $\xi = te^{i2\varphi}$, is a pure normalized momentum-squeezed vacuum state with squeezing parameter $t \in [0,\infty)$, that is rotated counterclockwise by a phase $\varphi \in [0,\pi)$ and that is subsequently displaced by $\alpha \in \mathbb{C}$. Here, $\hat{D}(\alpha) = \exp(\alpha a^\dagger - \alpha^* a)$ is the displacement operator and $S(\xi) = \exp\left\{\left[\xi(a^\dagger)^2 - \xi^* a^2\right]/2\right\}$ is the squeezing operator. Note that $t = 0$ corresponds to heterodyne detection, whereas homodyne detection is obtained in the limit $t \to \infty$. If the POVM element $\Pi(\alpha)$ is detected on mode B of the two-mode squeezed vacuum state (9.3), then mode A collapses into the state $|\beta,\omega = se^{-i2\varphi}\rangle$, which is a pure momentum-squeezed state with squeezing parameter

$$s = \frac{1}{2}\ln\left[\frac{1+e^{2t}\cosh(2r)}{\cosh(2r)+e^{2t}}\right] \tag{9.17}$$

that is rotated clockwise by phase φ and that is displaced by

$$\beta = \frac{\sinh(2r)}{2}\left[(z_+ + z_-)\,\alpha^* + (z_+ - z_-)\,e^{-i2\varphi}\alpha\right], \tag{9.18}$$

where $z_\pm = \left[\cosh(2r) + \exp(\pm 2t)\right]^{-1}$. Thus, the obtained conditional state,

$$\rho_{A|\alpha} = \mathrm{Tr}_B\left[\Pi_B(\alpha)\,\rho_0\right]/q(\alpha) \tag{9.19}$$

is again a convex mixture of the form (9.6) where $|\phi_1\rangle = |\beta,\omega\rangle$, $|\phi_2\rangle = |0\rangle$ and

$$\zeta_{1_\alpha} = \frac{pu(\alpha)}{\pi q(\alpha)}, \quad \zeta_{2_\alpha} = \frac{(1-p)v(\alpha)}{\pi q(\alpha)}. \tag{9.20}$$

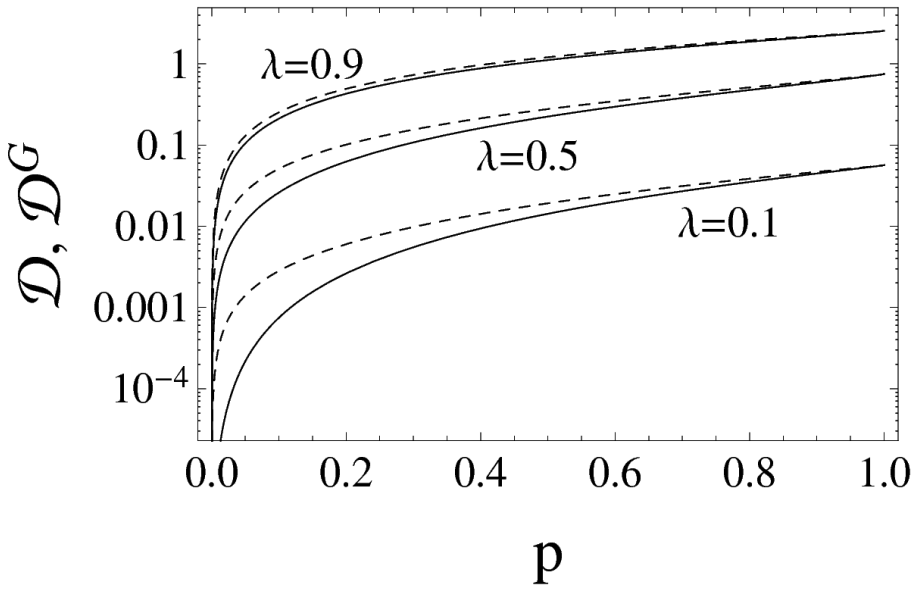

Figure 9.2: Logarithmic plot of quantum discord (solid curve) and Gaussian quantum discord (dashed curve) versus the probability p for the CV Werner state (9.5) with (from bottom to top) $\lambda = 0.1, 0.5, 0.9$. All the quantities plotted are dimensionless. Taken from **[IV]**. Copyright (2012) by The American Physical Society.

Here $q(\alpha) = [pu(\alpha) + (1-p)v(\alpha)]/\pi$ is the probability density of obtaining the measurement outcome α, $u(\alpha) = \langle \alpha, \xi | \rho_B^{\rm th}(\lambda) | \alpha, \xi \rangle$, where $\rho_B^{\rm th}(\lambda)$ is given in Eq. (9.4), and $v(\alpha) = |\langle 0|\alpha, \xi\rangle|^2$. The latter function $v(\alpha)$ can be computed straightforwardly using the formula [234]

$$\langle 0|\alpha, \xi = te^{i2\varphi}\rangle = \frac{\mathrm{e}^{-\frac{|\alpha|^2}{2} + \frac{\tanh(t)}{2}\mathrm{e}^{i2\varphi}\alpha^{*2}}}{\sqrt{\cosh(t)}}. \tag{9.21}$$

The overlap $|\langle \phi_1|\phi_2\rangle|^2 = |\langle 0|\beta, \omega = s\mathrm{e}^{-i2\varphi}\rangle|^2$ appearing in eigenvalues (9.7) can be calculated exactly along the same lines.

One can use the $\mathcal{P}$ function (section 2.2) representation of the thermal state, and the optical equivalence theorem (2.90) to express the thermal state as

$$\rho_B^{\rm th}(\lambda) = \frac{1-\lambda^2}{\pi\lambda^2} \int_{\mathbb{C}} \mathrm{e}^{-\frac{1-\lambda^2}{\lambda^2}|\varsigma|^2} |\varsigma\rangle\langle\varsigma| d^2\varsigma. \tag{9.22}$$

From this, we get the function $u(\alpha)$ in the form

$$u(\alpha) = \frac{1-\lambda^2}{\pi\lambda^2} \int_{\mathbb{C}} \mathrm{e}^{-\frac{1-\lambda^2}{\lambda^2}|\varsigma|^2} |\langle 0|\alpha - \varsigma, \xi\rangle|^2 d^2\varsigma, \tag{9.23}$$

where we used the property of displacement operators $D(-\varsigma)D(\alpha) = \exp[(\varsigma^*\alpha - \varsigma\alpha^*)/2]D(\alpha - \varsigma)$. Using once again the formula (9.21) to express the overlap $|\langle 0|\alpha - \varsigma, \xi\rangle|^2$ and performing the integration over ς we arrive at the formula

$$\begin{aligned} u(\alpha) \;=\; & \frac{1-\lambda^2}{\cosh(t)\sqrt{1-\lambda^4\tanh^2(t)}} \exp\left\{ -\frac{\left(1-\lambda^2\right)\left[1-\lambda^2\tanh^2(t)\right]}{1-\lambda^4\tanh^2(t)}|\alpha|^2 \right. \\ & \left. + \frac{\left(1-\lambda^2\right)^2\tanh(t)}{2\left[1-\lambda^4\tanh^2(t)\right]}\left(\mathrm{e}^{-i2\varphi}\alpha^2 + \mathrm{e}^{i2\varphi}\alpha^{*2}\right) \right\}. \end{aligned} \tag{9.24}$$

Substituting the obtained explicit expressions for functions $u(\alpha), v(\alpha)$ and $q(\alpha)$ into Eqs. (9.20) and using the explicit expression for the overlap $|\langle \phi_1|\phi_2\rangle|^2 = |\langle 0|\beta, \omega = s\mathrm{e}^{-i2\varphi}\rangle|^2$ we get from

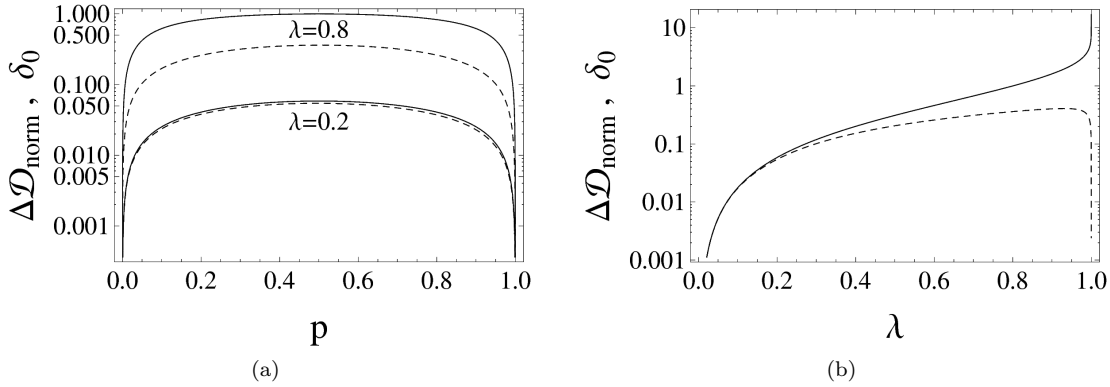

(a) (b)

Figure 9.3: Normalized gap $\Delta\mathcal{D}_{\rm norm}$ [Eq. (9.31)] between Gaussian discord and optimal discord (dashed curve) and non-Gaussianity δ_0 (solid curve) of the CV Werner state (9.5), plotted as functions of (a) the probability p for different values of λ ($\lambda = 0.2$ and 0.8 from bottom to top), and of (b) the squeezing factor λ (at $p = 0.5$). The plots are in logarithmic scale. All the quantities plotted are dimensionless. Taken from **[IV]**. Copyright (2012) by The American Physical Society.

Eq. (9.7) the eigenvalues and hence the entropy $\mathcal{S}\left(\rho_{A|\alpha}\right)$ of the conditional state $\rho_{A|\alpha}$. Subsequent averaging of the entropy over the density $q(\alpha)$ finally yields the Gaussian conditional entropy

$$\mathcal{H}^{G}_{\{\Pi(\alpha)\}}(A|B) = \int_{\mathbb{C}} q(\alpha)\mathcal{S}\left(\rho_{A|\alpha}\right) d^2\alpha \tag{9.25}$$

as a function of the squeezing parameter t and phase φ of the Gaussian measurement (9.15). Due to the complicated dependence of the conditional entropy $\mathcal{S}\left(\rho_{A|\alpha}\right)$ on α, the remaining integration over the complex plane $\mathbb{C}$, where $d^2\alpha \equiv d(\mathrm{Re}\alpha)d(\mathrm{Im}\alpha)$, has to be performed numerically. Likewise, minimization of the entropy (9.25) with respect to variables t and φ also requires numerics. This analysis reveals that, within the Gaussian POVM set, the entropy is minimized by homodyne detection on mode B. The resulting plots of Gaussian discord and the true quantum discord (9.14) (the latter obtained by photon counting on B) are shown in Figure 9.2. The figure clearly shows that apart from trivial cases $p = 0, 1$ the Gaussian discord is always strictly larger than the discord (9.14), meaning that general Gaussian measurements are strictly suboptimal (or, in other words, non-minimally disturbing) for the extraction of nonclassical correlations in the non-Gaussian state (9.5).

To shine a light on this we examine the gap

$$\Delta\mathcal{D} \equiv \mathcal{D}^{G}(\rho_0) - \mathcal{D}(\rho_0)\,, \tag{9.26}$$

which quantifies how much Gaussian measurements overestimate the total quantum correlations with a measure of non-Gaussianity δ_0 of state (9.5) [242]. The measure is defined as the quantum relative entropy between ρ_0 and a Gaussian state τ_0 with the same first and second moments, and it was shown in [242] that this can be rewritten as

$$\delta_0 = \mathcal{S}\left(\tau_0\right) - \mathcal{S}\left(\rho_0\right) \tag{9.27}$$

where $\mathcal{S}\left(\rho_0\right)$ is given in (9.10). To find $\mathcal{S}\left(\tau_0\right)$, we note that ρ_0 has zero first moments but possesses a covariance matrix of the form

$$\Gamma_0 = \begin{pmatrix} C & 0 & S & 0 \\ 0 & C & 0 & -S \\ S & 0 & C & 0 \\ 0 & -S & 0 & C \end{pmatrix} \tag{9.28}$$

with $C = p\cosh(2r) + (1-p)$, $S = p\sinh(2r)$. Using equations (2.114) and (2.115) the von Neumann entropy of the Gaussian state τ_0 can be then written as [61]

$$\mathcal{S}(\tau_0) = (\nu+1)\ln\left(\frac{\nu+1}{2}\right) - (\nu-1)\ln\left(\frac{\nu-1}{2}\right)\,, \tag{9.29}$$

where $\nu = \sqrt{[1-(1-2p)^2\lambda^2]/(1-\lambda^2)}$ is the doubly-degenerate symplectic eigenvalue of the covariance matrix Γ_0. The non-Gaussianity δ_0 is a concave function of p and increases with λ, diverging in the limit of infinite squeezing. In the regime of low squeezing, $\lambda \ll 1$, a series expansion (up to the quadratic term in λ) returns an approximate expression for the non-Gaussianity,

$$\delta_0^{(\lambda \ll 1)} \approx (-1+p)p\lambda^2[-1+\ln(p(1-p))+2\ln\lambda].$$

Clearly, the gap in discord (9.26) corresponds to the conditional entropy term given by homodyning, so $\Delta\mathcal{D} = \mathcal{H}_{\Pi^G(\alpha)}(A|B)$. In the low squeezing regime, we can also expand in series (up to the quadratic term in λ) the integrand in (9.25), so as to obtain an approximate analytic expression for the gap,

$$\Delta\mathcal{D}^{(\lambda \ll 1)} \approx \pi^{-1}(p-1)p\lambda^2[1-\gamma-\ln 2+\ln(p(1-p))+2\ln\lambda],$$

where $\gamma \approx 0.577$ is Euler's constant. Defining the ratio

$$\Phi_\lambda = \frac{\pi\left[\ln\left(\frac{4}{\lambda^2}\right)+1\right]}{\ln\left(\frac{8}{\lambda^2}\right)+\gamma-1} \tag{9.30}$$

between the approximate expressions for δ_0 and $\Delta\mathcal{D}$ (at $p = 0.5$), we see that the linearly dependent relationship $\delta_0 \approx \Phi_\lambda \Delta\mathcal{D}$ holds with good approximation for small λ. In other words, for low squeezing (say $\lambda \lesssim 0.2$), the (normalized) gap

$$\Delta\mathcal{D}_{\text{norm}} = \Phi_\lambda \Delta\mathcal{D} \tag{9.31}$$

between optimal Gaussian (homodyne) and globally optimal non-Gaussian (photon counting) measurements for the extraction of nonclassical correlations, correctly characterizes and quantitatively reproduces the non-Gaussianity δ_0 of the considered state (9.5). Interestingly,

$$\lim_{\lambda\to 0}\frac{\delta_0}{\Delta\mathcal{D}} \equiv \Phi_0 = \pi\,.$$

This intriguing relationship between the non-Gaussianity of ρ_0 and the overestimation of the Gaussian discord does not hold up for larger values of λ. The discrepancy between the two parameters becomes extreme in the limit $\lambda \to 1$ when the non-Gaussianity measure δ_0 diverges while the gap in discord $\Delta\mathcal{D}$ vanishes. Figure 9.3 compares the gap thoroughly.

Finite versus infinite-dimensional POVMs

One may argue that an even simpler non-Gaussian state than that given in Eq. (9.5) can be found possessing a strictly lower discord for a non-Gaussian measurement than for the best Gaussian measurement. For instance, the optimal measurement minimizing the discord in the qubit Werner state [87], studied in the seminal paper on quantum discord [7], is a simple non-Gaussian projection onto the first two Fock states $|0\rangle$ and $|1\rangle$. One can easily check that the optimization over all Gaussian measurements gives a strictly higher discord. Let us stress that the nonclassical correlations captured by discord are fundamentally different for the CV Werner state (9.5) considered here and for the qubit Werner state. Namely, although our CV Werner [238] is formally a qubit-like state, the globally optimal POVM has an infinite number of elements given by projectors onto all Fock states. Moreover, it is not difficult to show that no POVM measurement on mode B possessing a finite number N of elements Ω_i, $i = 1,\ldots,N$ can nullify the conditional entropy $\mathcal{H}(A|B)$ and hence also be globally optimal. Namely, the conditional state corresponding to detection of the element Ω_i has to be a pure state, that is, $\rho^\Omega_{A|i} = \text{Tr}_B[\rho_0\Omega_i] = |\chi_i\rangle\langle\chi_i|$ in order for the entropy of the conditional state to vanish. Now, consider the element $\Omega_0 \equiv \mathbb{1}_B - \sum_{i=1}^N \Omega_i$. The corresponding conditional state $\rho^\Omega_{A|0} = \text{Tr}_B[\rho_0\Omega_0] = \rho_{0,A} - \sum_{i=1}^N |\chi_i\rangle\langle\chi_i|$, where $\rho_{0,A}$ is obtained from Eq. (9.11) by replacing B with A, cannot have neither zero, nor one, nor even any finite number of strictly positive eigenvalues, as this would imply that the state $\rho_{0,A}$ also has a finite number of strictly positive eigenvalues which is not the case (see equation (9.12)).

Therefore, for any finite N the conditional state $\rho^\Omega_{A|0}$ is definitely a mixed state possessing strictly positive entropy and hence resulting in a strictly positive and therefore suboptimal

conditional entropy (i.e. not an optimised value for quantum discord). Consequently, the globally optimal POVM of the qubit Werner state is only two-component and thus the qubit Werner state is only a trivial embedding of a two-qubit state into an infinitely-dimensional two-mode state space carrying *only* qubit-type non-Gaussian nonclassical correlations. In contrast, the CV Werner state (9.5) carries genuinely CV non-Gaussian nonclassical correlations that can be optimally extracted only by a *non-Gaussian* POVM measurement with an *infinite* number of elements: in this particular case, photon counting.

Extension to mixtures of n Gaussian states

Before going further let us note that, for a state of the form (9.6), the global optimality of photon counting (for the calculation of quantum discord) follows immediately from the fact that the projection of one of its modes onto a Fock state projects the other mode onto the same Fock state. As a consequence the conditional entropy achieves the minimum possible value $\mathcal{H}_{\{\Pi(m)\}}(A|B) = 0$ and the discord is of the form (9.14). It is not difficult to find more general mixed states with the same property, for instance, states with the structure

$$\rho_q = \sum_{m,n=0}^{\infty} q_{mn} |mm\rangle\langle nn|, \tag{9.32}$$

with $q^*_{nm} = q_{mn}$, $\sum_{m=0}^{\infty} q_{mm} = 1$ and the matrix Q with elements $q_{ij,kl} = q_{ik}\delta_{ij}\delta_{kl}$ being positive-semidefinite.

A particular example of such states is a convex mixture of an arbitrary number of two-mode squeezed vacua (9.3) with different squeezing parameters λ_i obtained for $q_{mn} = \sum_i p_i \left(1 - \lambda_i^2\right) \lambda_i^{m+n}$, where p_i are probabilities and $\lambda_i \neq \lambda_j$ for $i \neq j$. We remark that for *all* non-Gaussian states of the form (9.32) the quantum discord can be computed exactly.

Other nonclassicality indicators

We can also explore the value of other measures on the state ρ_0. We shall show here that the ameliorated measurement induced disturbance and the so-called relative entropy of quantumness coincide with the discord on state ρ_0.

Measurement-induced disturbance

As in the previous chapter, the non-trivial task in calculating the AMID of a quantum state is the optimisation of the classical mutual information (equation (7.47)) after a measurement. We first note that the classical mutual information between A and B after bi-local measurements on a quantum state $\hat{\rho}_{AB}$ is upper bounded as [223]

$$\mathcal{I}_c\left(\rho_0\right) \leq \min\left\{\mathcal{S}(\rho_{0,A}), \mathcal{S}(\rho_{0,B}), \mathcal{I}_q\left(\rho_0\right)\right\}. \tag{9.33}$$

It is important to note that this bound is not tight! What we shall do is to find the minimal upper bound in (9.33) and then find measurements that achieve it. Since $\mathcal{S}(\rho_{0,A}) = \mathcal{S}(\rho_{0,B})$ for the state (9.5), we need to compare $\mathcal{S}(\rho_{0,B})$ with $\mathcal{I}_q\left(\rho_0\right)$ which can be done using majorization theory for infinite-dimensional density matrices [98]. Consider two such density matrices $\mathbf{A}$ and $\mathbf{B}$ with $a_1, a_2, \ldots$ and $b_1, b_2, \ldots$ being their non-zero eigenvalues arranged in a decreasing order and repeated according to their multiplicity. If some of the matrices, for example, $\mathbf{A}$ has only a finite number k of non-zero eigenvalues, we set $a_{k+1} = a_{k+2} = \ldots = 0$. We then say that $\mathbf{A}$ is more mixed than $\mathbf{B}$, and write $\mathbf{A} \succ \mathbf{B}$, if

$$\sum_{i=1}^{k} a_i \leq \sum_{i=1}^{k} b_i, \quad k = 1, 2, \ldots. \tag{9.34}$$

It holds further [98], that if $\mathbf{A} \succ \mathbf{B}$ then their von Neumann entropies satisfy $\mathcal{S}(\mathbf{A}) \geq \mathcal{S}(\mathbf{B})$. Taking now the eigenvalues $\tilde{\nu}_j$, $j = 0, 1, \ldots$ given in Eq. (9.12) instead of eigenvalues a_i, and $\nu_{1,2}$ given in Eq. (9.9) instead of eigenvalues b_i, one easily finds that they satisfy Eq. (9.34). This implies that the density matrices ρ_0 and $\rho_{0,B}$ of Eqs. (9.5) and (9.11) satisfy $\rho_{0,B} \succ \rho_0$ and

therefore $\mathcal{S}(\rho_{0,B}) \geq \mathcal{S}(\rho_0)$. Hence, one gets $\mathcal{I}_q(\rho_0) \geq \mathcal{S}(\rho_{0,B})$ which leads, using the inequality (9.33), to the upper bound on the classical mutual information in the form $\mathcal{I}(p_{AB}) \leq \mathcal{S}(\rho_{0,B})$.

We then ask what measurements if any could achieve this upper bound, and the answer is photon counting. One finds that

$$\mathcal{H}(p_A) = \mathcal{H}(p_B) = \mathcal{H}(p_{AB}) = \mathcal{S}(\rho_{0,A}) = \mathcal{S}(\rho_{0,B}) \tag{9.35}$$

which gives the classical mutual information in the form $\mathcal{I}_c(\rho_0) = \mathcal{S}(\rho_{0,B})$. Hence, the latter inequality is saturated by photon counting which finally yields $\mathcal{A}(\rho_0) = \mathcal{S}(\rho_{0,B}) - \mathcal{S}(\rho_0) = \mathcal{D}(\rho_0)$, that is, AMID coincides with the quantum discord, (9.14).

Relative entropy of quantumness

The Relative Entropy of Quantumness is defined as the relative entropy between the quantum state $\hat{\rho}_{AB}$ and the closest classically correlated state (Section 7.5). In [227], it was shown that the REQ could be expressed as

$$Q(\hat{\rho}_{AB}) = \min_{\{\Pi_A \otimes \Pi_B\}} \left[\mathcal{H}(p_{AB}) - \mathcal{S}(\hat{\rho}_{AB})\right], \tag{9.36}$$

where the minimization is performed over local measurements Π_A and Π_B. As with the measurement induced disturbance, we take the approach of finding a suitably tight bound on the joint Shannon entropy $\mathcal{H}(p_{AB})$ which must satisfy the inequalities $\mathcal{H}(p_{AB}) \geq \mathcal{H}(p_B) \geq \mathcal{S}(\rho_{0,B})$. Using the previous result, we see that the optimal measurement must be photon counting, as in that case $\mathcal{H}(p_{AB}) = \mathcal{S}(\rho_{0,B})$ and the lower bound is saturated. As a result we see that all of the non-classicality measures coincide as

$$\mathcal{D}(\rho_0) = \mathcal{A}(\rho_0) = Q(\rho_0) = \mathcal{S}(\rho_{0,B}) - \mathcal{S}(\rho_0). \tag{9.37}$$

9.3 General case

Let us now move to the analysis of nonclassical correlations in a generic CV Werner state (9.2) with $\mu \neq 0$, complementing the seminal analysis of nonclassical correlations in a two-qubit Werner state performed in [7, 192, 222]. This can be interesting in particular because, in contrast to the qubit case, there can potentially exist PPT entangled CV Werner states [238].

In the present general case we do not have any tight bounds, similar to those of the previous section, allowing us to perform exact optimizations in the calculation of discord, MID (AMID) and REQ. For this reason, we cannot prove the global optimality of photon counting or any other measurement strategy analytically. We then resort to computing upper bounds on discord, AMID[2] and relative entropy of quantumness, obtained for (possibly unoptimised) measurements in the local eigenbasis of the reduced state(s) of the two-mode CV Werner state. Interestingly, all the upper bounds on the different quantities again coincide as we show later in this Section: this hints at the conjecture that they might be indeed tight for the considered states, although we cannot provide conclusive evidence of this claim. We also derive nontrivial lower bounds for the nonclassical correlations.

Upper and lower bounds on discord

We consider a nonoptimized upper bound on quantum discord defined for a density matrix ρ as

$$\mathcal{U}(\rho) = \mathcal{S}(\rho_B) - \mathcal{S}(\rho) + \mathcal{H}_{\text{eig}}(A|B), \tag{9.38}$$

where $\mathcal{H}_{\text{eig}}(A|B)$ is the conditional entropy for the measurement of mode B in the local eigenbasis of the reduced state ρ_B. For the general CV Werner state of (9.2), tracing ρ over mode A gives the reduced state

$$\rho_B = p\rho_B^{\text{th}}(\lambda) + (1-p)\rho_B^{\text{th}}(\mu), \tag{9.39}$$

where ρ^{th} is defined in Eq. (9.4). This state is diagonal in the Fock basis with eigenvalues

$$g_m = p\left(1-\lambda^2\right)\lambda^{2m} + (1-p)\left(1-\mu^2\right)\mu^{2m} \tag{9.40}$$

[2] In this case the upper bound on AMID is simply the nonoptimized measurement-induced disturbance (MID).

that give, after substitution into Eq. (9.8), the marginal entropy $\mathcal{S}(\rho_B)$ appearing in Eq. (9.38).

The local eigenbasis is a Fock basis and so the projection on it corresponds again, even in the present general case, to photon counting. The conditional state $\rho_{A|m} = \mathrm{Tr}_B\left[|m\rangle_B\langle m|\rho\right]/p_B(m)$, where $p_B(m) = {}_B\langle m|\rho_B|m\rangle_B$, obtained by projecting mode B onto Fock state $|m\rangle$ reads explicitly

$$\rho_{A|m} = \frac{p\left(1-\lambda^2\right)\lambda^{2m}|m\rangle_A\langle m| + (1-p)(1-\mu^2)\mu^{2m}\rho_A^{\mathrm{th}}(\mu)}{p_B(m)} \tag{9.41}$$

with $p_B(m) = p\left(1-\lambda^2\right)\lambda^{2m} + (1-p)(1-\mu^2)\mu^{2m}$. It has the eigenvalues

$$\eta_n^{(m)} = \frac{p\left(1-\lambda^2\right)\lambda^{2m}\delta_{mn} + (1-p)(1-\mu^2)^2\mu^{2(m+n)}}{p_B(m)}, \tag{9.42}$$

where δ_{mn} is the Kronecker symbol, that give the following entropy of the conditional state

$$\begin{aligned}\mathcal{S}\left(\rho_{A|m}\right) &= -\frac{(1-p)\left(1-\mu^2\right)^2\mu^{2m}}{p_B(m)}\left\{\ln\left[\frac{(1-p)\left(1-\mu^2\right)^2}{p_B(m)}\right]\right. \\ &\quad \left.\times\left(\frac{1}{1-\mu^2}-\mu^{2m}\right)+\ln\left(\mu^2\right)\left[\frac{m}{1-\mu^2}+\frac{\mu^2}{\left(1-\mu^2\right)^2}-2m\mu^{2m}\right]\right\} \\ &\quad -\eta_m^{(m)}\ln\eta_m^{(m)}. \end{aligned} \tag{9.43}$$

From which, one obtains the conditional entropy from $\mathcal{H}_{\mathrm{eig}}(A|B) = \sum_{m=0}^{\infty} p_B(m)\mathcal{S}\left(\rho_{A|m}\right)$.

It remains to calculate the global entropy of the state (9.2). For this purpose it is convenient to express the state as

$$\rho = \sum_{m,n=0}^{\infty} M_{mn}|m,m\rangle\langle n,n| + \sum_{m\neq n=0}^{\infty} e_{mn}|m,n\rangle\langle m,n|, \tag{9.44}$$

where

$$\begin{aligned} M_{mn} &= p\left(1-\lambda^2\right)\lambda^{m+n} \\ &\quad +(1-p)\left(1-\mu^2\right)^2\mu^{2(m+n)}\delta_{mn}, \end{aligned} \tag{9.45}$$

$$e_{mn} = (1-p)\left(1-\mu^2\right)^2\mu^{2(m+n)}. \tag{9.46}$$

The state (9.2) thus possesses the eigenvalues e_{mn} corresponding to the eigenvectors $|m,n\rangle$, $m \neq n = 0,1,\ldots$ and the remaining eigenvalues ($\equiv f_l$) are the eigenvalues of the infinite-dimensional matrix M with elements (9.45). This gives the global entropy

$$\begin{aligned}\mathcal{S}(\rho) &= -\frac{2\mu^2(1-p)}{1+\mu^2}\left\{\ln\left[(1-p)\left(1-\mu^2\right)^2\right]\right. \\ &\quad \left.+\frac{2\ln(\mu)\left(1+\mu^2+2\mu^4\right)}{1-\mu^4}\right\} - \sum_{l=0}^{\infty} f_l\ln f_l. \end{aligned} \tag{9.47}$$

The eigenvalues f_l of matrix M appearing in the last expression of the previous equation cannot be calculated analytically and one has to resort to numerical diagonalization of a sufficiently large truncated matrix. Hence, one gets using Eq. (9.47), and expressions for $\mathcal{H}_{\mathrm{eig}}(A|B)$ and $\mathcal{S}(\rho_B)$, the sought upper bound (9.38) on the true quantum discord.

The true discord can be also bounded from below in the following way. Let us observe first, that apart from the trivial case $p = 0$ (corresponding to a product state) all other CV Werner states have nonclassical correlations as they possess a strictly positive quantum discord $\mathcal{D}(\rho) > 0$. This can be proven using the sufficient condition on strict positivity of quantum discord [204] according to which $\mathcal{D}(\rho) > 0$ for a state ρ if at least one off-diagonal block $\rho_{ij}^{(B)} \equiv {}_B\langle i|\rho|j\rangle_B$, $i \neq j$ is not normal, i.e., it does not commute with its adjoint. In the present case of the Werner state (9.2) we have explicitly $\rho_{ij}^{(B)} = p\left(1-\lambda^2\right)\lambda^{i+j}|i\rangle_B\langle j|$. Assuming $p > 0$ and $0 < \lambda < 1$ this gives immediately a nonzero commutator

$$\begin{aligned}\left[\rho_{ij}^{(B)}, \left(\rho_{ij}^{(B)}\right)^{\dagger}\right] &= p^2\left(1-\lambda^2\right)^2\lambda^{2(i+j)}\left[|i\rangle_B\langle i| - |j\rangle_B\langle j|\right] \\ &\neq 0 \quad \text{for } i\neq j,\ p\neq 0, \end{aligned} \tag{9.48}$$

as required.

An explicit, non-tight lower bound can be derived that is nonnegative (and thus nontrivial) at least on some subinterval of probabilities p. Namely, assume a POVM on mode B given by a collection of rank-1 operators $\{|\psi_j\rangle\langle\psi_j|\}$. If the component $|\psi_i\rangle\langle\psi_i|$ is detected on mode B in the state (9.2), then mode A collapses into the normalized conditional state

$$\rho_{A|i} = \frac{p|\phi_i\rangle_A\langle\phi_i| + (1-p)\langle\psi_i|\rho_B^{\rm th}(\mu)|\psi_i\rangle\rho_A^{\rm th}(\mu)}{p_i}, \tag{9.49}$$

where $|\phi_i\rangle_A$ is a pure unnormalized state that is not specified here and $p_i = \langle\psi_i|\rho_B|\psi_i\rangle$ with ρ_B given in Eq. (9.39) is the probability of measuring the outcome i. The state is a convex mixture of a pure state and a thermal state. Making use of the concavity of the von Neumann entropy $\mathcal{S}\left(\sum_j p_j\rho_j\right) \geq \sum_j p_j\mathcal{S}(\rho_j)$ and the fact that the entropy vanishes on pure states we arrive at the following inequality:

$$\mathcal{S}\left(\rho_{A|i}\right) \geq \frac{(1-p)}{p_i}\langle\psi_i|\rho_B^{\rm th}(\mu)|\psi_i\rangle\mathcal{S}\left(\rho_A^{\rm th}(\mu)\right). \tag{9.50}$$

By multiplying both sides of the inequality by p_i and summing over i one finds the classical conditional entropy to be lower bounded as $\mathcal{H}_{\{|\psi_i\rangle\langle\psi_i|\}}(A|B) \geq (1-p)\mathcal{S}\left[\rho_A^{\rm th}(\mu)\right]$ which, using the definition of discord (7.8), finally yields the lower bound

$$\mathcal{L}(\rho) = \mathcal{S}(\rho_B) - \mathcal{S}(\rho) + (1-p)\,\mathcal{S}\left[\rho_A^{\rm th}(\mu)\right]. \tag{9.51}$$

In what follows we evaluate the upper and lower bounds in Eqs. (9.38) and (9.51), respectively, for two particularly important two-parametric subfamilies of the set of CV Werner states.

Examples

The case $\lambda = \mu$

We first consider the case where $\lambda = \mu$, which is of interest as this is perhaps the closest continuous variable analogue to the discrete Werner state. The reduced state (9.39) is just a thermal state $\rho_B = \rho_B^{\rm th}(\lambda)$ with a well-known entropy

$$\mathcal{S}(\rho_B) = -\frac{\ln\left(1-\lambda^2\right)}{(1-\lambda^2)} - \frac{\lambda^2}{1-\lambda^2}\ln\left(\frac{\lambda^2}{1-\lambda^2}\right). \tag{9.52}$$

It can be shown that the CV Werner state (9.2) with $\lambda = \mu > 0$ is entangled for any $p > 0$ [238]. The upper bound (9.38) and lower bound (9.51) on quantum discord are depicted in Figure 9.4. Note that in this and in the following plots, only nonzero values of the lower bound (9.51) will be shown.

The case $\lambda = \mu^4$

The case for which $\lambda = \mu^4$ is interesting because the CV Werner state (9.2) runs through three different separability regions as the parameter p increases [238]:

1. If $p \leq p_{\rm sep} \equiv \frac{(1-\mu^2)^2}{2(1-\mu^2+\mu^4)}$, then the state ρ is separable (dark gray strip in Figure 9.5).

2. If $p_{\rm sep} < p \leq p_{\rm PPT} \equiv \frac{\left(1-\mu^2\right)^2}{(1-\mu^2)^2+(1-\mu^8)\mu^2}$, the state ρ is PPT (i.e., it has positive partial transposition) and it is unknown whether it is bound entangled or separable (light gray strip in Figure 9.5).

3. If $p > p_{\rm PPT}$, then the state ρ is non-PPT and therefore entangled (white region in Figure 9.5).

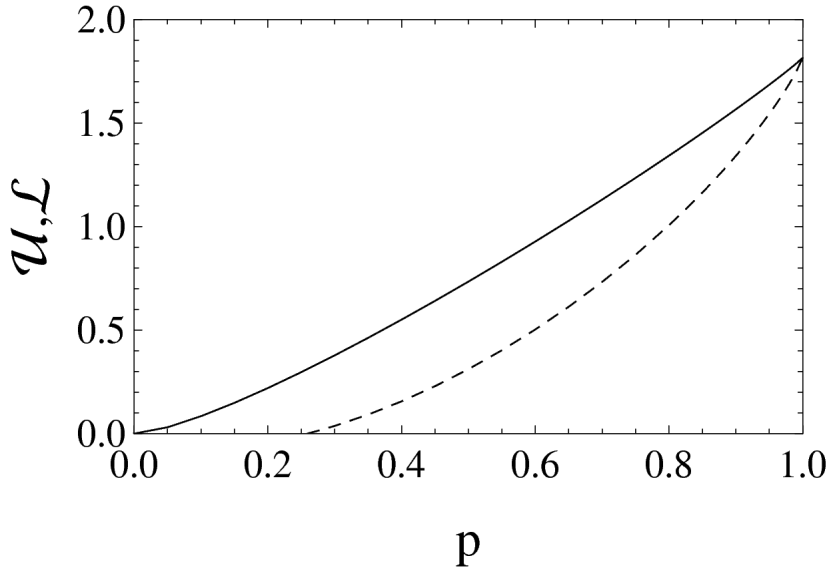

Figure 9.4: Upper bound $\mathcal{U}$ (solid curve) and lower bound $\mathcal{L}$ on quantum discord versus probability p for the CV Werner state (9.2) with $\lambda = \mu = 0.8$. All the quantities plotted are dimensionless. Taken from [**IV**]. Copyright (2012) by The American Physical Society.

Other nonoptimized nonclassicality indicators

Next we focus on the determination of the nonoptimized (upper bound) version of AMID. This is given by the MID and is achieved by performing photon number measurements on both modes yielding the joint probability distribution $p_{AB}(m,n) = {}_{AB}\langle mn|\rho|mn\rangle_{AB}$. Its marginal distributions $p_A = p_B$ coincide with the eigenvalues of the reduced states (9.40), i.e., $p_A(m) = p_B(m) = g_m$ whence we get the equality between local Shannon and von Neumann entropies

$$\mathcal{H}\left(p_A\right) = \mathcal{H}\left(p_B\right) = \mathcal{S}\left(\rho_A\right) = \mathcal{S}\left(\rho_B\right). \tag{9.53}$$

Hence MID simplifies to

$$\mathcal{M}(\rho) = \mathcal{H}\left(p_{AB}\right) - \mathcal{S}\left(\rho\right). \tag{9.54}$$

The global Shannon entropy can be derived easily by noting that the eigenvalues (9.42) of the conditional state (9.41) satisfy $\eta_n^{(m)} = p_{AB}(m,n)/p_B(m)$ thus representing a conditional probability $p_{AB}(n|m)$ of detecting n photons in mode A given m photons have been detected in mode B. This implies immediately that $\mathcal{H}_{\mathrm{eig}}(A|B) = \mathcal{H}\left(p_{AB}\right) - \mathcal{S}\left(\rho_B\right)$, where we have used Eq. (9.53) and the equality $p_A(m) = p_B(m)$. Substituting from here for $\mathcal{H}\left(p_{AB}\right)$ into Eq. (9.54) finally leads to the equality of the upper bound on discord (9.38) and MID (7.42)

$$\mathcal{M}(\rho) = \mathcal{U}(\rho). \tag{9.55}$$

Note that the two coincident quantities also provide an upper bound for the relative entropy of quantumness of the states (9.2). Note further that the lower bound (9.51) on discord is also a lower bound for the other measures of nonclassical correlations such as AMID, MID, and relative entropy of quantumness, since quantum discord is in general smaller than those mentioned quantities for arbitrary bipartite quantum states.

9.4 Partially transposed CV Werner state

One of the main technical disadvantages of the CV Werner state with $\mu \neq 0$ is that its eigenvalues, and consequently its global von Neumann entropy, cannot be calculated analytically. Interestingly, this ceases to be the case if the state is partially transposed. Then, one can find regions of parameters p, λ and μ for which the partial transposes are positive-semidefinite, and so represent a legitimate quantum state in their own right. Thus, one obtains another, sometimes simpler to treat family of non-Gaussian quantum states for which we can get further with analytical tools than in the case of the original state.

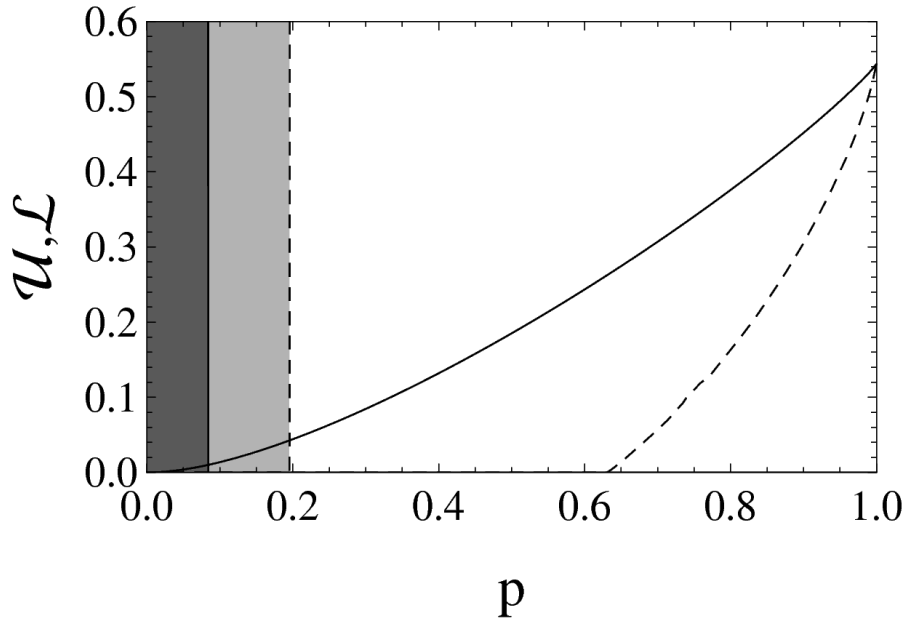

Figure 9.5: Upper bound $\mathcal{U}$, Eq. (9.38) (solid curve), and lower bound $\mathcal{L}$, Eq. (9.51) (dashed curve), on quantum discord versus probability p for the CV Werner state (9.2) with $\lambda = \mu^4$ and $\mu = 0.8$. The dark gray shaded region corresponds to separable states, the light gray shaded region corresponds to PPT states with unknown separability properties, and the white region corresponds to entangled non-PPT states. The boundary probabilities $p_{\rm sep}$ and $p_{\rm PPT}$ are depicted by vertical solid line and dashed line, respectively. All the quantities plotted are dimensionless. Taken from **[IV]**. Copyright (2012) by The American Physical Society.

Let us illustrate this on a simple example of the CV Werner state (9.2) with $\lambda = \mu^2$. As was shown in Ref. [238] for

$$p = \frac{1-\lambda}{2}, \tag{9.56}$$

the partial transposition $\rho^{T_A} \equiv \tilde{\rho}$ of the Werner state ρ with respect to mode A,

$$\tilde{\rho} = \mathcal{N} \sum_{m,n=0}^{\infty} \lambda^{m+n} \left(|n,m\rangle\langle m,n| + |m,n\rangle\langle m,n| \right), \tag{9.57}$$

possesses the following nonnegative nonzero eigenvalues

$$a_m = 2\mathcal{N}\lambda^{2m}, \quad m = 0,1,\ldots, \tag{9.58}$$

$$b_{mn} = 2\mathcal{N}\lambda^{m+n}, \quad m > n = 0,1,\ldots, \tag{9.59}$$

where $\mathcal{N} = \left(1-\lambda^2\right)(1-\lambda)/2$, and is therefore a valid two-mode density matrix corresponding to a different non-Gaussian state. Direct substitution of the eigenvalues into Eq. (9.8) gives the analytical expression for the global entropy of $\tilde{\rho}$ of the form

$$\mathcal{S}(\tilde{\rho}) = -\left[\ln(2\mathcal{N}) + \frac{1+3\lambda}{1-\lambda^2}\lambda \ln\lambda \right]. \tag{9.60}$$

Tracing the state (9.57) over mode A one gets the reduced state of mode B

$$\tilde{\rho}_B = \mathcal{N} \sum_{m=0}^{\infty} \left(\lambda^{2m} + \frac{\lambda^m}{1-\lambda} \right) |m\rangle_B\langle m| \tag{9.61}$$

with entropy

$$\begin{aligned} \mathcal{S}(\tilde{\rho}_B) = & -\left[\mathcal{N} \sum_{m=0}^{\infty} \left(\lambda^{2m} + \frac{\lambda^m}{1-\lambda} \right) \ln\left(\lambda^m + \frac{1}{1-\lambda} \right) \right. \\ & \left. + \ln(\mathcal{N}) + \frac{\lambda(1+3\lambda)}{2(1-\lambda^2)} \ln\lambda \right]. \end{aligned} \tag{9.62}$$

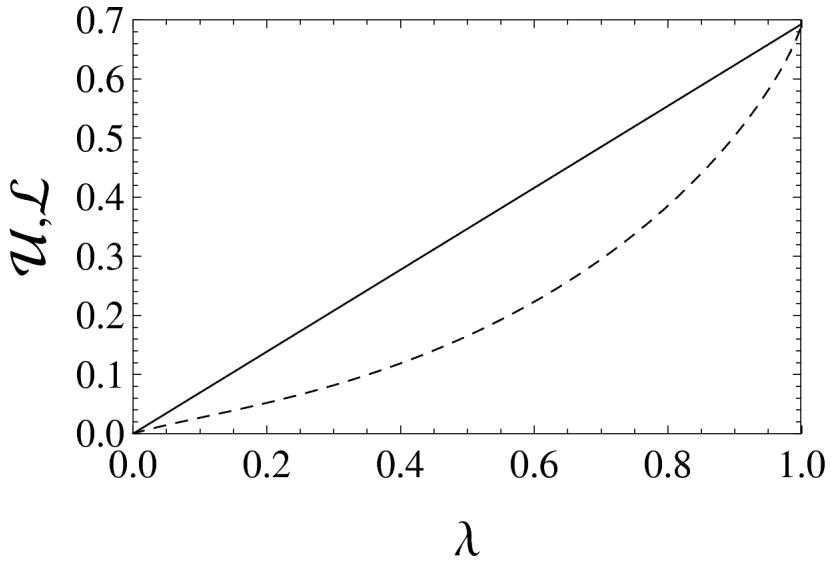

Figure 9.6: Upper bound $\mathcal{U}$, Eq. (9.66) (solid curve), and lower bound $\mathcal{L}$, Eq. (9.67) (dashed curve), on quantum discord versus squeezing parameter $\lambda = \tanh r$ for the partially transposed CV Werner state (9.57). All the quantities plotted are dimensionless. Taken from **[IV]**. Copyright (2012) by The American Physical Society.

Similarly one can find a reduced state $\tilde{\rho}_A$ of mode A which coincides with the reduced state (9.61) and yields the local entropy $\mathcal{S}(\tilde{\rho}_A) = \mathcal{S}(\tilde{\rho}_B)$.

Upon detecting m photons in mode B in the state (9.57), mode A collapses into the normalized conditional state

$$\tilde{\rho}_{A|m} = \frac{\mathcal{N}}{\tilde{p}_B(m)} \left(\lambda^{2m} |m\rangle_A\langle m| + \lambda^m \sum_{k=0}^{\infty} \lambda^k |k\rangle_A\langle k| \right), \tag{9.63}$$

where

$$\tilde{p}_B(m) = \mathcal{N}\lambda^m \left(\lambda^m + \frac{1}{1-\lambda} \right) \tag{9.64}$$

is the probability of detecting m photons on mode B in the state (9.57). After some algebra, the corresponding nonoptimized conditional entropy $\tilde{\mathcal{H}}_{\rm eig}(A|B) = \sum_{m=0}^{\infty} \tilde{p}_B(m)\mathcal{S}\left(\tilde{\rho}_{A|m}\right)$ attains then the form

$$\tilde{\mathcal{H}}_{\rm eig}(A|B) = \mathcal{S}(\tilde{\rho}) - \mathcal{S}(\tilde{\rho}_B) + \lambda \ln 2, \tag{9.65}$$

where we have used Eqs. (9.60) and (9.62). Substituting finally the latter formula into Eq. (9.38) we arrive at a very simple analytical expression for the upper bound on the quantum discord of the state (9.57),

$$\mathcal{U}(\tilde{\rho}) = \lambda \ln 2. \tag{9.66}$$

Even for the partially transposed CV Werner state $\tilde{\rho}$, it is possible to derive a nontrivial lower bound on quantum discord. Repeating the algorithm leading to Eq. (9.51) for the state (9.57), one gets the lower bound in the form:

$$\mathcal{L}(\tilde{\rho}) = \mathcal{S}(\tilde{\rho}_B) - \mathcal{S}(\tilde{\rho}) + \left(\frac{1+\lambda}{2} \right) \mathcal{S}\left[\rho_A^{\rm th}\left(\sqrt{\lambda} \right) \right]. \tag{9.67}$$

The upper bound (9.66) and lower bound (9.67) on discord are depicted in Figure 9.6 as a function of the parameter λ. Note that in this case they are quite close to each other, with the lower bound being always faithful in the whole considered parameter space. Also, nonclassical correlations in this PPT state (which may be separable or at most contain bound entanglement) are quite weak (yet always nonzero), increasing slowly with the squeezing r (recall that $\lambda = \tanh r$) and converging to the small, finite value $\ln 2$ in the limit $r \to \infty$. As for other nonclassicality

indicators, we get equivalent results. Moving for instance to the evaluation of the MID, one gets the joint photon-number distribution for the state (9.57) to be

$$\tilde{p}_{AB}(m,n) = \mathcal{N}\lambda^{m+n}(1+\delta_{mn}). \tag{9.68}$$

The Shannon entropy of the distribution reads

$$\mathcal{H}(\tilde{p}_{AB}) = \mathcal{S}(\tilde{\rho}) + \lambda \ln 2, \tag{9.69}$$

where the global entropy $\mathcal{S}(\tilde{\rho})$ is given in Eq. (9.60). The marginal distributions on each mode coincide and they are given by Eq. (9.64). Hence for the state $\tilde{\rho}$ also, the local Shannon and von Neumann entropies satisfy Eq. (9.53). Making use of the latter equality in the definition of MID we can express it as

$$\mathcal{M}(\tilde{\rho}) = \mathcal{H}(\tilde{p}_{AB}) - \mathcal{S}(\tilde{\rho}) = \lambda \ln 2, \tag{9.70}$$

where in the derivation of the second equality we used Eq. (9.69). Thus, as for the generic CV Werner state of the previous section, for the considered partially transposed CV Werner state the MID coincides with the upper bound on discord associated with local photon counting, i.e., $\mathcal{M}(\tilde{\rho}) = \mathcal{U}(\tilde{\rho})$.

9.5 Summary of Chapter 9

In this chapter, we have explored the behaviour of the most important measures of non-classical correlations on a simple family of two mode non-Gaussian continuous variable states. In some simple cases, we were able to provide analytic solutions and saw some interesting phenomena. Curiously, in the case of state ρ_0, we found that for even a slight non-Gaussian element (e.g. in the regime where p is close to unity but still not quite), the optimal measurement to perform in the evaluation of the quantum discord is non-Gaussian photon detection. Although for the pure Gaussian two mode squeezed vacuum ($p = 1$) photon counting also provides an optimal value for the discord, so does homodyne detection, and it is conjectured that the discord is always minimal with Gaussian POVMs on Gaussian states. This opens up the possibility that even an infinitesimal step into the non-Gaussian realm requires a non-Gaussian measurement. The considered states constitute probably the simplest example of bipartite states possessing genuinely non-Gaussian CV non-classical correlations besides entanglement. For the state ρ_0 we were also able to see how the gap between Gaussian discord and Discord varied with the non-Gaussianity of the state.

For general continuous variable Werner states, we were able to provide loose upper and lower bounds and we are tempted to conjecture that the upper bound does in fact yield the true quantum discord for all CV Werner states. Finally, we constructed a non-trivial non-Gaussian state which is positive under partial transposition and whose upper and lower bounds are easily computable. The correlations in this state were shown to be quite weak and remain finite even in the limit of infinite squeezing. Our study provides evidence of a trend for quantum correlations to be generally limited in the absence of (distillable) entanglement, as originally noted for Gaussian states.

Nonclassicality and non-Gaussianity are two of the most important resources for the optimization and realistic implementation of present-day and next-generation quantum technology [243, 244]. In this chapter we have taken an important first step to explore the interplay between the two in physically relevant CV states. An important next target for future work would be to study the structure of nonclassical correlations in other practically useful states deviating from Gaussianity, such as photon-subtracted states. Comparing the performance of non-Gaussian measurements, such as photon counting, with that of Gaussian strategies, such as homodyne and heterodyne detection, for accessing nonclassical correlations, and studying how the gap between the two scales with the non-Gaussianity of the states [242], and with other nonclassical parameters widely used in quantum optics, could provide novel insight into the nature of quantumness (in its broadest sense) and its potential exploitation for CV quantum information.

Part IV

Concluding Remarks

Chapter 10

Conclusions and Outlook

Before summarising this thesis, we first provide some ideas for further research related to the content of this thesis.

10.1 Suggestions for further investigation

Obvious Extensions

There are a number of ways in which the work of this thesis can be extended. There are, of course, fairly obvious suggestions to begin with. We could use the methods of Chapter 5 to explore which operations are best for distilling entanglement in Gaussian states. Regarding non-classicality measures, we could try to delve further into an analysis of non-Gaussian states. Other than the Werner state of Chapter 9, there is nothing known about the behaviour of these correlations in non-Gaussian states.

The direction of future research into the Gaussian Intrinsic Information of Chapter 6 is clearest of all. It is known that the measure is always zero on separable states, but it has not yet been rigorously proven that the measure is non-increasing under Gaussian local operations and classical communication. It seems most plausible that the Gaussian Intrinsic Information does possess this property and a sketch of an argument can be given. The effect of GLOCC will be to increase the symplectic eigenvalues of the transformed Gaussian state. This in turn will increase the strength of correlations with Eve's purification - terms proportional to $\sqrt{\nu_{A,B}^2 - 1}$ in equation (6.20). Thus any measurement that Eve performs will have a stronger effect on the state shared by Alice and Bob. It seems likely then that Eve would have more power to decrease their mutual information further.

Other properties should also be analysed. It seems highly unlikely that the measure will be convex, as the set of Gaussian states is not convex, but the measure may be additive. The measure shares a lot of similarities with the squashed entanglement and so may share similar properties.

However, my personal opinion is that there may be an interesting link between the Gaussian measure and the work carried out on Gaussian discord. More shall be said on this shortly.

Finding eigenvalues of non-Gaussian states

One plausible extension to the work carried out in Chapter 5 is that one could potentially find analytic eigenvalues of non-Gaussian states, built as mixtures of Gaussian states. This involves the use of the multivariable Hermite polynomials (Appendix A) and is best demonstrated by a simple example.

One considers a non-Gaussian state $\hat{\rho}$ made up of a mixture of two Gaussian states $\hat{\rho}_1$ and $\hat{\rho}_2$ i.e.

$$\hat{\rho} = p_1\hat{\rho}_1 + p_2\hat{\rho}_2 \tag{10.1}$$

where $p_1 + p_2 = 1$. In order to diagonalise $\hat{\rho}$ a unitary transformation U is required, that transforms the state to the diagonal matrix M

$$U\hat{\rho}U^\dagger = p_1 U\hat{\rho}_1 U^\dagger + p_2 U\hat{\rho}_2 U^\dagger = M. \tag{10.2}$$

Now to the point. *If* the matrix $\hat{\rho}$ can be diagonalised by Gaussian unitaries, then there must exist a symplectic matrix S that acts upon the covariance matrices γ_1 and γ_2 (of $\hat{\rho}_1$ and $\hat{\rho}_2$ respectively) such that, when we generate the density matrix elements using the multivariable Hermite polynomials, the matrix appears readily in the diagonal form M.

If we consider $\hat{\rho}_1$ and $\hat{\rho}_2$ to be single mode Gaussian states, then we can derive a simple recursion formula for the generation of the (two variable) Hermite polynomials required for the density matrix elements, centred at $x_j = 0$ as in the appendices,

$$H^{\{\theta\}}_{a+1,b} = -2\theta_{12} a H^{\{\theta\}}_{a-1,b} - (\theta_{11} + \theta_{22})\, b H^{\{\theta\}}_{a,b-1}, \tag{10.3}$$

where θ is a two by two matrix created by suitable transformations of a covariance matrix. The density matrix elements of M would then be given by

$$M_{jk} = \frac{p_1}{\sqrt{\det\left[S\gamma_1 S^T + \mathbb{1}\right]}} H^{\{\theta^{(1)}\}}_{j,k} + \frac{p_2}{\sqrt{\det\left[S\gamma_2 S^T + \mathbb{1}\right]}} H^{\{\theta^{(2)}\}}_{j,k}. \tag{10.4}$$

Using the recursion relation, and the requirement that $M_{j,k} = 0$ if $j \neq k$, we arrive at conditions on $\theta^{(1)}$ and $\theta^{(2)}$ which are then carried back through to yield

$$\sum_{j=1}^{2} \frac{p_j}{\sqrt{\det\left[S\gamma_j S^T + \mathbb{1}\right]}} \left(S\gamma_j S^T + \mathbb{1}\right)^{-1} = K \tag{10.5}$$

where K is a diagonal matrix. One would then aim to solve this for symplectic matrix S. If the transformation U is a non-Gaussian unitary then one would expect equation (10.5) to have no solution. Other conditions may be found on K by considering that, for example, $\mathrm{Tr}\left[M\right] = 1$. If the state is in fact Gaussian ($p_1 = 1$ and $p_2 = 0$) then S is trivially the matrix that symplectically diagonalises γ_1.

If (10.5) can be solved for S then one could return to evaluation of the density matrix elements using the Hermite polynomials. It appears that some analytic solutions could perhaps be found, but even from a numerical programming point of view, if an equation such as (10.5) can be solved, then this would dramatically speed up the diagonalisation of density matrices.

Examining the link between quantum discord and local operations

The mysterious properties captured by measures such as the quantum discord appear to have an intimate relation to quantum entanglement, even if they do not exclusively evaluate entanglement. To a certain extent this is epitomised in the Koashi Winter relation

$$\mathcal{E}_F\left(\hat{\rho}_{AB}\right) + \mathcal{J}^{\leftarrow}\left(\hat{\rho}_{AC}\right) = \mathcal{S}\left(\hat{\rho}_A\right). \tag{10.6}$$

As stated by Koashi and Winter, the von-Neumann entropy of the reduced state $\hat{\rho}_A$ can be thought of as the capacity of Alice's subsystem to form correlations with those held by Bob and Charlie.

In a recent publication by Streltsov *et al.* [206], it was shown that if two states (here called A and C) initially have no quantum correlations, it is possible to perform a local (quantum) operation on one subsystem to create non-classical correlations between the two subsystems. That is, the state goes from having zero discord to non-zero discord.

The example in particular is that the initial state is described by

$$\hat{\rho}_{AC} = \frac{1}{2}\left(|00\rangle\langle 00| + |11\rangle\langle 11|\right) \tag{10.7}$$

and the local operation on C transforms the state to

$$\hat{\rho}_{A'C'} = \frac{1}{2}\left(|00\rangle\langle 00| + |1+\rangle\langle 1+|\right) \tag{10.8}$$

where $|+\rangle = (1/\sqrt{2})\left(|0\rangle + |1\rangle\right)$ thereby creating quantum discord between A and C. In [206] the authors discussed non-unital maps as a way of explaining the phenomenon, but it is in fact far more easy to understand if we consider the full purification of the state (10.7). As has been

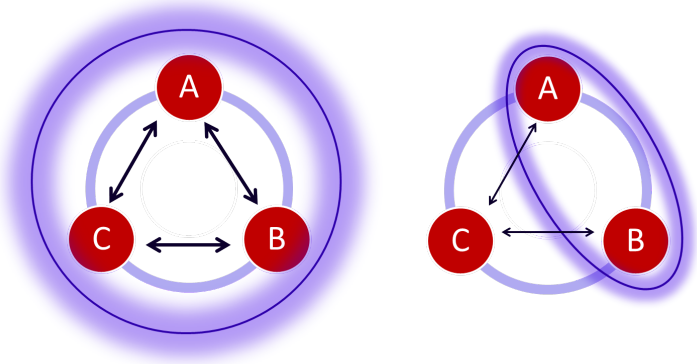

Figure 10.1: Initially no two subsystems are entangled (blue glowing circle) but all systems are strongly classically correlated (black arrows) and the entanglement across any bipartition of the pure state is maximum. After the local operation on C, the entropy of C decreases. No entanglement can form between A(B) and C as there was none to begin with so only classical correlations can be there, and weaker than previously. However, the capacity of $A(B)$ to be correlated is not used up by this so entanglement must emerge between A and B. From the other direction, the local measurement on C can be seen as a non-local measurement on A and B.

said previously, a mixed state can be considered as an admission of ignorance on the researcher's behalf. The pure state

$$|\mathrm{GHZ}\rangle = \frac{1}{\sqrt{2}}\left(|000\rangle + |111\rangle\right) \tag{10.9}$$

satisfies $\mathrm{Tr}_B\left[|\mathrm{GHZ}\rangle\right] = \hat{\rho}_{AC}$ and so we choose to explore the GHZ state after the interaction. Now we have all the statistical correlations in one place. As the global state is pure, across any bipartition the entropies are the same so

$$\mathcal{S}\left(\hat{\rho}_A\right) = \mathcal{S}\left(\hat{\rho}_{BC}\right), \quad \mathcal{S}\left(\hat{\rho}_B\right) = \mathcal{S}\left(\hat{\rho}_{AC}\right), \quad \mathcal{S}\left(\hat{\rho}_C\right) = \mathcal{S}\left(\hat{\rho}_{AB}\right) \tag{10.10}$$

where $\mathcal{S}\left(\hat{\rho}\right)$ is the von-Neumann entropy of the state $\hat{\rho}$ and the logarithm is to the base 2 to normalise as is standard in the qubit literature. In the GHZ state initially, there is entanglement between each of the bipartitions (quantified by the Entanglement of Formation $\mathcal{E}_F$):

$$\mathcal{E}_F\left(\hat{\rho}_{AB,C}\right) = \mathcal{E}_F\left(\hat{\rho}_{A,BC}\right) = \mathcal{E}_F\left(\hat{\rho}_{B,AC}\right) = 1 \tag{10.11}$$

However, if knowledge of any one of the three subsystems is missing, there is no entanglement between the other two - but classical correlations are maximal according to the Koashi-Winter relation. By classical correlations, we mean one way classical correlations $\mathcal{J}^{\leftarrow}\left(\hat{\rho}_{AB}\right)$ where the arrow implies the optimal measurement is performed on B. Consequently

$$\mathcal{E}_F\left(\hat{\rho}_{AB}\right) = \mathcal{E}_F\left(\hat{\rho}_{AC}\right) = \mathcal{E}_F\left(\hat{\rho}_{BC}\right) = 0; \tag{10.12}$$

$$\mathcal{J}^{\leftarrow}\left(\hat{\rho}_{AC}\right) = \mathcal{J}^{\rightarrow}\left(\hat{\rho}_{AC}\right) = 1 \tag{10.13}$$

$$\mathcal{J}^{\leftarrow}\left(\hat{\rho}_{AB}\right) = \mathcal{J}^{\rightarrow}\left(\hat{\rho}_{AB}\right) = 1 \tag{10.14}$$

$$\mathcal{J}^{\leftarrow}\left(\hat{\rho}_{BC}\right) = \mathcal{J}^{\rightarrow}\left(\hat{\rho}_{BC}\right) = 1 \tag{10.15}$$

and

$$\mathcal{S}\left(\hat{\rho}_A\right) = \mathcal{S}\left(\hat{\rho}_B\right) = \mathcal{S}\left(\hat{\rho}_C\right) = 1. \tag{10.16}$$

Let us now consider what must happen after a local measurement on C. If Alice had no knowledge of Bob or Charlie, then the probability distribution yielded from her part of the state $\hat{\rho}_A = \mathrm{Tr}\left[\hat{\rho}_{BC}\right]$ will be blissfully unchanged (she implicitly averages over everything that could happen to states B or C by not knowing anything about them). Consequently $\mathcal{S}\left(\hat{\rho}_{A'}\right) = \mathcal{S}\left(\hat{\rho}_A\right)$. A similar argument holds to get $\mathcal{S}\left(\hat{\rho}_{B'}\right) = \mathcal{S}\left(\hat{\rho}_B\right)$.

In fact, the only "local" distribution to be affected by the local measurement (which preserves the purity $\mathrm{Tr}\left[\hat{\rho}^2_{A'B'C'}\right] = \mathrm{Tr}\left[\hat{\rho}^2_{ABC}\right] = 1$ as nothing is lost to any more environment

qubits) is that of $\hat{\rho}_C$. In the case at hand, after the local operation, the entropy of $\hat{\rho}_{C'}$ is given by $\mathcal{S}(\hat{\rho}_C) = y$ where

$$y = \frac{\ln[8] - \sqrt{2}\coth^{-1}\left[\sqrt{2}\right]}{\ln[4]}. \tag{10.17}$$

At this point, the entropy of $\mathcal{S}(\hat{\rho}_{C'}) < \mathcal{S}(\hat{\rho}_C)$. That is, the capacity of Charlie's part of the state to form correlations has decreased. As the state $\hat{\rho}_C$ was initially separable from $\hat{\rho}_A$, a local operation on $\hat{\rho}_C$ can do nothing to create entanglement between A and C. Thus, in this case, the only correlations that $\hat{\rho}_{C'}$ can form are classical, and they are weaker than previously.

$$\mathcal{S}(\hat{\rho}_{C'}) = \mathcal{E}_F(\hat{\rho}_{A'C'}) + \mathcal{J}^{\rightarrow}(\hat{\rho}_{B'C'}) = \mathcal{J}^{\rightarrow}(\hat{\rho}_{B'C'}) = y; \tag{10.18}$$

$$\mathcal{S}(\hat{\rho}_{C'}) = \mathcal{E}_F(\hat{\rho}_{B'C'}) + \mathcal{J}^{\rightarrow}(\hat{\rho}_{A'C'}) = \mathcal{J}^{\rightarrow}(\hat{\rho}_{A'C'}) = y. \tag{10.19}$$

However, Alice and Bobs' local distributions remain unchanged - how could they change if they have never been interacted with? Thus their respective capacities for forming correlations remain unchanged. $\mathcal{S}(\hat{\rho}_{A'}) = \mathcal{S}(\hat{\rho}_A) = 1$ and $\mathcal{S}(\hat{\rho}_{B'}) = \mathcal{S}(\hat{\rho}_B) = 1$.

The entanglement between A and C remains unchanged, although the classical correlations between A and C have altered.

$$\mathcal{S}(\hat{\rho}_{A'}) = \mathcal{E}_F(\hat{\rho}_{A'B'}) + \mathcal{J}^{\leftarrow}(\hat{\rho}_{A'C'}). \tag{10.20}$$

The classical correlations between A and C are given by $\mathcal{J}^{\leftarrow}(\hat{\rho}_{A'C'}) = 1 - y$ which is a decrease in the classical correlations available to $\hat{\rho}_{A'}$. The consequence is that the remaining capacity for Alice's correlations must be filled - by becoming entangled with Bob!

The point is that the discord in $\hat{\rho}_{A'C'}$ emerges almost as a side effect of the change in local entropy of Charlie's state. A local operation on C has preserved the purity of the global state, but decreased the entanglement $\mathcal{E}_F(\hat{\rho}_{A'B',C'}) < \mathcal{E}_F(\hat{\rho}_{AB,C})$. The entanglement between $\mathcal{E}_F(\hat{\rho}_{A,BC})$ and $\mathcal{E}_F(\hat{\rho}_{B,AC})$ stay the same. The result is to reduce the classical correlations between Alice (Bob) and Charlie. However, the capacity of Alice (Bob) for forming correlations is unchanged so the consequence is that they become entangled. This is verified by direct calculation using the formula from [245]. The mutual information $\mathcal{I}_q(\hat{\rho}_{AC})$ is reduced from 1 to y but one way classical correlations are decreased further. In fact

$$\mathcal{D}^{\leftarrow}(\hat{\rho}_{A'C'}) = \mathcal{I}_q(\hat{\rho}_{A'C'}) - \mathcal{J}^{\leftarrow}(\hat{\rho}_{AC}) = 2y - 1 \tag{10.21}$$

$$\mathcal{D}^{\rightarrow}(\hat{\rho}_{A'C'}) = \mathcal{I}_q(\hat{\rho}_{A'C'}) - \mathcal{J}^{\rightarrow}(\hat{\rho}_{AC}) = 0. \tag{10.22}$$

Interestingly, we could think about this from the other direction - as opposed to performing a local operation on C we could perform a complementary non-local entangling operation directly on A and B. That is, a local operation is *equivalent* to an entangling operation on AB. This is due to the fact that the global state $\hat{\rho}_{ABC}$ is pure before and after the interaction:

$$\mathcal{S}(\hat{\rho}_{AB}) = \mathcal{S}(\hat{\rho}_C) \tag{10.23}$$

$$\mathcal{S}(\hat{\rho}_{A'B'}) = \mathcal{S}(\hat{\rho}_{C'}). \tag{10.24}$$

The initial transformation was of the form $\hat{\rho}_{A'B'C'} = \hat{E}\hat{\rho}_{ABC}\hat{E}^T$ where

$$\hat{E} = \mathbb{1}_A \otimes \mathbb{1}_B \otimes \begin{pmatrix} 1 & 1/\sqrt{2} \\ 0 & 1/\sqrt{2} \end{pmatrix} \tag{10.25}$$

but could also be performed by a transformation

$$\hat{E}' = \hat{M}_{AB} \otimes \mathbb{1}_C \tag{10.26}$$

where

$$\hat{M}_{AB} = \begin{pmatrix} 1 & 0 & 0 & 0 \\ 0 & 0 & 0 & 0 \\ 0 & 0 & 0 & 0 \\ 1/\sqrt{2} & 0 & 0 & 1/\sqrt{2} \end{pmatrix}. \tag{10.27}$$

Note, the transformations $\hat{E}$ and $\hat{E}'$ are *not* unitary.

Ultimately, this example shows just how much is missed when one does not look at the whole picture. It seems highly likely that a similar analysis could explain a rather baffling effect - the distribution of entanglement between separate parties by means of a separable ancilla. This has been explored in the qubit [181] and continuous variable [182, 183] regimes. In essence, Alice holds particles A and C which are separable from particle B ($\mathcal{E}_F(\hat{\rho}_{AC,B}) = 0$). She forces them to interact in a unitary way (CNOT gate in the qubit case [181] and beamsplitter in the CV case [182, 183]). Alice then sends particle C to Bob who performs another unitary interaction, and at the end, A is entangled with BC ($\mathcal{E}_F(\hat{\rho}_{A,BC}) > 0$). The counterintuitive aspect is that C is separable from AB at all times. A, B and C together from a mixed state.

This phenomenon has been studied very recently in relation to discord in [246] and [247]. However, neither reference considers the role of the environment. Instinctively, it seems that if one was to include extra modes such that the global state $\hat{\rho}_{ABC\ldots}$ was pure, then the protocol may reduce to nothing more than a clever form of entanglement swapping. The local entropies of A, C and the purifying modes are altered by the first interaction, which changes their respective capacities for forming correlations. A similar effect is seen after the interaction between B and C. It seems entirely plausible that in much the same way as the previous GHZ example, the alterations in local entropies create the entanglement between Alice and Bob with the discord emerging as a side effect.

Most interesting of all is the consideration of the Gaussian Intrinsic Information of Chapter 6 with the Koashi-Winter relation. Analysis so far of GLEMS suggests that the optimal measurement for Eve to perform to minimise the information shared between Alice and Bob is that which maximises the one way classical correlations $\mathcal{J}^{\leftarrow}(\hat{\rho}_{AE})$ (or $\mathcal{J}^{\leftarrow}(\hat{\rho}_{BE})$). Such a possibility would make sense, as by maximising classical correlations with A and B, the entanglement between A and B as measured by the entanglement of formation is minimised. The relation between our measure of entanglement and quantum discord needs to still be explored.

Ultimately, there is an overwhelming impression that deep down, quantum entanglement and other non-classical correlations are two sides of the same coin. They are intimately related and tell two entwined yet different stories.

10.2 Summary

This thesis has had three foci. Firstly, it was shown that Quantum Non-Demolition interactions between Gaussian states could be used in conjunction with non-Gaussian operations such as photon subtraction to increase entanglement in Gaussian states. This was demonstrated in great detail with the two mode squeezed vacuum, whereby the interactions transformed the pure state into a mixed state with higher entanglement. This investigation was primarily motivated by the question as to whether it would be possible to increase the entanglement in two entangled atomic ensembles, for use in quantum memory devices and quantum repeaters. It is thought that, although theoretically feasible, there are still a number of experimental hurdles to overcome.

Secondly, a potential entanglement measure for Gaussian states was introduced. This measure has a deep operational meaning within quantum cryptography. Alice and Bob wish to acquire a secret key about which a foe, Eve, knows nothing. However, Eve possesses all of the information required to purify the quantum state shared by Alice and Bob and performs measurements and local Gaussian operations to minimise the amount of shared classical correlations that Alice and Bob can obtain from the quantum state. The measure is then an upper bound on the secret key rate.

The second half of this thesis has introduced other types of nonclassical correlations that may exist in bipartite quantum states. At present this is still very much an emerging field in theoretical quantum information, and very little has been done in the continuous variable setting. We introduced the Gaussian Ameliorated Measurement Induced Disturbance, profiled its behaviour on two mode Gaussian states, and then compared it to other measures of nonclassical correlations. Following this, a full analysis was made of the continuous variable Werner state which acts as a simple example of a non-Gaussian state, and the obvious first step into the non-Gaussian realm.

These considerations should convince the reader that continuous variable entanglement in Gaussian states and continuous variable non-classicality measures are still the basis of a very much active and lively field of research. It is hoped that the results of this thesis, and the

suggestions for future work, may advance understanding of the intertwined fates of quantum entanglement and non-classical correlations beyond.

Appendix **A**

Multivariable Hermite Polynomials

In order to calculate the density matrix elements of a Gaussian state, the multivariable Hermite polynomials are an invaluable tool. It is common knowledge that the one dimensional Hermite polynomials are defined as

$$H_n(y) = (-1)^n e^{y^2} \left(\frac{\partial}{\partial y}\right)^n e^{-y^2} \tag{A.1}$$

and the multivariable Hermite polynomials [248] are a simple extension:

$$H^{\{\Theta,\Delta\}}_{r,s,t,v}(y_1,y_2,y_3,y_4) = (-1)^{r+s+t+v} \exp\left[\mathbf{y}^T\Theta\mathbf{y} + \Delta\mathbf{y}\right] \frac{\partial^r}{\partial y_1^r}\frac{\partial^s}{\partial y_2^s}\frac{\partial^t}{\partial y_3^t}\frac{\partial^v}{\partial y_4^v} \exp\left[-\mathbf{y}^T\Theta\mathbf{y} - \Delta\mathbf{y}\right] \tag{A.2}$$

where $\mathbf{y} = (y_1, y_2, y_3, y_4)^T$. The matrix Θ, when applied to Chapter 5, is a 4×4 matrix related to the covariance matrix of the Gaussian state. Traditionally, in the definition of the Hermite polynomials, the Δ term does not appear, but it is useful to include it above, as in Chapter 5 the Δ term is a row vector related to any displacements in the Q function as a result of homodyne measurements.

The density matrix elements of a quantum state can be generated by the Q function of that state. If the state is Gaussian, then the most general form of $\mathcal{Q}(\alpha,\beta)$ (a two mode Gaussian state) is

$$\mathcal{Q}(\alpha,\beta) = \frac{\sqrt{\det\Theta'}}{\pi^2} \exp\left[-\frac{\Delta'\Theta'^{-1}\Delta'^{\dagger}}{4}\right] \exp\left[-\mathcal{R}^{\dagger}\Theta'\mathcal{R} - \Delta'\mathcal{R}\right] \tag{A.3}$$

where $\mathcal{R} = (\alpha, \alpha^*, \beta, \beta^*)^T$ and $\Theta' = \left(\mathbf{U}\gamma\mathbf{U}^{\dagger} + \mathbb{1}\right)^{-1}$ where γ is a covariance matrix and $\mathbf{U}$ is as in Equation (5.13). Δ' is related to any displacements.

The density matrix elements of any two mode quantum state are generated as

$$\rho_{rstv} = \langle r|\langle s|\hat{\rho}|t\rangle|v\rangle = \frac{(2\pi)^2}{\sqrt{r!s!t!v!}} \left(\frac{\partial^{r+t}}{\partial\alpha^{*r}\partial\alpha^t}\right)\left(\frac{\partial^{s+v}}{\partial\beta^{*s}\partial\beta^v}\right)\left[\mathcal{Q}(\alpha,\beta)\, e^{|\alpha|^2+|\beta|^2}\right]\Big|_{\alpha=\beta=0} \tag{A.4}$$

which for Gaussian states is written

$$\rho_{rstv} = \frac{4\sqrt{\det\Theta'}}{\sqrt{r!s!t!v!}} \left(\frac{\partial^{r+t}}{\partial\alpha^{*r}\partial\alpha^t}\right)\left(\frac{\partial^{s+v}}{\partial\beta^{*s}\partial\beta^v}\right) \exp\left[-\mathcal{R}^{\dagger}\left(\Theta' - \frac{1}{2}\mathbb{1}\right)\mathcal{R} - \Delta'\mathcal{R}\right]\Big|_{\alpha=\beta=0}. \tag{A.5}$$

The $\frac{1}{2}\mathcal{R}^{\dagger}\mathbb{1}\mathcal{R}$ contribution in the exponent takes care of the $\exp\left[|\alpha|^2 + |\beta|^2\right]$ term in Equation (A.4). The matrix elements in the exponent are not yet in the correct arrangement for compatibility with the definition of the multivariable Hermite polynomials (A.2). At present we have exponents of the form

$$\left(\alpha^*, \alpha, \beta^*, \beta\right)\left(\Theta' - \frac{1}{2}\mathbb{1}\right)\begin{pmatrix}\alpha\\ \alpha^*\\ \beta\\ \beta^*\end{pmatrix}$$

when it would be far more desirable to have the form

$$\left(\alpha^*, \beta^*, \alpha, \beta\right) \Theta \begin{pmatrix} \alpha^* \\ \beta^* \\ \alpha \\ \beta \end{pmatrix}.$$

For this, it is useful to note that

$$\begin{pmatrix} \alpha^* \\ \beta^* \\ \alpha \\ \beta \end{pmatrix} = \underbrace{\begin{pmatrix} 0 & 1 & 0 & 0 \\ 0 & 0 & 0 & 1 \\ 1 & 0 & 0 & 0 \\ 0 & 0 & 1 & 0 \end{pmatrix}}_{\mathbf{D}^\dagger} \begin{pmatrix} \alpha \\ \alpha^* \\ \beta \\ \beta^* \end{pmatrix}, \quad \left(\alpha^*, \alpha, \beta^*, \beta\right) \underbrace{\begin{pmatrix} 1 & 0 & 0 & 0 \\ 0 & 0 & 1 & 0 \\ 0 & 1 & 0 & 0 \\ 0 & 0 & 0 & 1 \end{pmatrix}}_{\mathbf{B}^\dagger} = \left(\alpha^*, \beta^*, \alpha, \beta\right) \tag{A.6}$$

and then

$$\Theta = \mathbf{B}\left(\Theta' - \frac{1}{2}\mathbb{1}\right)\mathbf{D}, \tag{A.7}$$

from which the $\mathbf{C}^{(ij)}$ of Equation (5.19) in Chapter 5 is defined. Similarly, the Δ of equation (A.2) is defined as

$$\Delta = \Delta'\mathbf{D}. \tag{A.8}$$

With that, the matrix elements of the Gaussian state are given by

$$\begin{aligned}
\rho_{rstv} &= \frac{4\sqrt{\det\Theta'}}{\sqrt{r!s!t!v!}} \exp\left[-\frac{\Delta'\Theta'^{-1}\Delta'}{4}\right] \exp\left[-\mathbf{y}^T\Theta\mathbf{y} - \Delta\mathbf{y}\right] \\
&\quad \times \exp\left[\mathbf{y}^T\Theta\mathbf{y} + \Delta\mathbf{y}\right] \frac{\partial^r}{\partial\alpha^{*r}} \frac{\partial^s}{\partial\beta^{*s}} \frac{\partial^t}{\partial\alpha^t} \frac{\partial^v}{\partial\beta^v} \exp\left[-\mathbf{y}^T\Theta\mathbf{y} - \Delta\mathbf{y}\right]\Big|_{\alpha=\beta=0} \\
&= \frac{4\sqrt{\det\Theta'}\,(-1)^{r+s+t+v}}{\sqrt{r!s!t!v!}} \exp\left[-\frac{\Delta'\Theta'^{-1}\Delta'^\dagger}{4}\right] \\
&\quad \times \exp\left[-\mathbf{y}^T\Theta\mathbf{y} - \Delta\mathbf{y}\right] H^{\{\Theta,\Delta\}}_{rstv}\left(\alpha^*, \beta^*, \alpha, \beta\right)\Big|_{\alpha=\beta=0} \\
&= \frac{4\sqrt{\det\Theta'}\,(-1)^{r+s+t+v}}{\sqrt{r!s!t!v!}} \exp\left[-\frac{\Delta'\Theta'^{-1}\Delta'^\dagger}{4}\right] H^{\{\Theta,\Delta\}}_{rstv}
\end{aligned} \tag{A.9}$$

where $\mathbf{y}^T = \left(\alpha^*, \beta^*, \alpha, \beta\right)$ and in the last line $H^{\{\Theta,\Delta\}}_{rstv} \equiv H^{\{\Theta,\Delta\}}_{rstv}(0,0,0,0)$.

An elegant recursion formula can be derived for the Hermite polynomials evaluated at $\mathbf{y} = 0$ by directly using (A.2) and substituting there e.g. $r+1$. By using Leibniz's rule, that states that if f and g are $n-$times differentiable functions then the n^{th} derivative of the product fg is given by

$$\left(\frac{\partial}{\partial x}\right)^n (fg) = \sum_{k=0}^{n} \binom{n}{k} \left(\frac{\partial}{\partial x}\right)^k f \left(\frac{\partial}{\partial x}\right)^{n-k} g, \tag{A.10}$$

a recursion relation is given as

$$\begin{aligned}
H^{\{\Theta,\Delta\}}_{r+1,s,t,v} =& \Delta_1 H^{\{\Theta,\Delta\}}_{r,s,t,v} \\
&- 2r\Theta_{11} H^{\{\Theta,\Delta\}}_{r-1,s,t,v} \\
&- s\left(\Theta_{12} + \Theta_{21}\right) H^{\{\Theta,\Delta\}}_{r,s-1,t,v} \\
&- t\left(\Theta_{13} + \Theta_{31}\right) H^{\{\Theta,\Delta\}}_{r,s,t-1,v} \\
&- v\left(\Theta_{14} + \Theta_{41}\right) H^{\{\Theta,\Delta\}}_{r,s,t,v-1},
\end{aligned} \tag{A.11}$$

where Δ_1 is the first component of vector Δ. Similar formulae can be derived for $H^{\{\Theta,\Delta\}}_{r,s+1,t,v}$ etc. by replacing the coefficients in (A.11). With the recursion relations it becomes very simple to calculate the Hermite polynomials. In particular, if $\Delta = 0$, then $H^{\{\Theta,0\}}_{0000} = 1$ but $H^{\{\Theta,0\}}_{1000} = H^{\{\Theta,0\}}_{0100} = H^{\{\Theta,0\}}_{0010} = H^{\{\Theta,0\}}_{0001} = 0$ and so from the recursion relations it is immediately seen that only density matrices for which the sum of the indices is an even number need be calculated. Furthermore, due to the requirement that the density matrix $\hat{\rho}$ is hermitian, there is a further symmetry $H^{\{\Theta,\Delta\}}_{rstv} = H^{*\{\Theta,\Delta\}}_{tvrs}$

Appendix **B**

Symplectic Diagonalisation of two-mode Gaussian states in standard form

We aim to find the symplectic matrix S that would diagonalise a two mode Gaussian state in standard form

$$\gamma = \begin{pmatrix} a & 0 & c_+ & 0 \\ 0 & a & 0 & c_- \\ c_+ & 0 & b & 0 \\ 0 & c_- & 0 & b \end{pmatrix} \tag{B.1}$$

where γ is defined as in Chapter 2, and the quantum vacuum has covariance matrix $\mathbb{1}$. The matrix S must satisfy $S\Omega S^T = \Omega$ where

$$\Omega = \begin{pmatrix} 0 & 1 & 0 & 0 \\ -1 & 0 & 0 & 0 \\ 0 & 0 & 0 & 1 \\ 0 & 0 & -1 & 0 \end{pmatrix}, \tag{B.2}$$

and bring the covariance matrix γ to the form $S\gamma S^T = \mathrm{diag}\left(\nu_A, \nu_A, \nu_B, \nu_B\right)$ where ν_A and ν_B are symplectic eigenvalues of γ.

For convenience, we define

$$\begin{aligned} D &= \left(a^2 - b^2\right)^2 + 4\left(ac_+ + bc_-\right)\left(bc_+ + ac_-\right) \\ \Delta &= a^2 + b^2 + 2c_+c_- \end{aligned} \tag{B.3}$$

and note that this allows the symplectic eigenvalues to be written as

$$\nu_{A,B} = \sqrt{\frac{\Delta \pm \sqrt{D}}{2}}. \tag{B.4}$$

We first note that the symplectic eigenvalues can be found as the eigenvalues of the matrix $|i\Omega\gamma|$. From this, it follows that the matrix S can be found as a product $S = \left(\oplus_{j=1}^{2} U^*\right) V^T$ [249, 250], where

$$U = \frac{1}{\sqrt{2}} \begin{pmatrix} i & -i \\ 1 & 1 \end{pmatrix} \tag{B.5}$$

and V contains in its columns the eigenvectors of $i\Omega\gamma$ chosen such that S is real and satisfies the symplectic condition $S\Omega S^T$. As we have the matrix γ in standard form, we can add the further constraint that S does not mix position and momentum quadratures, and so S takes the form

$$S = \sqrt{2} \begin{pmatrix} x_1 & 0 & x_2 & 0 \\ 0 & x_3 & 0 & x_4 \\ x_5 & 0 & x_6 & 0 \\ 0 & x_7 & 0 & x_8 \end{pmatrix}, \tag{B.6}$$

where the real parameters $x_1, \cdots, x_8$ are related to the eigenvectors u_{ν_A} and ω_{ν_B} of the matrix $i\Omega\gamma$ corresponding to the eigenvalues ν_A and ν_B. We find

$$u_{\nu_A} = \begin{pmatrix} ix_1 \\ x_3 \\ ix_2 \\ x_4 \end{pmatrix}, \quad \omega_{\nu_B} = \begin{pmatrix} ix_5 \\ x_7 \\ ix_6 \\ x_8 \end{pmatrix} \tag{B.7}$$

along with the equations

$$\begin{aligned} Mx_3 + \left(b^2 + c_+c_- - \nu_A^2\right) x_4 = 0, \\ Mx_7 + \left(b^2 + c_+c_- - \nu_A^2\right) x_8 = 0, \\ x_1 = \tfrac{ax_3 + c_- x_4}{\nu_A}, \\ x_2 = \tfrac{bx_4 + c_- x_3}{\nu_A} \\ x_5 = \tfrac{ax_7 + c_- x_8}{\nu_B}, \\ x_6 = \tfrac{bx_8 + c_- x_7}{\nu_B} \end{aligned} \tag{B.8}$$

where $M = (ac_+ + bc_-)$. The symplectic condition $S\Omega S^T = \Omega$ also gives the conditions

$$\begin{aligned} x_1x_3 + x_2x_4 = \tfrac{1}{2}, \\ x_5x_7 + x_6x_8 = \tfrac{1}{2}, \\ x_1x_7 + x_2x_8 = 0, \\ x_3x_5 + x_4x_6 = 0. \end{aligned} \tag{B.9}$$

Several cases must be distinguished depending on the relations between the parameters a, b, c_+, c_-.

Case 1: $a = b$ **and** $c_+ = -c_- = c > 0$ **(two mode squeezed thermal states)**

In this case one gets $\nu_A = \nu_B = \sqrt{a^2 - c^2}$ and

$$S_1 = \frac{1}{\sqrt{2}} \begin{pmatrix} z^{-1} & 0 & z^{-1} & 0 \\ 0 & z & 0 & z \\ -z & 0 & z & 0 \\ 0 & -z^{-1} & 0 & z^{-1} \end{pmatrix} \tag{B.10}$$

where $z = \sqrt[4]{\frac{a+c}{a-c}}$.

Case 2: $a = b$ **and** $c_+ > -c_-$

In this case one gets $\nu_A = \sqrt{(a + c_+)(a + c_-)}$ and $\nu_B = \sqrt{(a - c_+)(a - c_-)}$ and then covariance matrix γ is diagonalised by

$$S_2 = \frac{1}{\sqrt{2}} \begin{pmatrix} z_1^{-1} & 0 & z_1^{-1} & 0 \\ 0 & z_1 & 0 & z_1 \\ -z_2 & 0 & z_2 & 0 \\ 0 & -z_2^{-1} & 0 & z_2^{-1} \end{pmatrix} \tag{B.11}$$

where

$$z_1 = \sqrt[4]{\frac{a + c_+}{a + c_-}}, \quad z_2 = \sqrt[4]{\frac{a - c_-}{a - c_+}}. \tag{B.12}$$

For $c_+ = -c_- = c$, one gets $z_1 = z_2 = z$ and $S_2 = S_1$. Thus cases 1 and 2 are joined and we can say that (B.11) diagonalises γ when $a = b$ and $c_+ \geq 0$ and $c_- \leq 0$.

Case 3: $a > b$

In this case, we have $M > 0$ and $L_A < 0$ where we have defined

$$L_{A,B} = b^2 + c_+c_- - \nu_{A,B}^2 = \frac{b^2 - a^2 \mp \sqrt{D}}{2}. \tag{B.13}$$

We can then differentiate two subcategories:

a) If $bc_+ = -ac_-$ then we get

$$\nu_A = \sqrt{a^2 + c_+c_-}, \quad \nu_B = \sqrt{b^2 + c_+c_-} \tag{B.14}$$

and $L_B = 0$. Thus by solving (B.8) and (B.9) we arrive at

$$S_{3a} = \begin{pmatrix} \sqrt{\frac{\nu_A}{a}} & 0 & 0 & 0 \\ 0 & \sqrt{\frac{a}{\nu_A}} & 0 & \frac{c_+}{\sqrt{a\nu_A}} \\ \frac{c_-}{\sqrt{b\nu_B}} & 0 & \sqrt{\frac{b}{\nu_B}} & 0 \\ 0 & 0 & 0 & \sqrt{\frac{\nu_B}{b}} \end{pmatrix}. \tag{B.15}$$

This set of states is not an empty set of states. For instance, the covariance matrix with $a = 3$, $b = 2$, $c_+ = 2$ and $c_- = -4/3$ represents an entangled physical state satisfying $bc_+ + ac_- = 0$.

b) If $bc_+ + ac_- > 0$ we have $L_B > 0$ and if $bc_+ + ac_- < 0$ then $L_B < 0$. By solving equations (B.8) and (B.9) we get the matrix S_{3b} in the form (B.6) with

$$\begin{aligned} x_3 &= -\frac{L_A}{M}x_4, & x_7 &= -\frac{L_B}{M}x_8, \\ x_1 &= -\frac{aL_A - c_-M}{\nu_A M}x_4, & x_2 &= \frac{bM - c_-L_A}{\nu_A M}x_4, \\ x_5 &= -\frac{aL_B - c_-M}{\nu_B M}x_8, & x_6 &= \frac{bM - c_-L_B}{\nu_B M}x_8, \end{aligned}$$

$$\begin{aligned} x_4 &= M\sqrt{\frac{\nu_A}{2\left(aL_A^2 - 2c_-L_AM + bM^2\right)}}, \\ x_8 &= M\sqrt{\frac{\nu_B}{2\left(aL_B^2 - 2c_-L_BM + bM^2\right)}}. \end{aligned} \tag{B.16}$$

Case 4: $a < b$ In the case where $a < b$, the covariance matrix can be transformed into case 3 by applying a symplectic operation to swap the modes A and B. The symplectic matrix that then diagonalises the covariance matrix is given by $S_4 = \tilde{S}_3 T$, where $\tilde{S}_3$ is the same as S_3 but with a and b swapped, and T is given by

$$T = \begin{pmatrix} 0 & \mathbb{1}_2 \\ \mathbb{1}_2 & 0 \end{pmatrix}. \tag{B.17}$$

With the matrices $S_1, \cdots, S_4$ we can transform any two mode Gaussian covariance matrix in standard form into diagonal form.

Appendix C

Comment on measurements of Alice and Bob in Gaussian Intrinsic information

In Section 6.4, we discussed the merits born from swapping the order of the maximisation and minimisation in the definition of the Gaussian Intrinsic Information. That is, we asked whether $\tilde{\mu}_G(\hat{\rho}_{AB}) = \mu_G(\hat{\rho}_{AB})$ where

$$\tilde{\mu}_G(\hat{\rho}_{AB}) = \max_{\{\hat{\Pi}_A^G, \hat{\Pi}_B^G\}} \left(\min_{\hat{\Pi}_E^G} \left(\mathcal{I}(X : Y \downarrow Z) \right) \right), \tag{C.1}$$

and what advantages this would bring. If we assume for now that this is true, then the measurements that Alice and Bob perform are pure, so we need only optimise over rank one Gaussian POVMs.

The proof of this has come from Dr Ladislav Mišta and is as follows. The covariance matrices $\Gamma_{A,B}$ of a generic measurement (6.21) with mixed state seed elements can be expressed as $\Gamma_j = \Gamma_{p,j} + N_j$, where $\Gamma_{p,j}$ signifies a pure covariance matrix and $N_j = (\nu_j - 1)\Gamma_{p,j}$ is a positive semi-definite matrix, where $\nu_j \geq 1$ is a symplectic eigenvalue of Γ_j.

The outcome d_j, $j = A, B$ of a generic Gaussian POVM $\Pi_j^G(d_j)$ can therefore be expressed as $d_j = d_{p,j} + \chi_j$ where d_j is the outcome of a POVM with seed element $\Gamma_{p,j}$ and χ_A, χ_B are random variables associated with the classical correlation matrices N_A and N_B respectively. The conditional mutual information $\mathcal{I}\left(A : B|\bar{E}\right)$ of the distribution $P(d_A, d_B, d_{\bar{E}})$ then satisfies

$$\begin{aligned}
\mathcal{I}\left(A : B|\bar{E}\right) &= \mathcal{I}\left(\bar{E}A : B\right) - \mathcal{I}\left(\bar{E} : B\right) \\
&\leq \mathcal{I}\left(\bar{E}A_p : B\right) - \mathcal{I}\left(\bar{E} : B\right) \\
&= \mathcal{I}\left(A_p : B|\bar{E}\right) \\
&= \mathcal{I}\left(A_p : \bar{E}B\right) - \mathcal{I}\left(A_p : \bar{E}\right) \\
&\leq \mathcal{I}\left(A_p : \bar{E}B_p\right) - \mathcal{I}\left(A_p : \bar{E}\right) \\
&= \mathcal{I}\left(A_p : B_p|\bar{E}\right)
\end{aligned} \tag{C.2}$$

where $\mathcal{I}\left(A_p : B_p|\bar{E}\right)$ is the conditional mutual information between Alice and Bob from the distribution $P(d_{p,A}, d_{p,B}, d_{\bar{E}})$. In the first and fourth lines of (C.2) we have used the chain rule for the mutual information [185] and the inequalities in the second and fifth row follow from the fact that mixing $d_{p,j} \to d_{p,j} + \chi_j$ cannot increase mutual information between the outcomes of measurements on modes A & E (B & E) [185, 251].

From this it is apparent that Γ_A and Γ_B can be restricted to pure covariance matrices.

Appendix D

Reduction to covariant Rank-One POVMs in the analysis of Gaussian Ameliorated Measurement Induced Disturbance

In Chapter 8, we introduced the Gaussian Ameliorated Measurement Induced Disturbance (GAMID) denoted $\mathcal{A}^G(\hat{\rho}_{AB})$ which measures the gap between the quantum mutual information of a two mode Gaussian state and the highest value of the classical mutual information between the two parties after local Gaussian measurements.

For the two mode Gaussian states, we claimed that the only measurements that we need optimise over were covariant POVMS of the form given in equation (8.2) with pure seed states $\hat{\Pi}_j^G$. Here we prove that statement.

The measurement of local POVMs (8.2) on a Gaussian state $\hat{\rho}_{AB}$ gives the outcome $d = \left(d_A^T, d_B^T\right)^T$ distributed according to

$$P(d) = \mathrm{Tr}[\hat{\Pi}_A^G(d_A) \otimes \hat{\Pi}_B^G(d_B)\hat{\rho}_{AB}]. \tag{D.1}$$

Making use of the overlap formula for Wigner functions (2.73), the distribution can be expressed as

$$P(d) = (2\pi)^2 \int \mathcal{W}_{\hat{\Pi}_A^G(d_A)}(r_A)\mathcal{W}_{\hat{\Pi}_B^G(d_B)}(r_B)\mathcal{W}_{\hat{\rho}_{AB}}(r_A, r_B)\mathrm{d}^2 r_A \mathrm{d}^2 r_B. \tag{D.2}$$

This is simply a Gaussian integration and yields

$$P(d) = \frac{1}{\pi^2\sqrt{\det(\gamma + \gamma_A \oplus \gamma_B)}} e^{-d^T(\gamma+\gamma_A\oplus\gamma_B)^{-1}d}, \tag{D.3}$$

where $\gamma_{A,B}$ are CMs of the seed elements of POVMs (8.2) and γ is the CM of the state $\hat{\rho}_{AB}$. The CMs $\gamma_{A,B}$ can be expressed as $\gamma_j = \gamma_j^{(\pi)} + N_j$, where $\gamma_j^{(\pi)} = S_j^{-1}(S_j^T)^{-1}$ is a pure-state CM (S_j symplectically diagonalizes γ_j) and $N_j = (\nu_j - 1)\gamma_j^{(\pi)}$ is a positive-semidefinite matrix ($\nu_j \geq 1$ is a symplectic eigenvalue of γ_j).

This means that the outcome d_j with $j = A, B$ of a generic Gaussian POVM $\hat{\Pi}_j^G(d_j)$, with the seed element $\hat{\Pi}_j^G$ being a mixed state with covariance matrix γ_j, can be expressed as $d_j = d_j^{(\pi)} + \chi_j$. The symbol $d_j^{(\pi)}$ is the outcome of the POVM with a pure seed element having covariance matrix $\gamma_j^{(\pi)}$, and χ_A, χ_B are mutually uncorrelated random variables, uncorrelated with $d_A^{(\pi)}, d_B^{(\pi)}$ obeying Gaussian distributions with classical correlation matrices N_A and N_B respectively. Since such processing of variables $d_j^{(\pi)}$ cannot increase their Shannon mutual information due to the data processing inequality [251] we can restrict without loss of generality to optimisation over projections onto pure states.

So, of all the covariant measurements that could be performed on subsystems A and B, pure state covariant POVMs are optimal. However, does a pure state covariant measurement always beat all non-covariant Gaussian POVMs? We answer in the affirmative. Covariant measurements with pure state seed elements maximise the classical mutual information even

within the framework of a larger class of generally non-covariant Gaussian POVMs possessing the structure [220, 252]

$$\hat{\pi}_j^G(z_j) = \frac{p_j(y_j)}{2\pi}\hat{D}_j(d_j)\hat{\Pi}_j^G(y_j)\hat{D}_j^\dagger(d_j), \quad j = A, B, \tag{D.4}$$

and satisfying the completeness condition $\int_{z_j}\hat{\pi}_j^G(z_j)dz_j = \mathbb{1}_j$. Here $p_j(y_j)$ is a normalized distribution of the parameter y_j, $\hat{\Pi}_j^G(y_j)$ is a normalized Gaussian state with CM $\gamma_j(y_j)$ dependent on parameter y_j and $z_j = (d_j^T, y_j^T)^T$.

Upon measuring the POVM (D.4) on the Gaussian state $\hat{\rho}_{AB}$, one finds the outcomes z_A and z_B to follow the distribution $\mathcal{P}(z_A, z_B) = p_A(y_A)p_B(y_B)P(d, y_A, y_B)$, where the distribution $P(d, y_A, y_B)$ is obtained from Eq. (D.3) by replacing γ_j with $\gamma_j(y_j)$. Denoting the classical mutual information of the distribution $\mathcal{P}(z_A, z_B)$ and $P(d, y_A, y_B)$ as $\mathcal{I}\left(A(z_A) : B(z_B)\right)$ and $\mathcal{I}\left(A(y_A) : B(y_B)\right)$, respectively, one then has

$$\mathcal{I}\left(A(z_A) : B(z_B)\right) = \int \mathcal{I}\left(A(y_A) : B(y_B)\right) p(y_A)p(y_B)\mathrm{d}y_A\mathrm{d}y_B. \tag{D.5}$$

Hence it follows immediately that

$$\mathcal{I}_c^G(\hat{\rho}_{AB}) \leq \max_{\left(\hat{\pi}_A^G(z_A)\otimes\hat{\pi}_B^G(z_B)\right)} \mathcal{I}\left(A(z_A) : B(z_B)\right) = \mathcal{I}\left(A(y_A^0) : B(y_B^0)\right), \tag{D.6}$$

where we have to maximize over all Gaussian POVM elements $\hat{\pi}_j^G(z_j)$ and y_j^0 label the POVM elements $\hat{\Pi}_j^G(y_j^0)$, which maximize $\mathcal{I}\left(A(y_A) : B(y_B)\right)$. If we take these as seed elements of Gaussian POVMs (8.2), we construct local covariant POVMs which give mutual information $\mathcal{I}\left(A(y_A^0) : B(y_B^0)\right)$ and therefore achieve the classical mutual information $\mathcal{I}_c^G(\hat{\rho}_{AB})$.

References

[1] Y. Aharonov and D. Bohm. Significance of electromagnetic potentials in the quantum theory. Phys. Rev., 115:485, 1959.

[2] J. S. Bell. On the Einstein Podolsky Rosen paradox. Physics, 1:195, 1964.

[3] Edited by A. Bokulich and G. Jaeger. Philosophy of Quantum Information and Entanglement. Cambridge University Press, 2010.

[4] S. Hawking. The Universe in a Nutshell. Bantam Press, London, 2001.

[5] B. D'Espagnat. Conceptual Foundations of Quantum Mechanics. Addison-Wesley, United States, second edition, 1989.

[6] J. Von Neumann. Mathematical Foundations of Quantum Mechanics. Princeton University Press, 1955.

[7] H. Ollivier and W. Zurek. Quantum discord: a measure of the quantumness of correlations. Phys. Rev. Lett., 88:017901, 2001.

[8] A. Datta, A. Shaji, and C. M. Caves. Quantum discord and the power of one qubit. Phys. Rev. Lett., 100:050502, 2008.

[9] B. Julsgaard, A. Kozhekin, and E. Polzik. Experimental long-lived entanglement of two macroscopic objects. Nature, 413:400, 2001.

[10] B. Julsgaard, J. Sherson, J. Cirac, J. Fiurášek, and E. Polzik. Experimental demonstration of quantum memory for light. Nature, 432:482, 2004.

[11] C. Simon *et al.* . Quantum memories. The European Physical Journal D - Atomic, Molecular, Optical and Plasma Physics, 58:1, 2010.

[12] A. Einstein. On a heuristic viewpoint concerning the production and transformation of light (translation). Annalen der Physik, 17:132, 1905.

[13] U. Leonhardt. Essential Quantum Optics. Cambridge University Press, 2010.

[14] R. Y. Chiao and J. C. Garrison. Quantum Optics. Oxford University Press, 2008.

[15] M. O'Scully and M. Zubairy. Quantum Optics. Cambridge University Press, 1997.

[16] C. Gerry and P. Knight. Introductory Quantum Optics. Cambridge University Press, 2005.

[17] S. Barnett and P. Radmore. Methods in Theoretical Quantum Optics. Oxford Science Publications, 2002.

[18] R. Loudon. The quantum theory of light. Oxford University Press, 1973.

[19] D. Wallis and G. Milburn. Quantum Optics. Springer, 1995.

[20] L. Mandel and E. Wolf. Optical Coherence and Quantum Optics. Cambridge University Press, 1995.

[21] R. Glauber. The quantum theory of optical coherence. Phys. Rev., 130:2529, 1963.

[22] R. Glauber. Coherent and incoherent states of the radiation field. Phys. Rev., 131:2766, 1963.

[23] E. Schrödinger. Der stetige uebergang von der mikro- zur makromechanik. Naturwiss, 14:664, 1926.

[24] E. Schrödinger. Collected Papers in Wave Mechanics. Blackie and Son, 1928.

[25] A. Ferraro, S. Olivares, and M.G.A. Paris. Gaussian states in continuous variable quantum information. ArXiv:quant-ph/0503237, 2005.

[26] C.W. Gardiner. Quantum Noise. Springer, Berlin, 1991.

[27] W. Pauli. Die allgemeinen Prinzipien der Wellenmechanik,Handbuch der Physik. Springer, Berlin, 1933.

[28] W. Pauli. General Principles of Quantum Optics. Springer, Berlin, 1980.

[29] D. Stoler. Equivalence classes of minimum uncertainty packets. Phys. Rev. D, 1:3217, 1970.

[30] J. N. Hollenhorst. Quantum limits on resonant-mass gravitational-radiation detectors. Phys. Rev. D, 19:1669, 1981.

[31] C. M. Caves. Quantum-mechanical noise in an interferometer. Phys. Rev. D, 23:1693, 1981.

[32] R. M. Wilcox. Exponential operators and parameter differentiation in quantum physics. J. Math. Phys., 8:962, 1967.

[33] M. Lutzky. Parameter differentiation of exponential operators and the Baker-Campbell-Hausdorff formula. J. Math. Phys., 9:1125, 1968.

[34] M. Ban. Lie-algebra methods in quantum optics: The Liouville-space formulation. Phys. Rev. A, 47:5093, 1993.

[35] R. Loudon and P.L. Knight. Squeezed light. J. Mod. Opt., 34:709, 1987.

[36] E. Wigner. On the quantum correction for thermodynamic equilibrium. Phys. Rev., 40:749, 1932.

[37] J. Bertrand and P. Bertrand. A tomographic approach to Wigner's function. Foundations of Physics, 17:397, 1987.

[38] K. E. Cahill and R. J. Glauber. Ordered expansions in boson amplitude operators. Phys. Rev., 177:1857, 1969.

[39] K. E. Cahill and R. J. Glauber. Density operators and quasiprobability distributions. Phys. Rev., 177:1882, 1969.

[40] A. Wünsche. The complete Gaussian class of quasiprobabilities and its relation to squeezed states and their discrete excitations. Quantum and Semiclassical Optics: Journal of the European Optical Society Part B, 8:343, 1996.

[41] E. C. G. Sudarshan. Equivalence of semiclassical and quantum mechanical descriptions of statistical light beams. Phys. Rev. Lett., 10:277, 1963.

[42] R. Glauber. Photon correlations. Phys. Rev. Lett., 10:84, 1963.

[43] S. L. Braunstein and P. van Loock. Quantum information with continuous variables. Rev. Mod. Phys., 77:513, 2005.

[44] G. Adesso. Entanglement of Gaussian states. PhD thesis, University of Salerno, 2007.

[45] G. Adesso and F. Illuminati. Entanglement in continuous-variable systems: recent advances and current perspectives. J. Phys. A: Mathematical and Theoretical, 40:7821, 2007.

[46] C. Weedbrook *et al.* . Gaussian quantum information. ArXiv:1110.3234, 2011.

[47] J. Marcinkiewicz. Math.Z., 44:612, 1939.

[48] A. K. Rajagopal and E. C. G. Sudarshan. Some generalizations of the Marcinkiewicz theorem and its implications to certain approximation schemes in many-particle physics. Phys. Rev. A, 10:1852, 1974.

[49] J. Ivan, M. Kumar, and R. Simon. A measure of non-Gaussianity for quantum states. Quantum Information Processing, page 1, 2011.

[50] R. Simon, N. Mukunda, and B. Dutta. Quantum-noise matrix for multimode systems: U(n) invariance, squeezing and normal forms. Phys. Rev. A, 49:1567, 1994.

[51] M. A. Nielsen and I. L. Chuang. Quantum Computation and Quantum Information. Cambridge University Press, 2000.

[52] A. Einstein, B. Podolsky, and N. Rosen. Can quantum-mechanical description of physical reality be considered complete? Phys. Rev., 47:777, 1935.

[53] V. B. Braginsky and F. Ya. Khalili. Quantum nondemolition measurements: the route from toys to tools. Rev. Mod. Phys., 68:1, 1996.

[54] P. Grangier, J. A. Levenson, and J. P. Poizat. Quantum non-demolition measurements in optics. Nature, 396:537, 1998.

[55] S. Braunstein. Squeezing as an irreducible resource. Phys. Rev. A, 71:055801, 2005.

[56] J. Williamson. Am. J. Math., 58:141, 1936.

[57] G. Adesso, A. Serafini, and F. Illuminati. Entanglement, purity, and information entropies in continuous variable systems. Open Systems & Information Dynamics, 12:189, 2005.

[58] A. Serafini. Multimode uncertainty relations and separability of continuous variable states. Phys. Rev. Lett., 96:110402, 2006.

[59] H. Huang and G. S. Agarwal. General linear transformations and entangled states. Phys. Rev. A, 49:52, 1994.

[60] A. Serafini, F., and S. De Siena. Symplectic invariants, entropic measures and correlations of Gaussian states. J. Phys. B: Atomic, Molecular and Optical Physics, 37:L21, 2004.

[61] A. S. Holevo and R. F. Werner. Evaluating capacities of bosonic Gaussian channels. Phys. Rev. A, 63:032312, 2001.

[62] J. Fiurášek. Gaussian transformations and distillation of entangled Gaussian states. Phys. Rev. Lett., 89:137904, 2002.

[63] G. Giedke and J. I. Cirac. Characterization of Gaussian operations and distillation of Gaussian states. Phys. Rev. A, 66:032316, 2002.

[64] E. Schrödinger. Discussion of probability relations between separated systems. Mathematical Proceedings of the Cambridge Philosophical Society, 31:555, 1935.

[65] E. Schrödinger. Die gegenwärtige situation in der quantenmechanik. Naturwissenschaften, 23:807–812,823–828,844–849, 1935.

[66] J. D. Trimmer. The present situation in quantum mechanics: a translation of Schrödinger's "Cat Paradox" paper. Proceedings of the American Philosophical Society, 124:323, 1980.

[67] R. Horodecki and P. Horodecki. Quantum redundancies and local realism. Physics Letters A, 194:147, 1994.

[68] R. Horodecki and M. Horodecki. Information-theoretic aspects of inseparability of mixed states. Phys. Rev. A, 54:1838, 1996.

[69] N. J. Cerf and C. Adami. Negative entropy and information in quantum mechanics. Phys. Rev. Lett., 79:5194, 1997.

[70] R. Horodecki, P. Horodecki, and M. Horodecki. Quantum α-entropy inequalities: independent condition for local realism? Physics Letters A, 210:377, 1996.

[71] A. Ekert. Quantum cryptography based on Bell's theorem. Phys. Rev. Lett., 67:661, 1991.

[72] C. H. Bennett and S. J. Wiesner. Communication via one- and two-particle operators on Einstein-Podolsky-Rosen states. Phys. Rev. Lett., 69:2881, 1992.

[73] C. Bennett, G. Brassard, C. Crepeau, R. Jozsa, A. Peres, and W. Wootters. Teleporting an unknown quantum state via dual-classical and Einstein-Podolsky-Rosen channels. Phys. Rev. Lett., 70:1895, 1993.

[74] D. Boschi, S. Branca, F. De Martini, L. Hardy, and S. Popescu. Experimental realization of teleporting an unknown pure quantum state via dual classical and Einstein-Podolsky-Rosen channels. Phys. Rev. Lett., 80:1121, 1998.

[75] P. W. Shor. Polynomial-Time Algorithms for Prime Factorization and Discrete Logarithms on a Quantum Computer. Siam J. Comput., 26:1484, 1997.

[76] D. Deutsche. Quantum theory, the Church-Turing principle and the universal quantum computer. Proc. R. Soc. Lond. A, 400:97, 1985.

[77] R. Horodecki, P. Horodecki, M. Horodecki, and K. Horodecki. Quantum entanglement. Rev. Mod. Phys., 81:865, 2009.

[78] A. Aspect, P. Grangier, and G. Roger. Experimental tests of realistic local theories via Bell's theorem. Phys. Rev. Lett., 47:460, Aug 1981.

[79] A. Aspect, P. Grangier, and G. Roger. Experimental realization of Einstein-Podolsky-Rosen-Bohm *Gedankenexperiment* : a new violation of Bell's inequalities. Phys. Rev. Lett., 49:91, 1982.

[80] A. Aspect, J. Dalibard, and G. Roger. Experimental test of Bell's inequalities using time- varying analyzers. Phys. Rev. Lett., 49:1804, 1982.

[81] N. Brunner, N. Gisin, V. Scarani, and C. Simon. Detection loophole in asymmetric Bell experiments. Phys. Rev. Lett., 98:220403, 2007.

[82] J. Larsson. Bell's inequality and detector inefficiency. Phys. Rev. A, 57:3304, 1998.

[83] T. Scheidl *et al.* . Violation of local realism with freedom of choice. Proc. Natl. Acad. Sci. USA, 107:19708, 2010.

[84] P. R. Holland. The quantum theory of motion. Cambridge University Press, 1993.

[85] N. Gisin. Bell's inequality holds for all non-product states. Physics Letters A, 154:201, 1991.

[86] N. Gisin and A. Peres. Maximal violation of Bell's inequality for arbitrarily large spin. Physics Letters A, 162:15, 1992.

[87] R. F. Werner. Quantum states with Einstein-Podolsky-Rosen correlations admitting a hidden-variable model. Phys. Rev. A, 40:4277, 1989.

[88] A. Acín, T. Durt, N. Gisin, and J. I. Latorre. Quantum nonlocality in two three-level systems. Phys. Rev. A, 65:052325, 2002.

[89] J. F. Clauser, M. A. Horne, A. Shimony, and R. A. Holt. Proposed experiment to test local hidden-variable theories. Phys. Rev. Lett., 23:880, 1969.

[90] D. Greenberger, M. Horne, and A. Zeilinger. "Going beyond Bell's theorem" *in* Bell's Theorem, Quantum Theory, and Conceptions of the Universe. Kluwer Academic, Dordrecht, 1989.

[91] L. Masanes. All bipartite entangled states are useful for information processing. Phys. Rev. Lett., 96:150501, 2006.

[92] R. F. Werner and M. M. Wolf. Bound entangled Gaussian states. Phys. Rev. Lett., 86:3658, 2001.

[93] B. M. Terhal. Bell inequalities and the separability criterion. Physics Letters A, 271:319, 2000.

[94] M. B. Plenio and S. Virmani. An introduction to entanglement measures. Quant. Inf. Comput., 7:1, 2007.

[95] A. Peres. Separability criterion for density matrices. Phys. Rev. Lett., 77:1413, 1996.

[96] M. Horodecki, P. Horodecki, and R. Horodecki. Separability of mixed states: necessary and sufficient conditions. Physics Letters A, 223:1, 1996.

[97] R. Simon. Peres-Horodecki criterion for continuous variable systems. Phys. Rev. Lett., 84:2726, 2000.

[98] A. Wehrl. How chaotic is a state of a quantum system? Reports on Mathematical Physics, 6:15, 1974.

[99] T. Hiroshima. Majorization criterion for distillability of a bipartite quantum state. Phys. Rev. Lett., 91:057902, 2003.

[100] M. Horodecki and P. Horodecki. Reduction criterion of separability and limits for a class of distillation protocols. Phys. Rev. A, 59:4206, 1999.

[101] P. Horodecki. Separability criterion and inseparable mixed states with positive partial transposition. Physics Letters A, 232:333, 1997.

[102] D. Bruß and A. Peres. Construction of quantum states with bound entanglement. Phys. Rev. A, 61:030301, 2000.

[103] L. Duan, G. Giedke, J. I. Cirac, and P. Zoller. Inseparability criterion for continuous variable systems. Phys. Rev. Lett., 84:2722, 2000.

[104] V. Giovannetti, S. Mancini, D. Vitali, and P. Tombesi. Characterizing the entanglement of bipartite quantum systems. Phys. Rev. A, 67:022320, 2003.

[105] H. F. Hofmann and S. Takeuchi. Violation of local uncertainty relations as a signature of entanglement. Phys. Rev. A, 68:032103, 2003.

[106] H. F. Hofmann. Bound entangled states violate a nonsymmetric local uncertainty relation. Phys. Rev. A, 68:034307, 2003.

[107] C. Bennett, G. Brassard, S. Popescu, B. Schumacher, J. Smolin, and W. Wootters. Purification of noisy entanglement and faithful teleportation via noisy channels. Phys. Rev. Lett., 76:722, 1996.

[108] C. H. Bennett, D. P. DiVincenzo, J. A. Smolin, and W. K. Wootters. Mixed-state entanglement and quantum error correction. Phys. Rev. A, 54:3824, 1996.

[109] M. Horodecki, P. Horodecki, and R. Horodecki. Inseparable two spin- $\frac{1}{2}$ density matrices can be distilled to a singlet form. Phys. Rev. Lett., 78:574, 1997.

[110] C. H. Bennett, H. J. Bernstein, S. Popescu, and B. Schumacher. Concentrating partial entanglement by local operations. Phys. Rev. A, 53:2046, 1996.

[111] M. A. Nielsen. Conditions for a class of entanglement transformations. Phys. Rev. Lett., 83:436, 1999.

[112] T. Opatrný, G. Kurizki, and D.-G. Welsch. Improvement on teleportation of continuous variables by photon subtraction via conditional measurement. Phys. Rev. A, 61:032302, 2000.

[113] S. Olivares, M. G. A. Paris, and R. Bonifacio. Teleportation improvement by inconclusive photon subtraction. Phys. Rev. A, 67:032314, 2003.

[114] J. Eisert, D. Browne, S. Scheel, and M. Plenio. Distillation of continuous-variable entanglement with optical means. Ann. Phys. NY, 311:431, 2004.

[115] A. Lund and T. Ralph. Continuous-variable entanglement distillation over a general lossy channel. Phys. Rev. A, 80:032309, 2009.

[116] A. Kitagawa, M. Takeoka, M. Sasaki, and A. Chefles. Entanglement evaluation of non-Gaussian states generated by photon subtraction from squeezed states. Phys. Rev. A, 73:042310, 2006.

[117] A. Ourjoumtsev, A. Dantan, R. Tualle-Brouri, and P. Grangier. Increasing entanglement between Gaussian states by coherent photon subtraction. Phys. Rev. Lett., 98:030502, 2007.

[118] H. Takahashi, J. Neergaard-Nielsen, M. Takeuchi, M. Takeoka, K. Hayasaka, A. Furusawa, and M. Sasaki. Entanglement distillation from Gaussian input states. Nature Photonics, 4:178, 2010.

[119] R. Dong, M. Lassen, J. Heersink, C. Marquardt, and R. Filip. Continuous-variable entanglement distillation of non-Gaussian mixed states. Phys. Rev. A, 82:012312, 2010.

[120] A. Datta, L. Zhang, J. Nunn, N. K. Langford, A. Feito, M. Plenio, and I. A. Walmsley. Compact continuous-variable entanglement distillation. Phys. Rev. Lett., 108:060502, 2012.

[121] J. Eisert, S. Scheel, and M. Plenio. Distilling Gaussian states with Gaussian operations is impossible. Phys. Rev. Lett., 89:137903, 2002.

[122] M. Horodecki, P. Horodecki, and R. Horodecki. Mixed-state entanglement and distillation: is there a "bound" entanglement in nature? Phys. Rev. Lett., 80:5239, 1998.

[123] P. Horodecki and M. Lewenstein. Bound entanglement and continuous variables. Phys. Rev. Lett., 85:2657, 2000.

[124] J. Eisert, C. Simon, and M. B Plenio. On the quantification of entanglement in infinite-dimensional quantum systems. J. Phys. A: Mathematical and General, 35:3911, 2002.

[125] V. Vedral, M. B. Plenio, M. A. Rippin, and P. L. Knight. Quantifying entanglement. Phys. Rev. Lett., 78:2275, 1997.

[126] G. Vidal. Entanglement monotones. Journal of Modern Optics, 47:355, 2000.

[127] S. Popescu and D. Rohrlich. Thermodynamics and the measure of entanglement. Phys. Rev. A, 56:R3319, 1997.

[128] M. Horodecki, P. Horodecki, and R. Horodecki. Limits for entanglement measures. Phys. Rev. Lett., 84:2014, 2000.

[129] M. Horodecki M. J. Donald and O. Rudolph. The uniqueness theorem for entanglement measures. J. Math. Phys., 43:4252, 2002.

[130] G. Vidal and J. I. Cirac. Irreversibility in asymptotic manipulations of a distillable entangled state. Phys. Rev. A, 65:012323, 2001.

[131] P. M. Hayden, M. Horodecki, and B. M. Terhal. The asymptotic entanglement cost of preparing a quantum state. J. Phys. A: Mathematical and General, 34:6891, 2001.

[132] M. Horodecki, A. Sen(De), and U. Sen. Rates of asymptotic entanglement transformations for bipartite mixed states: maximally entangled states are not special. Phys. Rev. A, 67:062314, 2003.

[133] G. Vidal, W. Dür, and J. I. Cirac. Entanglement cost of bipartite mixed states. Phys. Rev. Lett., 89:027901, Jun 2002.

[134] I. Devetak and A. Winter. Distilling common randomness from bipartite quantum states. IEEE Trans. Inf. Th., 50:3183, 2004.

[135] M. B. Hastings. Superadditivity of communication capacity using entangled inputs. Nat. Phys., 5:255, 2009.

[136] G. Giedke, M. M. Wolf, O. Krüger, R. F. Werner, and J. I. Cirac. Entanglement of formation for symmetric Gaussian states. Phys. Rev. Lett., 91:107901, 2003.

[137] M. M. Wolf, G. Giedke, O. Krüger, R. F. Werner, and J. I. Cirac. Gaussian entanglement of formation. Phys. Rev. A, 69:052320, 2004.

[138] P. Marian and T. A. Marian. Entanglement of formation for an arbitrary two-mode Gaussian state. Phys. Rev. Lett., 101:220403, 2008.

[139] A. Miranowicz and S. Ishizaka. Closed formula for the relative entropy of entanglement. Phys. Rev. A, 78:032310, 2008.

[140] S. Friedland and G. Gour. An explicit expression for the relative entropy of entanglement in all dimensions. J. Math. Phys., 52:052201, 2011.

[141] X. Chen. Gaussian relative entropy of entanglement. Phys. Rev. A, 71:062320, 2005.

[142] K. Zyczkowski, P. Horodecki, A. Sanpera, and M. Lewenstein. Volume of the set of separable states. Phys. Rev. A, 58:883, 1998.

[143] G. Vidal and R. F. Werner. Computable measure of entanglement. Phys. Rev. A, 65:032314, 2002.

[144] M. B. Plenio. Logarithmic negativity: a full entanglement monotone that is not convex. Phys. Rev. Lett., 95:090503, 2005.

[145] M. Christandl and A. Winter. "Squashed Entanglement": an additive entanglement measure. J. Math. Phys., 45:829, 2004.

[146] R Alicki and M Fannes. Continuity of quantum conditional information. J. Phys. A: Mathematical and General, 37:L55, 2004.

[147] H.-J. Briegel, W. Dür, J. I. Cirac, and P. Zoller. Quantum repeaters: the role of imperfect local operations in quantum communication. Phys. Rev. Lett., 81:5932, 1998.

[148] A. I. Lvovsky, B. C. Sanders, and W. Tittel. Optical quantum memory. Nature Photonics, 3:706, 2009.

[149] L. Duan, J. I. Cirac, P. Zoller, and E. S. Polzik. Quantum communication between atomic ensembles using coherent light. Phys. Rev. Lett., 85:5643, 2000.

[150] B. Julsgaard. Entanglement and quantum interactions with macroscopic gas samples. PhD thesis, University of Aarhus, Denmark, 2003.

[151] D. Browne, J. Eisert, S. Scheel, and M. Plenio. Driving non-Gaussian to Gaussian states with linear optics. Phys. Rev. A, 67:062320, 2003.

[152] J. Sherson, A. S. Sørensen, J. Fiurášek, K. Mølmer, and E. S. Polzik. Light qubit storage and retrieval using macroscopic atomic ensembles. Phys. Rev. A, 74:011802, 2006.

[153] J. F. Sherson and K. Mølmer. Polarization squeezing by optical Faraday rotation. Phys. Rev. Lett., 97:143602, 2006.

[154] C. A. Muschik, K. Hammerer, E. S. Polzik, and J. I. Cirac. Efficient quantum memory and entanglement between light and an atomic ensemble using magnetic fields. Phys. Rev. A, 73:062329, 2006.

[155] Y. Aharonov and L. Vaidman. Properties of a quantum system during the time interval between two measurements. Phys. Rev. A, 41:11, 1990.

[156] R. García-Patrón, J. Fiurášek, and N. J. Cerf. Loophole-free test of quantum nonlocality using high-efficiency homodyne detectors. Phys. Rev. A, 71:022105, 2005.

[157] S. Zhang and P. van Loock. Local Gaussian operations can enhance continuous-variable entanglement distillation. Phys. Rev. A, 84:062309, 2011.

[158] V. V. Dodonov, O. V. Man'ko, and V. I. Man'ko. Photon distribution for one-mode mixed light with a generic Gaussian Wigner function. Phys. Rev. A, 49:2993, 1994.

[159] G. Adam. Density matrix elements and moments for generalized Gaussian state fields. Journal of Modern Optics, 42:1311, 1995.

[160] O. V. Manko and G. Schrade. Photon statistics of two-mode squeezed light with Gaussian Wigner function. Physica Scripta, 58:228, 1998.

[161] K. Nemoto and S. L. Braunstein. Equivalent efficiency of a simulated photon-number detector. Phys. Rev. A, 66:032306, 2002.

[162] J. Eisert and M. M. Wolf. Gaussian Quantum Channels. Imperial College Press, London, 2007. Quantum Information with Continous Variables of Atoms and Light.

[163] C. Shannon. Communication theory of secrecy systems. Bell System Technical Journal, 28:656, 1948.

[164] W. Diffie and M. E. Hellman. New directions in cryptography. IEEE Trans. Inf. Th., 22:644, 1976.

[165] U. Maurer and S. Wolf. Secret-key agreement over unauthenticated public channels - part I: definitions and a completeness result. IEEE Trans. Inf. Th., 49:822, 2003.

[166] M. Kreißig. Information-theoretical secret-key agreement and bound information. Master's thesis, Universitat Politecnica de Catalunya, 2009.

[167] I. Csiszar and J. Korner. Broadcast channels with confidential messages. IEEE Trans. Inf. Th., 24:339, 1978.

[168] U. Maurer and S. Wolf. Unconditionally secure key agreement and the intrinsic conditional information. IEEE Trans. Inf. Th., 45:499, 1999.

[169] N. Gisin, R. Renner, and S. Wolf. Linking Classical and quantum key agreement: is there a classical analog to bound entanglement? Algorithmica, 34:389, 2002.

[170] N. Gisin and S. Wolf. Linking classical and quantum key agreement: is there "bound information". In Mihir Bellare, editor, Advances in Cryptology - CRYPTO 2000, volume 1880 of Lecture Notes in Computer Science, page 482. Springer Berlin / Heidelberg, 2000.

[171] A. Acín, J. I. Cirac, and Ll. Masanes. Multipartite bound information exists and can be activated. Phys. Rev. Lett., 92:107903, 2004.

[172] L. Mišta Jr. and N. Korolkova. Gaussian multipartite bound information. ArXiv:1108.0578, 2011.

[173] G. M. D'Ariano, P. Perinotti, and M. F. Sacchi. Informationally complete measurements and group representation. Journal of Optics B: Quantum and Semiclassical Optics, 6:S487, 2004.

[174] M. Christandl, R. Renner, and S. Wolf. A property of the intrinsic mutual information. Proceedings ISIT 2003, Yokohama, Japan, page 258, 2003.

[175] C. Shannon. A mathematical theory of communication. Bell System Technical Journal, 27:623, 1948.

[176] J. Fiurášek and L. Mišta. Gaussian localizable entanglement. Phys. Rev. A, 75:060302(R), 2007.

[177] A. Ferraro, L. Aolita, D. Cavalcanti, F. M. Cucchietti, and A. Acín. Almost all quantum states have nonclassical correlations. Phys. Rev. A, 81:052318, 2010.

[178] E. Knill and R. Laflamme. Power of one bit of quantum information. Phys. Rev. Lett., 81:5672, 1998.

[179] B. P. Lanyon, M. Barbieri, M. P. Almeida, and A. G. White. Experimental quantum computing without entanglement. Phys. Rev. Lett., 101:200501, 2008.

[180] A. Datta. Studies on the role of entanglement in mixed-state quantum computation. PhD thesis, University of New Mexico, 2008.

[181] T. S. Cubitt, F. Verstraete, W. Dür, and J. I. Cirac. Separable states can be used to distribute entanglement. Phys. Rev. Lett., 91:037902, 2003.

[182] L. Mišta and N. Korolkova. Distribution of continuous-variable entanglement by separable Gaussian states. Phys. Rev. A, 77:050302, 2008.

[183] L. Mišta and N. Korolkova. Improving continuous-variable entanglement distribution by separable states. Phys. Rev. A, 80:032310, 2009.

[184] C. Shannon. A mathematical theory of communication. Bell System Technical Journal, 27:379, 1948.

[185] T. M. Cover and J. A. Thomas. Elements of Information Theory. John Wiley & Sons Inc., United States, 1991.

[186] W. H. Zurek. Quantum optics, experimental gravitation and measurement theory. Plenum, New York, 1983.

[187] S. M. Barnett and S. J. D. Phoenix. Entropy as a measure of quantum optical correlation. Phys. Rev. A, 40:2404, 1989.

[188] B. Groisman, S. Popescu, and A. Winter. Quantum, classical, and total amount of correlations in a quantum state. Phys. Rev. A, 72:032317, 2005.

[189] N. J. Cerf and C. Adami. Negative entropy and information in quantum mechanics. Phys. Rev. Lett., 79:5194, 1997.

[190] N. J. Cerf and C. Adami. Quantum extension of conditional probability. Phys. Rev. A, 60:893, 1999.

[191] B. Schumacher and M. A. Nielsen. Quantum data processing and error correction. Phys. Rev. A, 54:2629, 1996.

[192] D. Girolami, M. Paternostro, and G. Adesso. Faithful nonclassicality indicators and extremal quantum correlations in two-qubit states. J. Phys. A: Mathematical and Theoretical, 44:352002, 2011.

[193] L. Henderson and V. Vedral. Classical, quantum and total correlations. J. Phys. A: Mathematical and General, 34:6899, 2001.

[194] B. Dakić, V. Vedral, and Č. Brukner. Necessary and sufficient condition for nonzero quantum discord. Phys. Rev. Lett., 105:190502, 2010.

[195] A. Datta. A condition for the nullity of quantum discord. ArXiv:1003.5256, 2011.

[196] S. Luo, S. Fu, and N. Li. Decorrelating capabilities of operations with application to decoherence. Phys. Rev. A, 82:052122, 2010.

[197] Z. Xi, X. Lu, X. Wang, and Y. Li. Necessary and sufficient condition for saturating the upper bound of quantum discord. ArXiv:1111.3837, 2011.

[198] C. Zhang, S. Yu, Q. Chen, and C. H. Oh. Observable estimation of entanglement of formation and quantum discord for bipartite mixed quantum states. Phys. Rev. A, 84:052112, 2011.

[199] Yu S, C. Zhang, Q. Chen, and C. H. Oh. Tight bounds for the quantum discord. ArXiv:1102.1301, 2011.

[200] S. Luo. Quantum discord for two-qubit systems. Phys. Rev. A, 77:042303, 2008.

[201] M. S. Sarandy. Classical correlation and quantum discord in critical systems. Phys. Rev. A, 80:022108, 2009.

[202] J. Maziero, L. C. Céleri, R. M. Serra, and V. Vedral. Classical and quantum correlations under decoherence. Phys. Rev. A, 80:044102, 2009.

[203] F. Galve, G. L. Giorgi, and R. Zambrini. Maximally discordant mixed states of two qubits. Phys. Rev. A, 83:012102, 2011.

[204] B. Bylicka and D. Chruściński. Witnessing quantum discord in $2 \times N$ systems. Phys. Rev. A, 81:062102, 2010.

[205] D. Girolami and G. Adesso. Quantum discord for general two-qubit states: analytical progress. Phys. Rev. A, 83:052108, 2011.

[206] A. Streltsov, H. Kampermann, and D. Bruß. Behavior of quantum correlations under local noise. Phys. Rev. Lett., 107:170502, 2011.

[207] M. Koashi and A. Winter. Monogamy of quantum entanglement and other correlations. Phys. Rev. A, 69:022309, 2004.

[208] Felipe F. Fanchini, Marcio F. Cornelio, Marcos C. de Oliveira, and Amir O. Caldeira. Conservation law for distributed entanglement of formation and quantum discord. Phys. Rev. A, 84:012313, 2011.

[209] F. F. Fanchini, L. K. Castelano, M. F. Cornelio, and M. C. de Oliveira. Locally inaccessible information as a fundamental ingredient to quantum information. New Journal of Physics, 14:013027, 2012.

[210] V. Madhok and A. Datta. Interpreting quantum discord through quantum state merging. Phys. Rev. A, 83:032323, 2011.

[211] D. Cavalcanti, L. Aolita, S. Boixo, K. Modi, M. Piani, and A. Winter. Operational interpretations of quantum discord. Phys. Rev. A, 83:032324, 2011.

[212] M. Horodecki, J. Oppenheim, and A. Winter. Partial quantum information. Nature, 436:673, 2005.

[213] M. Horodecki, J. Oppenheim, and A. Winter. Quantum state merging and negative information. Communications in Mathematical Physics, 269:107, 2007.

[214] D. Slepian and J. Wolf. Noiseless coding of correlated information sources. IEEE. Transac. Inf. Th., 19:471, 1973.

[215] D. Yang, M. Horodecki, and Z. D. Wang. An additive and operational entanglement measure: conditional entanglement of mutual information. Phys. Rev. Lett., 101:140501, 2008.

[216] M. B. Plenio and V. Vitelli. The physics of forgetting: Landauer's erasure principle and information theory. Contemporary Physics, 42:25, 2001.

[217] L. Szilárd. On the reduction of entropy in a thermodynamic system by the interference of intelligent beings. Z. Phys., 53:840, 1929.

[218] W. Zurek. Quantum discord and Maxwell's demons. Phys. Rev. A, 67:012320, 2003.

[219] M. F. Cornelio, M. C. de Oliveira, and F. F. Fanchini. Entanglement irreversibility from quantum discord and quantum deficit. Phys. Rev. Lett., 107:020502, 2011.

[220] P. Giorda and M. G. A. Paris. Gaussian quantum discord. Phys. Rev. Lett., 105:020503, 2010.

[221] G. Adesso and A. Datta. Quantum versus classical correlations in Gaussian states. Phys. Rev. Lett., 105:030501, 2010.

[222] S. Luo. Using measurement-induced disturbance to characterize correlations as classical or quantum. Phys. Rev. A, 77:022301, 2008.

[223] S. Wu, U. V. Poulsen, and K. Mølmer. Correlations in local measurements on a quantum state, and complementarity as an explanation of nonclassicality. Phys. Rev. A, 80:032319, 2009.

[224] A. Datta and S. Gharibian. Signatures of nonclassicality in mixed-state quantum computation. Phys. Rev. A, 79:042325, 2009.

[225] M. Piani, P. Horodecki, and R. Horodecki. No-local-broadcasting theorem for multipartite quantum correlations. Phys. Rev. Lett., 100:090502, 2008.

[226] J. Maziero, L. C. Celeri, and R. M. Serra. Symmetry aspects of quantum discord. ArXiv:1004.2082, 2011.

[227] K. Modi, T. Paterek, W. Son, V. Vedral, and M. Williamson. Unified view of quantum and classical correlations. Phys. Rev. Lett., 104:080501, 2010.

[228] A. SaiToh, R. Rahimi, and M. Nakahara. Nonclassical correlation in a multipartite quantum system: two measures and evaluation. Phys. Rev. A, 77:052101, 2008.

[229] S. Bravyi. Entanglement entropy of multipartite pure states. Phys. Rev. A, 67:012313, 2003.

[230] M. Piani, S. Gharibian, G. Adesso, J. Calsamiglia, P. Horodecki, and A. Winter. All nonclassical correlations can be activated into distillable entanglement. Phys. Rev. Lett., 106:220403, 2011.

[231] J. Peřina and J. Křepelka. Multimode description of spontaneous parametric down-conversion. Journal of Optics B: Quantum and Semiclassical Optics, 7:246, 2005.

[232] J. Peřina and J. Křepelka. Multimode description of stimulated parametric down-conversion. Optics Communications, 265:632, 2006.

[233] J. Peřina and J. Křepelka. Joint probability distributions of stimulated parametric down-conversion for controllable nonclassical fluctuations. Optics Communications, 281:4705, 2008.

[234] J. Peřina. Quantum statistics of linear and nonlinear optical phenomena. Kluwer,Dordrecht, 1991.

[235] I. M. Gelfand and A. M. Yaglom. Computation of the amount of information about a stochastic function contained in another such function. Usp. Mat. Nauk, 12:3, 1957.

[236] A. Serafini, O.C.O. Dahlsten, D. Gross, and M. B. Plenio. Canonical and micro-canonical typical entanglement of continuous variable systems. J. Phys. A: Mathematical and Theoretical, 40:9551, 2007.

[237] A. Al-Qasimi and D. F. V. James. Comparison of the attempts of quantum discord and quantum entanglement to capture quantum correlations. Phys. Rev. A, 83:032101, 2011.

[238] L. Mišta, R. Filip, and J. Fiurášek. Continuous-variable Werner state: separability, nonlocality, squeezing, and teleportation. Phys. Rev. A, 65:062315, 2002.

[239] A. P. Lund, T. C. Ralph, and P. van Loock. Entangled non-Gaussian states formed by mixing Gaussian states. Journal of Modern Optics, 55:2083, 2008.

[240] D. Chruściński and A. Kossakowski. Class of positive partial transposition states. Phys. Rev. A, 74:022308, 2006.

[241] C. Rodó, G. Adesso, and A. Sanpera. Operational quantification of continuous-variable correlations. Phys. Rev. Lett., 100:110505, 2008.

[242] M. G. Genoni, M. G. A. Paris, and K. Banaszek. Quantifying the non-Gaussian character of a quantum state by quantum relative entropy. Phys. Rev. A, 78:060303(R), 2008.

[243] Z. Merali. Quantum computing: the power of discord. Nature, 474:24, 2011.

[244] M. G. Genoni and M. G. A. Paris. Quantifying non-Gaussianity for quantum information. Phys. Rev. A, 82:052341, 2010.

[245] W. K. Wootters. Entanglement of formation of an arbitrary state of two qubits. Phys. Rev. Lett., 80:2245, 1998.

[246] H. Kampermann A. Streltsov and D. Bruß. Quantum cost for sending entanglement. ArXiv:1203.1264, 2012.

[247] T. K. Chuan, J. Maillard, K. Modi, T. Paterek, M. Paternostro, and M. Piani. Role of quantumness of correlations in entanglement distribution. ArXiv:1203.1268, 2012.

[248] A. Erdélyi *et al.* . Bateman Manuscript Project: Higher Transcendental Functions Volume 2. McGrawhill Book Company, 1953.

[249] A. Serafini, G. Adesso, and F. Illuminati. Unitarily localizable entanglement of Gaussian states. Phys. Rev. A, 71:032349, 2005.

[250] S. Pirandola, A. Serafini, and S. Lloyd. Correlation matrices of two-mode bosonic systems. Phys. Rev. A, 79:052327, 2009.

[251] A. Kolmogorov. On the Shannon theory of information transmission in the case of continuous signals. IRE Transactions on Information Theory, 2:102, 1956.

[252] L. Mišta and J. Fiurášek. Mixed-state localizable entanglement for continuous variables. Phys. Rev. A, 78:012359, 2008.